New insights into the thioredoxin-dependent redox regulation in the cyanobacterium *Synechocystis* sp. PCC 6803

Trabajo presentado para optar al grado de
Doctor en Ciencias Biológicas por el Licenciado

Alejandro Mata Cabana

Sevilla, septiembre 2010

Directores:

Dr. Francisco Javier Florencio Bellido
Catedrático de Bioquímica y Biología Molecular

Dra. Anna Marika Lindahl
Científico Titular del Consejo Superior de Investigaciones Científicas

“El tiempo es el ladrón de la memoria"
La torre oscura I. El pistolero
Stephen King

“La única razón por la que una persona escribe una historia, es porque a través de ella puede entender el pasado”
Stephen King

"Time's the thief of memory"
The Dark Tower I. The Gunslinger
Stephen King

“The only reason a person writes a story, because through it you can understand the past”
Stephen King

INDEX

INDEX

FIGURE INDEX

TABLE INDEX

ABREVIATIONS

1-DE	One dimension electrophoresis
2-DE	Two dimension electrophoresis
AAA^+	ATPases Associated with a variety of cellular Activities
ADP	Adenosine diphosphate
Ap	Ampicillin
ATP	Adenosine triphosphate
ATS	Activated thiol-Sepharose
BSA	Bovine serum albumin
CBB	Coomassie brilliant blue
Ci	Curie
DNA	Deoxyribonucleic acid
dNTPs	Deoxyribonucleotide triphosphate mix
DTT	Dithiothreitol
E	Einstein
EDTA	Ethylenediaminetetraacetic acid
FAD	Flavin Adenine Dinucleotide
FPLC	Fast Protein Liquid Chromatography
FTR	Ferredoxin dependent Thioredoxin Reductase
g	Gravity (acceleration)
gDNA	Genomic DNA
Grx	Glutaredoxin
GS	Glutamine synthetase
GSH	Glutathione
GSSG	Oxidised glutathione
GST	Glutathione *S*-transferase
GTP	Guanosine triphosphate
HEPES	4-(2-hydroxyethyl)-1-piperazineethanesulfonic acid
IAM	Iodoacetamide
ICAT	Isotope-Coded Affinity Tag
IEF	Isoelectric focusing
IPTG	Isopropyl-β-Thio Galactopyranoside
kDa	Kilodalton
Km	Kanamycin
LC-MS	Liquid chromatography-mass spectrometry

m/z	Mass/charge
MALDI-TOF	Matrix-assisted laser desorption/ionization – Time of flight
Mb	Mega base
MS	Mass spectrometry
mBBr	Monobromobimane
NADH	Nicotinamide adenine dinucleotide
NADPH	Nicotinamide adenine dinucleotide phosphate
NCBI	National Center for Biotechnology Information
NEM	*N*-Ethylmaleimide
NTR	NADPH dependent Thioredoxin Reductase
OD	Optical density
ORF	Open Reading Frame
PCC	Pasteur Culture Colection
PCR	Polymerase chain reaction
P_i	Inorganic phosphate
PM	Plasma membrane
PMF	Peptide mass fingerprinting
PMSF	Phenyl methyl sulfonyl fluoride
Prx	Peroxiredoxin
PSI	Photosystem I
PSII	Photosystem II
RNA	Ribonucleic acid
RNS	Reactive nitrogen species
ROS	Reactive oxygen species
rpm	Revolutions per minute
SDS	Sodium dodecyl sulfate
SDS-PAGE	Sodium dodecyl sulfate polyacrylamide gel electrophoresis
Sp	Spectinomycin
St	Streptomycin
TM	Thylakoid membrane
tRNA	Transfer RNA
Trx	Thioredoxin
USP	Universal stress protein
v/v	Volume/volume
w/v	Weight/volume
WT	Wild type

X-gal	Bromo-chloro-indolyl-galactopyranoside

NITROGENOUS BASES

A	adenine
C	cytosine
G	guanine
T	thymine

AMINO ACIDS

A	Ala	alanine	L	Leu	leucine
R	Arg	arginine	K	Lys	lysine
N	Asn	asparagine	M	Met	methionine
D	Asp	aspartic acid	F	Phe	phenilalanine
C	Cys	cysteine	P	Pro	proline
E	Glu	glutamic acid	S	Ser	serine
Q	Gln	glutamine	T	Thr	threonine
G	Gly	glycine	W	Trp	tryptophan
H	His	histidine	Y	Tyr	tyrosine
I	Ile	isoleucine	V	Val	valine

INTRODUCTION

INTRODUCTION

1. Cyanobacteria

Cyanobacteria form a diverse group of oxygenic photosynthetic prokaryotes, which are major contributors to global photosynthetic productivity (Ting *et al.*, 2002). Cyanobacteria are widely distributed: many are aquatic, but some are land-living, and their habitats include extreme environment, such as hot springs, deserts and polar regions. Some species are even found in symbiosis with fungi, ferns or cycads. Cyanobacteria play a central ecological role as primary producers in the Earth's carbon cycle. The nitrogen-fixing species also figure prominently in the nitrogen cycle. Moreover, as the only organisms ever to have evolved coupled photosystems, which harvest electrons from water and produce dioxygen, they also stand out in our planet's redox history (Knoll, 2008).

Life on Earth originated at least 3500 My ago and possibly much earlier. Between 2450-2320 My ago cyanobacteria should have been important primary producers in the world's oceans, and they could have emerged even earlier. The cyanobacterial production of molecular oxygen transformed the environment in a way that made novel physiologies and morphologies, including animals, possible (Knoll, 2008). The modern chloroplast is believed to have evolved from cyanobacteria, through a primary endosymbiotic event between a eukaryotic cell and an ancestral oxygenic photosynthetic prokaryote. Hence, the photoautotrophy was introduced to eukaryotes and, then, cyanobacteria contributed further to the environmental transformation of land as well as the sea (Knoll, 2008).

Cyanobacteria are monophyletic but morphologically diverse. The traditional taxonomic classifications focused on morphology and development, and divided these bacteria into five principal groups (Rippka *et al.*, 1979). Group I (formerly Chroococcales) and II (Pleurocapsales) are unicellular coccoids. Cells of Group I divide by binary fission, whereas those of Group II can also undergo multiple fission to produce small, easily dispersed cells called baeocytes. Cyanobacteria of Groups III-V form filaments of varying morphological complexity. Filamentous cyanobacteria of Group III (Oscillatoriales) have only vegetative cells, but in Group IV (Nostocales) and

V (Stigonematales), vegetative cells can differentiate into morphologically and ultrastructurally distinct heterocysts; cells that are specialized in nitrogen fixation under aerobic conditions. They may also differentiate into akinetes, resting cells that survive environmental stresses such as cold and desiccation, depending on growth conditions. In addition, filaments of Group V have complicated branching patterns. Their developmental variety and complexity are thus among the most highly developed in prokaryotes (Tomitani *et al.*, 2006). Molecular phylogenies of the cyanobacteria support some but not all of these groupings. The phylogenetic kinship of taxa that share features, like cell differentiation or multiple fissions, find support in molecular analyses. However, unicellular and simple filamentous cyanobacteria do not constitute monophyletic groups (Knoll, 2008) (Fig. 1).

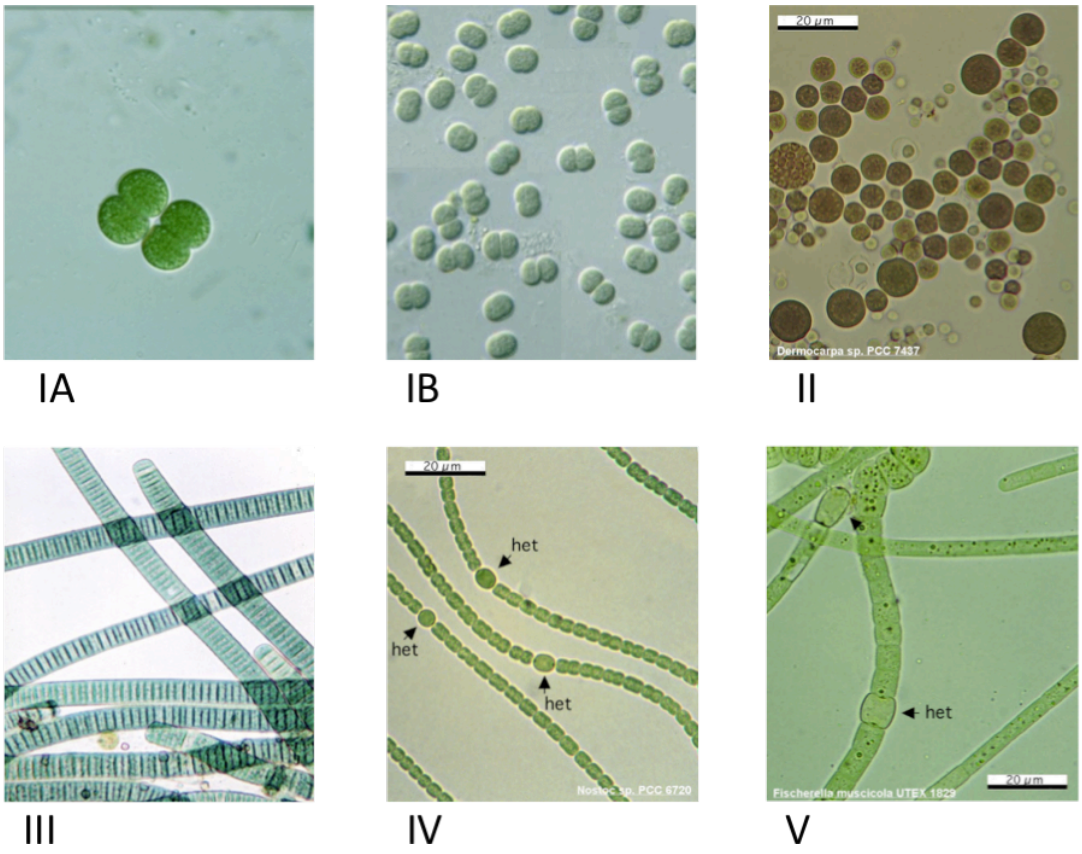

Figure 1. Morphological diversity of Cyanobacteria. A selected member represents each cyanobacterial group. IA and IB. Group I: *Synechocystis* sp. PCC 6803. II. Group II: *Dermocarpa* sp. PCC 7437. III. Group III: *Oscillatoria* MC. IV. Group IV: *Nostoc* sp. PCC 6720. V. Group V: *Fischerella muscicola* UTEX 1829.

Cyanobacteria are classified as Gram-negative bacteria since they have a cell envelope consisting of a plasma membrane, peptidoglycan layer, and outer

membrane (Hoiczyk and Hansel 2000). However, these organisms are unique among Gram-negative bacteria, because they also have an internal system of thylakoid membranes, where the large protein complexes of the photosynthetic and respiratory electron transfer chains reside. Therefore, the cyanobacteria are considered more complex than typical Gram-negative bacteria (Liberton *et al.*, 2006). An ongoing controversy regarding these organisms has concerned the exact morphology of the thylakoid membranes, its biogenesis and its physical relationship with the plasma membrane (Liberton *et al.*, 2006; van de Meene *et al.*, 2006).

From a metabolic view, all cyanobacteria are capable to grow photoautotrophically and some of them can use a reduced carbon source to develop a heterotrophic or mixotrophic growth. As in plants, the atmospheric CO_2 fixation is performed by the Calvin cycle. However, cyanobacteria have an incomplete Krebs cycle because of the lack of the 2-oxoglutarate dehydrogenase enzymatic complex. This feature gives an anabolic role to the Krebs cycle owing to the fact that 2-oxogutarate provides carbon skeletons for nitrogen assimilation. The oxidative pentose phosphate cycle is the main metabolic pathway of carbohydrate catabolism (Stanier and Cohen-Bazire, 1977). Moreover, cyanobacteria can use nitrate, nitrite and ammonium as nitrogen source (Guerrero and Lara, 1987). However, some cyanobacterial strains are also able to use urea, certain aminoacids, or molecular atmospheric nitrogen (N_2) (Stewart, 1980; Flores and Herrero, 1994). The N_2-fixing strains need to separate the nitrogen fixation and photosynthesis to avoid the irreversible inactivation of the nitrogenase enzyme by molecular oxygen. This separation can be achieved temporally (Fay, 1992) or spatially, by differentiating some vegetative cells into heterocysts where the N_2 assimilation is performed (Wolk, 1982).

From 1996 until now several full genome sequences of different cyanobacterial species have been made public (Cyano-Base, www.kazusa.or.jp/cyano/cyano.html). The genome of the unicellular cyanobacterium *Synechocystis* sp. PCC 6803 (Kaneko *et al.*, 1996) was the first to be sequenced from a photosynthetic organism. The G+C content is very variable and ranges from 32 to 71%. Most of the studied strains are highly polyploid, having around 12 copies of chromosome per cell (Labarre *et al.*, 1989). The sizes of the cyanobacterial genomes

range from 9.20 Mb (*Nostoc punctiforme*) to 1.66 Mb (*Prochlorococcus* MED4), which is considered the minimum genome size required for encoding the components of the oxygenic photosynthetic apparatus in addition to the enzymes of basic metabolism (Dufresne *et al.*, 2005). The genome sequence of the filamentous heterocyst-forming nitrogen-fixing cyanobacterium *Anabaena* sp. PCC 7120 (CyanoBase) has provided valuable information about the genes related to heterocyst differentiation and the process of nitrogen fixation (Kaneko *et al.* 2001). Many cyanobacteria are capable of integrating exogenous DNA stably into their genome (transformation) by means of homologous recombination processes (Porter, 1986). In addition, some genetic transfer techniques have been developed, such as conjugation (Wolk *et al.*, 1984; Flores and Wolk, 1985) or electroporation (Thiel and Poo, 1989). These features make certain cyanobacterial strains adequate model organisms for molecular studies.

The cyanobacterium used to carry out the present research was the unicellular *Synechocystis* sp. PCC 6803, which belongs to the cyanobacterial Group I.

1.1 *Synechocystis* sp. PCC 6803

Synechocystis sp. PCC 6803 (hereafter *Synechocystis*) is a model organism, which displays a unique combination of highly desirable molecular genetic, physiological, and morphological characteristics. This species is spontaneously transformable, incorporates foreign DNA into its genome by double-homologous recombination, grows under many different physiological conditions (*i.e.*, photoauto-, mixo- and heterotrophycally), and has a short duplication time. These features combined with the fact that its entire genome has been sequenced (Kaneko *et al.*, 1996) makes this species an ideal experimental system to answer questions regarding photosynthesis and the biogenesis and maintenance of thylakoid membranes, the sites of solar energy capture and energy transduction (van de Meene *et al.*, 2006).

1.1.1 Structure of *Synechocystis* sp. PCC 6803

Synechocystis cells are spherical immediately after cell division. During

growth, the cells elongate and an incipient septum invaginates into the cytoplasm. The septum continues to furrow inwards until the cytoplasm is divided producing two daughter cells. The mature cell wall is comprised of the periplasmic space, the peptidoglycan layer, the outer membrane, and the S-layer. Frequently, a second division, in a perpendicular plane to the first, begins before the two daughter cells are separated. At all stages of the cell cycles, the pairs of thylakoid membranes appear mainly to progress around the cell as concentric layers close to the plasma membrane. In addition, layers of thylakoid membranes form large loops or traverse the central cytoplasm. Thylakoid membranes converge at various sites close to the cytoplasmic membrane creating contoured arrays of these membranes. During cell division the thylakoid membranes expand to accommodate the invaginating septum. The arrangement of the thylakoid membrane pairs optimizes the surface area for membrane-associated processes, such as respiration and photosynthesis, and accommodates the large number of proteins complexes involved in these processes, including phycobilisomes. The mechanisms that regulate thylakoid organization are unknown. However, it is possible that unidentified anchoring and/or cytoskeletal proteins are involved. (van de Meene *et al.* , 2006). (Fig. 2)

Thylakoid membrane biogenesis remains an outstanding question in cyanobacteria. These membranes do not seem to be simple invaginations of the cytoplasmic membrane, it has been argued that there are not even any physical connections between thylakoid and cytoplasmic membranes (Liberton *et al.*, 2006). The thylakoid center is a distinctive cylindrical structure with thylakoid membrane sheets associated along its length. These centers are observed in association with thylakoid membrane pairs in the peripheral regions of the cell. In addition, they are closely associated with the cytoplasmic membrane and their cores appear to be continous with the periplamic space. The function of thylakoid centers is unknown, but likely play a role in the thylakoid membranes biogenesis (van de Meene *et al.*, 2006). Lipid bodies are abundant in *Synechocystis* and their distribution is restricted to locations between the thylakoid membranes pairs and adjacent to the cytoplasmic membrane. This location suggests a role in thylakoid maintenance and biogenesis (van de Meene, *et al.*, 2006). It is possible that there are occasional transient dynamic connections between the two membrane systems. Another possibility is that lipids and proteins may be exchanged between cytoplasmic and thylakoid membranes by

vesicle trafficking, but vesicles have not been observed in *Synechocystis*. However in the cyanobacterium *Microcoleus* sp. small membrane bound vesicles have been reported. Nevertheless, the *Synechocystis* plasma membrane harbours a homologue of the *Arabidopsis thaliana* protein Vipp1 (Vesicle Inducing Protein in Plastids 1), which is essential for thylakoid biogenesis in plants as well as in *Synechocystis* (Mullineux, 2008).

The interior of the *Synechocystis* cell contains components that are readily observed in most cyanobacterial cells. These include polygonal carboxysomes that contain the RuBP-carboxylase enzyme tightly packed in crystalline arrays (Price *et al.*, 2008). Cyanophycin granules, a nitrogen reserve composed of nonribosomally-synthesized arginine and aspartic acid polypeptides (Simon, 1987) are also found. Other storage structures include polyhydroxyalkanoate (PHA) granules, glycogen granules and polyphosphate bodies, which function in the storage of reduced carbon and phosphorus, respectively. In the cytoplasm there are the DNA-containing regions and a large number of ribosomes. Ribosomes are in the majority excluded from the areas between the thylakoid membranes, appearing instead in the central cytoplasmic region of the cell and between thylakoid and plasma membranes. They have also been observed to be associated with sheet-like structures in the interior of the cell, which appear to be continuous with the inner thylakoid membranes. This suggests a role in direct co-translational protein insertion into the thylakoid membranes. (Liberton *et al.*, 2006; van de Meene *et al.*, 2006). (Fig. 2)

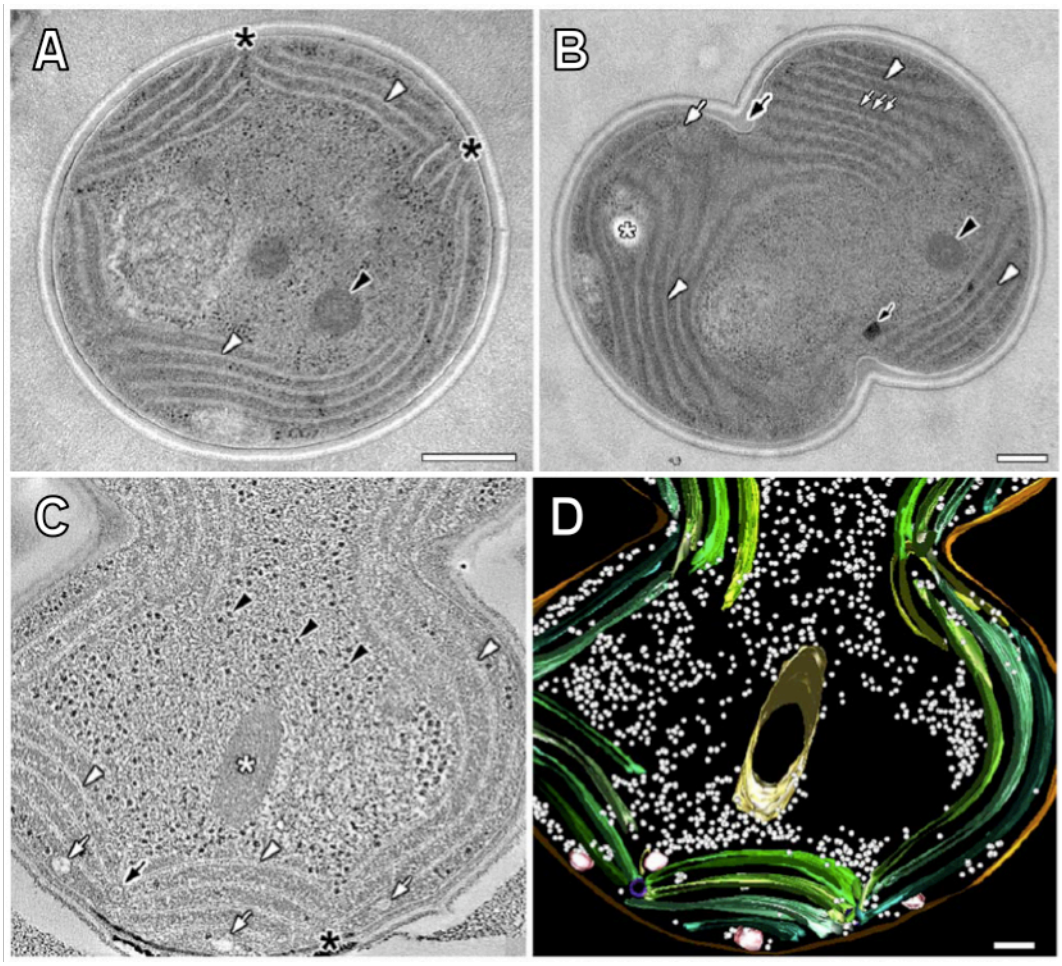

Figure 2. *Synechocystis* cell structure. A-B. Standard transmission electron microscopy of a non dividing cell **(A)** and a cell in early division **(B)**. The *white arrowheads* indicate the peripheral arrays of thylakoid membrane pairs. The *black asterisk* points the convergence of arrays of thylakoid membranes adjacent to cytoplasmic membranes. The cytoplasmic inclusions are marked as: *black arrowheads*, the carboxysomes; *small black arrows*, the polyphosphate bodies; *white asterisk*, a PHA granule; and *large white arrow*, a lipid body. In B the *small white arrows* indicate the phycobilisomes and the *large black arrow* the invaginating septum of dividing cell. **C**. Tomographic slice from a dividing cell. The marked structures are: thylakoid membranes pairs (*white arrowheads*); thylakoid membranes convergence (*black asterisk*); a thylakoid center (*black arrow*); carboxysome (*white asterisk*); ribosomes (*black arrowheads*); lipid bodies (*white arrows*). **D**. 3-D Model of C. The structures are coloured differently: thylakoid membranes pairs (*green*); a thylakoid center (*blue*); lipid bodies (*pink*); ribosomes (*white*); the carboxysome (*yellow*), and the cytoplasmatic membrane (*brown*). Taken from van de Meene *et al.*, 2006.

2. Photosynthesis and oxidative stress

2.1 Photosynthesis

All higher life on Earth depends on the oxygenic photosynthesis, since this process produces all the oxygen in the atmosphere. The photosynthesis converts the light energy from the sun into chemical energy. The organisms that perform oxygenic photosynthesis are plants, green algae and cyanobacteria. All of them contain two photosystems, photosystem I (PSI) and photosystem II (PSII), which operate in series in the photosynthetic electron transport chain. (Fig. 3)

The energy conversions occurring in photosynthetic organisms are divided into the light reactions, which convert the light energy into an electrochemical gradient, which is used to synthesise the high-energy substrates ATP and NADPH, and the dark reactions that consume ATP and NADPH for the production of carbohydrates by CO_2 fixation. The light reactions take place in the thylakoid membranes and are catalysed by four large multiprotein complexes: PSI, PSII, cytochrome b_6f and ATP synthase. (Fig. 3)

PSI and PSII contain the reaction centres, in which the charge separation takes place. PSII catalyses the water spliting and the electron transfer from water to plastoquinone (PQ) (Vassiliev and Bruce, 2008). Plastoquinone is a small liposoluble molecule that can move freely through the membrane. In each charge separation event, one electron is extracted from the Mn-cluster, and oxygen is evolved after 4 positive charges have been accumulated. During this process, 4 H^+ are released into the lumen of the thylakoids. The electron is transferred from the chlorophyll P_{680} in PSII by a chain of electron carriers to PQ. After two charge separation events, PQ is completely reduced, takes up two protons from the cytoplasm and leaves PSII as plastoquinol (PQH_2). The PQH_2 serves as mobile electron and proton carrier and is in constant equilibrium with the PQ pool in the membrane. It donates two electrons and two protons to the cytochrome b_6f complex, which releases 2 protons inside of the thylakoid, and subsequently reduces 2 molecules of plastocyanin (PC). Plastocyanin is a soluble protein located in the lumen of the thylakoids. In some cyanobacteria, cytochrome c_6 replaces PC (De la Rosa *et al.*, 2002). The two additional protons

pumped across the membrane by the cytochrome b_6f complex contribute to the establishment of a proton gradient across the thylakoid membrane. The reduced PC/ cytochrome c_6 serve as mobile electron carriers between the cytochrome b_6f complex and the PSI.

PSI catalyses the electron transfer across the membrane between the PC/ cytochrome c_6 and ferredoxin. When the light energy reaches and excites the chlorophyll P_{700} in PSI, an electron is ejected and transferred to a terminal Fe-S cluster, located at the cytoplasmic side of PSI. Thereafter, the electron is transferred from the Fe-S cluster to ferredoxin. Under iron deficiency, flavodoxin can replace ferredoxin as a soluble electron carrier (Nield *et al.*, 2003). The electron transfer process is completed by the reduction of the P_{700}^+ al the lumenal side by the PC/cytochrome c_6. Finally, ferredoxin or flavodoxin transfers the electron to the ferredoxin $NADP^+$ reductase (FNR), which reduces $NADP^+$ to NADPH. (Fromme and Grotjohann, 2008a; DeRuyter and Fromme, 2008).

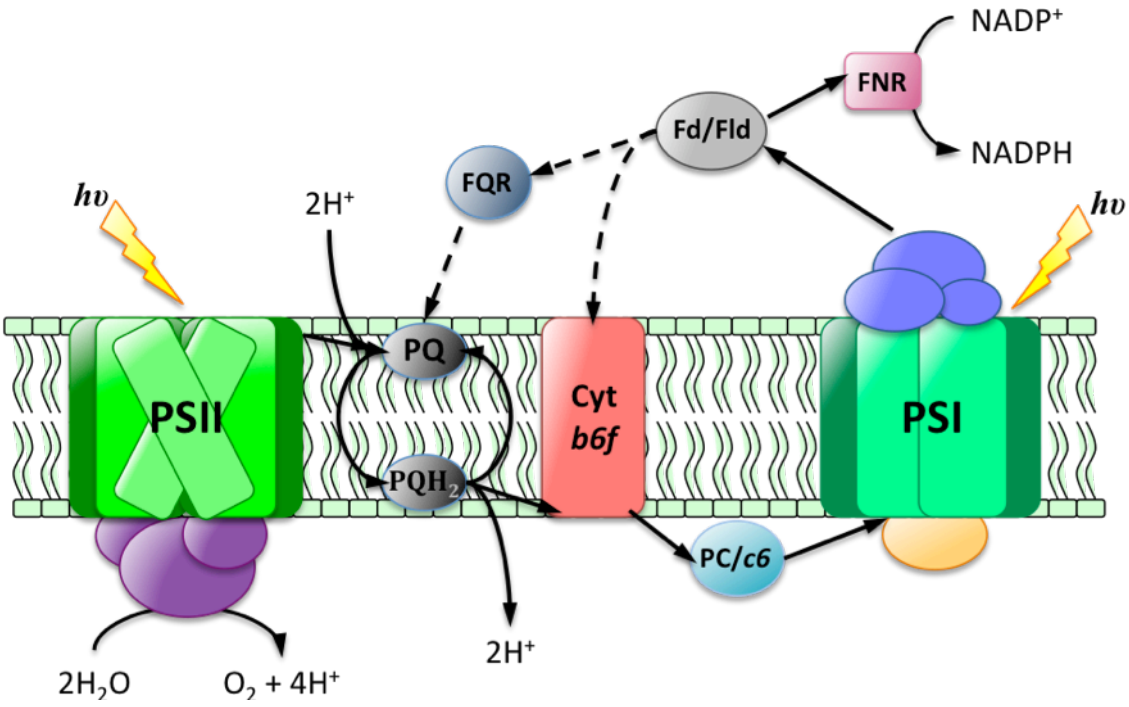

Figure 3. Photosynthetic electron transfer. The electron is transferred from H_2O to NADPH in the lineal non cyclic flux across different elements: PSII, photosystem II; PQ/PQH_2, oxidised/reduced plastoquinone; Cyt b_6f, cytochrome b_6f complex; PC/c_6, plastocyanin/cytochrome c_6; PSI, photosystem I; Fd/Fld, ferredoxin/flavodoxin; FNR, ferredoxin $NADP^+$ reductase. In the cyclic flux (dash line) the electron may be transferred from Fd/Fld directly to Cyt b_6f or to PQ by means of the FQR, ferredoxin-quinol reductase.

The electrochemical proton gradient generated by the electron transfer reactions is used by the ATP synthase to produce ATP from ADP and P_i. In the dark reactions the ATP and NADPH are used to fix CO_2 in the Calvin cycle, and other anabolic reactions. (Fromme and Grotjohann, 2008a; DeRuyter and Fromme, 2008).

The electron transfer performed by the three membrane protein complexes, PSI, PSII and cytochrome b_6f, is a linear non-cyclic flux. However, there is also a cyclic alternative pathway, in which the electron returns to PQ from ferredoxin through a ferredoxin-quinol reductase (FQR) or by direct transfer. Therefore, the cytochrome b_6f pumps the two protons into the lumen, thereby generating ATP, but NADPH is not produced. In this manner, the cell is thought to regulate the ATP/NADPH balance in response to certain stress (Bandall and Manasse, 1995).

Cyanobacteria contain large membrane attached but extrinsic antenna complexes, the phycobilisomes. The phycobilisome pigments absorb strongly in the 550-660 nm region, thereby complementing the spectral region covered by chlorophyll a in the blue and red regions. Therefore, the phycobilisome allows cyanobacteria to absorb green light and to use the full spectrum of visible light for photosynthesis. The phycobilisomes mainly serve as antenna for PSII, but can also move to PSI in a process of state transitions balancing the excitation between the photosystems, adapting to variable light conditions. The structure of the phycobilisome can be described as a set of rod like stacks of disks that radiate from a central core of tightly packed disks. The pigment composition is formed by: allophycocyanin, preferentially located in the core; phycocyanin, which forms the inner part of the rods; and phycoerythrin, located in the periphery of rods. (Fromme and Grotjohann, 2008b). The phycobilisome pigments are responsible for the cyan colour of cyanobacteria.

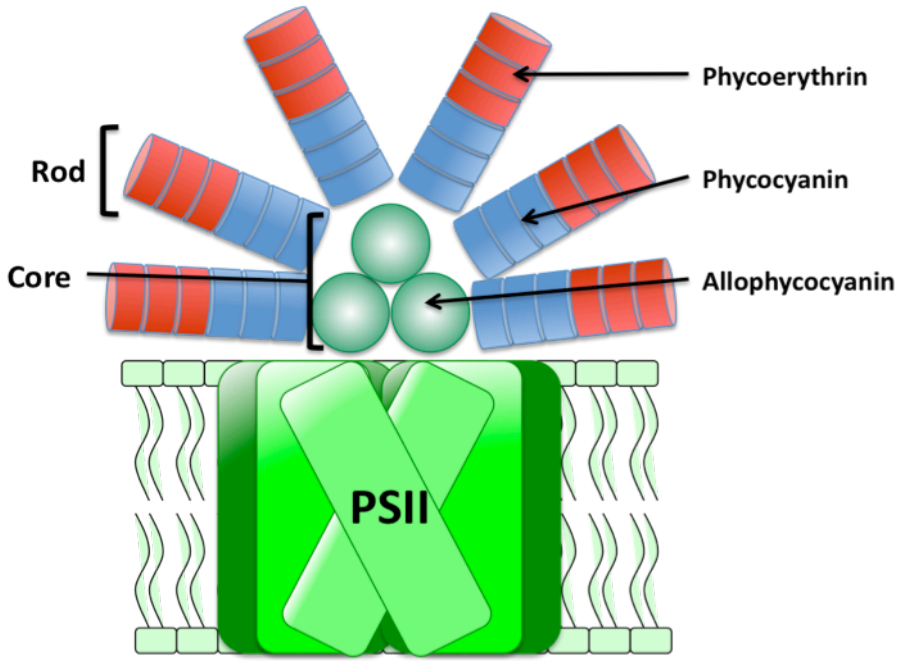

Figure 4. Phycobiliome. The phycobilisome is formed by rods and core. In the rods are the phycocianin and the phycoerythrin. In the core is the allophycocyanin.

Photosynthesis constitutes the primordial energetic process in cyanobacteria, but some strains are capable of growing in darkness through respiration using a reduced carbon source. Cyanobacteria perform the reactions of photosynthesis and respiration in the same compartment and both processes also share some components of the electron transfer, such as PC and the cytochrome b_6f complex (Paumann *et al.*, 2005). However, the cyanobacteria can separate these processes due to the development of an internal membrane system. Hence, the photosynthetic components are located in the thylakoid membrane and the respiratory ones in both thylakoid and cytoplasmic membranes (Gantt, 1994). Furthermore, the cyanobacterial respiration is inhibited by light (Brown and Webster, 1953), and, hence, photosynthesis and respiration are temporarily separated as well.

2.2 Production of reactive oxygen species and the concept of oxidative stress

The evolution of aerobic life has had the consequence that organisms have to cope with the damaging effects of oxygen on the metabolic pathways, which had originally evolved in an anoxic environment. Reactive oxygen species (ROS) are

unavoidably generated as intermediates of O_2 reduction, or by energisation of ground state molecular oxygen. ROS, including singlet oxygen ($^1O_2$), the superoxide anion (O_2^-), hydrogen peroxide (H_2O_2) and the hydroxyl radical ($^\bullet OH$) are powerful oxidising agents. Singlet oxygen ($^1O_2$) is produced by energy input to oxygen and is highly reactive, has a short half life in cells and reacts with target molecules (proteins, pigments, and lipids) in the immediate neighbourhood. The three oxygen reduction intermediates (O_2^-, H_2O_2, and $^\bullet OH$) have different intrinsic properties, and therefore possess different reactivities, toxicity levels and targets (D'Autréaux and Toledano, 2007). Both O_2^- and $^\bullet OH$ have an unpaired electron that renders them highly reactive with biomolecules. Because O_2^- is negatively charged, it does not diffuse through membranes. It oxidizes the $[4Fe–4S]^{2+}$ clusters to $[3Fe–4S]^{1+}$ releasing iron (Fe^{2+}). The hydroxyl radical is so reactive that reaction rates become diffusion limited. Even if H_2O_2 is less reactive than the other ROS it can be reduced to hydroxyl radical via the Fenton reaction ($Fe^{2+} + H_2O_2 \rightarrow OH^- + FeO^{2+} + H^+ \rightarrow Fe^{3+} + OH^- + {}^\bullet OH$) and, thus, is potentially highly damaging. Even though DNA is not the direct target of H_2O_2 and O_2^-, in contrast to $^\bullet OH$, these are nevertheless considered as potential mutagens, because they can engender the release of the Fenton-active ferrous iron, thus leading to the production of hydroxyl radicals, which can cause extensive DNA lesions. Organisms have developed various enzymatic and non-enzymatic defence mechanisms against ROS-induced damage. When the balance between oxidant production and antioxidant levels is perturbed, the organisms have to face an oxidative stress that generates different damages leading to cell death in bacteria and diverse pathologies in higher organisms (Imlay, 2003; Latifi *et al.*, 2009).

In aerobic organisms respiration produces intracellular ROS inside the cells. Molecular oxygen is able to diffuse passively into the cell and is reduced to superoxide anion and H_2O_2 via the oxidation of flavoproteins, such as the NADH dehydrogenase II (NdhII) in *Escherichia coli* (Imlay, 2003). The oxygenic phototrophic organisms do not only need to manage the oxidative stress resulting from respiration, as heterotrophic organisms, but also that produced during photosynthetic electron transfer. Singlet oxygen ($^1O_2$) is formed by the transfer of excitation energy from excited chlorophylls to oxygen. This oxygen species was considered the primary cause of photodamage to PSII, but now is thought to inhibit the repair of PSII inactivated by light. When the light intensity, and consequently the

excitation pressure, exceeds the rate of utilisation not only the $^1O_2$ production increases, but also other ROS can be formed. In this case, the oxygen is reduced, instead of ferredoxin, on the acceptor side of PSI resulting in the formation of the superoxide radical, which can be further converted to H_2O_2 and hydroxyl radicals (Nishiyama *et al.*, 2006; Latifi *et al.*, 2009).

Exposure of PSII to strong light severely inactivates this photosystem. This phenomenon has been called 'photoinhibition'. PSII photoinhibition has been shown to involve damage of the oxygen-evolving complex by strong blue light or UV light and release of manganese ions. Photosynthetic organisms are able to overcome photodamage by the rapid and efficient repair of PSII. A prerequisite for repair is the degradation of the D1 protein, which together with the D2 protein constitutes the reaction centre of PSII. Recently, it has been demonstrated that photoinhibition is exclusively a light-dependent process and that the target of ROS is the *de novo* synthesis of D1 in the repair step. Some cyanobacteria are able to replace the constitutive form of D1 with an alternative and more resistant isoform of this protein, allowing the bacteria to overcome photoinhibitory damage to PSII (Nishiyama *et al.*, 2006; Latifi *et al.*, 2009). Phycobilisomes are another possible target of ROS. H_2O_2 induces the interruption of energy transfer between the core and the terminal emitter of phycobilisomes in *Synechocystis* PCC 6803, which suggests that the phycobilisomes core is disassembled under oxidising conditions (Liu *et al.*, 2005; Latifi *et al.*, 2009).

Cyanobacteria have developed diverse strategies to avoid the production of ROS or to enhance their disposal. There are three mechanisms of energy dissipation as prevention strategies. The first is a blue light-induced non-photochemical quenching that requires the interaction between the orange caratenoid protein (OCP), a soluble caratenoid containing protein widely distributed among cyanobacterial species, and the phycobilisome core (Kirilovsky, 2007). The second one is related to the high light-inducible proteins (HLIPs), also designated small CAB-like proteins (SCPs), and their association with PSII dissipating the excess energy absorbed (Xu *et al.*, 2004). A third mechanism of energy dissipation is carried out by the iron stress-induced protein IsiA (CP43') under iron starvation conditions (Latifi *et al.*, 2009). In addition, some components of the electron transfer chain have been

shown to be important for tolerating oxidative stress. Cytochrome oxidases are thought to help removing excess electrons (Schubert *et al.*, 1995). Another way of avoiding excessive excitation of PSI is the use of alternative electron transfer pathways to get rid of electrons in excess downstream PSI, for example the plastoquinol terminal oxidase (PTOX) in the cyanobacterium *Synechococcus* WH8102 (Bailey *et al.*, 2008). The stromal (or cytosolic) extrinsic PSI subunit PsaE was recently suggested to play a regulatory role in preventing electron leakage from PSI to oxygen, thereby avoiding photo-oxidative damage (Jeanjean, *et al.*, 2008).

Once, ROS have been produced, as a second strategy, nonenzymatic antioxidants may prevent their accumulation. α-tocopherol and carotenoids are the most important nonenzymatic antioxidants in phototrophs. Cyanobacteria possess a wide variety of carotenoids like myxoxanthophyll, β-carotene, and its derivatives (zeaxanthin, echinenone). These pigments absorb energy from excited chlorophyll or from $^1O_2$ (Edge *et al.*, 1997). Cyanobacteria also possess antioxidant enzymes for detoxification of ROS. Superoxide dismutase (SOD) catalyses the disproportionation of O_2^- to H_2O_2 and oxygen. The decomposition of H_2O_2 to molecular oxygen and water is catalysed by catalases. Peroxidases reduce hydrogen peroxide to water. Catalases exclusively decompose H_2O_2, whereas peroxidases may use a broad range of peroxides as substrates. Several studies have reported the implication of SODs in protective processes in cyanobacteria (Lafiti *et al.*, 2009). Catalase-orthologues have been found in 20 cyanobacterial genomes. A catalase-peroxidase activity has been purified and characterised in *Synechococcus* PCC 7942 and *A. nidulans* (Mutsuda *et al.*, 1996; Obinger *et al.*, 1997) The activity of the bifunctional catalase-peroxidase KatG has been studied in *Synechocystis* sp. PCC 6803 (Tichy and Vermaas, 1999; Smulevich *et al.*, 2006). In *Synechocystis* sp. PCC 6803 two glutathione peroxidase-like proteins have also been characterised (Gaber *et al.*, 2004). Peroxiredoxins were recently identified and characterised in cyanobacteria. They constitute a family of thiol-specific antioxidant proteins that can catalyse the reduction of H_2O_2, alkyl hydroperoxides and peroxynitrite (Wood *et al.*, 2003). (Reviewed by Latifi *et al.*, 2009; Bernroitner *et al*., 2009).

3. Redox signalling and redox regulation in cyanobacteria

Redox regulation was defined in Buchanan and Balmer (2005) as a reversible posttranslational alteration in the properties of a protein, typically the activity of an enzyme, as a result of change in its oxidation state. The activation of various regulators in response to an increase in ROS concentrations can often modulate the transcription of a subset of genes, allowing an appropriate response to the stress sensed. In cyanobacteria homologous proteins to SoxR and SoxS of *E. coli* have been reported. In *E. coli* SoxR acts as a redox sensor that is activated by superoxide and activates the SoxS transcription. SoxS induces the expression of a dozen genes including detoxification enzymes (SOD) and DNA repair proteins (reviewed by Storz and Imlay, 1999; and Latifi *et al.*, 2009). In *Synechocystis* sp. PCC 6803 the induction of the regulator PerR by peroxide has been shown. PerR is a repressor that is able to inactivate its own transcription and that of the peroxiredoxin PrxII, since both share the same promotor (Kobayashi *et al.*, 2004). The inactivation of PerR abolishes the repression of a set of genes including the dps-homologue *mrgA*, the peroxiredoxin *prxII* and *isiA* (Li *et al.*, 2004). However, PerR does not regulate the majority of the genes that respond to oxidative stress in cyanobacteria. Histidine kinases have been shown to be involved in H_2O_2 sensing (Kanesaki *et al.*, 2007). Hik33 regulates many more genes than does PerR, although both co-regulate a set of genes. A number of peroxide-induced genes are regulated neither by Hik33 nor by PerR, indicating that other, as yet unknown, regulators are involved (Latifi *et al.*, 2009).

3.1 Cysteine reactivity

The chemistry of thiols underlies many processes in cellular redox signalling (Cooper *et al.*, 2002), hence, this type of signalling frequently implies the post-translational protein modification of cysteine residues that have a regulatory function (Cooper *et al.*, 2002). Cysteine is one of the least frequently occurring amino acids in proteins from all three superkingdoms. Thus, on average cysteine accounts for about 2% of the amino acids in eukaryotic proteins and about 1% in proteins from eubacteria and archaea (Pe'er *et al.*, 2004). The cysteine thiol group can adopt different forms depending on the gain (reduction) or loss (oxidation) of electrons and these reactions may lead to a change in the protein function. Reactive oxygen and

nitrogen species (ROS and RNS, respectively) can induce redox signals by means of the modification of cysteine residues. An individual enzyme may respond differently to diverse stimuli by differential modification of a single cysteine. Thus, this residue can be considered a signal transducer (Cooper *et al*., 2002).

Typically, the reactive cysteine thiol (Cys-SH) is present in its thiolate form ($Cys\text{-}S^-$). This ionised form is susceptible to oxidation by compounds, such as H_2O_2, organic hydroperoxides and hypochlorous acid. A product of such oxidation is the sulfenic acid (Cys-SOH). In many cases, the cysteine thiolate and sulfenate forms undergo rapid condensation with other thiols to form disulfide bonds (Fig. 5). The resulting disulphides can be intramolecular, with another cysteine from the same protein, or intermolecular, with a cysteine from another protein or a small molecule, such as glutathione or free cysteine (Poole and Nelson, 2008). The covalent attachment of glutathione to protein cysteines through a mixed disulfide bond is known as *glutathionylation* (Poole *et al.*, 2004). The disulfide bonds resulting from cysteine oxidation play important roles in protein structure and oligomerization, as well as enzyme activity regulation. The RNS, including nitric oxide (NO) and peroxynitrite (ONOOH), can mediate S-nitrosation yielding S-nitrosothiol (Cys-SNO) and S-nitration yielding S-nitrothiol ($Cys\text{-}SNO_2$), respectively (Fig. 5). Nearly all of these oxidative modifications are reversible through reduction catalysed by enzymes, such as thioredoxins or glutaredoxins. However, in certain proteins, the microenvironment may stabilize the cysteine sulfenic acid and this form could in turn be sensitive to hyperoxidation yielding sulfinic ($R\text{-}SO_2H$) and sulfonic acid ($R\text{-}SO_3H$) (Cooper *et al.*, 2002: Poole and Nelson, 2008). While cysteine sulfinic acid can be reverted to the thiol form by the enzyme sulfiredoxin (Poole *et al.*, 2004: Poole and Nelson, 2008), hyperoxidation to sulfonic acid is believed to be irreversible.

Protein cysteines differ in reactivity and not all cysteines are susceptible to modification. The properties of the protein microenvironment, which control cysteine reactivity and stability, are not completely understood. However, it seems to be clear that the cysteine pK_a plays an important role. Any cysteine modification involves an initial thiol deprotonation, suggesting a lowered sulfhydryl pK_a for the modifiable cysteines (Salsbury *et al.*, 2008). Salsbury *et al.* have calculated the mean

pK_a for modifiable cysteine residues as compared to non-modifiable ones and found this value to be 6.9 for the reactive cysteines and 8.14 for the control cysteines (Salsbury *et al.*, 2008). Thus, these values are consistent with the oxidation mechanism of cysteine. The decrease in pK_a is influenced by the presence of titratable, polar residues in the cysteine microenvironment, although this shift is sometimes observed in the absence of this kind of residues. In the latter case, a subtle polar interaction influenced by local backbone conformation and local hydrogen-bonding patterns appears to be determinant. The histidines are overrepresented in this microenvironment and are thought to constitute an important feature in this context. In addition, the presence of threonine residues has been related with such a pK_a shift (Salsbury *et al.*, 2008).

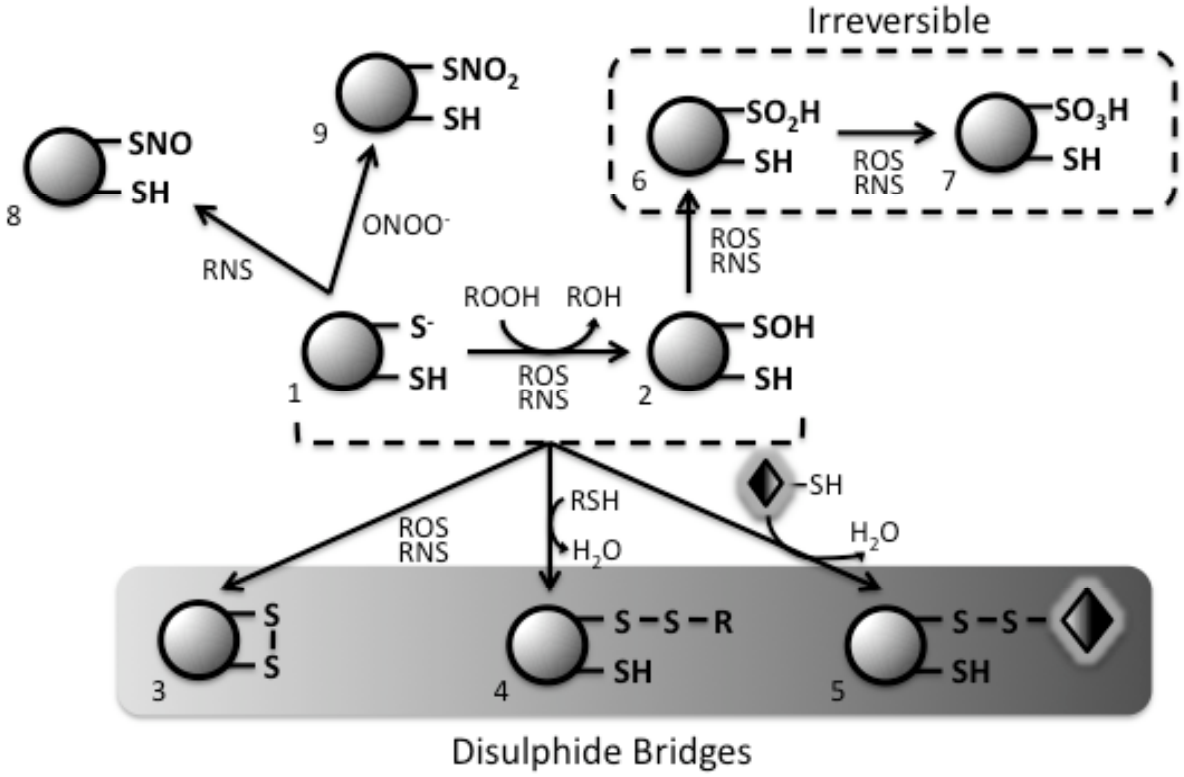

Figure 5. Reactive cysteine modifications. The thiol group (1) in its ionized form, the thiolate anion (Cys-S^-), is susceptible to oxidation by reactive oxygen species (ROS) or reactive nitrogen species (RNS) to yield sulfenic acid, Cys-SOH (2). The thiolate and sulfenate can form intramolecular disulfide bridges (3) or intermolecular disulfide bridges by condensation with other thiols belonging to a small organic molecule (4) or another protein (5). In certain cases, the sulfenic acid is sequentially hyperoxidised to sulfinic acid, Cys-SO_2H (6), and irreversibly to sulfonic acid, Cys-SO_3H (7). RNS also mediate the S-nitrosation yielding S-nitrosothiol, Cys-SNO (8), and S-nitration by peroxynitrite ($ONOO^-$) yielding S-nitrothiol, Cys-SNO_2 (9).

The cysteine sulfenic acid (Cys-SOH) plays an important role in redox signalling for many proteins. In these cases, the protein structure may ensure the stability of this cysteine form to maintain its reactivity and, hence, its signalling capacity. Thus, the Cys-SOH microenvironment is characterised by the lack of nearby reduced cysteines and the presence of local hydrogen-bonding residues, which stabilise the sulfenate form (Poole *et al.*, 2004; Salsbury *et al.*, 2008).

3.2 Cyanobacterial thioredoxin systems

In photosynthetic organisms, several enzymes involved in CO_2-fixation are activated by the reduction of a cystine-bridge formed by two vicinal cysteines. This reduction is mediated by a thioredoxin (Trx), which receives reducing equivalents from the photosynthetic electron transport. Thioredoxins are present in nearly all living organisms, though their abundance and diversity are particularly striking in plants and photosynthetic bacteria (Baumann and Juttner, 2002; Meyer *et al.*, 2005). They are characterised by their low molecular mass (around 12 kDa) and conserved compact architecture. The Trx active site contains a conserved sequence motif (–W**C**GP**C**–), which constitutes a highly reactive dithiol/disulphide. The Trxs convert disulphides to dithiols in their respective target enzymes, thereby modulating their activities.

Trx was initially identified in *E. coli* as a hydrogen donor to ribonucleotide reductase (RNR) (Laurent *et al.*, 1964). The first evidence for Trx in photosynthetic organisms came from studies of the ferredoxin-dependent activation of fructose-1,6-bisphosphatase, which belongs to the Calvin-Benson cycle of CO_2 assimilation in chloroplasts (Buchanan, 1980; Buchanan *et al.*, 2002; Florencio *et al.*, 2006). In plants two chloroplast Trxs named Trx *f* and Trx *m* were identified. Both are light-dependent regulators of several carbon metabolism enzymes (Schürmann and Jacquot, 2000; Lemaire *et al.*, 2007). Trx *f* was found to be responsible for the fructose-1,6-biphosphatase regulation, and Trx *m* activates the NADP malate dehydrogenase (Buchanan, 1980; Buchanan *et al.*, 2002). Later, plants and algae were found to possess cytosolic (Florencio *et al.*, 1988) as well as mitochondrial Trxs (Laoi *et al.*, 2001). The full genome sequences of *Arabidopsis thaliana* and other plants have revealed several more types of Trxs and multiple genes for nearly each type of Trx (Balmer and Buchanan 2002; Meyer *et al.*, 2005). Thus, plastids contain the *f*-, *m*-, *x*-,

y- type Trxs. In addition, there are Trx-like proteins such as CDSP32 and Lilium 1 to 5 (Meyer *et al.*, 2005). *H*-type Trxs are present in the cytosol and mitochondria; and *o*-type Trxs are present only in mitochondria (Jacquot *et al.*, 2009).

The first evidence for Trx in cyanobacteria was found in *Anabaena* sp. PCC 7119, in which two Trx-like activities were described (Yee *et al.*, 1981). One of them corresponded to a *m*-type Trx, which was the first to be cloned from cyanobacteria (Gleason and Holmgren, 1981). The increasing number of complete cyanobacterial genome sequences has allowed the identification, cloning and characterisation of several others Trxs in cyanobacteria. The phylogenetic analysis of amino acid sequences has revealed four distinct groups of Trx in cyanobacteria. Three groups are shared between cyanobacteria and photosynthetic eukaryotes and include *m*-type (also known as TrxA), *x*–type (TrxB) and *y*–type (TrxQ). The fourth group, TrxC, is unique to cyanobacteria. As a rule, large cyanobacerial genomes, for example that of *Anabaena* sp. PCC 7120, contain more Trxs than smaller ones, for example the *Prochlorococcus marinus* MED4 genome. The *m*-type is the only one present in all cyanobacteria, and in the marine species *Prochlorococcus marinus* MED4, MIT9313 and SS120 there are no additional Trxs. All the Trx *m* from cyanobacteria have a high degree of sequence identity around the active site. The *x*-type Trx (TrxB) is absent from the marine species and is also missing in the genomes of *Thermosynechococcus elongatus* BP-1 and *Gloeobacter violaceus*. The cyanobacterial Trx *x* sequences display some variation, but the consensus active site (WCGPC) is the same as for the *m*-type. The *y*-type Trx has the typical active site, too. The most prominent feature of the cyanobacterial Trx *y* sequences is the presence of numerous glutamine residues, particularly in the C-terminal half of the protein. For this reason the Trx *y* from *Synechocystis* sp. PCC 6803 was named TrxQ (Pérez-Pérez *et al.*, 2006). TrxC is characterised by a different active site sequence (WCGLC) and is present in all examined genomes except in those of the marine cyanobacteria. No activity or function has so far been ascribed to this class of Trx (Florencio *et al.*, 2006). The cellular protein levels for each type of Trx have been determined in *Synechocystis* sp. PCC 6803. The four Trxs are expressed simultaneously under standard photoautotrophic growth conditions. The values for TrxA, B, C and Q were 2,5 ± 0,4, 0,16 ± 0,01, 2,4 ± 0,1 and 0,046 ± 0,003 ng per µg total protein, respectively. Hence, TrxA and C are quite abundant proteins, with cellular concentrations similar to those of *E. coli* Trx1. TrxB is 16 times less abundant and present in amounts compatible with those of *E. coli* Trx2. TrxQ is more than 50 times less abundant than Trxs A and C

(Florencio *et al.*, 2006).

There are two types of Trx reduction system, the NADPH dependent thioredoxin reductase (NTR) and ferredoxin dependent thioredoxin reductase (FTR) systems. The NTR is present in heterotrophic as well as in photosynthetic organisms, but FTR is only in chloroplasts of photosynthetic eukaryotes as well in cyanobacteria (Florencio *et al.*, 2006). FTR is a 20 to 25 kDa heterodimer composed of one variable and one catalytic subunit. The primary structure of the catalytic subunit is highly conserved including six cysteines. Four of them ligate a Fe-S cluster and the remaining two form the adjacent redox-active disulfide bridge of the active site (Sun *et al.*, 2001; Jacquot *et al.*, 2009). The primary structure of the variable subunit differs significantly in different species. The main function of this subunit seems to be the stabilisation of the catalytic subunit, particularly of its active site region. The catalytic subunit receives electrons from the photosynthetic electron transport via ferredoxin and transforms this signal into a dithiol signal reducing Trxs. Given that Trx reduction requires two electrons and ferredoxin is a one-electron donor, a two-step mechanism has been proposed involving a one-electron reduced intermediate: a transient covalent complex between FTR and Trx (Walters *et al.*, 2005; Jacquot *et al.*, 2009). This reaction mechanism suggests simultaneous interaction of FTR with both ferredoxin and Trx (Jacquot *et al.*, 2009). All oxygenic photosynthetic organisms except for the cyanobacteria *Gloeobacter violaceus* and the three species of *Prochlorococcus marinus* possess the FTR reduction system. *Gloeobacter violaceus*, which lacks thylakoid membranes, adapts poorly to the environment and is extremely sensitive to changes in light intensity. The *Prochlorococcus* species live in a stable habitat. Therefore, there is no need for light-dependent metabolic regulation and, consequently, no requirement for a link between light and the Trx redox state. Among the remaining species of cyanobacteria the catalytic subunit is well conserved, particularly the six cysteines residues involved in the function of the protein. The gene encoding this subunit in *Synechocystis* sp. PCC 6803 seems to be essential. The sequences of the variable subunit are less conserved among cyanobacteria (Florencio *et al.*, 2006).

NTR is a homodimer with subunits of approximately 320 residues in plants that contain a redox-active CxxC motif. The subunit is divided into two similar

domains, one that binds the FAD and one that binds NADPH. The redox-active disulfide is located in the NADPH domain and is in close contact with the isoalloxazine moiety of FAD (Dai *et al.*, 1996; Jacquot *et al.*, 2009). The mechanism of reduction involves conformational changes, which enable NADPH to reduce FAD. FAD then reduces the disulfide, followed by a large domain rotation in order to enable the reduction of Trx by a disulphide-dithiol exchange reaction (Lennon *et al.*, 2000; Jacquot *et al.*, 2009). A NTR fused to a Trx domain, analogous to the one described in *Mycobacterium tuberculosis* (Wieles *et al.*, 1995), was identified in the chloroplast of rice and *Arabidopsis thaliana* (Serrato *et al.*, 2004). This kind of NTR is known as NTRC. The NTR system in cyanobacteria is much more diverse than in photosynthetic eukaryotes. At least three different groups of NTR can be discerned in cyanobacteria based on sequence comparison. These groups are clearly separated from the cytosolic/mitochondrial NTRs of plants and algae (Florencio *et al.*, 2006). In some cyanobacteria NTRC is also present, for example in *Anabaena* sp. PCC 7120. Interestingly, this cyanobacterium possesses in its genome another gene encoding a NTR located immediately upstream of a gene which codes for an unusual Trx. This suggests that the NTRC has arisen from the pre-endosymbiotic fusion between a NTR gene and a neighbouring Trx gene of an ancestral photosynthetic prokaryote (Florencio *et al.*, 2006).

Recently, a comparative study on the NTR and FTR reduction systems has been carried out in the cyanobacterium *Synechocystis* sp. PCC 6803. In this study the authors conclude that the NTR system is linked to antioxidant reactions while the FTR system controls the cell growth (Hishiya *et al.*, 2008). These findings raise the question of the origin of FTR and the evolution of redox regulation (Schürmann and Buchanan, 2008).

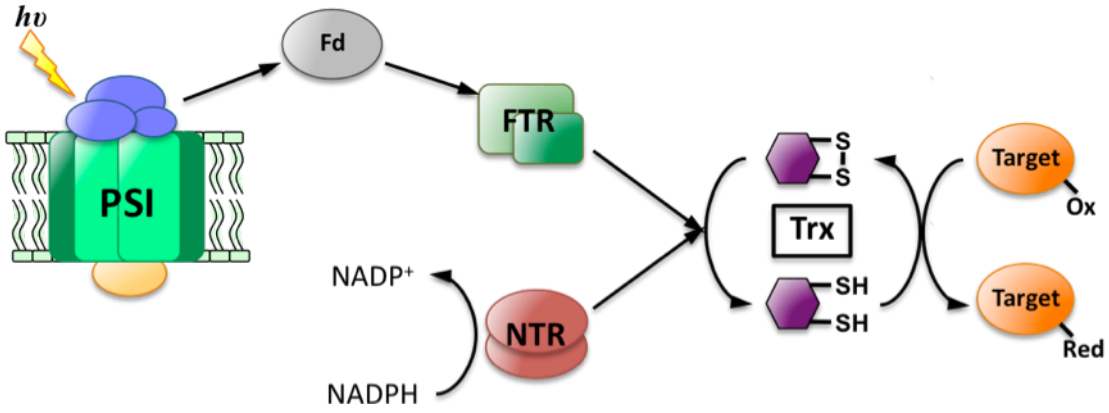

Figure 6. Trx reduction systems. Trx can be reduced by the FTR (ferredoxin dependent thioredoxin reductase) or the NTR (NADPH dependent thioredoxin reductase) system. FTR receives the electrons from the photosynthetic electron transport via ferredoxin and reduces the disulfide bound of the Trx. NADPH reduces the NTR that acts reducing the Trx. The reduced Trx possesses two thiol groups in its active site that allow it to reduced different protein targets.

Another thiol-based oxidoreductase enzyme is the glutaredoxin (Grx). Grxs are small proteins, which belong to the Trx superfamily exhibiting a similar overall 3D structure. Two molecules of glutathione (GSH) are necessary to reduce a Grx forming a molecule of oxidased glutathione (GSSG). GSH is regenerated by the glutathione reductase enzyme (Lemaire *et al.*, 2007). Grxs are able to reduce other proteins and mixed disulfides between proteins and GSH. These oxidoreductases are conserved in most eukaryotes and prokaryotes, except in some bacterial or archaeal phyla (Couturier *et al.*, 2009). Two families of glutaredoxins have been described: dithiolic glutaredoxins (which have two cysteines in their catalytic site) and monothiolic glutaredoxins (which only have one cysteine in their catalytic site). *Synechocystis* possesses two dithiolic glutaredoxins (GrxA and GrxB) and one monothiolic (GrxC) (López-Maury *et al.*, 2009; Pérez-Pérez *et al.*, 2009). In some cases the Trx and Grx function might be redundant.

4. Disulphide proteomes

Previous to the proteomics studies several cyanobacterial functions were suggested to undergo redox regulation (Florencio *et al.*, 2006). A thiol reductant-dependent activity was reported for cyanophycin synthetase in *Anabaena cylindrica*

(Simon, 1976) and for RNA polymerase in *Anabaena* sp. PCC 7120 (Schneider *et al.*, 1987). The glucose-6-phosphate dehydrogenase of *Anabaena* sp. PCC 7120 is inhibited *in vitro* by the Trx m (Gleason, 1996). A possible role of Trxs as signal transducers between the photosystems and a transcription factor in the transcription of *psbAII* and *psbAIII* genes in *Synechococcus* sp. PCC 7942 has been suggested (Sippola and Aro, 1999). The reduction of the peroxiredoxin 2-Cys Prx from *Synechocystis* by an *E. coli* Trx was shown *in vitro* (Yamamoto *et al.*, 1999). However, the biochemical approaches towards the Trx function have had a limited contribution to the global knowledge on the redox regulation in cyanobacteria. The comparative studies of Trx targets in other organisms might be informative, but there are important metabolic differences and evolutionary divergence that make the comparison with the cyanobacterial proteins difficult. Thus, it was necessary to develop new approaches to extend the knowledge on enzymatic activities, which undergo redox regulation in cyanobacteria.

Disulphide proteomes may be defined widely as sets of proteins, which contain cysteines that exhibit changes in their redox state (Lindahl and Kieselbach, 2009). Several proteomics approaches have been developed to search for proteins with reactive, accessible cysteines in order to reveal new targets of redox regulation and signal transducers. These methods were originally designed for analyses of soluble Trx targets. Methods have also been developed to study the disulphides proteome without the aid of redox enzymes (Lindahl and Kieselbach, 2009). This is the case of studies based on the mobility shifts on SDS-PAGE under non-reducing versus reducing conditions (Ströher and Dietz, 2008) or the analysis of the protein cysteine sensitivity to S-thiolation (Hochgräfe *et al.*, 2007). Disulphide proteomics analyses have provided useful insights into different redox regulated cellular processes. However, it should be kept in mind that complementary studies are necessary to confirm the physiological relevance of the results.

4.1 Methodology

The two main methods that use Trxs as tools for analysis of the disulphide proteome are the thiol labelling procedure and the thioredoxin affinity chromatography (Lindahl and Kieselbach, 2009).

The first method involves the labelling of thiols with the fluorescent compound monobromobimane (mBBr) (Yano *et al.*, 2001; 2002), radioactive iodoacetamide (^{14}C-IAM) (Marchand *et al.*, 2004) or reagents with different masses such as IAM and DMA (Schilling *et al.*, 2004). In this method, the free thiols are firstly blocked using alkylation reagents such as IAM or NEM. Thereafter, disulphide reduction by Trx gives rise to new free thiols, which are susceptible to labelling by the dye mBBr, that binds covalently to thiols, radioactive alkylation by ^{14}C-IAM or differential alkylation by IAM or DMA. Proteins with labelled thiols are separated using IEF/SDS-PAGE, detected and identified by mass spectrometry. Targets labelled with mBBr may be detected by an analysis of the UV images comparing Trx-reduced and unreduced samples. The radioactivity of the ^{14}C-IAM labelled thiols is detected by autoradiography. In the differential alkylation approach the 2D electrophoresis gels are analysed using MALDI-TOF-MS and the reduced cysteines are detected by the mass shifts due to the different alkylation agents used for thiol labelling. The mBBr method has relatively low sensitivity, which limits its application to the detection of abundant Trx targets. The sensitivity of the other two approaches is higher and similar between them. An advantage of differential alkylation is that it could prevent false positives due to proteins comigrating in the same 2-DE gel spot, by direct identification of the peptides that contain the reactive cysteine. In addition, it allows assignment of redox active cysteine within the amino acid sequence of a target protein (Lindahl and Kieselbach, 2009). The labelling approaches have the advantage that they may be adapted to monitor the *in vivo* redox state of proteins and to quantify the fluctuations. However, they potentially yield false positives *in vitro*, due to the high concentration of Trx used, which may reduce oxidised thiols belonging to non-target proteins (Montrichard *et al.*, 2009).

Trx affinity chromatography is based on the stabilisation of the mixed disulfide bond intermediate formed during the Trx reduction of its protein targets (Motohashi *et al.*, 2001; Balmer *et al.*, 2003; Lindahl and Florencio, 2003). This mechanism involves a two-step oxidation of the cysteine residues belonging to the Trx active site. In the first step the Trx N-terminal catalytic cysteine forms a mixed disulphide bond intermediate with the target (Fig. 7). Consecutively, the Trx C-terminal cysteine breaks this mixed bond by means of a second nucleophilic attack.

Finally, the products of the reaction are the reduced target and the oxidised Trx. Under normal conditions the mixed disulphide intermediate is labile, but if the second cysteine is replaced with another amino acid, *e.g.* serine or alanine, the mixed intermediate can be stabilised. Thus the monocysteinic Trx is a useful tool to study the proteins interacting with Trx (Buchanan and Balmer, 2005; Lindahl and Kieselbach, 2009)

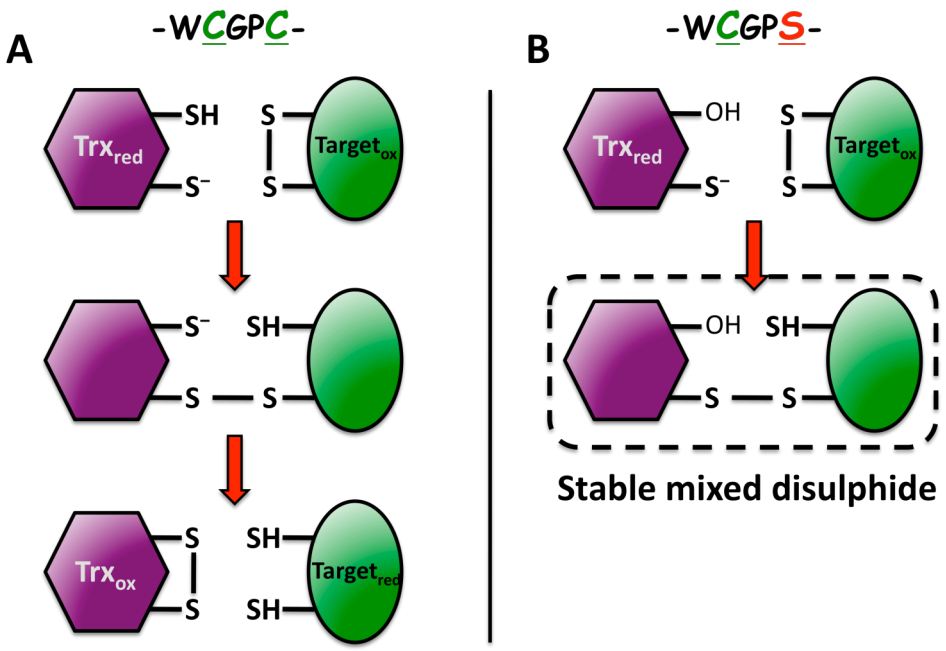

Figure 7. Mechanism of Trx-target reduction. In the WT Trx **(A)** the catalytic cystein of the active site (-WCGPC-) reduces a oxidised cystein of the protein target an forms the mixed disulphide bond intermediate, then the second cystein of Trx performs a nucleophilic attack that breaks the mixed bond resulting the reduced target and the oxidised thioredoxin. In the monocysteinic Trx **(B)** the labile mixed intermediate is stabilised because of the replacement of the second cysteine with a serine in the Trx active.

This strategy was first described for a screening *in vivo* in yeast (Verdoucq *et al.*, 1999) and was later adapted for column-affinity *in vitro* by immobilising the monocysteinic Trx on a Sepharose matrix (Motohashi *et al.*, 2001; Balmer *et al.*, 2003). A variant of this technique was developed in our laboratory (Lindahl and Florencio, 2003; Lindahl and Florencio, 2004), in which the monocysteinic Trx is not permanently bound to the matrix. Instead it is bound to a nickel-affinity chromatography matrix through a histidine tag. Therefore, the mixed Trx-target

complexes are purified by nickel affinity and eluted using imidazole, without breaking the disulphide bonds (Fig. 8). Separation of eluted complexes is performed on 2-D SDS-PAGE under non-reducing/reducing conditions. The mixed disulphides remain intact in the first dimension but, before the second dimension, this bond is broken by DTT treatment. Thus, in this step the Trx and its targets are separated and migrate independently in the second dimension SDS-PAGE. Hence, the thioredoxin targets migrate slower in the first dimension than in the second due to the extra mass of the Trx. Contaminants and non-target subunits can be discriminated since they migrate equally in the first and the second dimension and line up on the diagonal in the stained gel. The targets are located below the diagonal (Fig. 8). Sometimes appear spots above the diagonal, which correspond to proteins with an intramolecular disulphide bond. This approach has a limitation in the identification of protein targets with a molecular weight similar to that of Trx, because of the high amount of this protein used in the analyses. Therefore, the risk of contamination of these protein spots by Trx is elevated. The Trx affinity chromatography methods have the advantage of the enrichment of targets that allows the visualization of these proteins in Coomassie stained gels.

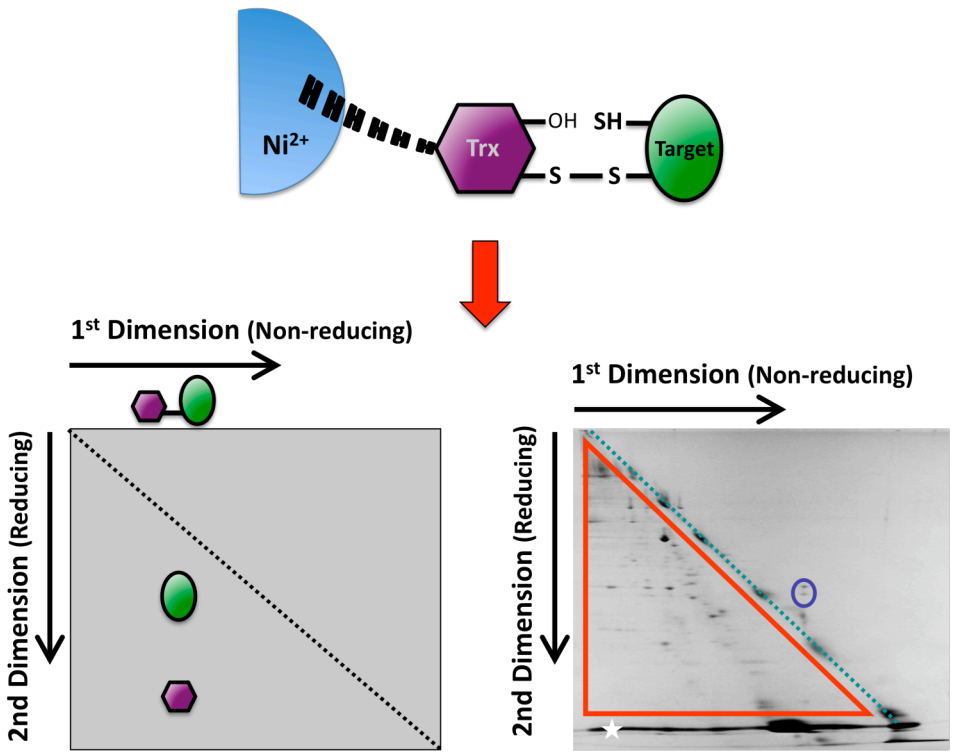

Figure 8. Isolation of Trx-targets by Trx affinity chromatography. The complexes formed by the monocysteinic his-tagged thioredoxin and its targets are

purified by means of Nickel-affinity chromatography. The complexes migrate in a first non-reducing dimension, after that the mixed disulphide bonds are broken using the reductive agent DTT. The broken complexes migrate in a second reducing dimension where the targets of Trx are separated. The non-target protein form a diagonal line (dashed line), the targets are located below this diagonal (marked with a red triangle), proteins with an intramolecular disulphide bond migrate above the diagonal (blue circle) and the free thioredoxins form a line (marked with a white star) in the 12 kDa region in the gel.

4.2 Analysis of disulphide proteome in prokaryotes (Except cyanobacteria)

Apart from studies in cyanobacteria, most of the disulphide proteomic studies in prokaryotes have been performed in the gram-negative model bacterium *Escherichia coli* and in the gram-positive model bacterium *Bacillus subtilis*. Despite the fact that Trx was originally identified in *E. coli* in 1964 (Laurent *et al*., 1964), Trx-dependent disulphide proteomic approaches have been developed and applied principally in photosynthetic organisms (see Buchanan and Balmer, 2005; Florencio *et al*., 2006; Lindahl and Kieselbach, 2009). The *E. coli* genome encodes two Trxs, three Grxs and two Grx-like proteins (Grx4 and NrdH). Out of these, the only essential protein is Grx4, which has a unique function, possibly related to Fe-S cluster assembly. Although Trxs and Grxs play fundamental roles as electron donors in *E. coli*, they are largely redundant (Meyer *et al*., 2009). The *trxA* and *trxC* genes in *E. coli* encode the Trx1 and Trx2, respectively. While none of the *trx* genes is required for viability in *E. coli*, Trx1 is essential in several other bacteria, *e.g*., *Rhodobacter sphaeroides*, *Bacillus subtilis*, *Anacystis nidulans* and *Synechocystis* sp. PCC 6803 (Zeller and Klug, 2006).

Long before the proteomics era, biochemical and genetic studies have described some targets of redoxins in *E. coli*. Initially, Trx was identified as an electron donor for ribonucleotide reductase, a key enzyme in DNA synthesis (Laurent *et al*., 1964). Since, various other functions have been attributed to prokaryotic Trxs and Grxs as electron donors to enzymes reducing methionine sulfoxide or participating in reductive sulphate assimilation (Gleason and Holmgren, 1988). For example, Trx1, Trx2 and Grx1 donate reducing equivalents to the *E. coli* PAPS reductase, the enzyme responsible for reduction of 3'-phosphoadenylylsulfate to

sulfite (Lillig *et al*. 1999), whereas Grx2 is an efficient electron donor for arsenate reductase (ArsC), which catalyses the reduction of arsenate to arsenite (Shi *et al.*, 1999).

An interesting example of redox regulation discovered in *E. coli* before disulphide proteomics is the oxidative activation of the molecular chaperone Hsp33, which contains four conserved cysteines prone to formation of disulphide bridges (Jakob *et al*., 1999). Another example is the bacterial transcription factor OxyR, which serves as a peroxide-sensitive thiol-based redox sensor and controls the expression of several genes involved in the antioxidant response (Zheng *et al*., 1998; Åslund *et al.*, 1999). Among the genes controlled by OxyR are a peroxidase, AhpC, and its reductase, AhpF, first described in *Salmonella typhimurium* (Christman *et al*., 1985). AhpC belongs to the family of peroxiredoxins, which catalyse reduction of H_2O_2 and alkyl hydroperoxides through reversible disulphide formation (Poole, 2005).

The first global study of proteins interacting with Trx in *E. coli* was based on a Tandem Affinity Purification (TAP) strategy, expressing a TAP-tagged version of Trx1 in *E. coli* cells with a *trxA*$^-$ knockout genetic background (Kumar *et al.*, 2004). However, it should be noted that the TAP-tagged Trx1 used in this study possessed the wild type active site, including both cysteines, and would hence not form stable mixed disulphides. Therefore, the target proteins isolated and identified did not necessarily interact with the Trx through thiol chemistry, but rather through electrostatic and/or hydrophobic interactions, forming multiprotein complexes. In this context, it is worth mentioning that *E. coli* Trx1 was previously found to be an essential structural subunit of the bacteriophage T7 DNA polymerase, independently of the Trx active site cysteines (Huber *et al*., 1986) Furthermore, Trx1 is required for the assembly of several filamentous phages (Russel and Model 1985). Nevertheless, some of the targets identified in the study using a TAP-tagged Trx (Kumar *et al.*, 2004) were found later in studies of *E. coli* using different disulphide proteome approaches (Leichert and Jakob, 2004; Brandes *et al*., 2007; Leichert *et al*., 2008).

The principal method used to analyse the disulphide proteome in *E .coli* involves a differential thiol-trapping technique combined with 2-DE gel analysis, in which the cysteines that were oxidised in the cell are reduced and thereafter

carbamidomethylated by radioactively labelled ^{14}C-IAM (iodoacetamide) (Leichert and Jakob, 2004; Brandes *et al.*, 2007). A quantitative thiol proteome study was carried out combining this method with ICAT chemistry (Leichert *et al.*, 2008). Hence, these approaches were used to monitor the thiol status of cellular protein under normal growth conditions as well as under different oxidative stress conditions. The redox-sensitive proteins identified in *E. coli* can be classified into three categories belonging to antioxidant mechanisms, intermediary metabolism or regulation processes. Most of these proteins have a role in the intermediary metabolism. The glyceraldehyde-3-phosphate dehydrogenase (GapA) has been detected reproducibly in the different studies. The redox regulation of GapA has been suggested to involve glutathionylation of its active site cysteine 149 (Cotgreave *et al.*, 2002). Notably, the metabolism of amino acids and related molecules is highly represented by, for example, MetE (cobalamin-independent methionine synthase), IlvC (ketol-acid reductoisomerase, plays a central role in the biosynthesis of isoleucine and valine), AlaS (alanyl-tRNA synthetase), PheT (phenylalanyl-tRNA synthetase beta-subunit) or GlyA (serine hydroxymethyltransferase). The reversible thiol oxidation of MetE after oxidative stress has been shown to be responsible for inhibition of methionine biosynthesis (Hondorp and Matthews, 2004). The peroxiredoxins AhpC and Tpx, as well as the reductase of AhpC (AhpF), are reproducibly shown in the studies and belong to the antioxidant enzymes. Several regulatory proteins have been shown to be redox thiol-sensitive, such as, TufA (elongation factor Tu), ProQ (regulator of ProP, involved in osmoregulation) or YhiF (transcriptional regulator). Other thiol-modified proteins shown in *E. coli* are the aconitase B (AcnB) and different ribosomal subunits.

Recently, a study was published in which thiol- and disulphide-containing proteins from *E. coli* were selected by using an Activated Thiol-Sepharose (ATS) chromatography (Hu *et al.*, 2010). ATS is a thiol-specific resin that possesses an activated disulphide structure, which is able to react and to form covalent mixed disulphides with thiolic groups. The procedure involves a denaturation step with urea prior to purification, thus the thiols detected under normal conditions do not necessarily belong to reactive cysteines. More interesting are the proteins that contain disulphide bonds or thiol groups under oxidative stress generated by menadione treatment. Amongst the identified proteins, ribosomal proteins, amynoacyl-tRNA synthetases, and metabolic and antioxidant enzymes were

prominent (Hu *et al*., 2010).

An approach similar to that used in *E. coli* (Leichert and Jakob, 2004) was developed, but instead of radioactive labelling, a fluorescent reagent was introduced (Hochgräfe *et al.*, 2005). This method was applied for analysis of the cysteine redox state of cytoplasmic *B. subtilis* proteins under normal growth conditions and upon oxidative stress induced by diamide, H_2O_2 or O_2^- (Hochgräfe *et al.*, 2005). The redox-sensitve proteins identified under normal growth were, among others, the antioxidant system made up of the peroxirredoxin AhpC and its reductase (AhpF), the thioredoxin TrxA and the phosphoadenosine phosphosulfate reductase (CysH). The proteins with thiol modification were found to be specific for each oxidative stress condition, but five proteins were identified under all conditions. These were the peroxiredoxins AhpC and Tpx, and the proteins belonging to the amino acid metabolism LeuC (large subuit of 3-isopropylmalate dehydratase), ArgC (N-acetylgutamate gamma-semialdehyde dehydrogenase) and MtnA (methylthionucleoside-1-phosphate isomerase). Other proteins with thiol modification were detected under several but not all of the oxidative conditions tested. Some of these play a role in the amino acid metabolism, such as MetE, AroA (3-deoxy-D-arobino-heptulosonate 7-phosphate synthase) and LeuD (large subuit of 3-isopropylmalate dehydratase). Other proteins detected reproducibly were the PfkA (6-phosphofructokinase) and some enzymes of the nucleotide metabolism, such as GuaB (inosine-monophosphate dehydrogenase) and PurA (adenylosuccinate synthase). There were also proteins modified in only one of the oxidative stress treatments, for example IlvC and GlyA, which belong to the amino acid metabolism or the elongation factor Tu (TufA). These proteins coincided with those identified in *E. coli*. The same approach has been used to test the oxidative effect of the quinones in *B. subtilis.* However, the only redox-sensitive protein identified was the glyceraldehyde-3-phosphate dehydrogenase (GapDH) (Liebeke *et al.*, 2008).

A different technique was developed in *B. subtilis* to analyse the protein S-thiolation by cysteine (called S-cysteinylation) under condition of disulfide stress using diamide treatment. By in vivo [^{35}S]cysteine labelling in the presence of chloramphenicol and 2-DE, six proteins showed S-cysteinylation in response to diamide stress (Hochgräfe *et al.*, 2007). Four of these, GuaB, MetE, PpaC and the

protein YwaA with similarity to branched-chain amino acid aminotransferases, were already reported in the previously mentioned study.

The same fluorescence labelling approach described for *B. subtillis* (Hochgräfe *et al.*, 2005) was used to study the reversibly oxidised thiols of cytoplasmic proteins in *Staphylococcus aureus* during normal growth and under oxidative stress induced by diamide and H_2O_2 treatments (Wolf *et al.*, 2008). Amongst the proteins identified under normal growth condition were the peroxiredoxin system AhpC/AhpF, dihydrolipoyl dehydrogenase PdhD of the pyruvate dehydrogenase complex, and a probable cysteine desulfurase Csd. Diamide treatment results in a global oxidation of many cysteine residues in intracellular proteins of *S. aureus*. Many of these have been previously detected in *B. subtilis* as well as in *E. coli*, *e.g.*, AhpC/AhpF system, MetE, GlyA, IlvD, LeuD, LeuD, GuaB and GapA. Eighteen different proteins with thiol oxidation after H_2O_2 stress were identified. The largest number belongs to the intermediary metabolism, for example, AldA (aldehyde dehydrogenase), MetE and the CTP synthase PyrG. Moreover, proteins implicated in oxidative stress and peroxide detoxification, such as the thioredoxin system composed by the thioredoxin TrxA and its reductase TrxB, the Tpx peroxiredoxin and the glutathione peroxidase homologue BsaA. The regulatory protein Spx was also observed to be redox-sensitive.

A study of S-thiolation has been carried out in *S. aureus* where two proteins were identified that are modified by S-cysteinylation (Pöther *et al.*, 2009); the acetoine reductase and a hypothetical lipoprotein. Results with lower confidence levels suggest S-cysteinylation of a glycyl-tRNA synthetase, a phosphoribosylaminoidazole-succinocarboxamide synthase, a pyruvate kinase, a triosephosphate isomerase and SarA. In the same study, Pöther *et al.*, 2009 analyse the intramolecular and intermolecular disulfide bond formation as in *B. subtilis* as well as in *S. aureus*. Some proteins with intramolecular disulphide bond in *B. subtilis* are MetE GuaB, ArgF and Tpx. Proteins with intermolecular disulphide bonds include IlvC, HisI, HisB and AhpC in *B. subtilis* and AhpC, MetN-2, PurH and the glycyl-t-RNA synthetase GlyQS in *S. aureus*.

Mycobacterium tuberculosis and the obligate anaerobic photosynthetic green sulfur bacterium *Chlorobaculum tepidum* are other prokaryotes, where the disulphide

proteomes have been studied. In *M. tuberculosis* proteins with S-nitrosylation sensitive cysteines have been analysed (Rhee *et al.*, 2005). The Trx-interacting proteome has been studied in *C. tepidum* (Hosoya-Matsuda *et al.*, 2009). In both bacteria the majority of proteins identified are implicated in the intermediary metabolism, especially in the amino acid metabolism, *e.g.*, AsnB (asparagine synthase), SerA (3-phosphoglycerate dehydrogenase), GlnA1 (glutamine synthetase) and GltB (glutamate synthase) in *M. tuberculosis*, and serine hydroxymethyltransferase, S-adenosylmethionine synthetase and tryptophan synthase in *C. tepidum*. Antioxidant defense proteins are been shown in both cases, for example, the catalase KatG in *Mycobacterium* and the peroxiredoxins 2-Cys Prx and PrxQ in *C. tepidum*.

Many proteins are described, which possess reactive cysteines and, hence, might undergo a putative redox regulation, but notably, there is a high abundance of protein implicated in the metabolism of amino acids and related molecules. Bacteria have low molecular weight (LMW) thiols that act as thiol redox buffer and protect the protein cysteines against overoxidation by S-thiolation. Gram-negative bacteria have glutathione (GSH) as redox buffer, but many gram-positive bacteria lack genes for GSH biosynthesis. *B. subtilis* and *S. aureus* rely on different LMW thiols, such as bacillithiol (BSH), or even the free cysteine (Pöther *et al.*, 2009). Thus, it has been suggested that under oxidative stress it is necessary increase the cysteine pool to protect the cell from damage. A metabolome study carried out in *B. subtillis* revealed significant modifications in the cysteine and branched-chain amino acid biosynthesis pathways in response to diamide (Pöther *et al.*, 2009). A drastic depletion of cysteine and its precursors supports the idea of cysteine generation and S-thiolation of protein thiols after exposure to diamide. Under these stress conditions, cysteine biosynthesis is induced by derepression of the CymR regulon (Leichert *et al.*, 2003). The concentration of glycine, which is a precursor of serine, is reduced under oxidative stress and the synthesis of the glycyl-tRNA synthetase is also decreased (Leichert *et al.*, 2003; Pöther *et al.*, 2009). This might indicate an enhanced provision of glycine for serine synthesis, a cysteine precursor. The CymR-controlled MccA (YrhA) and MccB (YrhB) proteins participate in the conversion of methionine to cysteine and are induced under disulphide stress (Liechert *et al.*, 2003). The methionine synthase MetE is S-cysteinylated under diamide stress and inactivated by

S-thiolation in *E. coli* (Hondorp and Matthews, 2009; Hochgräfe *et al.*, 2007). The methionine pool is decreased in diamide treated cells. All these findings indicate a decreased conversion of cysteine to methionine (Pöther *et al.*, 2009).

4.3 The disulphide proteome in Photosynthetic organisms (Plants and Algae)

The thioredoxin redox control in alage and plants shows a high complexity because of the large number of Trx present in theses organism. The green algae *Chlamydomonas reinhardtii* contains 8 Trx genes, 5 plastidic Trx: 2 Trx *f*, 1 Trx *m*, 1Trx *x* and 1 Trx *y*; and three non-plastidic, 1 Trx *o* and 2 Trx *h*. The plant *Arabidopsis thaliana* contains 20 Trx genes in its genome, 9 of which encode proteins located in the chloroplast: 2 Trx *f*, 4 Trx *m*, 1 Trx *x* and 2 Trx *y*. Mitochondria harbour 2 Trx *o* and, in addition, 9 Trx *h* are distributed between several cell compartments (cytosol, mitochondria, endoplasmic reticulum) as well as outside the cell (Lemaire *et al.*, 2007). *Arabidopsis thaliana* contains in its genome 42 genes that encode Trx-like disulfide proteins (Meyer *et al.*, 2005). Among these are the chloroplastic proteins NTRC, CDSP32 and HCF164. CDSP32 contains two Trx domains and its expression is induced under drought stress and is able to reduce two chloroplastic peroxiredoxins. HCF164 is anchored to thylakoid membranes and required for the biosynthesis of cytochrome b6/f (Lemaire *et al.*, 2007). A new type of Trx called Trx *s* involved in the symbiosis process and was identified in the legume *Medicago truncatula* (Alkhalfioui *et al.*, 2008).

Before the development of proteomics approaches, there were several plant proteins known to undergo light-dependent redox regulation catalysed by Trx. The fructose-1,6-bisphosphatase (FBPase) was the first to be identified. Thereafter, more Trx-linked proteins belonging to different processes were detected, such as four additional proteins of the Calvin-Benson cycle, -namely phosphoribulokinase (PRK), sedoheptulose bisphosphatase (SBPase), NADP-glyceraldehyde 3-phosphate dehydrogenase (GADPH) and the Rubisco activase-. The NADP-malate dehydrogenase (NADP-MDH), the ATP synthase γ-subunit, the glucose 6-phosphate dehydrogenase, the acetyl-CoA carboxylase and ADP-glucose pyrophosphorylase were also found to be subject to Trx-dependent regulation (Montrichard *et al.*, 2009).

These findings linked the thioredoxins to the control of the Calvin-Benson cycle and the oxidative pentose phosphate pathway, fatty acid and starch synthesis. Some later biochemical studies provided evidence of regulation of germination, growth and development by Trx *h* in wheat (Montrichard *et al.*, 2009).

The main approaches used for disulphide proteomics in plants are the same as explained previously in the methodology section: thiol labelling and thioredoxin affinity chromatography, but some new strategies have also been developed. Targets of different subcellular compartments have been identified, including chloroplast, cytosol, mitochondria and nucleus. Different tissues of plant have been used in these studies from leafs (Lemaire *et al.*, 2007) to embryos of germinating barley grain (Marx *et al.*, 2003).

The disulphide proteomic studies in the chloroplast have resulted in a total of 136 potentially redox-regulated Trx-target proteins (Lindahl and Kieselbach, 2009). The target proteins reported participate in the major chloroplast metabolic pathways, for example, the photosynthetic electron transport, ATP synthesis, Calvin-Benson cycle and some biosynthetic pathways including starch synthesis, sulphur and nitrogen assimilation, and the synthesis of proteins, tetrapyrroles, chlorophillide and heme (Lindahl and Kieselbach, 2009).

Nineteen Trx-targeted proteins are found in the photosynthetic apparatus, such as the D1 protein (PsbA) of the PSII reaction centre (Ströher and Dietz, 2008). Chloroplastic Trxs could also be involved in the mechanism of state transition, which is based on the phosphorylation of LHCII mobile antenna by a redox dependent kinase. The cloning of the kinase phosphorylating LHCII in *Chlamydomonas* (Depége *et al.*, 2003) and *Arabidopsis* (Bellafiore *et al.*, 2005) revealed the presence of two conserved cysteines in the N-terminal part of the protein, which might be involved in a Trx-dependent regulation mechanism (Lemaire *et al.*, 2007). The activation of chloroplast ATP synthase by Trx via FTR has been known for a long time (Lemaire *et al.*, 2007) and there is evidence that it depends on the Trx-mediated reduction of a disulphide in the γ-subunit (Wu *et al.*, 2007). In addition, the results from independent screening studies in *Arabidopsis*, spinach, potato and *C. reinhardtii* show that also the α-, β-, δ-, and ε-subunits of CF1 are potential targets for regulation by

Trx (Motohashi and Hisabori, 2006; Balmer *et al.*, 2006; Lemaire *et al.*, 2004; Ströher and Dietz, 2008; Rey *et al.*, 2005; Balmer *et al.*, 2004; Lindahl and Kieselbach, 2009).

Nineteen *in vitro* targets of Trx participate directly or indirectly in the Calvin-Benson cycle, indicating that Trx regulates all Calvin-Benson cycle enzymes. Thus, Trx control might function as a main switch to activate this cycle upon illumination (Schürmann and Buchanan, 2008; Lemaire *et al.*, 2007; Lindahl and Kieselbach, 2009).

In the starch synthesis pathway the ADP glucose pyrophosphorylase has been identified in several independent proteomics studies (Lindahl and Kieselbach, 2009). Redox regulation of α–glucan water dikinase controls starch degradation in both photosynthetic and non-photosynthetic tissues (Mikkelsen *et al.*, 2005). The β-amylase was also detected by proteomics approaches (Balmer *et al.*, 2003). The first enzyme of the reductive assimilation of sulphate, the adenylylsulphate reductase (APS), was identified as a Trx-target in *C. reinhardtii* (Lemaire *et al.*, 2004); the chloroplast APS reductases have a C-terminal Trx-like domain, which is necessary for activity (Weber *et al.*, 2000). The biosynthesis of cysteine links sulphur assimilation and amino acid synthesis. In plants the O-acetylserine lyase (OASB) and the Cyp20-3 have been detected as Trx-targets, suggesting a redox regulation of the cysteine synthesis (Motohashi *et al.*, 2001; Motohashi *et al.*, 2003; Balmer *et al.*, 2003).

Some proteins involved in the nitrogen assimilation have been decribed as redox regulated. The chloroplastidic glutamine synthetase GLN2 has been detected in many screening studies of Trx targeted proteins (Motohashi *et al.*, 2003; Lemaire *et al.*, 2004; Marchand *et al.*, 2004). The cytosolic glutamine synthetase (GLN1;3) was also reported to be a target of Trx (Balmer *et al.*, 2003; Balmer *et al.*, 2004). Activation of the *Chlamydomonas* plastidic glutamine synthetase by *m*-type Trx has been shown (Florencio *et al.*, 1993). This enzyme is activated by reduction of an intramolecular disulphide in *C. lineata* (Choi *et al.*, 1999). The glutamate synthase (GOGAT) was also found to be regulated by Trx (Lichter and Häberlein, 1998).

The biosynthesis of tetrapyrroles is a multi-branched pathway and there is evidence that redox control via Trx is involved in several steps, for example, the activity of CHL1 subunit of Mg chelatase is stimulated upon reduction of a disulphide

bridge by Trx *f* (Ikegami *et al.*, 2007).

The protein metabolism is highly represented in the Trx-target screenings. Several ribosomal subunits and translation elongation factors, such as EF-Tu and EF-G, have been found. In addition, some proteins related to protein folding have been identified, for example, the chaperones CPN60 (Rubisco binding protein) and Hsp70, the chaperonine 20 or the immunophilins FKBP12, FKBP13, FKBP20-2, that catalyse the cis-trans isomerisation of prolyl peptide bonds. Other targets of Trx are related to protein degradation, e.g., the proteases ClpC and FtsH (Lindahl and Kieselbach, 2009). Disulphide proteome studies in plants and algae have identified some enzymes functioning in the oxidative stress response; and this is the case of several peroxiredoxins, glutathione peroxidases and the methionine sulfoxide reductases A and B1 (Lindahl and Kieselbach, 2009).

The majority of the chloroplastic disulphide proteome studies have been carried out by means of Trx affinity chromatography techniques. However, the screening performed using plant seeds and cereal grains involved mainly fluorescent thiol labelling (Montrichard *et al.*, 2009). The proteins found in these studies are enzymes of different key processes, such as starch metabolism, antioxidant defence and protein metabolism, including degradation, assembly and folding. Moreover, more specific targets have been found, including a desiccation-related protein, a seed maturation protein and some proteins in embryos of germinating barley grain (Marx *et al.*, 2003; Montrichard *et al.*, 2009). A strategy based on the quantitative ICAT method was employed to analyse the disulphide proteome linked to Trx in soluble proteins of barley seed embryo (Hägglund *et al.*, 2008). Ninety putative Trx-targets were identified, among which a notable number of ribosomal proteins were present. Other targets related to protein metabolism were several proteins functional in amino acid metabolism (*e.g.* the glycyl-tRNA synthetase), and enzymes catalysing protein folding and degradation. This work confirms the key role that redox regulation plays in protein metabolism (Montrichard *et al.*, 2009).

The Trx-affinity chromatography approach was used to analyse the Trx-linked proteins in the plant mitochondria (Balmer *et al.*, 2004b). Novel targets included proteins functional in photorespiration, citric acid cycle, lipid metabolism, electron

transport, membrane transport and hormone synthesis (Montrichard *et al.*, 2009).

4.4 The disulphide proteome in Cyanobacteria

The strategy used for analysis of the disulphide proteome in cyanobacteria was developed in *Synechocystis* sp. PCC 6803 and involved the purification of mixed disulphide complexes formed by a monocysteinic his-tagged Trx and its putative targets, followed by 2-D SDS-PAGE under non-reducing/reducing conditions (Lindahl and Florencio, 2003; Florencio *et al.*, 2006).

TrxA, TrxB and TrxQ have been used as bait in comparative screening studies of Trx-targets (Lindahl and Florencio, 2003; Pérez-Pérez *et al.*, 2006). There is little variation between the target proteomes using different Trx, indicating a low degree of target specificity *in vitro*. Thirty-nine Trx-targets in total were identified in *Synechocystis*. These targets organised in groups according to their function or the metabolic pathways, in which they participate, are shown in Table 1, which has been adapted from Florencio *et al.*, 2006.

Table 1. Thioredoxin target proteins identified in *Synechocystis* sp. PCC 6803.

ORF	Protein name
Carbon dioxide fixation	
slr0009	Rubisco large subunit (RbcL)
sll1031	Carboxysomal protein (CcmM)
sll1525	Phosphoribulokinase
Glycolysis and pentose phosphate pathway	
sll0018	Fructose-1,6-bisphosphate aldolase, class II
sll1342	Glyceraldehyde-3-phosphate dehydrogenase (Gap2)
slr0394	Phosphoglycerate kinase
sll1841	Pyruvate dehydrogenase subunit E2
sll1070	Transketolase

Glycogen metabolism	
sll0726	Phosphoglucomutase
slr1176	ADP-glucose pyrophosphorylase
sll1393	Glycogen synthase (Glg2)
sll0158	Glucan branching enzyme (GlgB)
slr1367	Glycogen phosphorylase
Sugar-nucleotide metabolism	
sll1212	GDP-mannose dehydratase
sll0576	Sugar-nucleotide epimerase
Sulphur metabolism	
slr1165	Sulfate adenylyltransferase
slr0963	Ferrredoxin-sulfite reductase
Nitrogen metabolism	
sll1499	Ferredoxin-GOGAT (GlsF)
sll1502	NADH-GOGAT (GltB)
slr0585	Argininosuccinate synthetase
slr1133	Argininosuccinate lyase
Tetrapyrrole biosynthesis	
sll1994	Porphobilinogen synthase
Oxidative stress response	
slr1198	1-Cys peroxiredoxin (1-Cys-Prx)
sll1621	YLR109-homologue (Type II Prx)
sll1987	Catalase-peroxidase (KatG)
Light harvesting	
ssr3383	Phycobilisome core linker (LC)
slr0335	Phycobilisome core-membrane linker (LCM)
sll1577	Phycocyanin β-subunit

RNA metabolism	
sll1789	RNA polymerase β'-subunit
sll1787	RNA polymerase β-subunit
sll1043	Polyribonucleotide nucleotidyl transferase
Protein synthesis and folding	
slr0557	Valyl-tRNA synthetase
slr1550	Lysyl-tRNA synthetase
slr1463	Translation elongation factor EF-G
sll1099	Translation elongation factor EF-Tu
sll1804	30S ribosomal protein S3
slr2076	60-kDa chaperonin 1 (GroEL)
Redox regulation	
slr0623	Thioredoxin (TrxA)
Unknown	
slr1855	Hypothetical protein

One third of these *Synechocystis* target proteins have homologues, which have been found as targets for Trx or Grx, in other photosynthetic organisms. These common targets emphasise the processes of carbon dioxide fixation, glycolysis, glycogen synthesis, nitrogen metabolism, oxidative stress response and protein synthesis and folding as principal subjects to redox control. Five enzymes were found as universal Trx or Grx targets in all three classes of photosynthetic organisms (plants, algae and cyanobacteria), namely Rubisco large subunit (RbcL), phosphoribulokinase, Type II Prx, the translation elongation factor EF-Tu and the 60 kDa chaperonin GroEL, which is also known as Rubisco-binding protein. The conservation of cysteines in these five proteins from chloroplasts and cyanobacteria, together with their presence in the target proteomes, suggests that they are early redox-regulated proteins in the perspective of molecular evolution (Florencio *et al.*, 2006).

A comparison with the disulphide proteome of other bacteria (mainly *E. coli* and *B. subtilis*) shows a low degree of overlap concerning cellular processes. Common processes include glycolysis, in which the glyceraldehyde-3-phosphate dehydrogenase is a highly conserved redox regulated target in all bacteria analysed, and oxidative stress response, where the peroxiredoxins are reproducibly identified. Protein synthesis and folding stand out for the detection of different t-RNA synthetases and the presence of the translation elongation factor EF-Tu, which is found as target of redox control in all the organism analysed. The type II peroxiredoxin is the other protein found in all photosynthetic organisms and all bacteria, in which this kind of studies have been performed. The glutamine synthetase has also been found as Trx-target in cyanobacteria *in vivo*, and in plant and non-photosynthetic bacteria this has been a recurrent target.

The differences between the disulphide proteomes of cyanobacteria and those of other organisms may have different reasons. Firstly, cyanobacteria possess specific cellular processes and structures absent from plants and from other prokaryotes, for example, the phycobilisomes and the carboxysomes. It seems obvious that the photosynthesis establishes a great difference with the non-phosynthetic prokaryotes and this is reflected in these proteomic studies. There are also some Trx-targets in plants that are not present in cyanobacteria; this is the case of the enzyme Rubisco activase (Florencio *et al.*, 2006). Other reasons may be the evolutionary divergence of the target protein between prokaryotes and eukaryotes. For example, the glucan branching enzyme (GlgB), phosphoglucomutase and sulphate adenylyl transferase from *Synechocystis* belong to families of prokaryotic enzymes, whereas their chloroplast counterparts have eukaryotic characteristics. The cysteines of the cyanobacterial GlgB, phosphoglucomutase and sulphate adenylyl transferase are amongst the many residues that differ between these proteins and the corresponding chloroplast enzymes (Florencio *et al.*, 2006). Furthermore, there are evolutionary changes, such as the insertion of regulatory Cys-containing motifs in the chloroplast fructose-1,6-bisphosphatase and the γ-subunit of the CF_1 ATP synthase, which are missing in the cyanobacterial homologues (Florencio *et al.*, 2006). One last reason is derived from the different methodology used in each organism. For example, most Trx proteomics studies on chloroplasts have employed isoelectric focusing for separation of target proteins, which hampers the identification of high molecular

mass proteins such as the GOGATs and the β- and β´-subunits of the RNA polymerase. On the other hand, the method used to isolate *Synechocystis* target proteins (Lindahl and Florencio, 2004) impedes identification of proteins in the range of 10 to 15 kDa molecular mass due to the presence of high amounts of recombinant *Synechocystis* Trx in this region, which would exclude for example the small subunit of Rubisco (Motohashi *et al.*, 2001; Florencio *et al.*, 2006).

The reported discrepancies between the cyanobacterial disulphide proteomes with respect to chloroplast on one hand and non-photosynthetic bacteria on the other might indicate that there is more to discover both in cyanobacteria and in the other organisms. Hence, it would be necessary to take further improved redox proteomic studies to understand the complete network of redox regulation in cyanobacteria. Since proteomic studies alone do not provide information on regulation of activity biochemical analyses are also required. There are proteins of low abundance, such as regulatory kinases and transcription factors, which elude detection using conventional proteomic techniques. To study the possible interactions between Trx and such proteins new approaches must be developed.

OBJECTIVES

OBJECTIVES

In order to extend the knowledge about redox signalling and the function of Trx in cyanobacteria we aimed at identifying the putative Trx-targets that, for different reasons, had been overlooked in previous studies on cyanobacteria Therefore, the main objective of this thesis was to complete the effort to characterise the Trx-target proteome of the cyanobacterium *Synechocystis* sp. PCC 6803. This general objective may be divided into the following subsidiary objectives:

I. **Membrane proteins from the cyanobacterium *Synechocystis* sp. PCC 6803 interacting with Trx**. We sought to develop a procedure in *Synechocystis* that would allow analysis of Trx-interactions with membrane proteins, since the proteomic approaches previously used to analyse putative Trx-targets had not been compatible with membrane-associated proteins. The aim was to identify targets in both thylakoid and plasma membranes.

II. **Trx-targets in the thylakoid lumen**. We set out to study the possible targets for Trx-mediated redox regulation in the soluble compartment contained within thylakoids, the lumen. Since the isolation of cyanobacterial thylakoid lumen is not possible, we decided to use chloroplast thylakoid lumen preparations from *Arabidopsis* and, thereafter, to search for proteins in *Synechocystis* homologous to the Trx-targets identified from *Arabidopsis*.

III. **Trx-mediated redox regulation of eukaryotic type Ser/Thr kinases in the cyanobacterium *Synechocystis* sp. PCC 6803**. Proteomic procedures used to identify Trx-targets are not sensitive enough to detect most components of signalling pathways. Thus, we decided to take on the search of this kind of proteins using a different approach and focused on the study of the Ser/Thr kinases in *Synechocystis* and their possible redox regulation.

Finally, we wanted to make an in-depth analysis of aspects related to the redox regulation *in vitro* and *in vivo* of some of the Trx-targets found. Thus, we decided to

address further the activity of Trx towards the peroxiredoxins **2-Cys Prx**, **1-Cys Prx** and **PrxQ2**, the universal stress protein **Usp1**, the protease **FtsH2** and the Ser/Thr kinase **SpkB**.

Part of the work exposed here has been published in the following articles:

Florencio FJ, Pérez-Pérez ME, López-Maury L, Mata-Cabana A, Lindahl M (2006) **The diversity and complexity of the cyanobacterial thioredoxin systems.** Photosynth Res 89:157-171

Mata-Cabana A, Florencio FJ, Lindahl M (2007) **Membrane proteins from the cyanobacterium Synechocystis sp. PCC 6803 interacting with thioredoxin.** Proteomics 7:3953-3963

Pérez-Pérez ME, Mata-Cabana A, Sánchez-Riego AM, Lindahl M, Florencio FJ (2009) **A comprehensive analysis of the peroxiredoxin reduction system in the Cyanobacterium Synechocystis sp. strain PCC 6803 reveals that all five peroxiredoxins are thioredoxin dependent.** J Bacteriol 191:7477-7489

Hall M, Mata-Cabana A, Akerlund HE, Florencio FJ, Schröder WP, Lindahl M, Kieselbach T (2010) **Thioredoxin targets of the plant chloroplast lumen and their implications for plastid function.** Proteomics 10:987-1001

RESULTS

I- MEMBRANE PROTEINS FROM THE CYANOBACTERIUM *Synechocystis* sp. PCC 6803 INTERACTING WITH THE THIOREDOXIN

Introduction

The disulphide proteomic methods developed until now have been very useful for the identification of a large number of cytosolic putative Trx-tagets in cyanobacterial as well as in plant cells. However, Meyer *et al.* (2005) pointed out that a limitation of the current strategies to identify thioredoxin target proteins is their incompatibility with membrane proteins. Consequently, about one-third of all cellular proteins (Wallin and von Heijne, 1998) would be beyond reach and perhaps several putative targets for redox regulation of membrane-associated processes, such as respiration, photosynthesis and ion transport, would be left undiscovered. The inherent difficulty of analysing membrane proteins lies in that they may either be integral to the lipid bilayer, and therefore include extended hydrophobic stretches, or strongly bound by electrostatic and/or hydrophobic interactions to integral membrane proteins (Santoni *et al.*, 2000). Thus, chromatographic procedures cannot be performed unless the proteins are solubilised using detergents, which partially replace the lipids, or extracted by organic solvents. Furthermore, a standard separation technique in the protocols applied for resolution of thioredoxin target proteins, IEF, is unsuitable for membrane proteins since these are particularly prone to precipitation at their isoelectric points (Santoni *et al.*, 2000; Wu and Yates, 2003).

More recently, Motohashi and Hisabori (2006) reported a method to screen for thylakoid-bound targets of the *Arabidopsis thaliana* thioredoxin-like enzyme HCF164, the catalytic moiety of which faces the thylakoid lumen. Octylglucoside-solubilised thylakoid proteins were subjected to thioredoxin-affinity chromatography using an immobilised monocysteinic version of HCF164 and, as a result, nine putative target proteins were identified on 1-DE. However, it should be kept in mind that solubilisation of membrane proteins prior to their contact with the monocysteinic thioredoxin might expose buried protein disulphides that are normally not accessible to react with thioredoxins or other enzymes. Another method, described by Balmer *et al.* (2006), involved differential labelling of protein thiols with mBBr following thioredoxin-mediated reduction of Triton X-100-solubilised thylakoid proteins. This strategy led to the identification of 14 thylakoid-bound thioredoxin targets, several of which were reported for the first time. However, since this method does not include a step that selects target proteins, the application of total thylakoid protein on IEF/SDS-

PAGE 2-DE probably permits the identification only of the most abundant target proteins.

In this study, we designed a new procedure to isolate membrane proteins interacting with thioredoxin by binding *in situ* to a monocysteinic His-tagged thioredoxin added directly to the intact membranes. Solubilisation of membrane proteins was performed after thioredoxin-target disulphide formation, in order to avoid the potential exposure of buried disulphides to the thioredoxin used as bait. Targets were subsequently selected by Ni-affinity chromatography and resolved on 2-D SDS-PAGE under non-reducing/reducing conditions, thus avoiding altogether the application of IEF. This procedure was performed on total membranes, including thylakoid and plasma membranes, from the cyanobacterium *Synechocystis* sp. PCC 6803 and, hence, completes the effort to characterise the thioredoxin target proteome in this organism.

Results and discussion

1. Subcellular localisation of TrxA

The cyanobacterial *m*-type thioredoxin, TrxA, was previously found to be associated with purified thylakoid membranes from *Synechocystis* sp. PCC 6803 (Srivastava *et al.*, 2005) and the thioredoxins m1, m2 and m4 were identified in a study mapping the *A. thaliana* peripheral thylakoid membrane proteome (Peltier *et al.*, 2002). Since the *Synechocystis* thioredoxin TrxA is a highly abundant protein that constitutes about 2.5 ng *per* mg of total cellular protein (Florencio *et al.*, 2006), it may be assumed that residual amounts could contaminate the membrane fractions, despite extensive purification (Srivastava *et al.*, 2005). In order to determine the proportion of TrxA associated with membranes in *Synechocystis* sp. PCC 6803, we performed Western blot analysis on the soluble and the total membrane fraction, obtained by centrifugation of broken cells, using antibodies raised against TrxA and, as a control, against GSI, another abundant *Synechocystis* protein (Fig. 9A). Under standard growth conditions about one-third of all TrxA was found to be present in the membrane fraction and, in contrast, only about 10% of all GS was found in this fraction (Fig. 9B),

indicating that a subpopulation of TrxA indeed is associated with membranes in *Synechocystis*. Thereafter, we aimed at testing the specificity of the TrxA association to the two different membrane types in cyanobacteria. To this end, we analysed the presence of TrxA in isolated thylakoid and plasma membranes, kindly provided by Birgitta Norling's laboratory (See the membranes preparation method: Norling B *et al.*, 1998), by western blot (Fig. 9C). TrxA appeared to be equally distributed between both membrane types (Fig. 9C). It should be noted that the antibodies used are specific for TrxA and do not recognise the other *Synechocystis* Trxs (Florencio *et al.*, 2006).

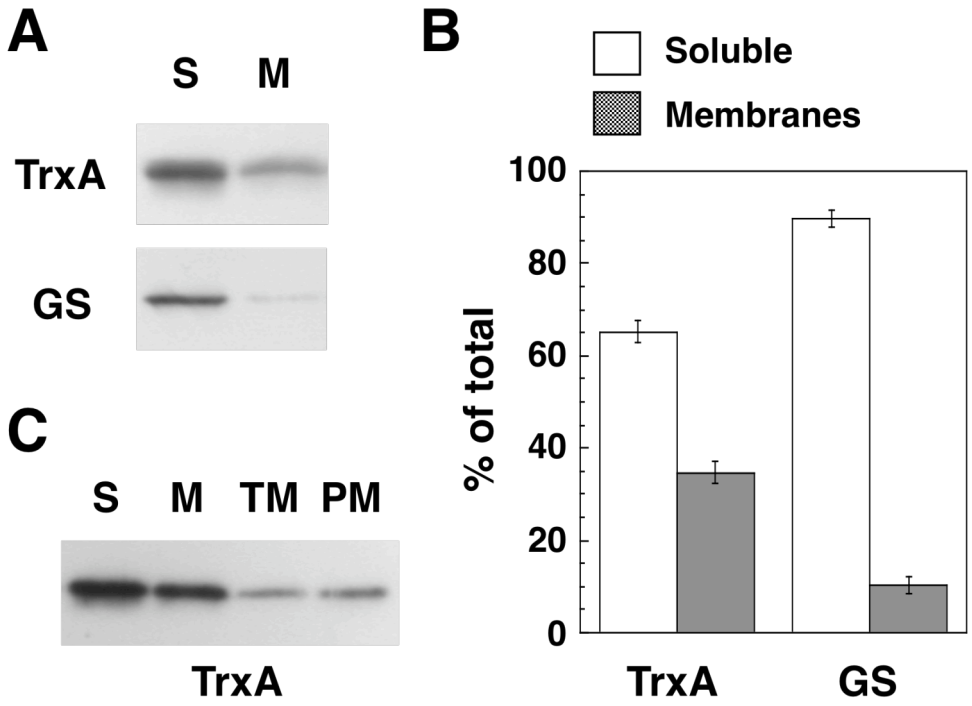

Figure 9. Distribution of the *Synechocystis* sp. PCC 6803 thioredoxin TrxA between soluble and membrane fractions. (A) Western blot analysis. Equivalent amounts of soluble (S) and membrane proteins (M), corresponding to 9 and 12 μg of protein respectively, were separated by SDS-PAGE and analysed by western blot using antibodies raised against TrxA and glutamine synthetase (GS). **(B)** Signals from western blots were quantified to determine the proportions of TrxA and GS associated with the membrane fraction, respectively. The data represent the means of the values obtained from two independent experiments using different cell cultures and the standard deviations are presented as error bars. **(C)** Western blot analysis. Equivalent amounts of soluble (S) total membrane (M), thylakoid membrane (TM) and plasma membrane proteins (PM) corresponding to 12 μg of protein respectively, were separated by SDS-PAGE and analysed by western blot using antibodies raised against TrxA.

2. Isolation of membrane proteins interacting with thioredoxin

Since considerable amounts of TrxA may be associated with membranes and little is known about membrane proteins interacting with thioredoxins, we aimed at developing a procedure for isolation and identification of membrane bound thioredoxin target proteins. To this end, we used the recombinant His-tagged monocysteinic version of TrxA, TrxA35, in which the second cysteine of the active site (WCGPC) had been replaced with a serine (WCGPS) to permit the formation of stable mixed disulphides with its putative target proteins. For sake of simplicity, proteins forming mixed disulphides with the thioredoxin are hereafter referred to plainly as 'thioredoxin targets'. However, it should be understood that conclusions about the physiological relevance of the redox state of the target protein cysteines and their possible interaction with thioredoxins or other enzymes could only be drawn after extensive experimental work implying, *e.g*. site-directed mutagenesis of these cysteines and studies of enzymatic activity.

Total membranes, including thylakoid and plasma membranes, prepared from *Synechocystis* sp. PCC 6803 cultures grown under standard conditions, were incubated with TrxA35 in order to allow formation of disulphide bonds with the membrane-bound target proteins *in situ* (Fig. 10). After this step it would be possible to solubilise the membranes directly using a non-ionic detergent and to subject the sample to Ni-affinity chromatography for isolation of peripheral and integral membrane proteins bound to TrxA35. However, we choose to fractionate the membranes prior to the chromatographic step in order to avoid overloading in subsequent separation steps implying 2-DE and, hence, to improve the possibilities of identifying target proteins. First, excess unbound TrxA35 and weakly associated membrane proteins were removed by centrifugation and the resulting supernatant is hereafter referred to as fraction I (Fig. 10). The elimination of excess TrxA35 at this stage of the procedure also prevents additional disulphide bond formation with targets during solubilisation. The pelleted membranes were washed with a buffer containing 0.75 M NaCl and 0.02% Triton X-100 to further remove peripheral membrane proteins associated by electrostatic and/or hydrophobic interactions and this wash supernatant was referred to as fraction II. Fraction III was obtained by solubilisation of the resuspended membrane pellet with 1.3% dodecylmaltoside (Fig. 10) and fraction IV by extraction of

insoluble proteins from fraction III with 8 M urea.

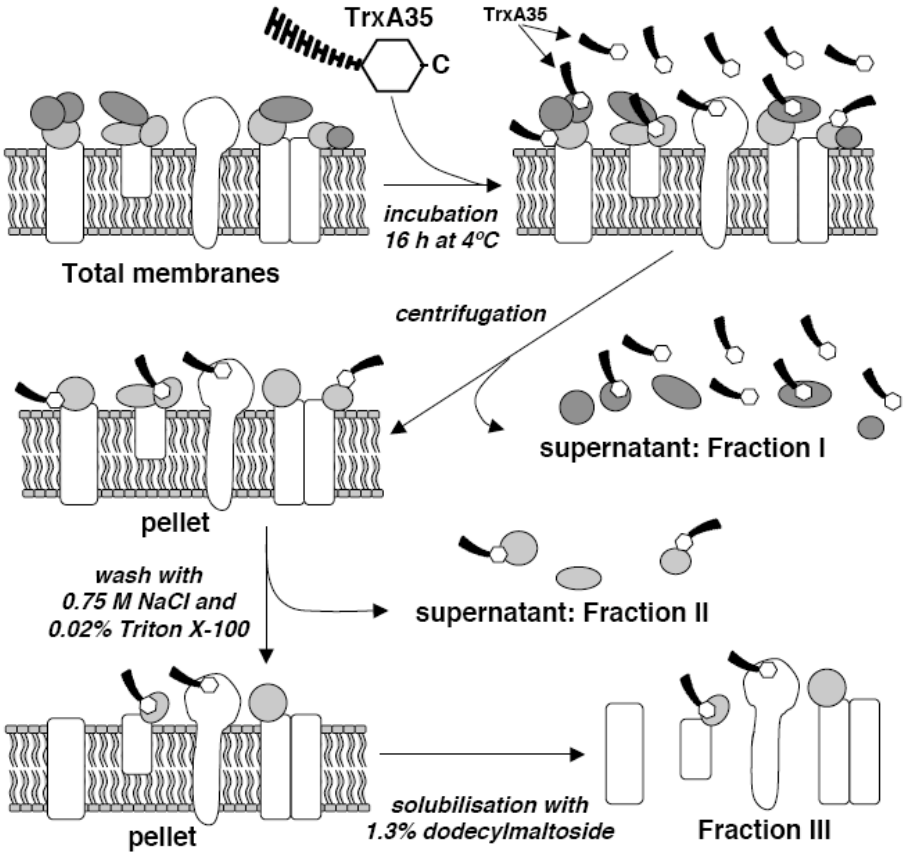

Figure 10. Schematic representation of the procedure for isolation of membrane proteins interacting with thioredoxin. The His_6-tagged recombinant thioredoxin, TrxA35, which carries a Cys-to-Ser mutation in its active site, was incubated for 16 hours with total *Synechocystis* membranes in order to allow disulphide formation *in situ* with its target proteins. Membranes were collected by centrifugation and the supernatant, which contained weakly associated membrane proteins and excess TrxA35, was denoted Fraction I. The membrane pellet was washed with 0.75 M NaCl and 0.02% Triton X-100 and the wash supernatant, which contained membrane-associated proteins, was termed Fraction II. Finally, the membranes, which contained integral and strongly bound peripheral proteins, were solubilised with 1.3% dodecylmaltoside, thus yielding Fraction III. TrxA35-target protein complexes from all fractions were isolated by Ni-affinity chromatography.

Each fraction was subjected to Ni-affinity chromatography in order to isolate the targets covalently bound to the His-tagged thioredoxin used as bait, TrxA35. The 1-DE protein profiles from this chromatographic procedure, including those of the starting material from each fraction (TP for total protein) is shown in Fig. 11A. Large amounts of phycobiliproteins are readily distinguished in the 16–20 kDa region of

fractions I and II, but are essentially removed from fraction III (Fig. 11A). Two of the most abundant proteins of fraction II were identified by PMF and found to be RbcL and the carboxysomal protein (CcmM), both indicating the presence of carboxysomes in this fraction (Fig. 11A). The two most abundant proteins of fraction III were identified as the β-subunit of the ATP synthase and the subunit NrtA of the nitrate/nitrite transporter (Fig. 11A). NrtA is known to be located in the *Synechocystis* plasma membrane (Pisareva *et al.*, 2007), whereas the ATP synthase β-subunit is found in both thylakoids (Srivastava *et al.*, 2005) and plasma membranes of *Synechocystis* sp. PCC 6803 (Huang *et al.*, 2006). Data supporting the identification of these proteins by PMF are provided in Table 2. Finally, TrxA35-target complexes from all fractions were eluted with imidazole and analysed by 1-DE under reducing conditions (Fig. 11A, right panel). The protein profiles suggested differences in target composition between the fractions, as judged by protein migration and intensity of CBB-staining. As expected, the highest amounts of the recombinant TrxA35 were found in the eluate from Ni-affinity chromatography of fraction I, which should contain the major part of excess unbound TrxA35 (Fig. 11A). Western blot analysis using antibodies directed against the known thylakoid proteins D1 of photosystem II and PsaC and PsaD of photosystem I showed that these were present only in fraction III (Fig. 11B), consistent with the assumption that this fraction should contain integral and strongly bound peripheral membrane proteins. In contrast, RbcL was mainly present in fractions I and II with only trace amounts visible in fraction III (Fig. 11B).

Table 2. Proteins indicated in Figure 11A identified by PMF

Fraction	Band [a)]	Protein	ORF [b)]	Mass [c)] exp./theor. (kDa)	Mowse score	Peptides matched	% seq. coverage
II	A	Rubisco large subunit (RbcL)	*slr0009*	55/52.5	138	11	27
II	B	Carboxysomal protein CcmM	*sll1031*	52/56.9	138	12	24
III	C	ATP synthase, β-subunit	*sll1329*	58/51.7	151	14	44
III	D	NrtA	*sll1450*	49/49.2	100	8	22

a) Band, protein band in Figure 11A, b) ORF, open reading frames according to the Cyanobase, c) Mass exp./theor., experimental and theoretical mass values

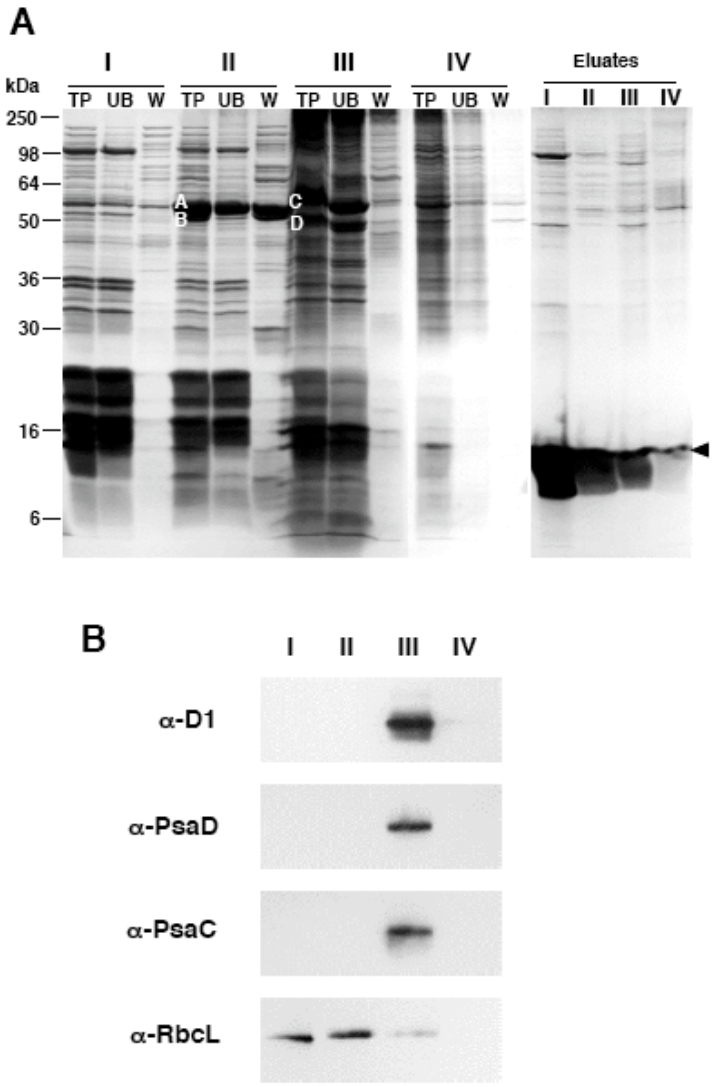

Figure 11. Analysis of 1-DE protein profiles from the process of isolation of *Synechocystis* sp. PCC 6803 membrane proteins interacting with thioredoxin. (A) Proteins were separated by 1-D SDS-PAGE under reducing conditions using 12% acrylamide gels and stained with CBB. For all of the fractions I, II, III and IV, volumes of 20 μl of total protein (TP) prior to chromatography, unbound protein (UB) from the Ni-affinity chromatography and proteins washed off the affinity matrix with 60 mM imidazole (W) were applied. For the eluates obtained by elution with 1 M imidazole, 30 μl were applied per lane following 30 min incubation with 20 mM DTT in order to efficiently break the thioredoxin-target mixed disulphides. The recombinant mutated thioredoxin used as bait, TrxA35, is indicated with a black arrowhead. Two of the most abundant proteins from fraction II (A and B, white letters) and two of the most abundant proteins from fraction III (C and D, white letters) were excised and identified by PMF. The identities were: A, Rubisco large subunit; B, carboxysomal protein CcmM; C, ATP synthase β-subunit; D, Nitrate/nitrite transporter subunit NrtA. **(B)** The presence of known thylakoid proteins in the fractions I, II, III and IV was examined by western blot against the photosystem II D1-protein and against the photosystem I PsaC- and PsaD-proteins. For D1, 4 μg of total protein from each fraction was loaded per lane and the antibody was used at 1:7000 dilution. For PsaC and PsaD, 6 μg of protein was loaded per lane and the antibodies were used at 1:3000 dilution. Signals were detected by enhanced chemiluminescence.

3. Resolution and identification of membrane-associated thioredoxin target proteins

Following the isolation procedure, we proceeded to resolve target proteins on 2-D SDS-PAGE using non-reducing conditions in the first dimension and reducing conditions in the second dimension as described previously (Lindahl and Florencio, 2004). Thus, thioredoxin-target mixed disulphides remained intact in the first dimension and were thereafter broken and the targets were liberated prior to their separation in the second dimension. Consequently, target proteins were more retained in the first dimension than in the second and, therefore, found below the diagonal defined by the molecular mass standard on 2-DE gels (Fig. 12). In most of the cases, the difference in migration between first and second dimensions corresponded to the mass of one TrxA35 molecule (15 kDa). However, in some cases target proteins appeared in several spots and the respective differences in migration suggested that these proteins were able to bind TrxA35 to more than one of their cysteines, as discussed in Pérez-Pérez *et al.* (2006). CBB-stained target proteins from fractions I, II and III were identified by PMF and are listed in Table 3. As a rule, we decided that to count as positively identified, a target should appear in the same fraction in at least two of the three independent experiments of complete isolation procedures performed. Only targets fulfilling this criterion are indicated in Fig. 12 and listed in Table 3. In fact, most of these targets were identified in all three experiments and several of them in more than one fraction. In Table 3, the highest MOWSE scores, sequence coverage and numbers of matched peptides obtained for each target are reported. For fraction IV, few targets were identified and none of them were unique to this fraction (Fig. 12 and Table 3). A total of 50 target proteins were identified (Table 3), 38 of which have previously not been reported as thioredoxin targets in *Synechocystis*. Their molecular masses range from 107 to 15 kDa and the attempts to identify some targets with lower molecular masses than that of the recombinant TrxA35 itself were unsuccessful. Ten of the newly identified *Synechocystis* targets have homologues, which have earlier been reported as thioredoxin targets in other organisms, and the references to the corresponding studies are listed in Table 3 as well as the references corresponding to the identified *Synechocystis* target proteins and their homologues in other organisms, as discussed in Florencio *et al.* 2006.

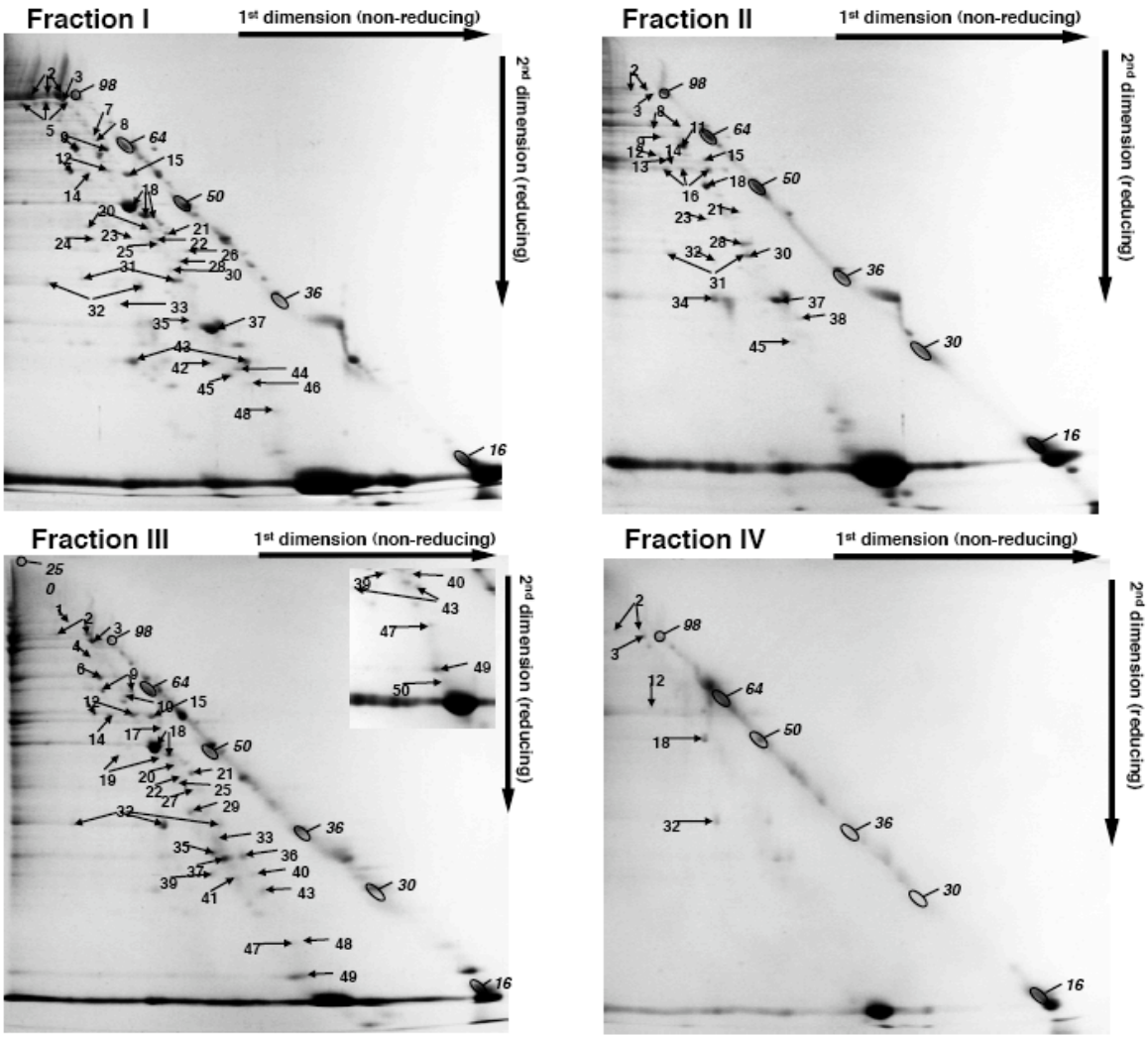

Figure 12. Resolution of membrane-associated thioredoxin target proteins by 2-D SDS-PAGE under non-reducing/reducing conditions. Fraction I was obtained by centrifugation of membranes following a 16-h incubation with the His-tagged mutated thioredoxin TrxA35. Fraction II was obtained by washing the resulting membrane pellet with 0.75 M NaCl and 0.02% Triton X-100. Fraction III was obtained by dodecylmaltoside-solubilisation of salt- and Triton X-100-washed membranes. Fraction IV was obtained by extraction of insoluble proteins from fraction III with 8 M urea. The four fractions were subjected to Ni-affinity chromatography and the thioredoxin-target mixed disulphides were eluted with 1 M imidazole. For the first dimension of 2-D SDS-PAGE 150 µl of each eluate was mixed with 10 µl prestained protein standard and the proteins were separated under non-reducing conditions using 10% acrylamide gel for fraction I and 12% for fractions II, III and IV. The second dimension was performed following reduction of thioredoxin-target mixed disulphides by 100 mM DTT and proteins were stained with CBB. Target proteins, characterised by their migration below the diagonal, were identified by PMF and appear numbered according to Table 3. The spots defining the diagonal corresponding to the pre-stained protein standard are encircled and labelled with the respective molecular masses in kDa with the numbers in italics. The insert corresponding to the fraction III shows part of a 12% acrylamide 2-D gel used to resolve target number 50, which cannot be seen on 10% acrylamide gels.

Table 3. *Synechocystis* sp. PCC 6803 membrane proteins interacting with thioredoxin

No[a)]	Protein	Cys[b)]	ORF[c)]	Fraction	Mass[d)] exp./theor. (kDa)	Mowse score	Peptides matched	% seq. coverage	Ref.[e)]
1	Preprotein translocase SecA*	3	*sll0616*	III	114/106.9	183	30	33	
2	Phycobilisome core-membrane linker polypeptide (L_{CM})	3	*slr0335*	I	101/100.2	173	32	37	A
				II		160	22	37	
				III		163	26	36	
				IV		144	14	14	
3	ClpC*	1	*sll0020*	I	93/91.1	129	15	21	1
				II		93	12	23	
				III		161	23	37	
				IV		139	14	22	
4	ClpB1*	1	*slr1641*	III	87/98.1	78	11	14	1
5	Polyribonucleotide nucleotidyl transferase, α-subunit	3	*sll1043*	I	90/77.9	219	22	35	B
6	FtsH*	1	*slr1604*	III	70/67.2	99	12	18	7
7	Aspartyl-tRNA synthetase*	3	*slr1720*	I	69/67.4	81	7	15	
8	Ferredoxin-sulfite reductase	7	*slr0963*	I	68/71.4	109	18	30	A
				II		161	18	38	
9	60-kDa chaperonin 1 (GroEL 1)	2	*slr2076*	I	62/57.5	183	26	44	A, 1, 2, 4
				II		127	17	37	
				III		175	18	38	
10	Transcription termination factor NusA*	1	*slr0743*	III	61/51.4	105	14	26	
11	Pyruvate dehydrogenase component E2	1	*sll1841*	II	62/44.9	148	18	53	B

12	ATP synthase, α-subunit*	2	*sll1326*	I	58/53.9	140	8	22	2, 4, 7
				II		77	10	28	
				III		109	15	37	
				IV		141	8	22	
13	Rubisco large subunit (RbcL)	11	*slr0009*	II	59/52.5	96	18	37	A, 4
14	ATPase of the AAA-family*	1	*slr0374*	I	57/56.4	140	11	22	
				II		188	26	46	
				III		170	19	40	
15	ATP synthase, β-subunit*	1	*sll1329*	I	58/51.7	235	17	51	2, 3, 7
				II		159	23	63	
				III		161	27	75	
16	Carboxysomal protein CcmM	9	*sll1031*	II	56/56.9	192	24	38	A
17	Type 2 NADH dehydrogenase, NdbC*	6	*sll1484*	III	55/56.8	91	13	37	
18	Elongation factor EF-Tu	1	*sll1099*	I	50/43.8	244	31	72	A, 1, 2, 4
				II		191	27	66	
				III		165	28	62	
				IV		89	8	24	
19	Oxyanion-translocating ATPase, ArsA*	2	*sll0086*	III	49/44.6	124	15	59	
20	Putative GTP-binding protein*	3	*sll0245*	I	46/39.3	144	8	31	6
				III		152	15	42	
21	Urea transporter, ATP-binding subunit (UrtD)*	1	*sll0764*	I	45/41.2	103	9	29	
				II		112	14	44	
				III		94	9	30	

22	RecA*	3	*sll0569*	I	44/37.8	119	10	36	
				III		88	8	28	
23	RNA polymerase, α-subunit*	2	*sll1818*	I	44/35.1	131	6	26	
				II		137	13	40	
24	Phosphoribulokinase	4	*sll1525*	I	44/37.9	89	13	31	B, 1, 4, 5
25	Twitching motility protein PilT*	3	*slr0161*	I	43/40.8	91	6	18	
				III		75	11	34	
26	Glyceraldehyde-3-phosphate dehydrogenase (GAPDH2)	5	*sll1342*	I	42/36.6	132	11	36	B, 1, 8
27	Hypothetical protein*	3	*slr0658*	III	42/37.7	114	14	55	
28	Pyruvate dehydrogenase component E1, α-subunit*	5	*slr1934*	I	38/38.1	231	32	64	2
				II		132	14	34	
29	Nitrate/nitrite transporter, ATP-binding subunit (NrtD)*	3	*sll1453*	III	38/36.5	139	12	48	
30	Pyruvate dehydrogenase component E1, β-subunit*	3	*sll1721*	I	38/35.7	89	12	33	2
31	30S ribosomal protein S2*	3	*sll1260*	I	37/30.1	132	11	39	
				II		95	15	46	
32	Universal stress protein Usp1*	4	*slr0244*	I	36/31.2	96	9	55	
				II		71	6	28	
				III		113	7	34	
				IV		88	7	33	
33	Universal stress protein Usp2*	4	*slr0670*	I	33/32.9	75	4	19	

				III		103	13	66	
34	β-type carbonic anhydrase*	4	*slr1347*	II	32/30.7	98	15	52	1, 5, 6
35	Glutathione-S-transferase*	1	*sll1545*	I	31/29.7	82	6	28	1, 6
				III		148	13	57	
36	Serine-O-acetyl transferase*	3	*slr1348*	III	31/27.5	93	7	30	
37	30S ribosomal protein S3	1	*sll1804*	I	30/27.0	165	17	58	A
				II		108	10	41	
				III		119	16	68	
38	50S ribosomal protein L3*	1	*sll1799*	II	30/22.7	86	10	60	
39	Hypothetical protein*	1	*slr1702*	III	29/27.3	131	11	53	
40	Heme oxygenase 1*	1	*sll1184*	III	29/27.0	79	11	45	
41	Phycobilisome rod-core linker polypeptide (L_{RC})*	1	*sll1471*	III	28/28.5	108	12	50	
42	Response regulator Rre1*	2	*slr1783*	I	27/31.5	129	7	35	
43	1-Cys peroxiredoxin	3	*slr1198*	I	26/23.6	117	10	43	A, 8
				III		75	8	31	
44	Transcription antitermination protein NusG*	1	*sll1742*	I	25/23.5	110	10	51	
45	Hypothetical protein ycf50*	1	*slr2073*	I	25/20.6	86	5	41	
				II		78	6	42	
46	Precorrin isomerase*	2	*slr1467*	I	24/24.7	84	5	31	
47	Acetolactate synthase, small subunit*	1	*sll0065*	III	21/18.9	121	9	61	
48	Phycocyanin β-subunit	3	*sll1577*	I	21/18.1	88	6	47	B
				III		103	9	76	

49	Hypothetical protein*	1	*sll1106*	III	18/18.0	80	8	46
50	Photosystem I protein PsaD*	1	*slr0737*	III	15/15.6	87	5	39

Proteins marked with an asterisk (*) are here identified as thioredoxin targets for the first time in *Synechocystis* sp. PCC 6803.
a) No., spot numbers in Figures 12
b) Cys, number of cysteines in the amino acid sequence
c) ORF, open reading frames according to the Cyanobase
d) Mass exp./theor., experimental and theoretical mass values
e) References to studies, where the thioredoxin-interacting protein has been reported as a thioredoxin target in cyanobacteria: (A) Lindahl and Florencio, 2003; (B) Pérez-Pérez *et al.*, 2006. Or reported in another organism: (1) Balmer *et al.*, 2003; (2) Balmer *et al.*, 2004b (3) Balmer *et al.*, 2006; (4) Lemaire *et al.*, 2004; (5) Marchand *et al.*, 2004; (6) Marchand *et al.*, 2006; (7) Motohashi and Hisabori, 2006; (8) Wong *et al.*, 2003.

The precise locations in *Synechocystis* thylakoid and/or plasma membranes have previously been determined (Srivastava *et al.*, 2005; Pisareva *et al.*, 2007; Huang *et al.*, 2002; Huang *et al.*, 2006) for 18 of the proteins identified as putative thioredoxin targets in the present study. These proteins, their locations and the corresponding references are listed in Table 4. Among the newly identified proteins four were predicted to be integral membrane proteins according to the TMHMM programme (http://www.cbs.dtu.dk/services/TMHMM-2.0). The FtsH protease encoded by the ORF *slr1604* (Fig. 12, spot no. 6) was predicted to have two transmembrane helices between residues 10 and 29 and residues 107 and 129. However, as pointed out by Pisareva *et al.* 2007, the first of these helices may actually correspond to an N-terminal signal peptide. The type 2 NADH dehydrogenase subunit NdbC, the nitrate/nitrite transporter subunit NrtD and the hypothetical protein encoded by the ORF *sll1106* (Fig. 12, spot nos. 17, 29 and 49) were predicted to possess one transmembrane helix each between residues 487–504, 293–315 and 53–75, respectively.

Table 4. Localisation of *Synechocystis* sp. PCC 6803 membrane proteins present in our study

No. [a)]	Protein	ORF [b)]	Location [c)]	Reference [d)]
1	Preprotein translocase SecA*	*sll0616*	TM	Srivastava *et al.*, 2005
2	Phycobilisome core-membrane linker polypeptide (L_{CM})	*slr0335*	PM	Pisareva *et al.*, 2007

3	ClpC*	*sll0020*	TM, PM	Srivastava *et al.*, 2005 Huang *et al.*, 2006
6	FtsH*	*slr1604*	PM	Pisareva *et al.*, 2007
8	Ferredoxin-sulfite reductase	*slr0963*	PM	Pisareva *et al.*, 2007
9	60-kDa chaperonin 1 (GroEL 1)	*slr2076*	TM	Srivastava *et al.*, 2005
12	ATP synthase, α-subunit*	*sll1326*	TM, PM	Srivastava *et al.*, 2005 Huang *et al.* 2002, 2006
13	Rubisco large subunit (RbcL)	*slr0009*	PM	Pisareva *et al.*, 2007
15	ATP synthase, β-subunit*	*sll1329*	TM, PM	Srivastava *et al.*, 2005 Huang *et al.*, 2006
16	Carboxysomal protein CcmM	*sll1031*	PM	Pisareva *et al.*, 2007
17	Type 2 NADH dehydrogenase, NdbC*	*sll1484*	PM	Pisareva *et al.*, 2007
18	Elongation factor EF-Tu	*sll1099*	TM	Srivastava *et al.*, 2005
24	Phosphoribulokinase	*sll1525*	TM	Srivastava *et al.*, 2005
26	Glyceraldehyde-3-phosphate dehydrogenase (GAPDH2)	*sll1342*	TM	Srivastava *et al.*, 2005
28	Pyruvate dehydrogenase component E1, α-subunit*	*slr1934*	TM	Srivastava *et al.*, 2005
41	Phycobilisome rod-core linker polypeptide (L_{RC})*	*sll1471*	TM	Srivastava *et al.*, 2005
48	Phycocyanin β-subunit	*sll1577*	TM, PM	Srivastava *et al.*, 2005 Huang *et al.*, 2006
50	Photosystem I protein PsaD*	*slr0737*	TM, PM	Srivastava *et al.*, 2005 Huang *et al.*, 2002

a) No., spot numbers in Figure 12, b) ORF, open reading frames according to the Cyanobase, c) Location. PM, plasma membrane; TM, thylakoid membrane,
d) References:

Huang F, *et al.* (2002) Proteomics of *Synechocystis* sp. strain PCC 6803. Identification of plasma membrane proteins. Mol Cell Proteomics 1:956-966

Huang F, *et al.* (2006) Proteomic screening of salt-stress-induced changes in plasma membranes of *Synechocystis* sp. strain PCC 6803. Proteomics 6:2733-2745

Pisareva T, *et al.* (2007) Proteomics of *Synechocystis* sp. PCC 6803. Identification of novel integral plasma membrane proteins. FEBS J 274:791-804

Srivastava R, *et al.* (2005) Proteomic studies of the thylakoid membrane of *Synechocystis* sp. PCC 6803. Proteomics 5:4905-4916

A schematic representation of the distribution of targets between the fractions I, II and III (Fig. 13A and Table 3) shows that each fraction contains unique target proteins. This underlines the convenience to fractionate the membranes, as described, prior to separation on 2-DE in order to reduce the number of protein species to be resolved on each gel. One fifth of the thioredoxin targets appeared in all three fractions, generally the most abundant target proteins such as the phycobilisome core-membrane linker (L_{CM}) and the translation elongation factor EF-Tu. Examination of the distribution of all hitherto identified thioredoxin targets in *Synechocystis* sp. PCC 6803 (Lindahl and Florencio, 2003; Pérez-Pérez *et al.*, 2006; and the present study) between the soluble cytosolic fraction and the total membranes reveals, somewhat surprisingly, that the majority of these targets are bound to membranes (Fig. 13B). Almost twice as many unique targets are associated with the membranes as compared to those present exclusively in the cytosol. It should be noted that three of the eight targets found in an extract of peripheral membrane proteins reported in (Lindahl and Florencio, 2003) were not identified in the present study, namely the RNA polymerase subunits β and β' and sulphate adenylyl transferase.

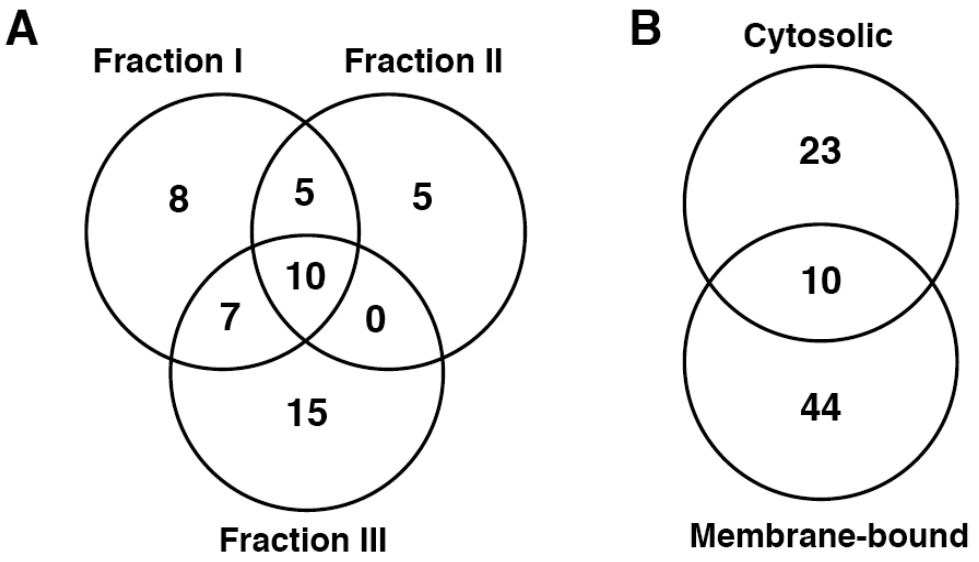

Figure 13. Trx-targets distribution in *Synechocystis.* (A) Distribution of the 50 thioredoxin targets in the present study between the different fractions of *Synechocystis* sp. PCC 6803 membrane proteins. **(B)** Distribution of all 77 *Synechocystis* thioredoxin targets identified to date (Lindahl and Florencio, 2003; Pérez-Pérez *et al.*, 2006 and the present study) between cytosol and membranes.

The presence of the ATP-binding subunits of several transporters, such as SecA, ArsA, UrtD and NrtD (spot nos. 1, 19, 21 and 29), in the thioredoxin membrane target proteome is intriguing and suggests that translocation across membranes could be regulated by means of redox-dependent modulation of the ATPase activities of the respective transporters, which deserves further studies. A closer look at the positions of the cysteines in the sequences of these proteins, which do not share homology, shows that some cysteines are located precisely in the ATPase sequence signatures and, hence, their redox states are likely to affect ATP-binding or ATPase activity. The second of the three cysteines of SecA is located in the ATPase Walker B motif (208-F<u>C</u>IIDEV-213) and two of the three cysteines of NrtD appear in the Walker A motif (52-<u>C</u>IIGHSG<u>C</u>GKS-62) (see Walker *et al.*, 1982 for a definition of these motifs). Another interesting category of membrane associated thioredoxin target proteins belongs to the AAA$^+$- family (ATPases associated with a variety of cellular activities), which constitutes a subfamily of the Walker-type NTPases (Neuwald *et al.*, 1999; Ogura and Wilkinson, 2001). ClpC, a regulatory subunit of the Clp-protease, and ClpB1 (spot nos. 3 and 4) share a single conserved cysteine, which is located in the so-called AAA$^+$ Sensor 1-domain (Neuwald *et al.*, 1999), also known as the motif C (Koonin, 1993). The FtsH protease (Fig. 12, spot no. 6), encoded by the ORF *slr1604*, is known to be integral to the *Synechocystis* sp. PCC 6803 plasma membrane (Pisareva *et al.*, 2007). The single cysteine of this AAA protease appears in the Walker B motif (255-<u>C</u>IVFIDEI-262) and this feature is shared not only with the other *Synechocystis* FtsH proteases, which are present in thylakoid- or plasma membranes in this organism (Srivastava *et al.*, 2005; Pisareva *et al.*, 2007), but also with the plant chloroplast homologues. In some of our experiments, we could also detect tryptic fragments by PMF corresponding to the *Synechocystis* thylakoid FtsH encoded by the ORF *sll1463*, although the MOWSE scores obtained were not high enough to unambiguously ascertain the identity. The FtsH proteases of photosynthetic organisms have recently attracted much attention for their roles in the turnover of the photosystem II D1-protein following light induced damage in cyanobacteria (Silva *et al.*, 2003) as well as in plants (Lindahl *et al.*, 2000; Sakamoto, 2006). A possible redox regulation of their activities could have profound implications for the maintenance of the photosynthetic apparatus and functioning of other membrane associated processes. Interestingly, ClpA (Balmer *et al.*, 2003) as well as two FtsH proteases (Motohashi and Hisabori, 2006) have previously been identified as thioredoxin targets in plant chloroplasts.

Finally, an uncharacterised member of the AAA⁺-family encoded by the ORF *slr0374*, which is present in a stress-responsive operon (Singh and Sherman, 2000; Singh and Sherman, 2002) was identified as a thioredoxin target (Fig. 12, spot no. 14). The only cysteine of this AAA⁺-protein, which is conserved among the cyanobacterial species, is present in the Walker A motif (262-LILGVPGCGKS-272). Common to all of these members of the AAA⁺-family is that they possess one single cysteine in their sequences, which implies that the oxidised state involves an intermolecular disulphide either with another protein or with a low molecular mass thiol compound such as glutathione. Glutathionylation has only recently been considered as a reversible post-translational modification in photosynthetic organisms (Masip *et al.*, 2006; Michelet *et al.*, 2006), whereas this mechanism for regulation is better characterised in mammalian systems. The localisation of the single cysteine within the amino acid sequence of these proteins has been represented in the Figure 14.

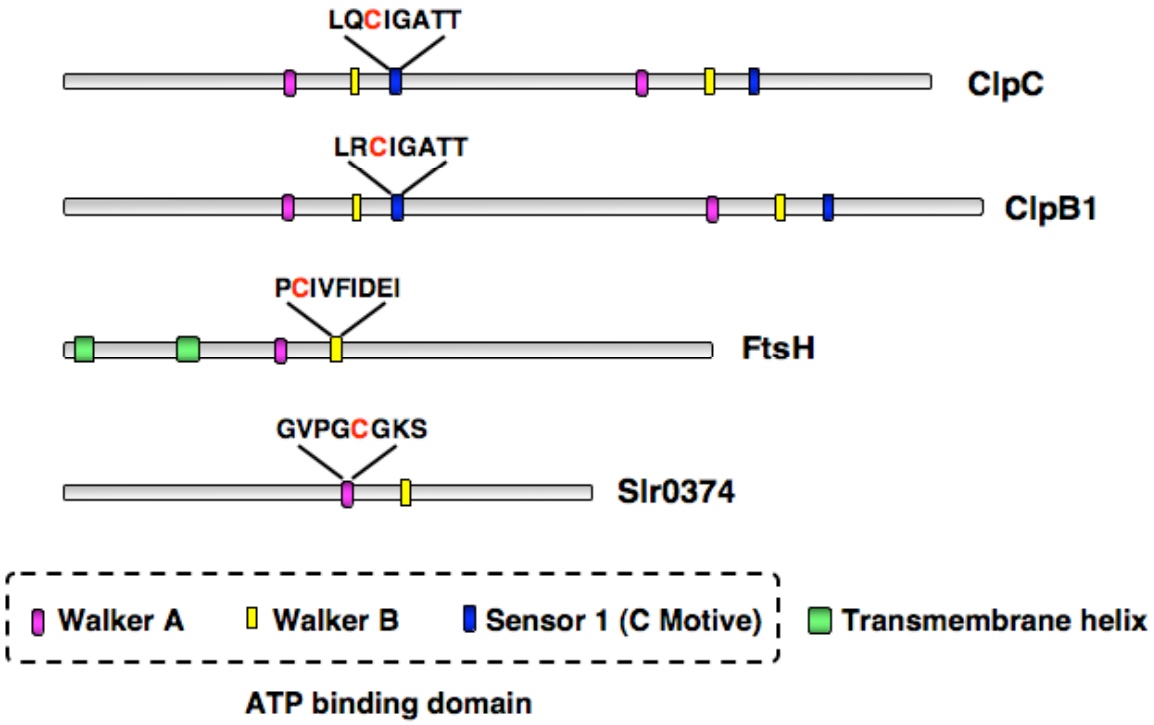

Figure 14. Cysteine localisation within the amino acid sequences of the AAA⁺-protein. The AAA⁺-proteins have been represented including the ATP binding domain and the cysteine residues have been located inside of it. The protein domains have been identified using the engine PROSITE SCAN (http://npsa-pbil.ibcp.fr/cgi-bin/npsa_automat.pl?page=npsa_prosite.html).

Two members of the universal stress protein-family (Usp) (Kvint *et al.*, 2003) were identified amongst the new membrane-associated thioredoxin targets (Fig. 12, spot nos. 32 and 33). The exact function of the Usp-domain is not clear, although it is known to possess autophosphorylating activity and can be found in many proteins from archae, bacteria and plants, either alone, in tandem or as a fusion with other domains (Kvint *et al.*, 2003). In *Escherichia coli*, Usp-expression is induced under various stress conditions such as moderate heat shock, nutrient starvation and exposure to uncouplers (Gustavsson *et al.*, 2002) and deletion of Usp-genes causes hypersensitivity to stress (Nachin *et al.*, 2005). The *Synechocystis* Usp's identified in this study both consist of two Usp-domains in tandem.

Concerning amino acid- and protein metabolism, as was observed previously in other studies (Florencio *et al.*, 2006; Montrichard *et al.*, 2009), a large number of proteins identified as thioredoxin targets were involved in such pathways. Three of them play a role in amino acid metabolism; namely the small subunit of acetolactate synthase, serine-O-acetyl transferase and aspartyl-tRNA synthetase, and have been found to interact with Trx for the first time in the present study. However, several tRNA syntheses have been shown previously to interact with Trx in *Synechocystis*, valyl-tRNA synthase (Lindahl and Florencio, 2004), lysyl-tRNA synthase (Pérez-Pérez *et al.*, 2006); in plants, glycyl-tRNA synthase and seryl-tRNA synthase (Häglund *et al.*, 2008); and in non-photosynthetic prokaryotes, phenylalanyl-tRNA synthase (Liechert and Jakob, 2004), alanyl-tRNA synthase (Liechert *et al.*, 2008) and glutamyl-tRNA synthase (Hochgräfe *et al.*, 2005). We have also found three ribosomal proteins, whereas as many as 30 different ribosomal proteins have been reported in studies of Trx-target proteins in plants (Montrichard *et al.*, 2009). Only the protein 60-kDa chaperonin 1 related with protein folding was identified here, however, diverse chaperones belonging to chloroplast and mitochondria have been reported in plants (Montrichard *et al.*, 2009; Lindahl and Kieselbach, 2009). ClpB, ClpC and FtsH are three proteins with protease activity, which have been defined as Trx target in the present study and previously in plants (Balmer *et al.*, 2003; 2004 and 2006).

Another thioredoxin target worth mentioning is the haeme oxygenase 1 (Fig. 12, spot no. 40), which functions in biosynthesis of open-chain tetrapyrroles (Sugishima *et al.*, 2004), such as phycobilin, utilised for light harvesting and as the

pigment of the phytochrome photoreceptors in cyanobacteria (Lamparter, 2004). Finally, we identified the PsaD subunit of the photosystem I multiprotein complex (Herranen *et al.*, 2004), which participates in the docking of the soluble electron carrier ferredoxin of the photosynthetic electron transport (Sétif *et al.*, 2002).

Following the proteomics assisted screening for Trx-target proteins in membranes we choose to study further the peripheral peroxiredoxins and USP-proteins and the integral FtsH.

4. Interactions of 1-Cys- and 2-Cys peroxiredoxins with TrxA in *Synechocystis*

Peroxiredoxins (Prx) are a ubiquitous group of thiol-dependent peroxidases, which require reduction by electron donors such as Trx, Grx or cyclophilins (König *et al*., 2002; Rouhier *et al*., 2001; Lee *et al*., 2001), though other enzymes have been shown to function as reductants for Prx such as NTRC in plants (Pérez-Ruiz *et al*., 2006) and the flavoprotein AhpF in non-photosynthetic bacteria (Poole, 2005). Based on their phylogeny as well as their catalytic mechanisms, Prx are classified into four groups; 2-Cys Prx, 1-Cys Prx, Type II Prx and PrxQ. The 2-Cys Prx contains two catalytic cysteines in its amino acid sequence, referred to as peroxidatic and resolving cysteines, and is a homodimeric enzyme where the two subunits are linked via a disulphide bond in the oxidised form (Baier and Dietz, 1996; König *et al*., 2002). Type II Prx and PrxQ are atypical 2-Cys Prx, since they possess two catalytic cysteines, but functions as a monomer. PrxQ, which is a homologue of the *E. coli* bacterioferritin comigraing protein (BCP), carries the two cysteines spaced by only four aminoacids and in type II Prx the cysteines are separated by 24 amino acids (Stork *et al*., 2009). The last group is the 1-Cys Prx containing a single conserved catalytic cysteine (Stacy *et al*., 1996; 1999).

The genome of the cyanobacterium *Synechocystis* encodes five Prx, which belong to each of the established groups (Stork *et al*., 2005): 2-Cys Prx (*slr0755*), 1-Cys Prx (*sll1198*), type II Prx (*sll1621*) and two PrxQ, PrxQ1 (*slr0242*) and PrxQ2 (*sll0221*). Different studies in cyanobacteria show that the mutant strains lacking some of these

enzymes are affected in the growth at elevated light intensities (Klughammer et al., 2004; Perelman et al., 2003; Hosoya-Matsuda et al., 2005; Kobayashi et al., 2004; Latifi et al., 2007).

The thioredoxin target proteomics studies in *Synechocystis* have only reported the 1-Cys Prx and type II Prx as putative Trx-interacting peroxiredoxins (Lindahl and Florencio, 2003; Pérez-Pérez *et al*., 2006; Florencio *et al*., 2006). The 2-Cys Prx has never been identified amongst the targets of any thioredoxin in *Synechocystis* and the explanation suggested was that this protein has a hydrophobic domain, which could anchor it to membranes, and hence it would be absent from cytosolic extracts (Pérez-Pérez *et al*., 2006). However, in the proteomic approach here described, in which membrane proteins were analysed, the only Prx found to interact with TrxA was the 1-Cys Prx (Fig. 12 and Table 3). Therefore, aiming at confirming the relationship of 1-Cys Prx with TrxA and searching for a possible interaction of the 2-Cys Prx with this Trx, both peroxiredoxins were expressed in *E. coli* and purified for further studies.

In order to analyse the localisation of 2-Cys Prx in *Synechocystis*, the purified protein was used to raise specific antibodies. Hence, cytosolic and membrane extracts from *Synechocystis* were prepared for western blot analyses of the possible location in membranes of 2-Cys Prx. However, no signal was obtained in the membrane fraction, whereas a strong signal was visualised in the cytosolic fraction (Fig. 15A). Thus, we could discard the anchoring of this peroxiredoxin in membranes and confirm its presence in the cyanobacterial cytosol (Fig. 15A). Since we were unable to detect this protein among the Trx-targets isolated from any cellular compartment resolved in gels and stained with CBB we thought that the protein staining might not be sensitive enough. Therefore, we decided to repeat the Trx-affinity chromatography using cytosolic extracts and to analyse the eluate resolved in non-reducing/reducing 2-D SDS-PAGE gels by means of western blot using the antibody against *Synechocystis* 2-Cys Prx. As shown in Fig. 15B the 2-Cys Prx was indeed present in the eluate and migrated below the diagonal, indicating the formation of the mixed disulphides with the monocysteinic TrxA35. Moreover, the 2-Cys Prx appeared distributed between two bands corresponding to two types of complexes; one in which the Prx bound one molecule of Trx and other in which it bound two molecules of Trx (Fig. 15B). Therefore, we could conclude that 2-Cys Prx was a putative Trx target, although it had

not been discerned in Coomassie gels. This suggested that the level of this protein in the cytosol of *Synechocistis* is low. We carried out an estimation of the 2-Cys Prx present in the *Synechocystis* cytosol by quantitative western blot and could determine a concentration of 0.11±0.02 ng/μg cytosolic protein for this peroxiredoxin. Previously reported concentrations for 1-Cys Prx and type II Prx were 6 ng/μg and 5 ng/μg cytosolic protein, respectively (Hosoya-Matsuda *et al*., 2005). Hence, the 2-Cys Prx is a minor Prx in the *Synechocystis* cell, as compared with the other two peroxiredoxins studied.

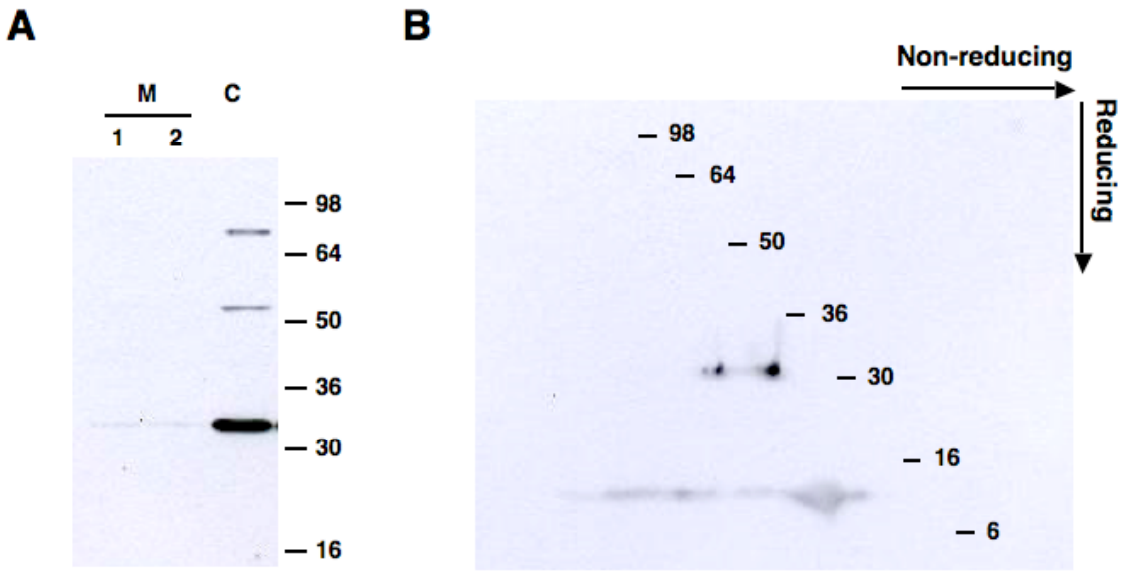

Figure 15. 2-Cys Prx location. (A) Twenty-five *(1)* and 50 *(2)* μg of membrane *(M)* and 15 μg of cytosolic *(C)* franctions from *Synechocystis* were resolved in a 12% acrylamide gel by 1-D SDS-PAGE under reducing conditions. The gel was analysed by western blot using specific antibodies raised against 2-Cys Prx in a dilution of 1:2000. **(B)** The TrxA35-target mixed complexes formed during the incubation of the monocysteinic Trx with the cytosolic protein fraction from *Synechocystis* were purified by nickel affinity chromatography. The putative targets were resolved by 2-D SDS-PAGE under non-reducing/reducing conditions. The gel was analysed by western blot using the antibody against 2-Cys Prx. A weak signal at 15 kDa corresponds to the high amounts of TrxA35 used as a bait cross-reacting slightly.

In order to study the oligomeric state of the 1-Cys Prx and 2-Cys Prx, they were separated in 1-D SDS-PAGE gels under reducing or non-reducing conditions. As expected, 2-Cys Prx migrated mainly as a dimer in the absence of reductant (Fig. 16). This is a result of the disulphide bond formed between the peroxidatic cysteine of a subunit and the resolving cysteine of another subunit during catalysis (Ellis and Poole,

1997). However, various oligomeric forms with a superior molecular weight were showed (Fig. 16), which might be explained as interactions between different dimers of this Prx. High molecular weight complexes have been well characterised in several organisms (Wood *et al*., 2003). Moreover, some of these complexes have been shown to have a chaperone activity in yeast (Jang *et al*., 2004). Under reducing conditions the treatment applied was perhaps not strong enough to reduce all the complexes to the monomeric form. 1-Cys Prx migrated mainly as a dimer and other complexes with a high molecular weight were also shown (Fig. 16). The catalytic mechanism of 1-Cys Prx is still unknown, but the migration under non-reducing conditions indicates that either of its two additional cysteines, apart from the peroxidatic cysteine, may participate in intermolecular disulphide formation (Hosoya-Matsuda *et al*., 2005).

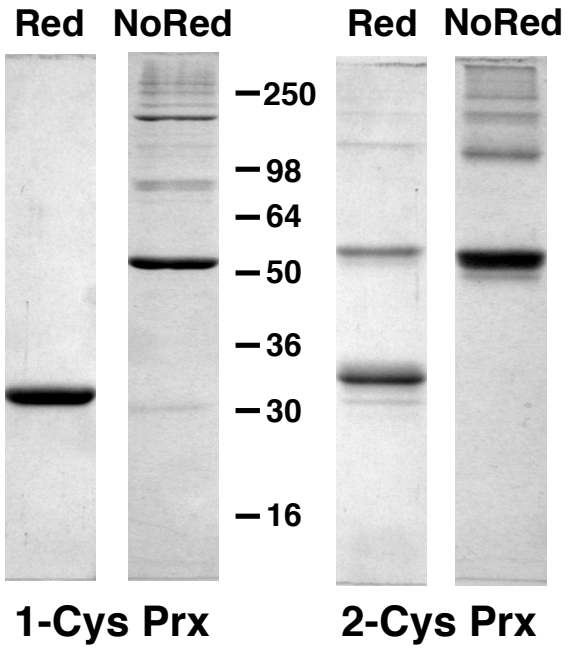

Figure 16. Electrophoretic migration of 2-Cys Prx and 1-Cys Prx. Three μg of each purified peroxiredoxin were resolved in a 12% SDS-PAGE gel under reducing **(Red)**, incubating the sample with a loading buffer containing final concentration of 350μM of 2-mercapto-ethanol, and non-reducing **(No Red)** conditions, using a loading buffer without any reductant.

The ability of 1-Cys Prx and 2-Cys Prx to interact physically with TrxA was analysed through incubation of the purified peroxiredoxin with the monocysteinic TrxA35 followed by electrophoretic separation under non-reducing conditions and western blot using the antibodies against TrxA (Fig. 17). Since TrxA35 also forms

homodimers in the absence of reductant, it was also incubated alone without Prx in order to distinguish the TrxA dimers from the Trx-Prx complexes. The result shows mixed disulphide formation between TrxA and both peroxiredoxins. These complexes were not only dimers, but also appeared as oligomers with a high molecular weight that may correspond to Trx interacting with various Prx molecules linked to each other or the bond formation between two or more Trx *per* Prx. Electrophoresis under reducing conditions abolished completely the complexes. The main bands obtained in the western blot have been referred in the Figure 17 with a letter. The bands signalled as *c* and *f* in the Figure 17 correspond to one molecule of Prx bound to one Trx molecule. The bands marked as *b* and *d* correspond in the western blot to a cross-linked reaction with the highly abundant 2-Cys Prx monomer and dimer respectively. The *a* band could be explained as one molecule of TrxA bound to a 2-Cys Prx dimer, although it could also be two molecules of TrxA bound to a single molecule of 2-Cys Prx. In the case of 1-Cys Prx the band named as *e* probably corresponds to a unique molecule of Prx bound to two molecules of TrxA, indicating the participation of some of the non-peroxidatic cysteines present in its amino acid sequence.

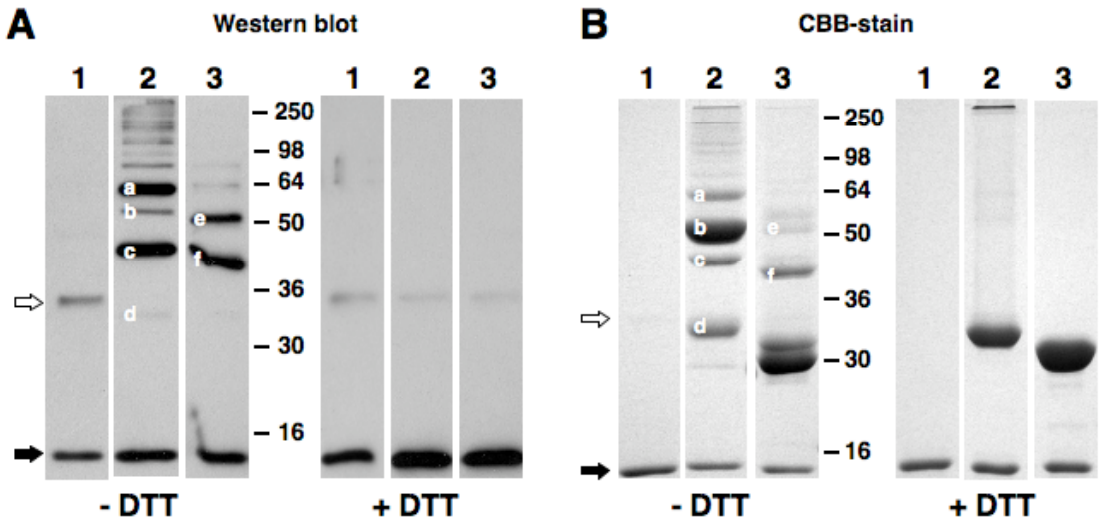

Figure 17. Analysis of the interaction between the peroxiredoxins 2-Cys Prx and 1-Cys Prx with the TrxA. (A) Twenty μg of each peroxiredoxin was incubated with 8 μg of the monocysteinic TrxA35 and a 1/30 dilution of the resulting reaction mixtures was resolved on 12% SDS-PAGE gel under non-reducing (-DTT) and reducing (+DTT) conditions. The thioredoxin was detected by western blotting using specific antibodies raised against TrxA. **(B)** In parallel, the reaction mixtures without dilution were applied on 12% acrylamide gels and stained with CBB. Lanes 1, TrxA35 alone; lanes 2, TrxA35 and 2-Cys Prx; lanes 3, TrxA35 and 1-Cys Prx. The black arrows mark the monomeric TrxA35 and the white arrows mark the TrxA35 homodimer. The main bands resulted in the western blot have been named with a letter from *a* to *f*. The meanings of the bands marked with letters are discussed in the text.

Once confirmed the interaction between these peroxiredoxins and the TrxA, we decided to test whether this interaction involves functional electron transfer. Hence, we analysed the peroxidase activity of the Prxs with wild type TrxA as electron donor. To this end, we incubated 5 μM of each Prx with 4 μM of TrxA reduced with a low (0.2 mM) concentration of DTT, and the reduction of H_2O_2 was monitored by the FOX (ferrous ion oxidation) colorimetric assay (Fig. 18). The DTT alone or together with TrxA did not produce appreciable rates of peroxidase activity (Fig. 18). Both Prx showed peroxidase activity, but the 2-Cys Prx was more efficient in decomposing the peroxide. Thus, this Prx scavenged about 70% of the initial H_2O_2 added (100 μM) in 10 min, whereas the 1-Cys Prx only removed 20% during the same time. After 20 min, the 2-Cys Prx had decomposed all the peroxide, whereas the 1-Cys Prx had scavenged only 30%. The measured activities were 1.7±0.1 nmol H_2O_2/min·nmol Prx for the 2-Cys Prx and 0.4±0.05 nmol H_2O_2/min·nmol Prx for the 1-Cys Prx.

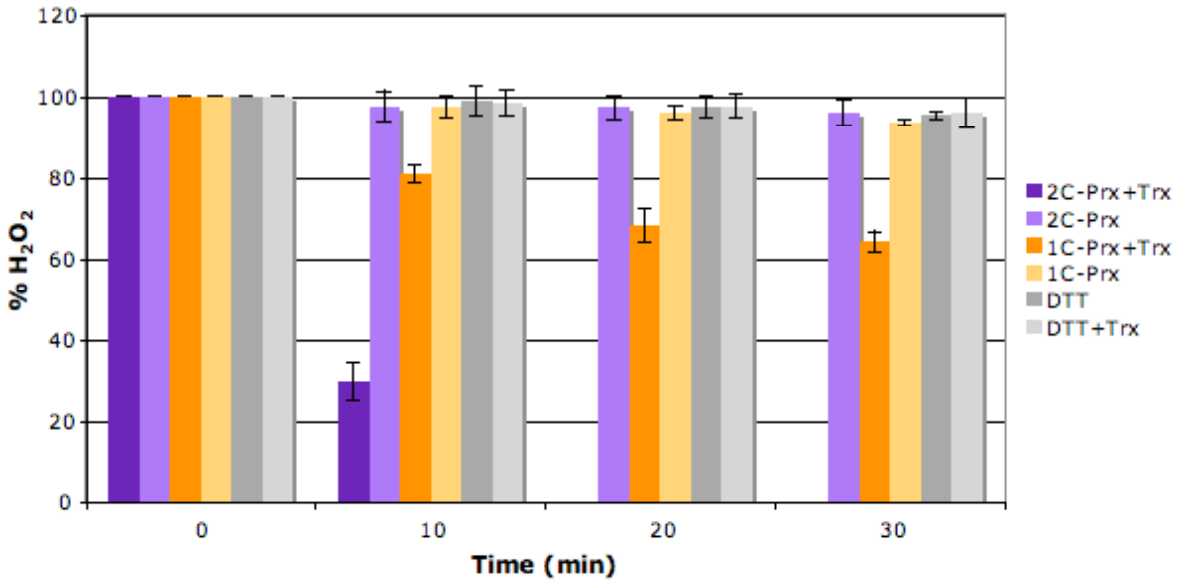

Figure 18. TrxA-dependent peroxidase activity of 2-Cys Prx and 1-Cys Prx. The decomposition of 100 μM H_2O_2 by 5 μM of each purified peroxiredoxin was measure using the FOX assay. The peroxidase activity was analysed in presence of the complete reduction system, 0.2 mM DTT + 4 μM TrxA + 5 μM Prx **(2C-Prx+Trx or 1C-Prx+Trx)**; or lacking the Trx **(2C-Prx or 1C-Prx)**, the Prx **(DTT+Trx)** or both of them **(DTT)**. The remaining H_2O_2 was measured at 0, 10, 20 and 30 min. The error bars represent the standard deviation.

5. The Universal Stress Protein (USP) and its interaction with Trx

Proteins of the Universal Stress Protein (USP) superfamily are present in diverse organisms ranging from archea and bacteria to plants, though they are rare in fungi and absent from animals (Kvint *et al*., 2003). The UspA protein from *E. coli* initially gave the name to the superfamily (Kvint *et al*., 2003) since the levels of this protein become elevated in response to a large variety of stress conditions, including starvation for carbon, nitrogen, phosphate, sulfate, and amino acids and exposure to heat, oxidants, metals, uncouplers of the electron transport chain, polymixin, cycloserine, ethanol and antibiotics (Gustavsson *et al*., 2002; Kvint *et al*., 2003; Nyström and Neidhart, 1994; Nachin *et al*., 2005). Usp-containing organisms are usually equipped with several *usp* genes (Nachin *et al*., 2005). They encode either a small Usp protein (around 14-15 kDa) harbouring one Usp domain, or a larger version (around 30 kDa) consisting of two Usp domains in tandem. There are also large proteins, in which the Usp domain is present together with another functional domain, typically an ion transporter or a Ser/Thr protein kinase (Kvint *et al*., 2003). *E. coli* have five small Usp Proteins and one tandem-type Usp (UspE). They have been divided into four different classes: UspA, UspC and UspD belong to class I, UspF and UspG belong to class II and the two Usp domains of UspE separate into classes III and IV (Kvint *et al*., 2003). UspA is a serine/threonine phosphoprotein with autokinase activity (Freestone *et al*., 1997) and its deletion produces a premature death during stasis (Nyström and Neidhart, 1994), whereas overproduction blocks the cell in a growth-arrested state (Nyström and Neidhart, 1996). Moreover, deletion of class I or class III/IV *usp* genes results in hypersensivity to DNA-damaging agents (Gustavsson *et al*., 2002). However, cells lacking the class II Usp are sensitive to uncouplers but not to DNA-damaging agents (Bochkareva *et al*., 2002), indicating that the functions of the class I and II may be distinct (Nachin *et al*., 2005). Nevertheless, molecular mechanisms for the Usp function in the cell are still undefined.

We discovered two Usp-like proteins amongst the putative targets of TrxA in *Synechocystis* membranes (Fig. 12, Fig. 19 and Table 3). Both Usp proteins migrated in the 2-D SDS-PAGE under non-reducing/reducing conditions distributed between several spots (Fig. 19). The different spots, which appeared below the diagonal corresponded to each Usp protein bound to one or more molecules of TrxA. The spots

resolved above the diagonal corresponded to intramolecular disulphide formation (Fig. 19). These data indicated that Usp's are able to form intra- and intermolecular disulphide bonds. The Usp proteins in cyanobacteria have not been studied, however, cyanobacterial genomes encode homologues of Usp domain-containing proteins (Kvint *et al*., 2003). The two Usp proteins here identified, named Usp1 and Usp2, are encoded by the ORF's *slr0244* and *slr0670*. Both proteins consist of two Usp domains in tandem, and have four cysteines in their amino acid sequences.

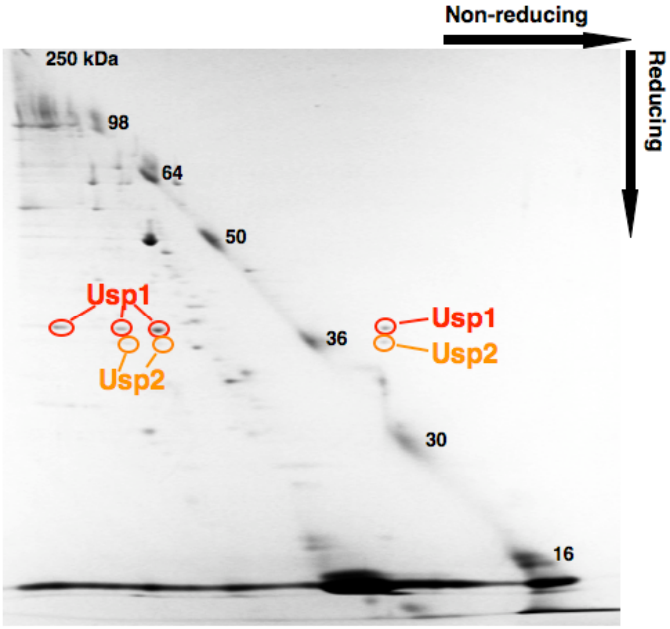

Figure 19. Positions of Usp1 and Usp2 in the 2-D SDS-PAGE under non-reducing/reducing conditions. The Usp proteins identified in the Fraction I of the membrane proteins interacting with TrxA (Fig. 12 and Table 3) have been located in the gel. The spots corresponding to Usp1 (encoded by *slr0244*) are encircled in red and the spots corresponding to Usp2 (encoded by *slr0670*) are encircled in orange.

In order to determine whether the TrxA is able to reduce Usp and whether this protein indeed undergoes redox regulation we expressed Usp1 in *E. coli* for purification.

Firstly, we decided to analyse the redox state of the Usp1 cysteines by observing the migration pattern in acrylamide gels in presence and absence of reducing agents, such as DTT and TrxA (Fig. 20). Under oxidising conditions Usp1 migrated mainly as oligomers with a very high molecular weight, suggesting the capacity of Usp1 to form intermolecular disulphide bonds (Fig. 20). In the absence of

any reductant, a monomeric form that migrated with a lower apparent molecular weight could also be seen, which may be the result of intramolecular disulphide formation (Fig. 20). When a reductant was added, the oligomeric forms disappeared rapidly and the band corresponding to the monomeric form of Usp1 increased. DTT at 2 mM concentration was enough to reduce the Usp1 completely. A fixed concentration of 0.1 mM of DTT was used as an electron donor for TrxA (Fig. 20B), since DTT at this concentration did not reduce much of the Usp1. A graphic representation of the TrxA-dependent increase of the monomeric form of Usp1 is shown (Fig. 20C), clearly showing the positive correlation between TrxA concentration and the monomer of Usp1. Therefore, we concluded that TrxA is a functional electron donor for Usp1 *in vitro*.

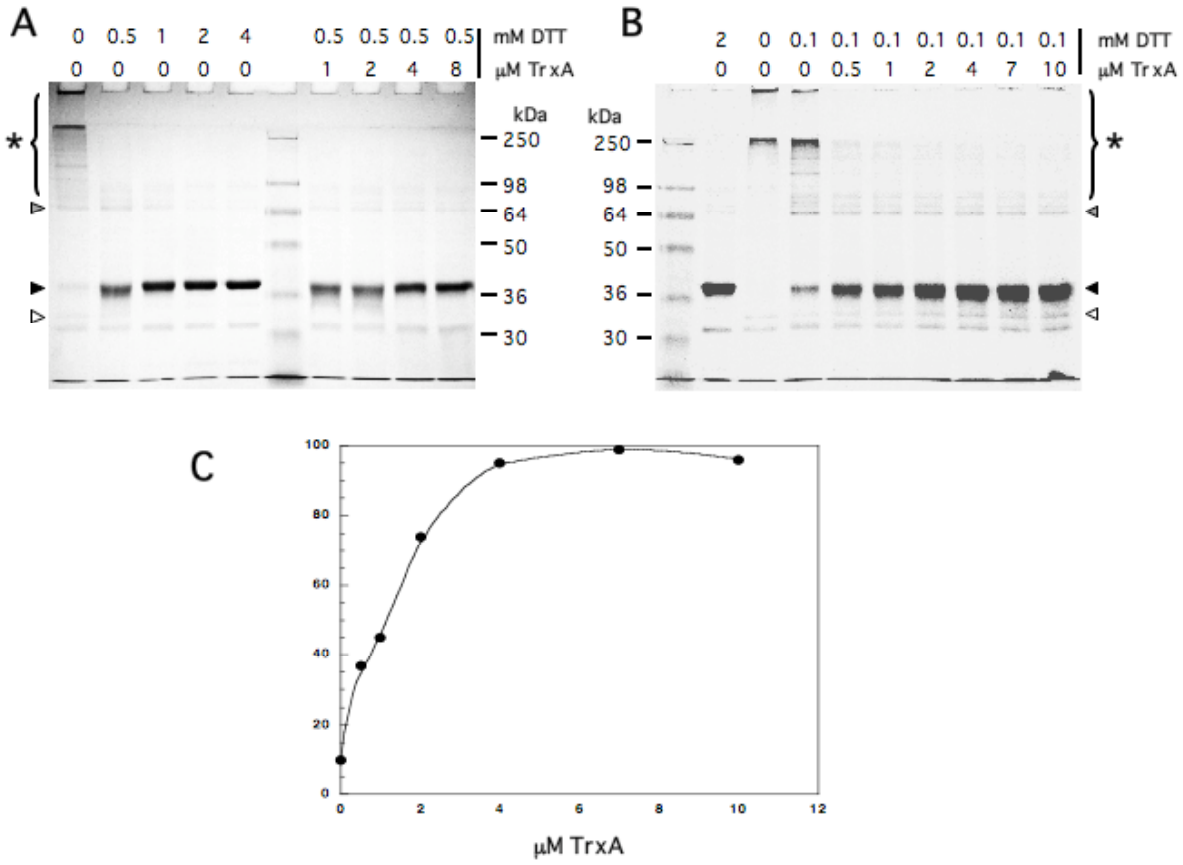

Figure 20. Reduction of Usp1 (*slr0244*) by DTT and TrxA. Three µg of purified Usp1 (*slr0244*) was incubated at 25ºC during 20 min in absence or presence of different reductant (DTT and TrxA). The result of incubation was resolved on 10% acrylamide gels by SDS-PAGE under non-reducing conditions. In **(A)** a gradient concentration of DTT and TrxA was tested, from 0 to 4 mM to DTT and 1 to 8 µM of TrxA with a fixed DTT concentration of 0.5 mM. In **(B)** the gradient concentration of TrxA is repeated from 0 to 10 µM, but the fixed concentration of DTT was 0.1 mM in this case. A control with 2 mM DTT was used. The black arrowhead marks the monomeric form of Usp, whereas the white

arrowhead marks an oxidised form of the monomeric Usp, the grey arrowhead marks the dimeric form of the Usp and the asterisk indicates the Usp at other oligomeric forms. **(C)** Graphic representation of Usp1 monomer apparition by means of TrxA-dependent reduction.

After verifying the capacity of TrxA to reduce the disulphides of Usp1, we wanted to test the reversibility of this kind of reduction, using the thiol oxidising reagents H_2O_2 and copper. Hence, the Usp1 protein was initially pre-reduced with a ten-fold saturating concentration (20 mM) of DTT and after elimination of DTT, the sample was oxidised using different concentrations of the reagents. H_2O_2 as well as Cu^{2+} were able to re-oxidise Usp1 (Fig. 21) as judged by the disappearance of the monomeric form and increase in the oligomeric forms of Usp1 (and the intramolecular disulphide). In the range of concentrations used, H_2O_2 oxidised more efficiently the Usp1 protein than Cu^{2+}. Therefore, the Usp1 cysteines undergo redox modification and are sensitive to treatment with thiol-oxidising agents.

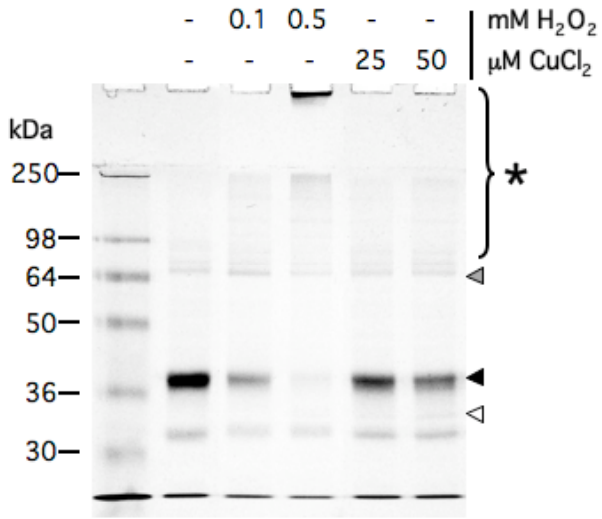

Figure 21. Re-oxidation of Usp1 (*slr0244*) using H_2O_2 and Cu^{2+}. Three µg of Usp were pre-reduced by 30 min incubation on ice with 20 mM DTT and thereafter concentrated and diluted on Vivaspin (cut-off 30 kDa) in 20 mM Tris-HCl (pH 8.0)/0.5 M NaCl until the DTT concentration was about 0.16 mM. Therefore, the reduced sample was re-oxidised at 25°C during 20min using H_2O_2 and $CuCl_2$ at the indicated concentrations and the proteins we resolved by SDS-PAGE in 10% acrylamide gels under non-reducing conditions. The black arrowhead marks the monomeric form of Usp, whereas the white arrowhead marks an oxidised form of the monomeric Usp. The grey arrowhead marks the dimeric form of the Usp and the asterisk indicates the Usp at other oligomeric forms.

Finally, we aimed at finding out if the redox modification of the Usp1 cysteines could alter the activity of this protein, though the precise function of this kind of protein remains unknown. However, autophosphorylation of UspA (Freestone *et al.*, 1997) and UspG (Weber and Jung, 2006) from *E. coli* using radioactively labelled GTP and ATP as phosphate donors has been reported. Hence, we tested whether *Synechocystis* Usp1 undergoes autophosphorylation and, if so, whether the autokinase activity is altered by treatment with a reducing agent. Following incubation of Usp1 with [γ-^{32}P]ATP with and without DTT, the samples were resolved on acrylamide gels under reducing conditions to avoid the formation of oligomers, which could make the interpretation difficult. The CBB stained gel is shown as loading control. The autoradiography of Usp1 samples with DTT at 15 and 30 min time of phosphorylation revealed the inhibition of this activity by disulphide reduction (Fig. 22). Therefore, we can affirm that the autophosphorylation of the Usp1 protein is redox-dependent.

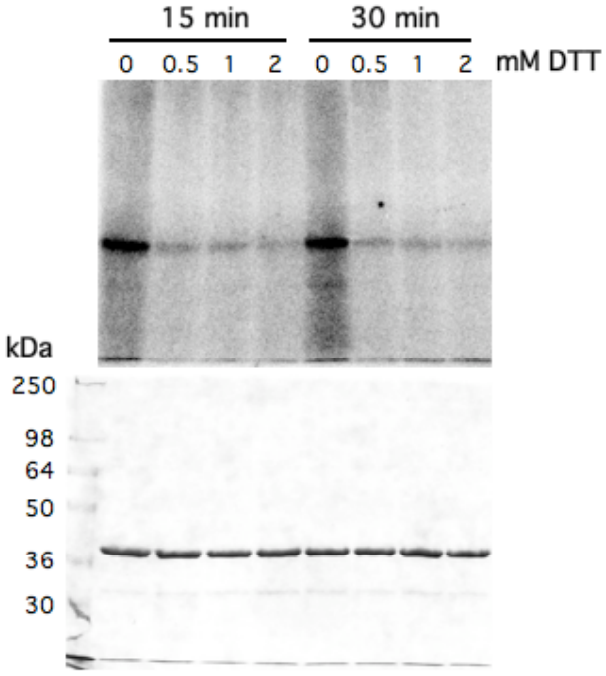

Figure 22. Autophosphorylation of Usp1 (*slr0244*) and the effect of the thiol redox state. The Usp samples were incubated during 20 min at 25ºC with and without of DTT at the indicated concentrations. After that, the autophosphorylation capacity of 3 μg of purified Usp protein in presence of 2 μCi [γ-^{32}P]ATP was tested at 15 and 30 min time of phosphorylation at 25ºC. The resulting samples were resolved on 10% acrylamide gels by SDS-PAGE under reducing conditions and analysed by autoradiography (upper picture) and CBB stain (lower picture).

6. The FtsH protease

A thylakoid homologue of the bacterial FtsH protease (Lindahl *et al*., 1996) was suggested some years ago to play a role in the light-induced turnover of the Photosystem II (PSII) D1 protein, based on studies *in vitro* using isolated PS II complexes and purified *Arabidopsis thaliana* FtsH1 (Lindahl *et al*., 2000). During catalysis PSII splits water to protons and molecular oxygen. An inevitable consequence of its activity associated with electron transfer and oxygen evolution is the production of highly oxidising species, such as tyrosine radicals, chlorophyll cations, and singlet oxygen, which cause irreversible damage to the PSII reaction centre proteins, resulting in loss of photosynthetic activity (Barber and Andersson, 1992; Aro *et al*., 1993). This inactivation process is sometimes referred to as "photoinhibition". As a rule, the higher the light intensity, the more frequent is the photoinhibition. Of all PSII subunits, the reaction centre D1 protein is the most prone to undergo damage and during the PSII repair process it is replaced through partial disassembly, selective proteolysis and insertion of a newly synthesised D1 subunit (Nishiyama *et al*., 2006). FtsH proteases constitute a subgroup of the AAA^+ (for ATPases Associated with a variety of cellular Activities) protein family (Sakamoto, 2006) and have been demonstrated *in vivo* to participate in D1 protein degradation related to PSII repair both in plant chloroplasts (Bailey, *et al*., 2002) and cyanobacteria (Silva *et. al*., 2003; Komenda *et al*., 2006). However, some aspects of this process are still unclear and so far there are no reports on regulation of the FtsH activity.

Four open reading frames (ORF´s) have been found to encode FtsH homologues in the *Synechocystis* sp. PCC 6803 genome. Two of these homologues, encoded by *slr1390* (FtsH1) and *slr1604* (FtsH3), are essential to the organism, whereas elimination of the one encoded by *sll1463* (FtsH4) does not lead to any phenotypic change (Mann *et al*., 2000). In contrast, the *slr0228* (FtsH2) insertion mutant displays an extremely light-sensitive phenotype and dies even at moderate light intensities as a result of impaired D1 protein degradation and failure to perform PS II repair (Nixon *et al*., 2005). Although the phenotypes differ amongst the mutants, the four FtsH are very similar and the percentage of identity between their amino acid sequences range from 48% to 66% and the percentage of similarity from 67% to 80%.

One of the putative membrane targets of TrxA identified here was the FtsH encoded by the ORF *slr1604*. Moreover, our data also indicate that the FtsH encoded by *sll1463* is captured by Trx, though the MOWSE scores obtained were not high enough to unambiguously ascertain identity. All four *Synechocystis* FtsH homologues possess a single cysteine in their amino acid sequences. This cysteine, which is also conserved in plant FtsH homologues, is located in the ATPase Walker B motif, suggesting that its redox state could affect ATP-binding or ATPase activity (Fig. 14). Modification of the redox state of a single regulatory cysteine may involve intermolecular disulphide formation, glutathionylation or oxidation to sulphenic acid, to mention a few examples (Cooper *et al*., 2002).

Aiming at confirming the *in vitro* interaction between the TrxA and the FtsH proteins and to study the putative redox regulation of the FtsH activity we analysed their presence in the eluates from the Trx affinity chromatography. Futhermore, we constructed *Synechocystis* mutant strains lacking FtsH2 and containing a version of FtsH2 in which the cysteine had been substituted by a serine.

Professor Peter J. Nixon kindly provided us with an FtsH antibody that recognises all four *Synechocystis* FtsH proteins. Using this antibody we could confirm the presence of this kind of protease amongst the TrxA35-target complexes purified by Ni-affinity chromatography from total membrane preparations (Fig. 23). Eluted proteins were resolved on a 1-D SDS-PAGE gel under reducing and non-reducing conditions (Fig. 23A). Under reducing conditions a unique band was clearly observed. This band could be composed by one or more isoforms of FtsH, since the four *Synechocystis* FtsH have a similar molecular weight (FtsH1 69.3 kDa, FtsH2 68.5 kDa, FtsH3 67.2 kDa and FtsH4 68.2 kDa). Indeed, in the non-reducing gel, in which the TrxA35 remains attached to its targets, the band corresponding to the FtsH-Trx mixed disulphide are actually two bands that migrate very closely. It may be due to slight differences in migration between the complexes formed by the TrxA35 with the different FtsH's. Moreover, bands corresponding to some oligomeric forms of FtsH were also visualised in the non-reducing gel. The remaining monomeric band of FtsH, which appeared in the non-reducing electrophoresis, could represent non-Trx-interacting FtsH subunits, which form complexes with other FtsH subunits that interact with Trx. In *E. coli* and plants the formation of homooligomers and

heterooligomers between different FtsH subunits have been reported (Akiyama *et al*., 1995; Sakamoto *et al*., 2003; Aluru *et al*., 2006). A heterooligomeric complex formation between FtsH2 and FtsH3 has been suggested in the PSII repair mechanism for *Synechocystis* (Nixon *et al*., 2010). Furthermore, FtsH is known to form supercomplexes with the HflKC in *E. coli* (Saikawa *et al*., 2004) and with the prohibitin complex in yeast (Steglich *et al*., 1999). Hence, it is possible that *Synechocystis* FtsH are forming different types of complexes and that the entire complex might be brought along, although not all subunits form mixed disulphides with TrxA35 (Fig. 23A). We also visualised by western blot using the α-FtsH antibody the FtsH signal in a 2-D SDS-PAGE gel run under non-reducing and reducing conditions (Fig. 23B). The major spot corresponding to FtsH appeared below the diagonal, indicating the *in situ* interaction with TrxA35. Most of the FtsH signal was located in the position where the protein interacts with only one molecule of Trx. This is consistent with the single cysteine present in the amino acid sequence of all four FtsH in *Synechocystis*.

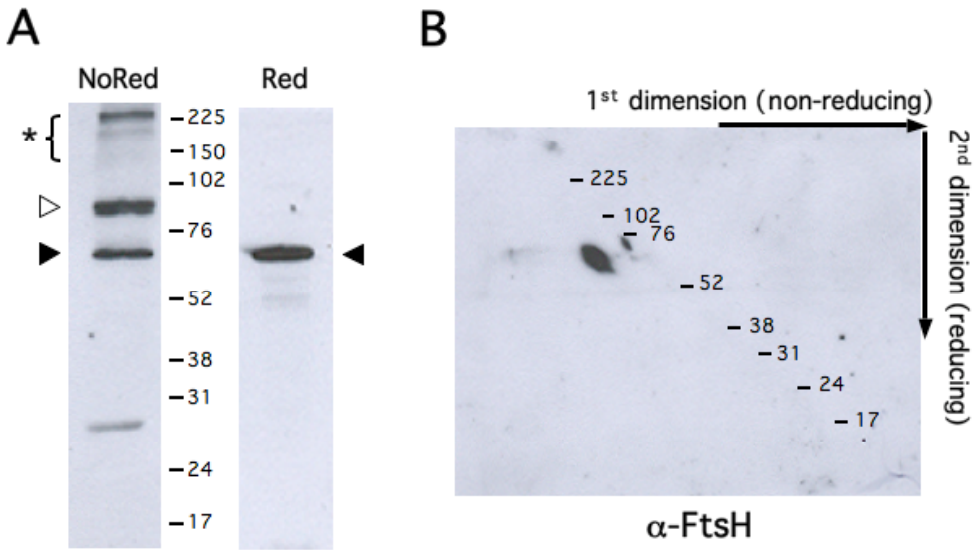

Figure 23. Presence of FtsH in the eluate of Fraction III. Trx-target complexes eluted from the Trx-affinity chromatography of Fraction III (Fig. 11 and 12)were analysed by western blot using antibodies recognises all FtsH from *Synechocystis*. **(A)** Ten µl of the eluate were resolved in a 10% acrylamide gel under non-reducing and reducing conditions. **(B)** The same volume of eluate was analysed by 2-D SDS-PAGE under non-reducing conditions in the first dimension and reducing conditions in the second one. The antibody against FtsH was used in a dilution of 1:5000. The black arrowhead indicates the FtsH band. White arrowhead marks the TrxA35-FtsH complexes. The asterisk point up larger complexes.

In order to elucidate whether the single cysteine plays a role in the regulation of the FtsH activity we proceeded to construct a *Synechocystis* mutant strain in which the FtsH2 is replaced with a FtsH version carrying a cysteine-to-serine substitution. Hence, we could compare the growth of this mutant strain at high light conditions with the WT strain and the mutant lacking the FtsH. It should be noted that only FtsH3 was reported as putative Trx target and we also had some indications about the possible interaction of the FtsH4 with TrxA. However, FtsH3 is essential and the FtsH4 mutant has not a distinct phenotype (Mann *et al*., 2000). FtsH1 is also essential and, hence, the only useful FtsH mutant for comparisons is the strain lacking FtsH2, which is unable to grow under high light conditions (Silva *et al*., 2003). Thus, we selected FtsH2 for construction of site-directed mutants, but firstly we wanted to test the capacity of this FtsH to interact *in situ* with TrxA35. To this end, professor Peter J. Nixon provided us with a *Synechocystis* strain, in which the endogenous FtsH2 was replaced with a protein fusion between FtsH2 and GST. This strain is hereafter referred to as the GST strain. We used a total membrane preparation from the GST strain aiming at reproducing the Trx affinity chromatography in order to probe the specific interaction of GST-FtsH2 with the thioredoxin TrxA35. Therefore, this approach allows us to distinguish the FtsH2 from the other FtsH in an acrylamide gel due to the increase in molecular weight added by the GST moiety. We monitored the presence of FtsH proteins in the different steps of the procedure by western blot using the α-FtsH antibody (Fig. 24A). Thus, we could observe that GST-FtsH2 is indeed present in the eluate, where the putative targets of Trx are. In this fraction were also other kinds of FtsH, present emphasising that FtsH2, as well as some of the other FtsH, are putative targets of Trx in *Synechocystis*. The migration in acrylamide gels under non-reducing and reducing conditions of the Trx-FtsH purified from WT and GST strains were compared (Fig. 24B). Under non-reducing conditions the migration patterns were very similar. A band corresponding to the GST-FtsH2 attached to the TrxA35 could not be seen, though high molecular mass forms seemed to appear in this lane. However, the free GST-FtsH2 band emerged under reducing condition, whereas it did not under non-reducing conditions, indicating a possible mixed disulphide with TrxA35 *in situ*. Thereafter, Trx-targets were resolved in 2-D SDS-PAGE under non-reducing conditions in the first dimension and reducing conditions in the second dimension, and the FtsH signal was analysed by western blot using the α-FtsH antibody as well as an α-GST antibody (Fig. 24C). In both cases the signal is divided in two spots, one of

which is located at the diagonal, corresponding to the non-Trx interacting proteins and the other located below the diagonal indicating the *in situ* interaction with TrxA35. The spot below the diagonal in the α-GST western blot was at the edge of the first dimension gel, suggesting the formation of large complexes containing the GST-FtsH2 fusion under oxidising conditions. Hence, we did not obtain conclusive data about the interaction between TrxA and FtsH2, but the formation of large complexes in the absence of thiol reductant and the presence of the highly conserved cysteine in its amino acid sequence would favour the idea of a possible redox regulation. Eventually, aiming at testing this possible regulation we constructed the FtsH2 knock out mutant strain (ΔFtsH2) and the mutant strain containing FtsH2, in which the cysteine was replaced with a serine, hereafter denoted the FtsH266 strain.

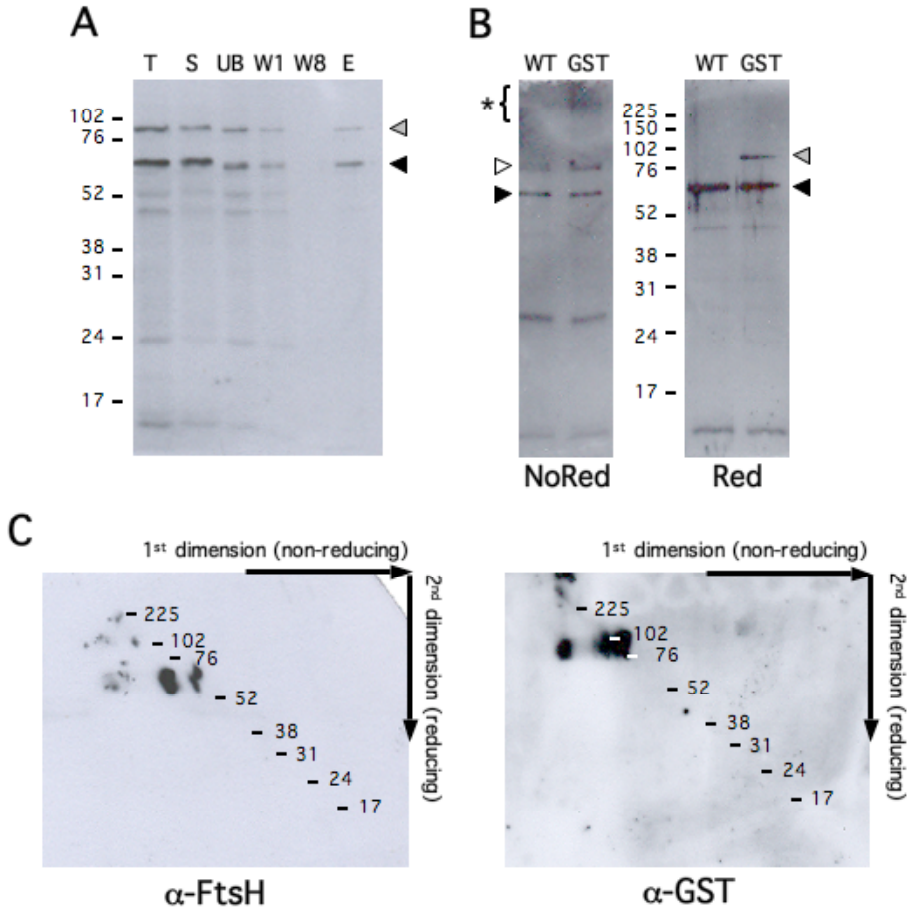

Figure 24. TrxA35 interaction with the GST-FtsH2 fusion. The total membrane thylakoid preparation from the GST strain of *Synechocystis* was subjected to the procedure described in Fig. 10. The presence of the FtsH proteins in the different steps of the purification was monitored by western blot using the antibody that recognises all the *Synechocystis* FtsH in a dilution of 1:5000 **(A)**. Pre-solubilised membranes (T), solubilised membranes (S), unbound proteins to Ni-affinity matrix (UB), the first (W1) and the last (W8) washes with 60mM imidazole, and the eluate obtained by elution with 1M imidazole (E). **(B)** Ten μl of the eluted fraction obtained from the WT and the GST strains resolved in a 1-DE 10% acrylamide gel under non-reducing and reducing conditions and analysed by

western blot using the FtsH antibody. The asterisk indicates high molecular mass forms. Ten µl of the eluate from the GST strain was also analysed by 2-D SDS-PAGE under non-reducing conditions in the first dimension and reducing conditions in the second. The FtsH proteins were visualised by western blot using the FtsH and GST antibodies **(C)**. The dilution used for the FtsH and the GST antibodies were 1:5000 and 1:20000, respectively.

The three strains (WT, ΔFtsH and FtsH266) were grown at 30ºC in BG11C medium under low light conditions (10 $\mu E \cdot m^{-2} \cdot s^{-1}$) and were thereafter transferred to high light (1000 $\mu E \cdot m^{-2} \cdot s^{-1}$) conditions. As expected the ΔFtsH mutant was not able to grow at high light, but the WT and FtsH266 did not show any differences in their growth (Fig. 25). Under high light the thioredoxin receives more electrons from the photosynthesic electron transfer chain and reduces its protein targets. The FtsH protease is also active under these conditions; therefore, the initial hypothesis was the activation of FtsH by Trx under light stress and inactivation under low light or in darkness. Data obtained by thermoluminescence measurements of the PSII activity (data not shown) also revealed the similarity between WT and FtsH266 strains. The C266S-version of FtsH2 would structurally resemble the reduced form of the wild type FtsH2 and, hence, our results support the idea that this corresponds to the active form *in vivo*. Whether the oxidised wild type FtsH2 is inactive remains to be established. Further investigations are necessary to clarify whether this cysteine has an implication in redox regulation.

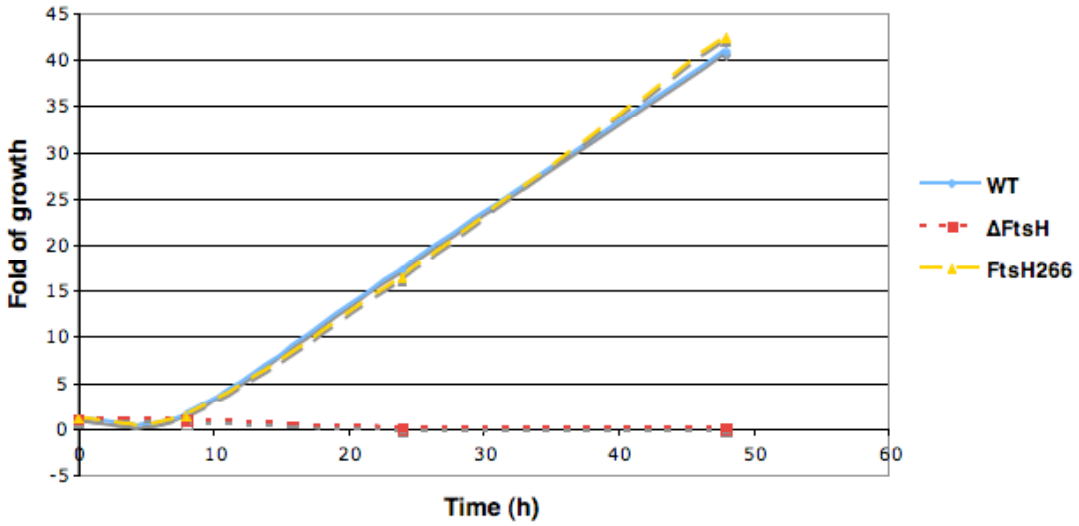

Figure 25. A growth of the *Synechocystis* FtsH mutant strains upon High Light conditions. WT (blue line), ΔFtsH and FtsH266 strains were grown at 30ºC in BG11C medium under high light (1000 $\mu E \cdot m^{-2} \cdot s^{-1}$) conditions and the growth was monitored by measuring the chlorophyll concentration of each strain in several time points.

II- THIOREDOXIN TARGETS IN THE THYLAKOID LUMEN

Introduction

The thylakoid lumen is where the water-splitting occurs and where the protons accumulate to form the thylakoid proton gradient that drives ATP synthesis in oxygenic photosynthesis. Since it is not possible to isolate intact thylakoids from cyanobacteria, the cyanobacterial thylakoid lumen has so far not been characterised. However, it is possible obtain thylakoid membrane preparations (Funk and Vermaas, 1999) and to purify the PSII and PSI multiproteic holocomplex (Tsiotis *et al*., 1995; Bricker *et al.*, 1998) and some luminal proteins have been detected. This is the case of the subunits of the oxygen-evolving complex (OEC), PsbP and PsbQ, which are associated to PSII (Thornton *et al*., 2004; Ishikawa *et al*., 2005). Other luminal proteins have been reported in cyanobacteria (Mulo *et al*., 2008), though their localisation and function have been inferred from plants and green algae.

The chloroplast thylakoid lumen is still a poorly characterised compartment, but obviously better known than the cyanobacterial lumen. Several proteomic studies of the lumen of plant chloroplasts have revealed that the lumenal proteome is composed by a small number of protein families, each represented by several members. The largest families are the PsbP-domain proteins and at least ten different immunophilins are present in the chloroplast lumen of *Arabidopsis thaliana* (Peltier *et al*., 2002; Schubert *et al*., 2002). There are also some luminal proteases, including several of the members of the family of tail-specific proteases such as the D1-processing protease and the D1-processing protease like protein (Schubert *et al*., 2002). Another protein family present in the plant thylakoid lumen is that of the pentapeptide repeat proteins. *Arabidopsis* posseses four genes encoding pentapeptide repeat proteins and two of these are lumenal proteins (Schubert *et al*., 2002). The function of most of the lumenal proteins still remains unknown, but there is evidence that many of them may act as auxiliary proteins involved in the assembly and the proper function of the different components of the photosynthetic machinery (Mulo *et al*., 2008).

In the thylakoid lumen there is a continuous production of ROS derived from the oxygen evolved and side reactions of the photosynthetic electron transport. These ROS must be scavenged to avoid damage to proteins as well as membrane lipids

(Peltier *et al*., 2002). Among the protective mechanisms, the dissipation of excess energy absorbed as heat represents one of the most important photoprotective mechanisms in thylakoid membranes of plants and algae (Jahns *et al*., 2009). Zeaxanthin is a carotenoid that plays a central role in the dissipation of excess excitation energy (nonphotochemical quenching, NPQ) in the antenna of PSII (Demmig *et al*., 1987; Niyogi *et al*., 1998). The violaxanthin deepoxidase (VDE), which is involved in the xanthophyll cycle catalysing the conversion of violaxanthin to zeaxanthin during the NPQ (Jahns *et al*., 2009), has been found in the lumen (Peltier *et al*., 2002; Schubert *et al*., 2002). The TL29 protein is a lumenal protein that sequence homology with the ascorbate peroxidases (APX) and, therefore, was annotated as a putative APX. However none of the analyses performed provided any evidence for a peroxidase activity associated with TL29 (Granlund *et al*., 2009). The only peroxidase found in the chloroplast lumen in plants is the peroxiredoxin Q (PrxQ) (Kieselbach and Schröder, 2003; Petersson *et al*., 2006), which would require a disulphide reductant for its activity.

Apart from PrxQ, another thiol-dependent enzyme localised in the thylakoid lumen of *Arabidopsis*, is the immunophilin FKBP13, which is inactivated *in vitro* by the *E. coli* Trx (Gopalan *et al*., 2004). Moreover, the *in vitro* interaction between the cytoplasmic Trx *h3* and two lumenal proteins, PsbO and the pentapeptide protein TL17 has been reported (Marchand *et al*., 2004; Marchand *et al*., 2006). Despite the evidence for a Trx-dependent redox regulation in the lumen of the chloroplast, no Trx has been found in this compartment. However, HCF164 is a Trx-like protein, which is anchored in the thylakoid membrane with its catalytic domain facing the lumen (Lennartz *et al*., 2001, Motohashi and Hisabori, 2006). HCF164 may be implied in a possible electron transport across the thylakoid membrane from the stroma to the lumen through disulphide-dithiol exchange (Porat *et al*., 2004). Reduction of the lumenal domain of HCF164 via Trx *m*, which is located in the stroma of the chloroplast, has been reported (Motohashi and Hisabori, 2006). A homologue of HCF164, denoted TxlA, has been found in cyanobacteria (Collier and Grossman, 1995). It should be mentioned that, hitherto, no systematic analysis of Trx-targets in the plant thylakoid lumen has been performed.

Given this scenario, we would have liked to search directly for possible targets

of Trx in the thylakoid lumen of *Synechocystis*. Since this is not possible we have nevertheless carried out a study of the soluble lumenal proteins from *Arabidopsis* interacting with TrxA from *Synechocystis* by means of a Trx-affinity chromatography approach. Subsequently, we have looked for proteins in *Synechocystis* homologous to the putative lumenal Trx-targets from *Arabidopsis* and the conserved cysteines in the sequences.

Results and discussion

1. Proteomic identification of putative Trx-targets from the *Arabidopsis* chloroplast lumen

In order to identify putative lumenal targets of Trx we used a Trx affinity chromatography approach as in Lindahl and Florencio, 2003 and 2004, in which the histidine-tagged monocysteinic version of the TrxA of *Synechocystis*, called TrxA35, is immobilised on a nickel affinity matrix. TrxA has been used previously in diverse Trx-targets screenings in cyanobacteria (Lindahl and Florencio, 2003; Lindahl and Florencio, 2004; Pérez-Pérez *et al*., 2006), since this enzyme has been shown to be a highly efficient bait for Trx-target proteins (Pérez-Pérez *et al*., 2006). The lumenal protein extracts from *Arabidopsis* used for the binding assays were provided by Thomas Kieselbach and the proteins able to interact with Trx formed a stable disulfide bond with the immobilised TrxA35. The matrix was washed with a low concentration of imidazole to remove the non-specifically bound proteins. The mixed TrxA35-target complexes were eluted using a high concentration of imidazole. The 1-DE profiles from this procedure are shown in the Figure 26A; the lumenal proteins before application to the column, unbound proteins, the removed proteins in the washing step, and the eluted proteins. A comparison of the lanes corresponding to the lumen fraction and the unbound proteins shows that some proteins are specifically bound to the matrix. The lane corresponding to the eluates displayed more than ten different proteins that potentially interact with TrxA35.

To resolve the lumenal proteins interacting with the Trx, the eluates were subjected to 2-D SDS-PAGE under non-reducing in the first dimension and reducing in

the second dimension as described. The target-TrxA35 mixed disulphide bonds remain intact in the non-reducing dimension, but the targets were released and separated from TrxA35 in the second dimension. Hence, the proteins that interacted with the TrxA35 migrate below the diagonal indicated by the pre-stained standard protein markers (Fig. 24B). The proteins that bind only a molecule of TrxA35 migrate in the first dimension with a shift of approximately 15 kDa. In some cases the shift is higher and may correspond to two or more molecules of Trx bound. This pattern is observed for some lumenal proteins, such as VDE, PrxQ and PsaN. The isolated Trx-target proteins were analysed by MALDI-TOF mass spectrometry and the identifications are presented in the Table 5. The numbers of the spots in Figure 26B correspond to the numbers indicated in the Table 5. As detailed in this table, all identified lumenal Trx-targets contain cysteine residues that are conserved in plants. Five of these lumenal proteins have been identified in other studies, which have examined interactions with Trx: the extrinsic PSII subunits PsbO1 and PsbO2 (Marchand *et al*., 2004; Marchand *et al*., 2006; Balmer *et al*., 2006), PsbP1 (Marchand *et al*., 2006; Balmer *et al*., 2006), the extrinsic PSI protein PsaN (Motohashi and Hisabori, 2006; Balmer *et al*., 2006) and the peroxiredoxin PrxQ (Marchand *et al*., 2006; Motohashi *et al*., 2001).

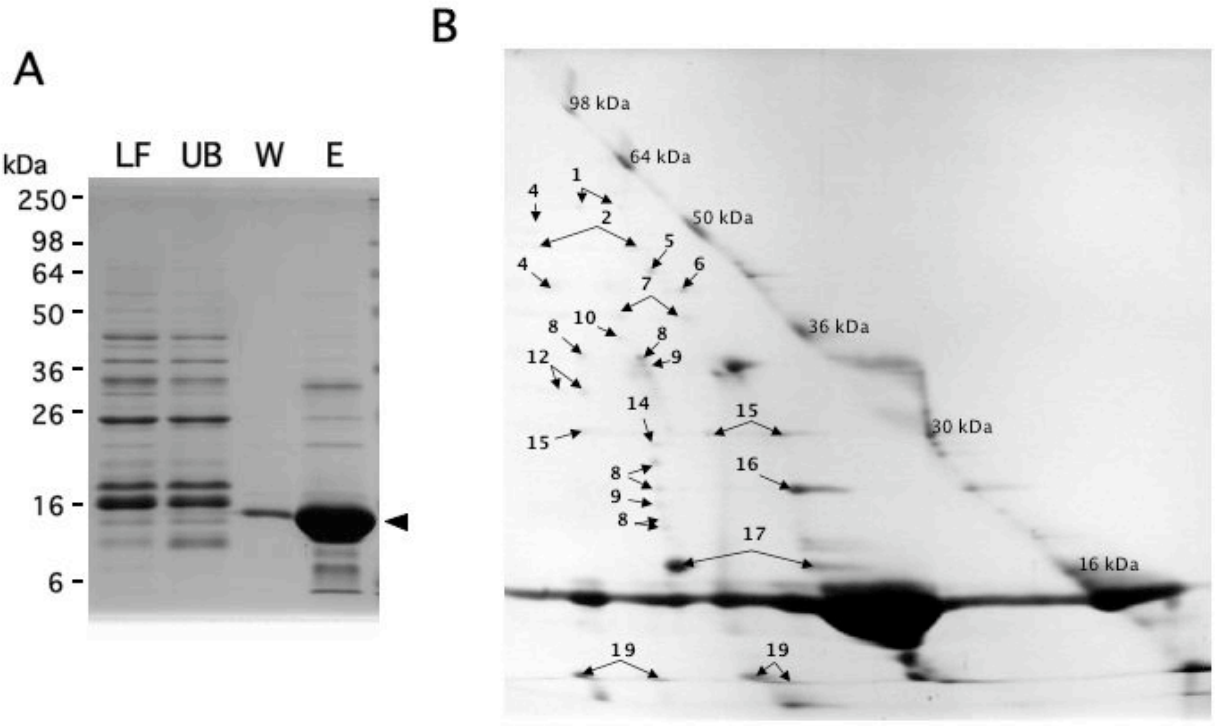

Figure 26. Thylakoid Trx-targets isolation. (A) Protein fractions from Trx affinity chromatography were separated by 1-D SDS-PAGE using a 12% polyacrylamide gel under reducing conditions and stained with CBB. For each fraction 25 μl was applied *per* lane. *LF* (lumenal fraction) corresponds to the total lumenal protein prior to binding to the matrix with the immobilised TrxA35. The *UB* (unbound protein) lane contains the non-retained proteins after the incubation with the TrxA35 matrix. In the lane *W* (wash) is the fraction obtained by washing with 60mM imidazole solution. The *E* (elution) lane corresponds to the eluate following addition of 1 M imidazole. The *black triangle* indicates the TrxA35 used as bait in the chromatography procedure. **(B)** Resolution of Trx lumenal targets derived from the affinity chromatography by 2-D SDS-PAGE under non-reducing/reducing conditions. For the first dimension separation, 150 μl of eluate was mixed with 10 μl SeeBlue pre-stained protein standard markers and the mixed Trx-target complexes were resolved under non-reducing conditions. Lanes were excised, incubated with 100 mM DTT and the target proteins, released from TrxA35, were separated by SDS-PAGE and stained with CBB. Separations in both dimensions were performed using 11% polyacrylamide gels. The target proteins, characterised by their migration below the diagonal, were identified by PMF. The numbers indicate identified spots and correspond to the number of proteins in Table 5. Molecular weights of standard markers are indicated in the diagonal of the gel.

Table 5. Trx targets detected in the lumenal chloroplast of *Arabidopsis*

No[a)]	Protein	Cys [b)]	Gene locus	Mass [c)] (kDa)	Mowse score	Peptides matched	% seq. coverage
1	C-terminal processing protease	5	*At4g17740.2*	54.5/42.6	153	18	47.2
2	Putative C-term. D1 processing	4	*At5g46390.2*	53/46	152	15	31.7
3	RuBisCo (LS)	9	*AtCg00490*	52.9/52.7	197	22	32.4
4	Violaxanthin de-epoxidase	13	*At1g08550.1*	51.9/39.8	141	12	25.8
5	Cyp38	1	*At3g01480.1*	47.9/38.2	202	18	54.8
6	Deg1	1	*At3g27925.1*	46.6/35.2	205	6	16
7	FNR2	6	*At1g20020.1*	41.1/35	95	14	33.9
8	PsbO1	2	*At5g66570*	35.1/26.5	206	17	45.8
9	PsbO2	2	*At3g50820*	35/26.5	156	17	50.8
10	Deg5	2	*At4g18370*	34.9/27	105	10	41.5
11	Plastid lipid associated protein	1	*At3g23400.1*	30.4/22.9	76	10	39.8
12	PIFI	7	*At3g15840*	29.7/Uk	97	5	16
13	FNR1	4	*At5g66190.2*	29.7/Uk	190	7	18

14	20 kDa PbsP protein	2	*At3g56650*	28.6/21.5	153	12	73.3
15	PsbP1	1	*At1g06680*	28/20.2	143	13	66.7
16	TL19	1	*At3g63535*	25/20	247	12	48
17	PrxQ	2	*At3g26060*	23.6/16.5	152	11	77.9
18	PsaN	4	*At5g64040*	19.3/9.7	143	2	22.4

a) No., spot numbers in Figures 26
b) Cys, number of cysteines in the amino acid sequence
c) Mass precursor/mature protein kDa

We performed a search for proteins in the *Synechocystis* genome homologous to the targets found in the lumenal preparation of *Arabidopsis* using the tools of the Cyanobase website (http://genome.kazusa.or.jp/cyanobase/). The results are showed in the Table 6, where we indicate the protein name, the corresponding ORF in the *Synechocystis* genome, the number of cysteines in the protein sequence of *Arabidopsis* conserved in the cyanobacterium, and the number of cysteines in the amino acid sequences in *Synechocystis*. In several cases, there is only one protein in *Synechocystis* corresponding to two or more in the plant, such as the PsbO and PsbP proteins. Only in the case of the protease Deg5 there are two possible homologues in *Synechocystis*, but the protease encoded by the ORF *slr1204* has been detected in the outer membrane of *Synechocystis* (Huang *et al*., 2004). Taken together, there are actually 8 *Synechocystis* proteins for 12 proteins in *Arabidopsis* (Table 6).

The PsbO, PsbP-like protein, PrxQ and one of the two putative homologues to Deg5 have at least one cysteine in their sequences, but only PsbO and PrxQ possess conserved cysteines, when compared with the *Arabidopsis* sequences. None of them have earlier been reported as Trx target in any proteomic study in cyanobaceria. However, the PrxQ peroxiredoxins from *Anabaena* sp. PCC 7120 and *Synechococcus elongatus* PCC 7942 have been showed to have a Trx-dependent peroxidase activity (Cha *et al*., 2007; Stork *et al*., 2009).

Water splitting and oxygen-evolving functions of PSII in plants are supported by a complex of luminal extrinsic proteins: PsbO, PsbP and PsbQ (Debus, 2000). In cyanobacteria, the PsbO protein is present, but PsbP and PsbQ are considered to be

structurally and functionally replaced by PsbU and PsbV (Hankamer *et al*., 2001; Enami *et al*., 2003; Eaton-Rye, 2005). However, in *Synechocystis* a PsbP-like protein has been identified to be a peripheral component of PSII, located at the lumenal side of the thylakoid membrane (Kashino *et al*., 2002) and is suggested to play a possible role in stabilisation of the charge separation in PSII through the interaction with the Mn cluster (Sveshnikov *et al*., 2007). PsbO is the only subunit of the OEC conserved in all organisms that performs oxygenic photosynthesis (Schriek *et al*., 2008). However, PsbO does not seem to be directly involved in the water oxidising reaction, since *ΔpsbO* mutant strains of *Synechocystis* sp. PCC 6803 (Burnap and Sherman, 1991) and *Synechococcus elongatus* PCC 7942 (Bockholt *et al*., 1991) are able to grow photoautotrophically. Diverse functions have been proposed, in which PsbO may be involved, such as maintenance of optimal concentration of Ca^{2+} and Cl^- for the OEC, stabilisation of PSII dimmers (De Las Rivas and Barber, 2004), regulation of D1 degradation (Lundin *et al*., 2007) or, even, a function similar to Trx in *Scenedesmus obliquus* (Heide *et al*., 2004). Although the real function of PsbO has not been determined, redox regulation could make sense in most of the functions proposed, but further investigations are necessary to confirm this hypothesis.

Table 6. *Synechocystis* proteins homologous to the Trx lumenal targets identified in *Arabidopsis*

No[a)]	Protein	ORF [b)]	Cys *A.thaliana* [c)]	Cys *Syn* [d)]	Conserved Cys [e)]
1	C-terminal processing protease	*slr0008*	5		
2	Putative C-term. D1 processing	*slr0008*	4		
5	Cyp38	*sll0408*	1		
6	Deg1	*sll1679*	1		
8	PsbO1	*sll0427*	2	3	2
9	PsbO2	*sll0427*	2	3	2
10	Deg5	*sll1679/slr1204*	2	0/1	
11	Plastid lipid associated protein	*sll1568*	1		
14	20 kDa PbsP protein	*sll1418*	2	1	
15	PsbP1	*sll1418*	1	1	
16	TL19	*sll1418*	1	1	

17	PrxQ	*sll0221*	2	2	1

a) No., spot numbers in Figures 26
b) ORF, open reading frames according to the Cyanobase
c) Cys *A. thaliana*, number of cysteines in the amino acid sequence of *Arabidopsis*
d) Cys *Syn*, number of cysteines in the amino acid sequence of *Synechocystis*
e) Conserved Cys, number of cysteines in the amino acid sequence of *Arabidopsis* conserved in *Synechocystis*

2. The PrxQ2 interaction with TrxA in *Synechocystis*

The peroxiredoxin PrxQ, together with the type II Prx, are called atypical 2-Cys Prx in order to distinguish them from the typical 2-Cys Prx, since they work as monomers in which the catalytic and resolving cysteines form the disulphide within the same polypeptide (Rouhier *et al*., 2004). The plant PrxQ is a lumenal protein (Petersson *et al*., 2006). This type of Prx is absent from animals. In prokaryotes, this enzyme is also named bacterioferritin comigratory protein (BCP). Some bacterial PrxQ isoforms lack the resolving cysteine (Stork *et al*., 2009). *E. coli* possesses a PrxQ, called Tpx. This enzyme has been well characterised (Cha *et al*., 1995; Hall *et al*., 2009) but its location is controversial. Firstly, it was described as a periplasmic protein (Cha *et al*., 1995; Link *et al*., 1997), but a more recent study locates it in the cytosol (Tao, 2008).

The *Synechocystis* genome possesses two ORFs that encode two PrxQ, *slr0242* (PrxQ1) and *sll0221* (PrxQ2). PrxQ2 contains a N-terminal extension that is predicted to be a signal peptide according to Signal P (http://www.cbs.dtu.dk/services/SignalP/). Thus, it could be transported into the thylakoid lumen or into the periplasm. PrxQ2 has been classified belonging to a phylogenetic subgroup of the cyanobacterial PrxQ homologues referred to as the GCT4 subcluster (Cha *et al*., 2007). Our sequence analyses showed that all cyanobacterial homologues from the GCT4 subcluster possess a previously unrecognised putative signal peptide. We have performed a sequence comparison of most of the cyanobacterial PrxQ by multiple alignment and obtained a phylogenetic tree from this alignment (Fig. 28). The alignment and the tree clearly show that all PrxQ with the N-terminal extension group in the same subcluster, in which the *Synechocystis* PrxQ2 is found (Fig. 28). This could indicate the existence of, at least, two PrxQ types, one of

which is composed by cytosolic PrxQ and another composed by PrxQ with a different location in the cyanobacterial cell, which may be in the thylakoid lumen or periplasm.

The *Synechocystis* PrxQ2 was expressed and purified from *E. coli* to study its capacity for *in vitro* interaction with TrxA. The PrxQ2 was expressed without the 34-amino-acid N-terminal extension, which is predicted to be a signal peptide according to the SignalP, version 3.0 (http://www.cbs.dtu.dk/services/SignalP/), and TargetP, version 1.1 (http://www.cbs.dtu.dk/services/TargetP/), programs. We wanted to analyse the oligomeric state of the purified PrxQ2 by means of non-reducing SDS-PAGE electrophoresis conditions (Fig. 27). The comparison of the migration of this protein under reducing and non-reducing electrophoresis shows that PrxQ2 is mainly in the monomeric state, although a weak dimer formation is detected. Under non-reducing conditions the PrxQ2 protein migrates with a lower apparent mass than under reducing conditions, indicating the formation of an internal disulphide bond in the polypeptide sequence (Fig. 27). This is in agreement with the study of Cha *et al.*, 2007, which showed that all four PrxQ from *Anabaena* sp. PCC 7120 form intramolecular disulphides.

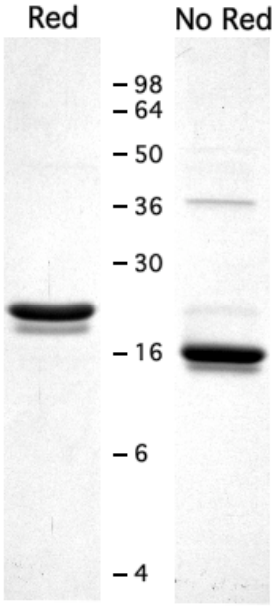

Figure 27. Electrophoretic PrxQ2 gel migration. Three μg of purified PrxQ2 without the signal peptide was resolved in a 15% SDS-PAGE gel under reducing **(Red)**, incubating the sample with a loading buffer containing a final concentration of 350 μM of 2-mercapto-ethanol, and non-reducing **(No Red)** conditions, using a loading buffer without any reductant.

A

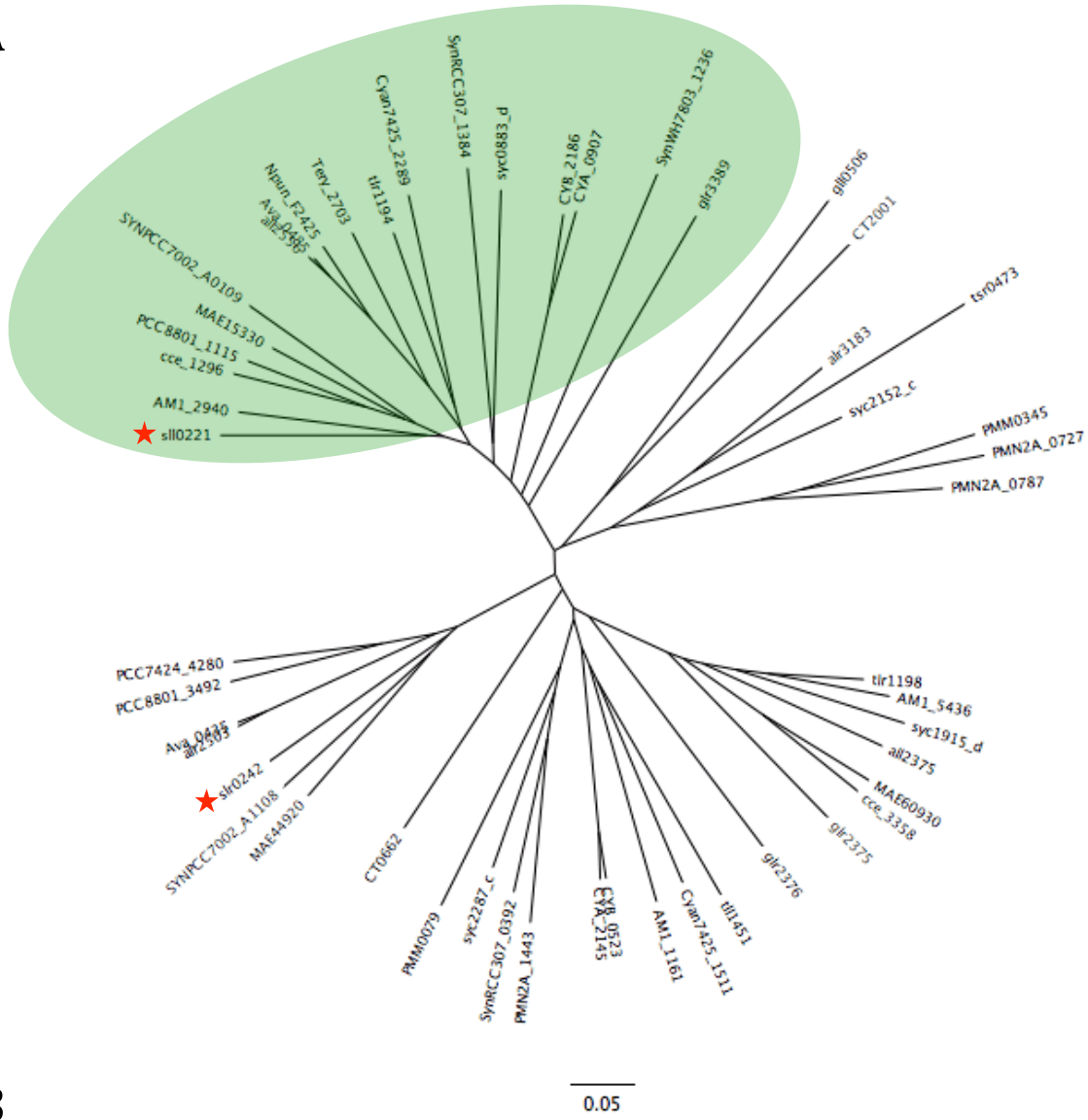

B

```
tlr1198          ----------------------------------------MALAVGTPAPPFTAK--DTQ
AM1_5436         ----------------------------------------MALTAGTAAPAFTTK--DTN
syc1915_d        ----------------------------------------MALTVGTAAPDFTAL--DDA
all2375          ----------------------------------------MPLAVGTDAPAFTVK--DTN
MAE60930         ----------------------------------------MALTVGTIAPNFTTT--DDT
cce_3358         ----------------------------------------MALAVGTVAPDFTTV--DDE
glr2375          ----------------------------------------MALNVGDKAPDFTAK--DTH
tll1451          ----------------------------------------MSLTAGAIAPPFELA--DAT
Cyan7425_1511    ----------------------------------------MTLNPGDSAPDFTLA--DAS
AM1_1161         ----------------------------------------MTLDIGDYAPEFTLP--NAD
CYB_0523         ----------------------------------------MPLAVGDPAPEFTLP--DAE
CYA_2145         ----------------------------------------MALAVGDPAPEFTLP--DAE
PMN2A_1443       ----------------------------------------MTLCIGDSAPDFTLP--NQD
SynRCC307_0392   ----------------------------------------MALQIGDPAPDFTLP--DQD
syc2287_c        ----------------------------------------MPLQVGDRAPDFTLP--DQQ
PMM0079          ----------------------------------------MALKVGDKAPEFNLK--DSF
glr2376          ----------------------------------------MSEPLNVGDPAPEFAAE--QTS
CT0662           ----------------------------------------MALLQAGQKAPEFTAK--DQD
MAE44920         ------------------------------M-----------TLEVGQKAPEFATP--NQR
SYNPCC7002_A1108 ------------------------------MT----------TLTIGQAAPDFALT--NAQ
slr0242          ------------------------------MAT---------ALETNQAPTFSAP--NAE
alr2503          ------------------------------MSN---------IPQAGQPAPDFSTP--DQN
Ava_0435         ------------------------------MSN---------FPQAGQPAPDFSTP--DQN
PCC8801_3492     ------------------------------MSN---------FPKIGEPAPNFAAK--NQK
PCC7424_4280     ------------------------------MSN---------LPQIGEKVPNFTGK--NQE
sll0221          MTSKKFSWPKTIIALLLTLGLWLGLA---DLPTYALGG--IQPELDQPAPLFTLP-STTG
AM1_2940         --MKPLRHHLTRICLVLGLIVSLVMA---APAAFAMGG--DPPPLDQPAPTFTLP-SNTG
cce_1296         ------MLRRQILAILLAIAV-IFSG--TQTPALALGG--PQPPLNESAPNFTLP-TNTG
PCC8801_1115     --MVSIMSRRSLFKWLLALCLTLFSSSFLITPALALGG--TQPPLNEPAPEFTLP-TNSG
MAE15330         ------MSRRQLLSFLIAVILAFFAF---IPDANALGG--PQPPLNQLAPDFTLP-TNTG
SYNPCC7002_A0109 ----MLQFFRTILITVVAIAFMWFPG----EAAIALGG--PQPELNQLAPEFTLL-GNDG
all2556          -----MISRRNFLHILLVSCFAVISWLNLPPTAYALGG--KLPPINQPAPDFTLP-TNTG
Ava_0485         -----MISRRNFLHILLVSCFAVISWLNFAPTAYALGG--KLPAINQPAPDFTLP-TNTG
Npun_F2425       -----MISRRTFLNILFASCISVISWLNFIPAADALGG--KLPAINQPAPEFTLP-TNTG
Tery_2703        -----MRSRRHFQTIFLVICLALITWLNFIPNAWALGG--KLPELDQPAPEFTLP-TNIG
tlr1194          -----MFLR-----SVLVALLSLILFLSPSAPSWALGG--ELPPLNAPADPFSLP-SSVN
Cyan7425_2289    --MSFSFRRR---FLLLACFLSLSLLL-PALPALALGG--DLPPLNQPAPPFALP-TNSG
SynRCC307_1384   ------MRRQEVLKL-LGALPLLALR---PRPAAAMGG--TLPALDQLAPDFDLESAGQT
SynWH7803_1236   ------MNRRQLLQSGLVAAAAITLR---PGKTWALGG--VAPEIGSSAPDFELAGTNLN
syc0883_d        ----MPVSRRQLLLSSLLALPALVLA---PRSAQALGG--PQPPVDEPAPDFSLP----T
CYB_2186         -------------MGLV---VGLLVGFGMTQPAWAQWGTTPLPPIGSPAPEFALP--DQS
CYA_0907         -------------MGLVGLFTALLVSWAGVQPALAQWGTTPLPQIGAPAPEFELP--DQS
glr3389          -------MRKLLLKSSLLFALLLAGP-----QAALLAA----PRVGEAAPAFELP---VA
glr0506          ------------------------------------MAIEVGRPAPDFTLD--GSQ
CT2001           ----------------------------------------MIEEGKIAPDFTLP--DST
alr3183          ----------------------------------------MPVKVGDSAPDFTLP--AQN
tsr0473          --------------------------------------------------------
syc2152_c        ----------------------------------------MAIAVGDVAPDFSLP--AQD
PMM0345          ----------------------------------------MQIGDKVPQFSLL--DQN
PMN2A_0727       ----------------------------------------MKLKVGDQIPSFSLK--DQK
PMN2A_0787       ----------------------------------------MPLKLGDQIPDFSLS--DQL
```

Figure 26. Cyanobacterial PrxQ amino acid sequences comparison. (A) Neighbour Joining Phylogenetic tree. **(B)** Partial sequence alignment of the PrxQ N-terminus. The sequences are from: *Synechocystis* sp. PCC 6803 (Sll0221 and Slr0242), *Anabaena* sp. PCC 7120 (All2375, All2556, Alr3183 and Alr2503), *Anabaena variabilis* (Ava_0485, Ava_0435), *Nostoc punctiforme* (Npun_F2425, Npun_R6477), *Thermosynechococcus elongatus* (Tlr1194, Tll1451, Tsr0473 and Tlr1198), *Gloeobacter violaceus* (Glr2375, Glr3389, Glr2376 and Gll0506), *Microcystis aeruginosa* (MAE15330, MAE44920 and MAE60930), *Prochlorococcus marinus* MED4 (PMM0345 and PMM0079), *Prochlorococcus marinus* str. NATL2A (PMN2A_0787, PMN2A_1443 and PMN2A_0727), *Synechococcus elungatus* PCC 6301 (Syc0883_d, Syc2152_c, Syc1915_d and Syc2287_c), *Synechococcus* sp. PCC 7002 (SYNPCC7002_A0109 and SYNPCC7002_A1108), *Synechococcus* sp. JA-2-3B'a(2-13) (CYB_0523 and CYB_2186), *Synechococcus* sp. JA-3-3Ab (CYA_2145 and CYA_0907), *Synechococcus* sp. RCC307 (SynRCC307_1384 and SynRCC307_0392), *Synechococcus* sp. WH 7803 (SynWH7803_1236), *Chlorobium tepidum* (CT2001 and CT0662), *Acaryochloris marina* (AM1_1161, AM1_5436 and AM1_2940), *Cyanothece* sp. ATCC 51142 (Cce_3358 and Cce_1296), *Cyanothece* sp. PCC 8801 (PCC8801_1115 and PCC8801_3492), *Cyanothece* sp. PCC 7425 (Cyan7425_2289 and Cyan7425_1511), *Cyanothece* sp. PCC 7424 (PCC7424_4280) and *Trichodesmium erythraeum* (Tery_2703). The *Synechocystis* PrxQ sequences are marked with a red star.

In order to verify the interaction between *Synechocystis* PrxQ2 and TrxA suggested by the proteomic study where the lumenal fraction of *Arabidopsis* was used, we incubated *in vitro* the purified PrxQ2 with the monocysteinic TrxA35 and analysed formation of the mixed disulphide complexes. Thereafter, the reaction mixtures were resolved on SDS-PAGE gels under non-reducing and reducing conditions (Fig. 29). The TrxA migration pattern was detected by western blotting using specific antibodies raised against this protein. In the absence of a reductant we could observe that the major part of TrxA remained in the monomeric form, but a minor fraction participates in the formation of TrxA dimers and mixed disulphides with PrxQ2. This demonstrated that TrxA and PrxQ2 could interact physically *in vitro* and suggests that TrxA probably could act as an efficient electron donor for the peroxiredoxin.

We assayed the peroxidase activity of PrxQ2 to test whether it could receive electrons and protons efficiently from TrxA. To this end, 5 μM of peroxiredoxin were incubated with 4 μM of TrxA reduced with a low (0.2 mM) concentration of the reductant DTT, and decomposition of H_2O_2 was measured using the ferrous ion oxidation (FOX) colorimetric assay (Fig. 30). As controls we used DTT alone and the incomplete system lacking Trx or Prx, respectively. None of these controls produced significant rates of H_2O_2 decomposition, however, PrxQ2 showed a clear peroxidase activity in presence of the complete reduction system (TrxA and DTT). After 10 minutes PrxQ2 had decomposed approximately 60% of the initial H_2O_2 (100 μM). The

calculated activity was 1.17±0.04 nmol H_2O_2/(min·nmol Prx). Hence, we conclude that PrxQ2 is a functional thioredoxin-dependent peroxiredoxin.

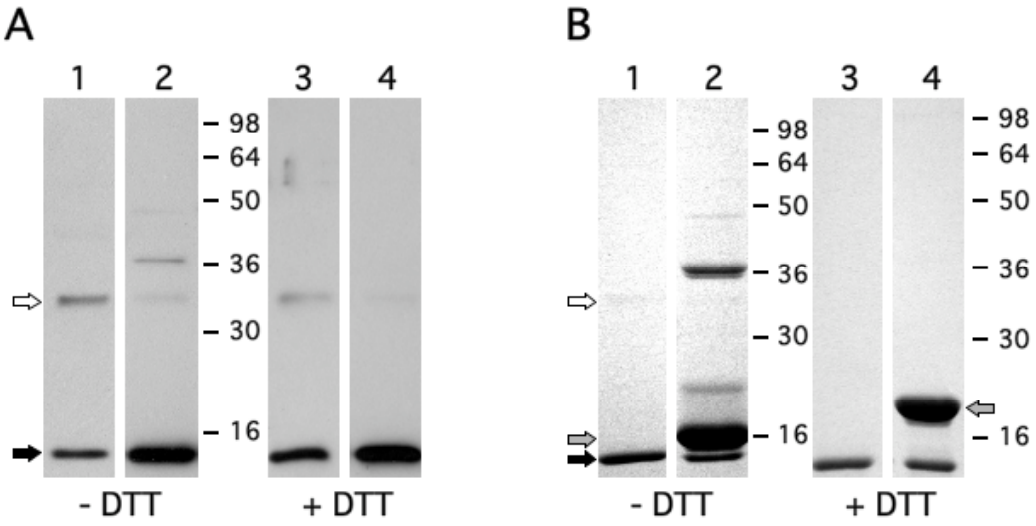

Figure 29. Analysis of the PrxQ2-TrxA interaction. Twenty μg of the PrxQ2 was incubated with 8 μg of the monocysteinic TrxA35 and a 1/30 dilution of the resulting reaction mixture was resolved on 12% SDS-PAGE gel under non-reducing (-DTT) and reducing (+DTT) conditions. The thioredoxin was detected by western blotting using specific antibodies raised against TrxA **(A)**. In parallel, the undiluted reaction mixture was subjected to electrophoresis in an identical gel and stained with CBB **(B)**. Lanes 1 and 3, TrxA alone. Lanes 2 and 4, TrxA incubated with PrxQ2. The black arrows mark the monomeric TrxA35. The white arrows mark the TrxA35 dimer and the grey arrows mark the PrxQ2 monomer.

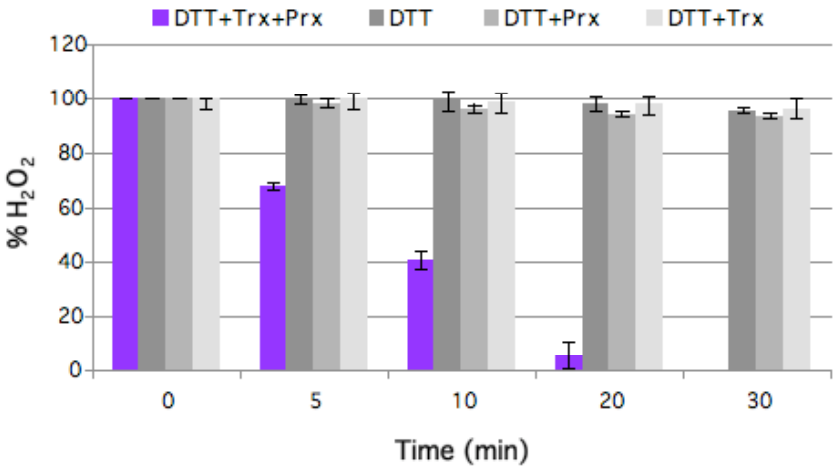

Figure 30. TrxA-dependent peroxidase activity of PrxQ2. The capacity of decomposition of 100 μM H_2O_2 by 5 μM of purified PrxQ2 was measure using the FOX assay. The peroxidase activity was analysed in presence of the complete reduction system, 0.2 mM DTT + 4 μM TrxA + 5 μM Prx **(DTT+Trx+Prx)**; or lacking the Trx **(DTT+Prx)**, the Prx **(DTT+Trx)** or both of them **(DTT)**. The remaining H_2O_2 was measured at 0, 5, 10, 20 and 30 min.

III- THIOREDOXIN-MEDIATED REDOX REGULATION OF A EUKARYOTE TYPE Ser/Thr KINASE IN THE CYANOBACTERIUM *Synechocystis* sp. PCC 6803

Introduction

Protein phosphorylation catalysed by protein kinases is a principal signalling mechanism that allows prokaryotes as well as eukaryotes to transduce extracellular signals and to adapt to changes in the environment. It is involved in the cell response to environmental stimuli by regulating gene expression and enzyme activities. In prokaryotes the predominant mechanism of signal transduction is the two-component system, in which a His kinase transfers a phosphate group to the Asp residue of an associated response regulator (Stock *et al*., 1990). On the other hand, in eukaryotes the cascades of phosphorylation signalling occur at Ser, Thr and Tyr residues and, therefore, Ser/Thr and Tyr kinases play a central role in signal transduction. Hence, protein phosphorylation was considered to have originated independently in prokaryotes and eukaryotes in order to meet their diverse cellular and environmental requirements. However, Ser/Thr kinases have been recently reported to be widespread amongst bacteria and archea (Krupa and Srinivasan, 2005). The first eukaryotic type Ser/Thr kinase in bacteria was identified in the Gram-negative bacterium *Myxococcus xanthus* (Muñoz-Dorado *et al*., 1991). Since then, the emergence of a great number of sequenced bacterial genomes has revealed the presence of Ser/Thr kinases in many other bacteria (Krupa and Srinivasan, 2005). Eventually, about 100 eukaryotic-like Ser/Thr protein kinases have been identified in *M. xanthus* (Kimura *et al*., 2009), suggesting an important role of these proteins in the cellular signalling of bacteria apart from the His kinases. Although Ser/Thr kinases were first discovered in eukaryotes and are more widely distributed amongst them, this type of kinases did not originate in eukaryotes. On the contrary, the presence of an ancestral Ser/Thr kinase prior to the divergence of eukaryotes, prokaryotes and archea during the evolution has been inferred (Leonard *et al*., 1998, Han and Zhang, 2001). The conservation of these sequences in bacterial genomes despite the limitation of their genomic size, during evolution suggests that their functions are essential for regulation of cellular activities (Krupa and Srinivasan, 2005). These kinases have been described to be composed by a kinase domain fused to different domains of diverse nature. The domain structures observed in bacteria are radically different from the ones observed in eukaryotic Ser/Thr kinases. The prokaryotic Ser/Thr kinases have been classified according the domain structures (Krupa and Srinivasan, 2005). The cellular functions of these protein kinasas are not well understood and their domain

organisation have been studied in an attempt to identify their probable biological role (Krupa and Srinivasan, 2005). Thus, there are Ser/Thr kinases with transmembrane domains, glyco-protease domains, peptidoglycan-binding domains, Glu/Gln binding domains, His kinase domains and several more. Most of these second domains are involved the signal transduction processes (Krupa and Srinivasan, 2005; Zhang *et al*., 2007) but there are also some domains with unknown functions, and they include DUF323, RDD and Pentapeptide repeats domains (Zhang *et al*., 2007).

In cyanobacteria the first Ser/Thr kinase was reported in *Anabaena* sp. PCC 7120 (Zhang, 1993). Since, the analysis of a growing number of sequenced cyanobacterial genomes has revealed a wide distribution of these kinases amongst them. The number of Ser/Thr kinase genes in cyanobacterial genomes is a fuction of the genome size, ecophysiology, and physiological properties of the organism (Zhang *et al*., 2007). However, Ser/Thr kinase genes are not ubiquitous in all cyanobacteria and they are completely absent in four *Prochlorococcus* strains and one marine *Synechococcus* WH8102. These cyanobacteria live in oligotrophic open ocean conditions without the need to respond to environmental conditions (Dufresne *et al*., 2005). In contrast, filamentous heterocystous cyanobacteria, which differentiate into heterocysts in response to the absence of combined nitrogen shown a high number of this type of kinase genes (Zhang *et al*., 2007). Fourteen types of additional functional domains have been found in cyanobacteria, which is many more than in other bacteria (Zhang *et al*., 2007). Zhang *et al*., 2007 classified the cyanobacterial Ser/Thr kinases according to structural characteristics into three families. Family I groups the kinases that do not possess any identifiable additional functional domain, apart from transmembrane domains. Family II consists of kinases that contain at least one additional domain but do not contain His kinase domain. Family III is composed by kinases that are also named as dual protein kinases due to they possess both N-terminal Ser/Thr kinase domain and C-terminal His kinase domain.

The *Synechocystis* sp. PCC 6803 genome contains 12 genes for putative eukaryotic-type protein kinase divided into two subfamilies: seven genes for homologues to eukaryotic Pkn2 kinase and five genes for ABC1 (Kaneko *et al*., 1996; Leonard *et al*., 1998). The seven Pkn2 type kinases have been named SpkA (Sll1575), SpkB (Slr1697), SpkC (Slr0599), SpkD (Sll0776), SpkE (Slr1443), SpkF (Slr1225) and

SpkG (Slr0152) (Kamei *et al*., 2001, 2002 and 2003). SpkA, SpkB, SpkC, SpkD and SpkF have been demonstrated to be functionally active protein kinases as they were able to autophosphorylate and phosphorylate artificial substrates (Kamei *et al*., 2001, 2002 and 2003). SpkE resulted to be a non-functional kinase and it was not possible to express SpkG in *E. coli* (Kamei *et al*., 2002). SpkF is a transmembrane kinase (Kamei *et al*., 2002) and amongst these seven Ser/Thr kinases only SpkB and SpkD possess an additional domain (Zhang *et al*., 2007). SpkB contains a pentapeptide repeat domain and SpkD a SH3b domain (Zhang *et al*., 2007). SH3b is a cell wall targeting domain (Lu et al., 2005) and the pentapeptide repeat domain has an unknown function (Zhang *et al*., 2007). Moreover, SpkB and SpkF possess in their N-terminal region a "Cys-motif" formed by four cysteines grouped in two pairs, suggesting a role in redox chemistry (Kamei et al., 2002). SpkA and SpkB have been functionally related to the *Synechocystis* cellular motility, since the respective mutant strains did not display phototactic movement (Kamei *et al*., 2001 and 2003). Moreover, SpkA has been reported to regulate the expression of genes in three operons that are responsible for the pili formation and cell motility in *Synechocsystis* (Panichkin *et al*., 2006).

An example of redox regulation of a Ser/Thr kinase in eukaryotes involves the thylakoid STT7 kinase. STT7 is a chloroplast protein kinase from *Chlamydomonas* responsible for LHCII phosphorylation during state transitions (Depège *et al*., 2003). State transitions are the mechanism by which the light excitation energy is redistributed with PSII or PSI (Bonaventura and Myers, 1969; Murata, 1969). This process involves the reversible association of the antenna complex (LHCII) between PSII and PSI (Allen, 1992). Under high light conditions LCHII dissociates from PSII and associates to PSI (Allen, 1992). The differential association of LHCII is mediated by the redox-dependent phosphorylation of LHCII subunits (Allen, 1992) carried out by STT7 in the chloroplast of *Chlamydomonas* (Depège *et al*., 2003). *Arabidopsis* possess a protein kinase orthologue to STT7 named STN7 (Bellafiore *et al*., 2005). The plants lacking STN7 are deficient in state transition and LHCII phosphorylation (Bellafiore *et al*., 2005). In plants the phosphorylations of LHCII was proposed to be regulated by a network involving redox control both via plastoquinone and the cytochrome *b6f* complex and via the thiol redox state of the chloroplast. Thus, the reduction by the plastoquinone and cytochrome *b6f* complex is necessary to activate the kinase under normal light conditions and it is inactivated by Trx-catalysed reduction under high

light (Rintamäki *et al*., 2000). A different mechanism has been described in cyanobacteria, in which the dephosphorylation of Ser/Thr residues in linker proteins accompanies disassembly of phycobilisomes and their degradation (Piven *et al*., 2005). This process would enable cyanobacteria to acclimatise to high light stress. However, the kinase responsible for this phosphorylation has not been identified. So far, regulation of kinase activity for eukaryotic-type Ser/Thr kinases in prokaryotes has not been described.

Since these types of regulatory proteins are not abundant in the cell, the proteomic approaches used hitherto are not sensitive enough to detect them. Thus, in order to find a possible relationship between redox signalling and protein phosphorylation pathways in cyanobacteria, we decided to analyse the effect of changes in the cysteine redox state on endogenous Ser/Thr kinase activities in *Synechocystis* WT and mutant strains lacking the Pkn2-type Ser/Thr kinases.

Results and discussion

1.Redox dependent protein phosphorylation in *Synechocystis*

In order to search for redox-dependent kinase activities in *Synechocystis,* we compared the protein phosphorylation pattern under different redox conditions. To reduce the complexity of the sample we decided to separate the membranes and soluble fractions. Both fractions were incubated with DTT, a disulphide reducing reagent, and two thiol oxidising reagents, $CuCl_2$ and H_2O_2. The membrane fraction was treated also with DCMU, which blocks the photosynthetic electron flow and is known to inhibit the chloroplast thylakoid protein phosphorylation. The phospho-proteins present in each fraction were radioactively labelled by incubation with 0.5 mM ATP, 5 μCi [γ-^{32}P]ATP and 10 mM NaF, a phosphatase inhibitor. In this kind of assay *de novo* phosphorylated proteins are labelled, however, the basal phosphorylation level is not revealed. The protein extracts were resolved by SDS-PAGE and the phosphorylation pattern was revealed by autoradiography. The result shows that copper treatment causes an inhibition of phosphorylation in the soluble fraction as well as in the membranes fraction (Fig. 31). Inhibition appeared to be more general in membranes,

whereas in the soluble fraction the loss of phosphorylation was specific for a protein, the molecular weight of which was about 90 kDa. Under DTT and H_2O_2 treatments there were no great differences with the exception of the appearance a new phosphorylated protein of about 55 kDa in the soluble fraction in the presence of DTT. Hence, one of the two thiols oxidising agents used displays the inhibition of at least one kinase in the soluble fraction and another one in the membrane fraction.

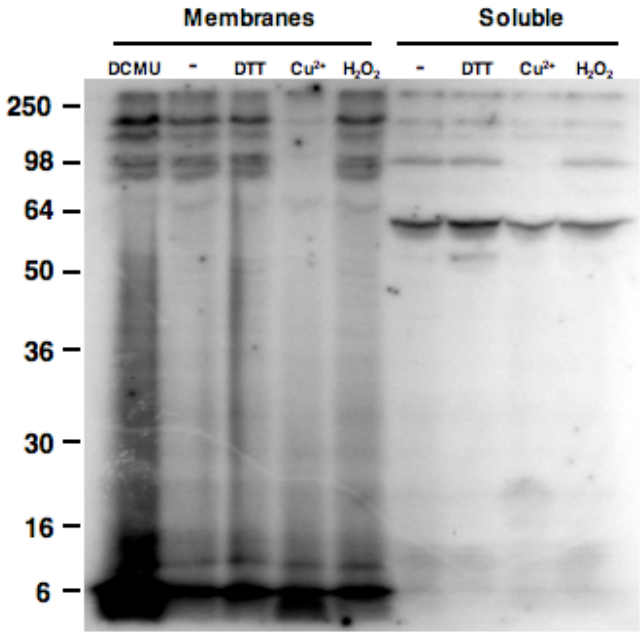

Figure 31. Phosphorylation of *Synechocystis* proteins in separate membranes/soluble fraction. Fifteen μg of chlorophyll of total membrane fraction and soluble fraction corresponding to 20 μg of chlorophyll were pre-incubated 15 min with some additions: 5 mM DTT, 50 μM $CuCl_2$, 0.1 mM H_2O_2 or 20 μM DCMU. After this treatment the samples were incubated for 30 min with 0.5 mM ATP, 5 μCi [γ-^{32}P]ATP and 10 mM NaF in order to label the phospho-proteins present in the fractions. The samples were resolved in a 12% acrylamide gel and the labelled proteins were detected by autoradiography.

Copper is able to catalyse disulphide bond formation and oxidised glutathione (GSSG) is another thiol oxidant that may play the same role and, hence, would reproduce the phosphorylation inhibition observed under $CuCl_2$ treatment. In order to analyse the sensitivity of phosphorylation to both oxidants, we carried out a titration with increasing concentrations of these two reagents (Fig. 32). Thus, we confirmed that copper as well as GSSG changed the phosphorylation pattern, reducing the number of phosphorylated proteins. Unlike the $CuCl_2$ treatment, in which the

phosphorylation of a protein of about 90 kDa disappeared specifically, the effect of GSSG was more general, showing a drastic global inhibition of phosphorylation at 10 mM treatment. However, for lower concentrations of GSSG (2.5 and 5 mM) the specific inhibition of the phosphorylation of a protein with high molecular weight was observed (Fig. 32). In both cases, relatively high concentrations (from 25 μM of $CuCl_2$ and 10 mM of GSSG) were necessary to yield visible effects. Moreover, the $CuCl_2$ produced an increase in labelling of a protein around 22 kDa. No increase in phosphorylation was observed upon GSSG treatment.

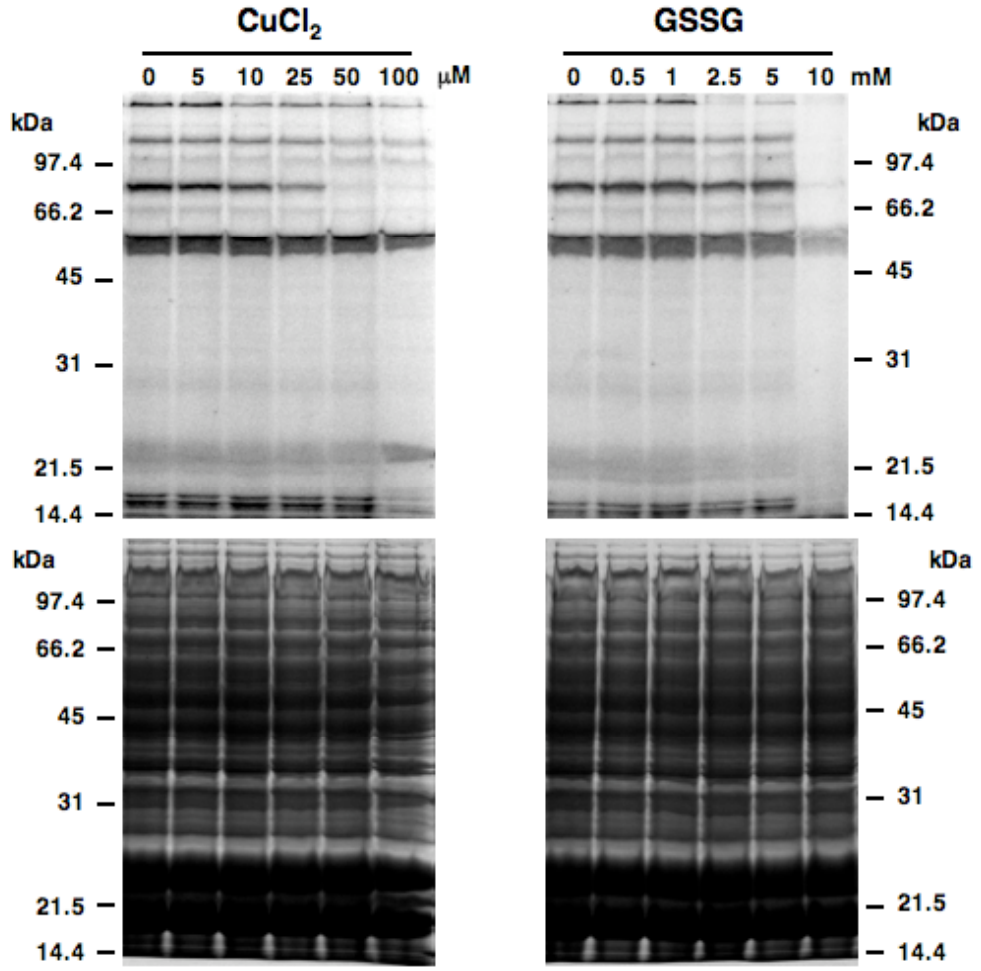

Figure 32. Phosphorylation sensibility to oxidant agents of *Synechocystis* cytosolic proteins. Before radioactive labelling, the *Synechocystis* cytosolic fraction was treated for 15 min with increasing concentrations of the thiol oxidants $CuCl_2$ (from 0 to 100 μM) and GSSG (from 0 to 10 mM). After the treatment the phosphorylation assay was performed incubating the samples with 0.5 mM ATP, 5 μCi [γ-^{32}P]ATP and 10 mM NaF in order to radioactively label the phospho-proteins present in the fractions. The samples were resolved in a 10% acrylamide gel, which was stained with Coomassie (lower panel), and the labelled proteins were detected by autoradiography (upper panel).

Aiming at elucidating the mechanism for redox regulation of the oxidant-sensitive kinase activity present in the *Synechocystis* cytosol, we wanted to test whether a reductant could restore the kinase activity (Fig. 33). Thus, we pre-treated a *Synechocystis* cytosol sample with $CuCl_2$ in order to inhibit the kinase and then, after elimination of Cu^{2+}, treated it with reducing agents, such as GSH (reduced glutathione), DTT and purified TrxA. As a result, DTT and TrxA, but not the GSH, were able to recover the phosphorylation of the 90 kDa protein. Hence, the phosphorylation of this protein depended on a redox-regulated kinase. The next step was to try to identify the kinase, which displayed such activity.

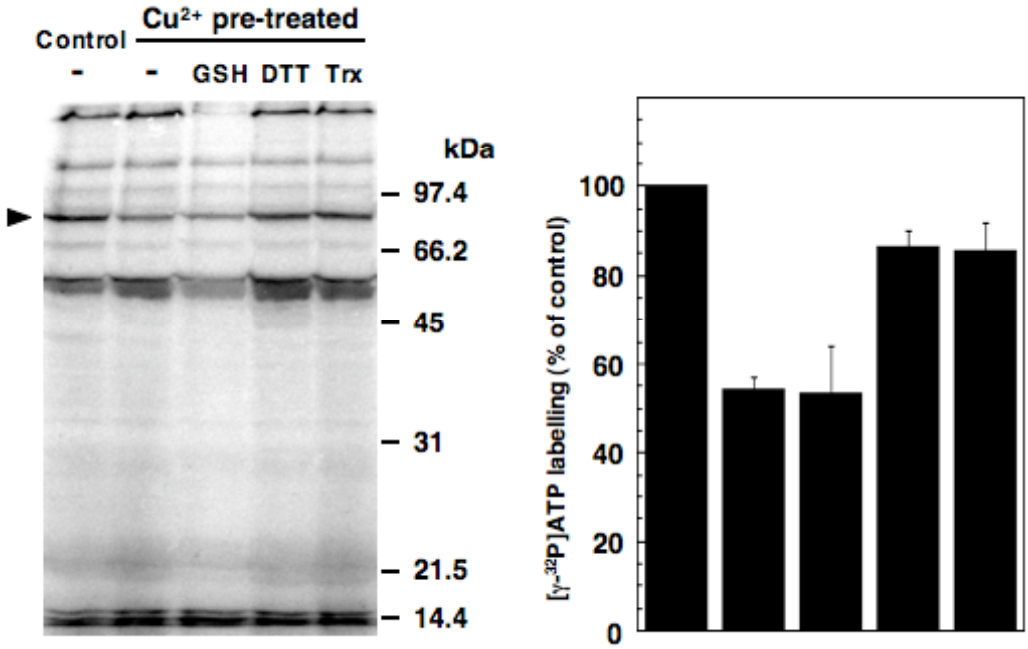

Figure 33. Reactivation of the 90 kDa protein phosphorylation by reductant agents. Cytosolic extracts of *Synechocystis* corresponding to 80 μg of chlorophyll was pre-oxidised for 15 min by 100 μM $CuCl_2$ and then the sample was diluted to 20 μg of chlorophyll and treated for 15 min with some reductant agents: 5 mM GSH, 5 mM DTT or 4 μM TrxA with 0.2 mM DTT. After the treatment the phosphorylation assay was performed incubating the samples with 0.5 mM ATP, 5 μCi [γ-^{32}P]ATP and 10 mM NaF in order to label the phospho-proteins present. The samples were resolved in a 10% acrylamide gel and the labelled proteins were detected by autoradiography (upper panel). A control without oxidising pre-treatment was loaded in the first lane as well as a control with the $CuCl_2$ treatment but without reductant in the second lane. The black arrowhead indicates the 90 kDa protein the phosphorylation of which that is specifically inhibited under oxidising conditions. In the right panel the arithmetic mean of the 90 kDa protein phosphorylation between three independent experiments is shown. 100% of phosphorylation is the one observed in the control lane.

The Two-Component system is the principal signal transduction system in bacteria (Mizuno et al., 1996), and the histidine kinases, which form part of this system, are the most common kinases in these organisms. Despite the main role of the histidine kinases we decided to start searching for Ser/Thr kinases mainly for two reasons. The first reason is that *Synechocystis* includes 44 putative genes for histidine kinases in its chromosome and three more in its plasmids (Murata and Suzuki, 2006), whereas the number of genes for Ser/Thr kinases is much smaller (7 Pkn2 type and 5 ABC1 type). The second reason is that the bond of the phosphoryl group to the histidine residue is more labile than to the serine and threonine (Matthews, 1995), making the histidine kinase phosphorylation more difficult to observe. Therefore, the phosphorylation observed in our experiments more likely corresponds to the Ser/Thr kinase activity in *Synechocystis*. Moreover, the histidine kinases are bifunctional having both kinase and phosphatase activities, and the phosphorylation signal in this transduction system is more transient than in the eukaryotic type (Klumpp and Krieglstein, 2002). The *Synechocystis* mutant strain collection of our laboratory contains the strains lacking each of the Ser/Thr kinases. It allowed us to analyse the soluble protein phosphorylation pattern of all mutants and to compare them with the pattern corresponding to the WT strain under normal, oxidising and reducing conditions (Fig. 34A). All mutants, including the ΔSpkE mutant (not shown), strains exhibited a phosphorylation pattern very similar to that of the WT strain, with the exception of the ΔSpkB mutant. In all cases the 90 kDa protein appeared phosphorylated under normal conditions and unphosphorylated under $CuCl_2$ treatment, but in the ΔSpkB this protein was unphosphorylated under all conditions, suggesting that the SpkB kinase could be responsible for this phosphorylation. It should be taken into account that SpkE was reported not to be a functional kinase (Kamei et al., 2002). With the exception of SpkD all *Synechocystis* Ser/Thr kinases possess in their amino acid sequence one or more cysteines residues, some of which are located in the kinase domain (Fig. 34B). SpkB and SpkF contain a Cys-motif in their N-terminal domain as described in Kamei *et al*., 2002. Thus, the Cys-motif could be related with the redox regulation of SpkB. However, the same Cys-motif is found in SpkF but no cytosolic phosphoproteins were missing in ΔSpkF. This might be explained by the presence of four transmembrane helix domains in its C-terminus, which should anchor it to the membrane and, hence it would be absent in the soluble protein preparations.

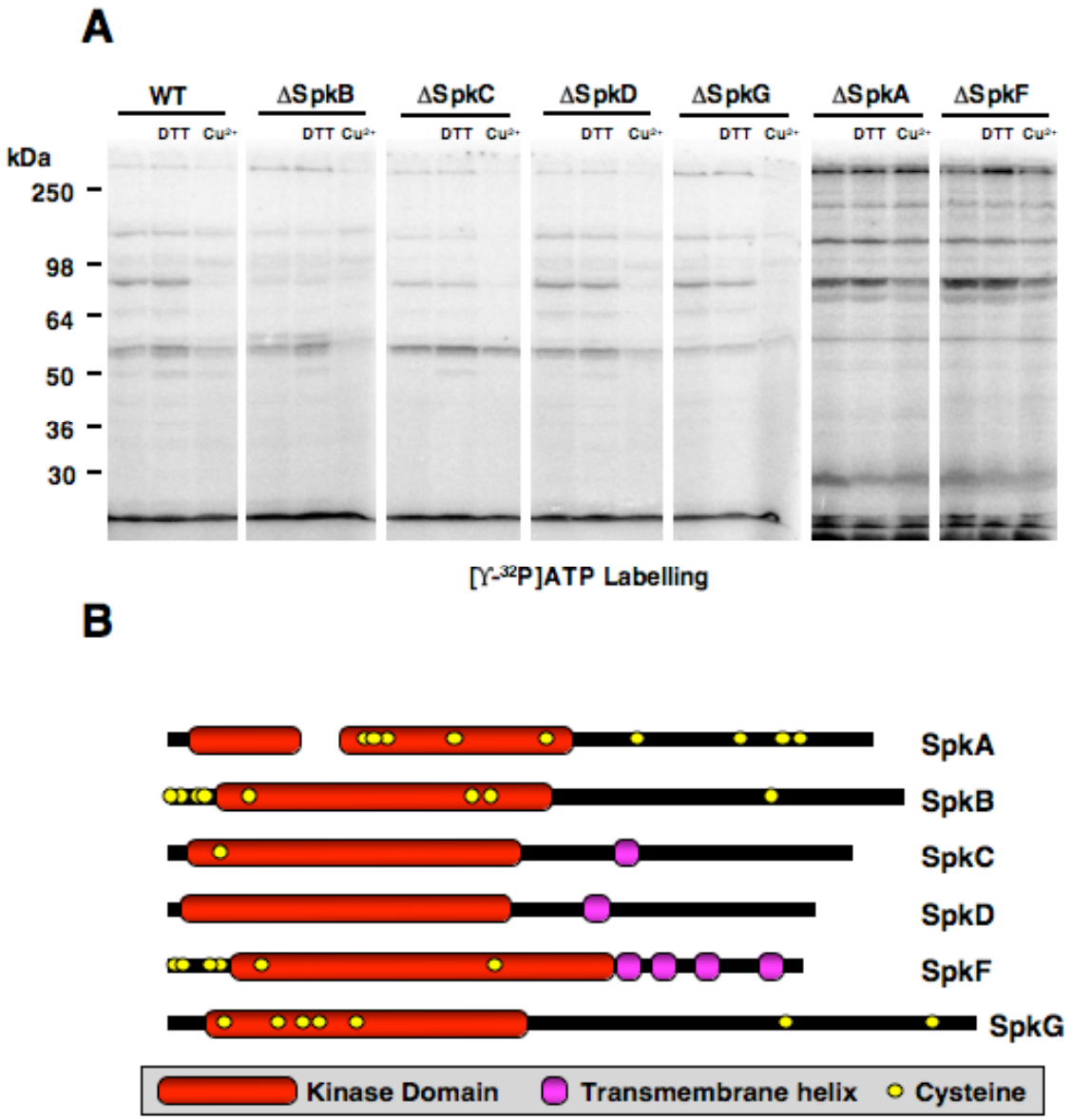

Figure 34. Pkn2 kinases of *Synechocystis*. (A) The phosphorylation pattern of cytosolic proteins from WT and mutant strains lacking the different Pkn2 type Ser/Thr kinases was observed under normal conditions and under reducing and oxidising treatment. Cytosolic extracts from each strain of *Synechocystis* corresponding to 20 μg of chlorophyll were treated for 15 min with 5 mM DTT, 100 μM $CuCl_2$ or without additions and thereafter incubated with 0.5 mM ATP, 5 μCi [γ-^{32}P]ATP and 10 mM NaF in order to label the phospho-proteins present in the fractions. Labelled proteins were detected by autoradiography. **(B)** Schematic representation of the different Pkn2 type Ser/Thr kinases in *Synechocystis*. The location of the kinase domain, transmembrane domain and the cysteines present in the amino acid sequence of each kinase are indicated.

2. SpkB redox regulation

SpkB has been related to cell motility, since the ΔSpkB mutant did not display phototactic movement (Kamei *et al*., 2003). This kinase is composed by the kinase domain followed by a pentapeptide repeat domain. In Zhang *et al*., 2007, the authors performed a phylogenetic analysis of the Ser/Thr kinases in cyanobacteria based on the catalytic domain. Despite the use of only the catalytic domain in this study, all cyanobacterial Ser/Thr kinases containing a pentapeptide repeat domain clustered together forming a subgroup of Ser/Thr kinases (Zhang *et al*., 2007). Here, we present a multiple alignment of some representative kinases of this subgroup including the *Synechocystis* SpkB (Fig. 33). In the alignment we can observe the existence of five completely conserved cysteines and one more highly conserved cysteine (in all sequences except one cysteine). Four of the totally conserved cysteine residues are grouped in pairs forming the so-called Cys-motif in the N-terminal domain. Some of the amino acids adjacent to these cysteines are highly conserved too. The high degree of conservation of the Cys-motif suggests a possibly important role in the protein activity, maybe involving redox regulation (Kamei *et al*., 2002). The other two remaining conserved cysteines are located within the kinase domain, where the first is present in the ATP binding domain. The pentapeptide domain is composed of several repeats of the following amino acid sequence: A(D/N)LXX. This domain is more diverse amongst the kinases from different organisms and a common pattern does not exist. The function of this domain remains unknown (Zhang *et al*., 2007). Based on the domain structure and phylogenetic data we propose that this kind of kinase constitutes a new sub-type of Pkn2 Ser/Thr kinases. So far, nothing is known about their functions, protein substrates or regulation. Other Ser/Thr kinases have been identified in bacteria that conserve the organization of a Cys-motif upstream the kinase domain, though the pentapeptide domain is replaced with other kinds of domains. This is the case of Pkn22 from *Anabaena*, where the pentapeptide repeat domain has been substituted with a PbHI, which is structurally similar, and the function is also unknown (Jenkins *et al*., 1998). In the case of PknG from *Mycobacterium tuberculosis,* this domain has been replaced with a tetratricopeptide repeat region, which mediates protein-protein interactions and the assembly of multiprotein complexes (D'Andrea and Regan, 2003) although a similar N-terminal

Cys-motif is conserved. This could suggest that the Cys-motif is a widely distributed regulator domain amongst Ser/Thr kinases.

In order to analyse the SpkB kinase activity and its putative redox regulation, we cloned the *slr1697* gene into the pET28a vector, where the expression of the cloned gene is subjected to IPTG control and a His-Tag is added to the protein. SpkB was expressed in the *E. coli* BL21DE3 strain and the kinase activity was detected in cytosolic extracts from *E. coli* cells as described in Kamei *et al*., 2001 and 2002 (Fig. 36). For this phosphorylation assay casein was used as artificial protein substrate. The casein alone and incubated with extracts of *E. coli* that was not expressing the kinase did not show appreciable phosphorylation of the substrate (Fig. 36). However, incubation with the *E. coli* extracts expressing SpkB resulted in a clear phosphorylation of casein, which decreased after $CuCl_2$ treatment, confirming the previous results obtained from *Synechocystis* extracts. Moreover, phosphorylation of a protein in the upper part of the gel (about 80 kDa) is observed. This may correspond to the autophosphorylation of SpkB, as suggested in Kamei *et al*., 2003.

Figure 35. Alignment of SpkB homologues. The Clustal X engine was used to perform the alignment of cyanobacterial SpkB homologous proteins. The sequences are from: *Synechocystis* sp. PCC 6803 (*slr1697*), *Cyanothece* sp. ATCC 51142 (*cce_2943*), *Microcystis aeruginosa* NIES-843 (*MAE_53550*), *Synechococcus* sp. PCC 7002 (*SYNPCC7002_A0446*), *Nostoc punctiforme* PCC 73102 (*Npun_R2916*), *Anabaena* sp. PCC 7120 (*alr3268*), *Trichodesmium erythraeum* IMS101 (*Tery_2064*) and *Lyngbya* sp. PCC 8106 (*L8106_12570*). The aminoacids that constitute the kinase domain are coloured in purple. The totally conserved cysteines are coloured in green and the pentapepteide repeats are in red. The ATP binding domain is indicated with a red box and the cysteines of SpkB from *Synechocystis* not totally conserved are indicated with a green box.

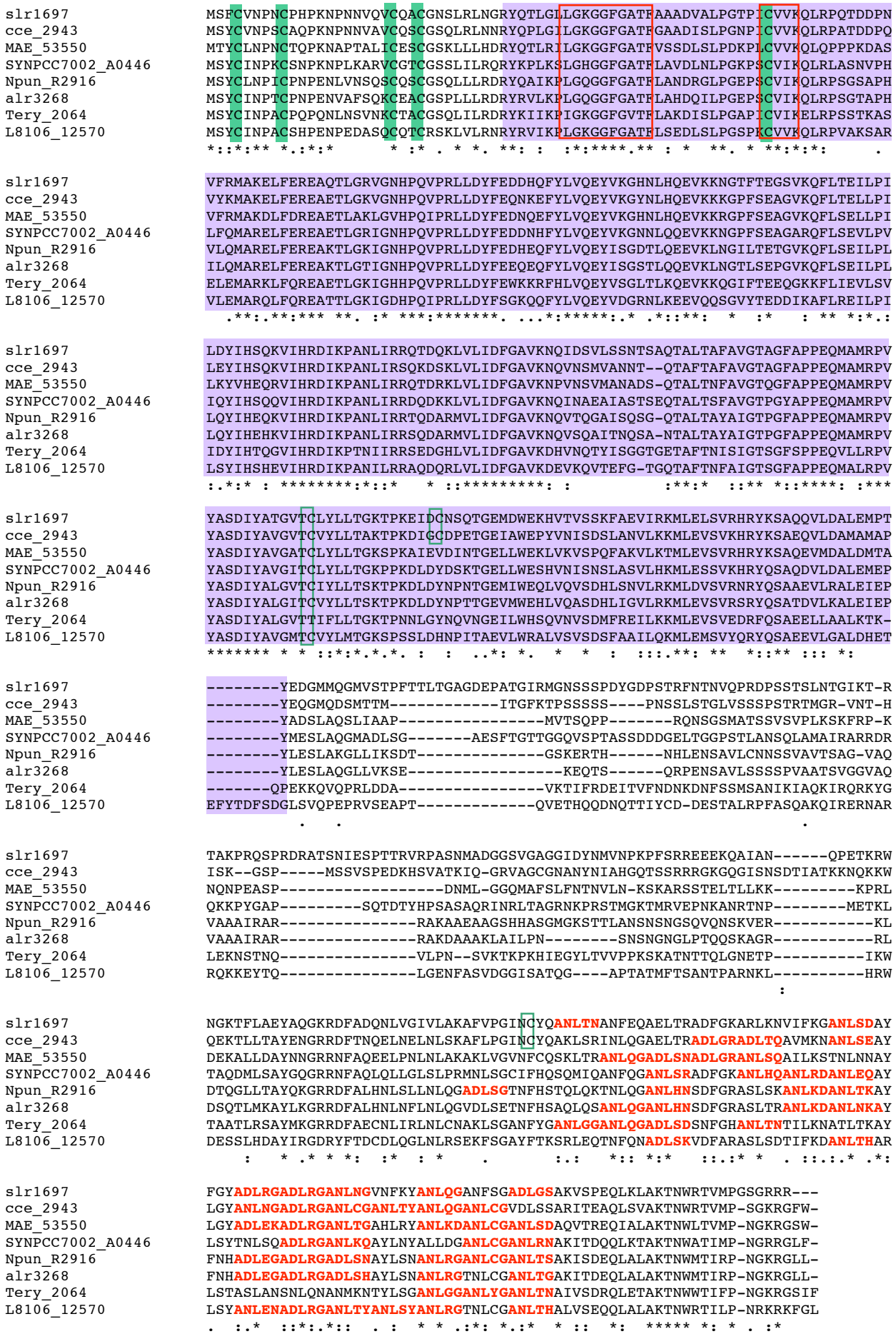
slr1697
cce_2943
MAE_53550
SYNPCC7002_A0446
Npun_R2916
alr3268
Tery_2064
L8106_12570

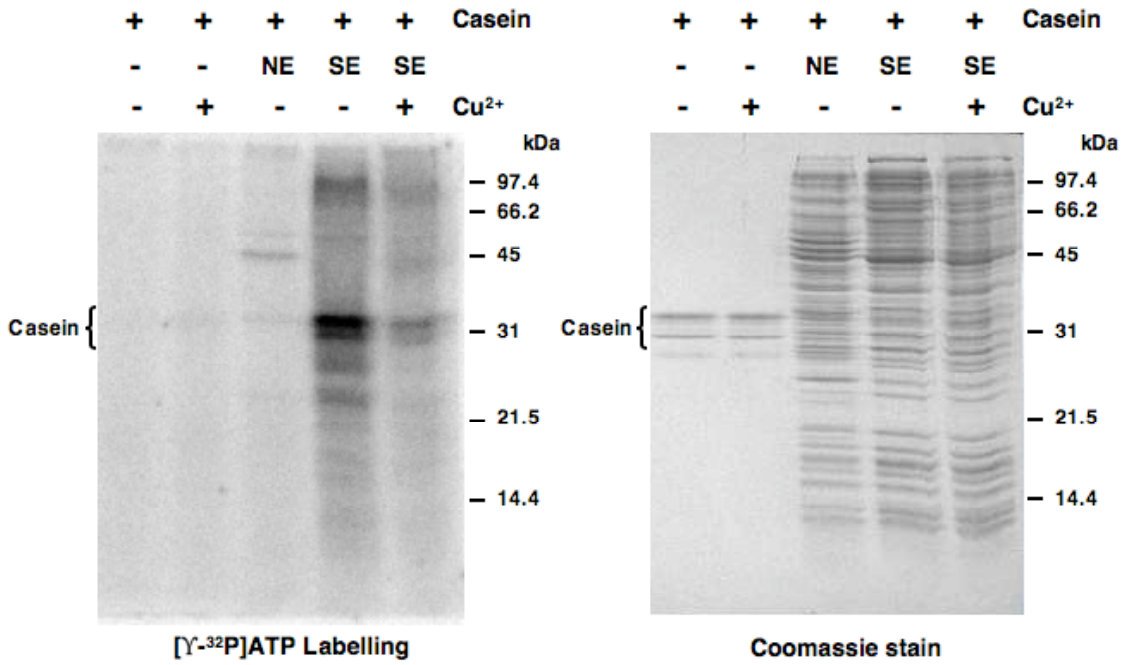

Figure 36. Activity of SpkB kinase expressed in *E. coli*. Kinase activity of SpkB was analysed performing a phosphorylation assay using 20 μg of *E. coli* cytosolic protein extracts from cells expressing (SE) or non-expressing (NE) the SpkB kinase of *Synechocystis* and 2.5 μg of casein as artificial kinase substrate. A sample of the *E. coli* expressing the kinase was pre-trated 15 min with 100 μM $CuCl_2$. The phosphorylation assay was performed incubating the samples with 0.5 mM ATP, 5 μCi [γ-^{32}P]ATP and 10 mM NaF in order to radioactive label the phospho-proteins. The samples were resolved in a 15% acrylamide gel, which was stained with Coomassie (right panel), and the labelled proteins were detected by autoradiography (left panel). A control with only casein in absence of *E. coli* extracts untreated and treated with $CuCl_2$, were loaded in the two first lanes of gel.

In order to purify recombinant SpkB from *E. coli* extracts we applied nickel affinity chromatography. However, SpkB could not be purified to homogeneity, though the majority of contaminants were removed. The identity of SpkB in the Coomassie-stained band was verified by MALDI-TOF analysis and peptide mass fingerprinting (PMF). The data for the identification of SpkB by PMF were MOWSE score: 189; number of peptides matched: 16; and sequence coverage: 29%. This partially purified preparation was used for phosphorylation assays, with casein as substrate (Fig. 37). Hence, the sensitivity of the semi-purified SpkB to oxidising treatment and the restoration of the kinase activity under reducing treatments was tested. Samples were pre-trated with either Cu^{2+} or GSSG in order to inactivate the kinase activity and attempts were made to reactivate with 5 mM DTT, 5 mM GSH or 4 μM TrxA (Fig. 37A). When the sample was treated with TrxA a low concentration of DTT (0.2 mM) was

used as electron donor. The phosphorylation assay showed that both Cu^{2+} and GSSG inhibited the kinase activity of SpkB and that this activity was efficiently restored by DTT and TrxA, but not by GSH (Fig 37A). This result is in agreement with the inactivation and reactivation of the kinase activity observed in *Synechocystis* cell-free extracts (Fig. 33). The inefficiency of the GSH treatment, as compared with DTT and TrxA may be explained by the redox potential of GSH, which is more positive than that of DTT and TrxA (Sevier and Kaiser, 2002). In order to test the concentration dependence on TrxA for restoration of the SpkB kinase activity we performed a titration using increasing concentrations of TrxA as reductant (Fig. 37B). In the control without TrxA, but with 0.2 mM DTT, part of the kinase activity was restored, although 1 μM TrxA was needed to reach the maximum level of casein phosphorylation. The maximum phosphorylation level reached upon restoration after $CuCl_2$ treatment was slightly higher than that of the untreated sample.

In order to test whether recombinant SpkB is able to phosphorylate the 90 kDa substrate protein, which is non-phosphorylated in the ΔSpkB mutant, we performed complementation assays. Hence, cytosolic extracts from the *Synechocystis* ΔSpkB mutant were incubated with increasing concentrations of purified recombinant SpkB (Fig. 38). The phosphorylation of the 90 kDa protein was specifically restored in the presence of low concentrations of exogenously added SpkB. With increasing amounts of SpkB, the 90 kDa protein phosphorylation was enhanced and new phosphorylated proteins appeared. One of them was most strongly labelled when the maximum concentration of SpkB was used (Fig. 38). This probably corresponds to the autophosphorylated SpkB, since the molecular weight matches with the observed one for SpkB of about 80 kDa. In conclusion, the exogenous addition of SpkB is able to replace *in vitro* the SpkB activity lacking in the mutant strain.

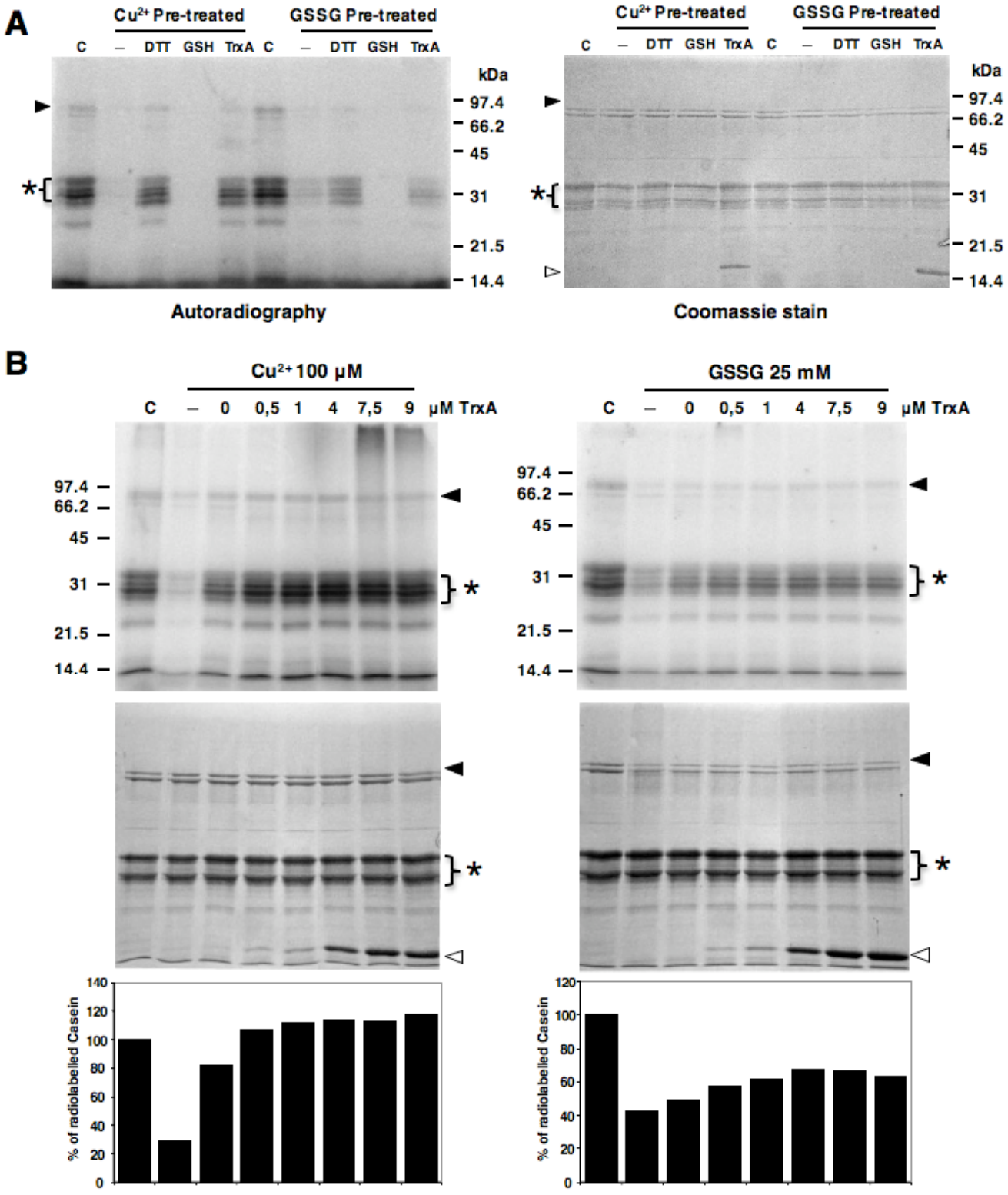

Figure 37. Kinase activity of partially-purified SpkB kinase expressed in *E. coli*. His-tagged SpkB was semi-purified by a one-step nickel affinity chromatography. The kinase activity of SpkB, its inactivation by oxidation and reactivation by reduction were tested performing the phosphorylation assay using 2.5 µg of casein as substrate. A concentrated sample of semi-purified SpkB was oxidised by the indicated concentrations of $CuCl_2$ and GSSG during 15 min and then was 10 times diluted for reactivation by

reductant agents. **(A)** The capacity of reactivate SpkB of different reducing agents was tested: 5 mM DTT, 5 mM GSH and 4 μM TrxA + 0.2 mM DTT. **(B)** Increasing concentrations of TrxA were used to reactivate the SpkB activity after oxidation with 100 μM $CuCl_2$ or 25 mM GSSG. 0.2 mM of DTT was used as electron donor to TrxA. In each case a control without any treatment (C) and without reactivation (-) was performed. Two μg of every sample was used to the phosphorylation assay and were resolved in 12 % acrylamide gels. The gels were stained by coomassie (lower panels) and the phosphorylation was detected by autoradiography (upper panels). The black arrowhead marks the supposed location of SpkB in coomassie gels and the autophosphorylation in autoradiography images. The white arrowhead marks the TrxA and the asterisk marks the casein. Below of the gels the graphic of the quantification of the radiolabelled casein has been represented.

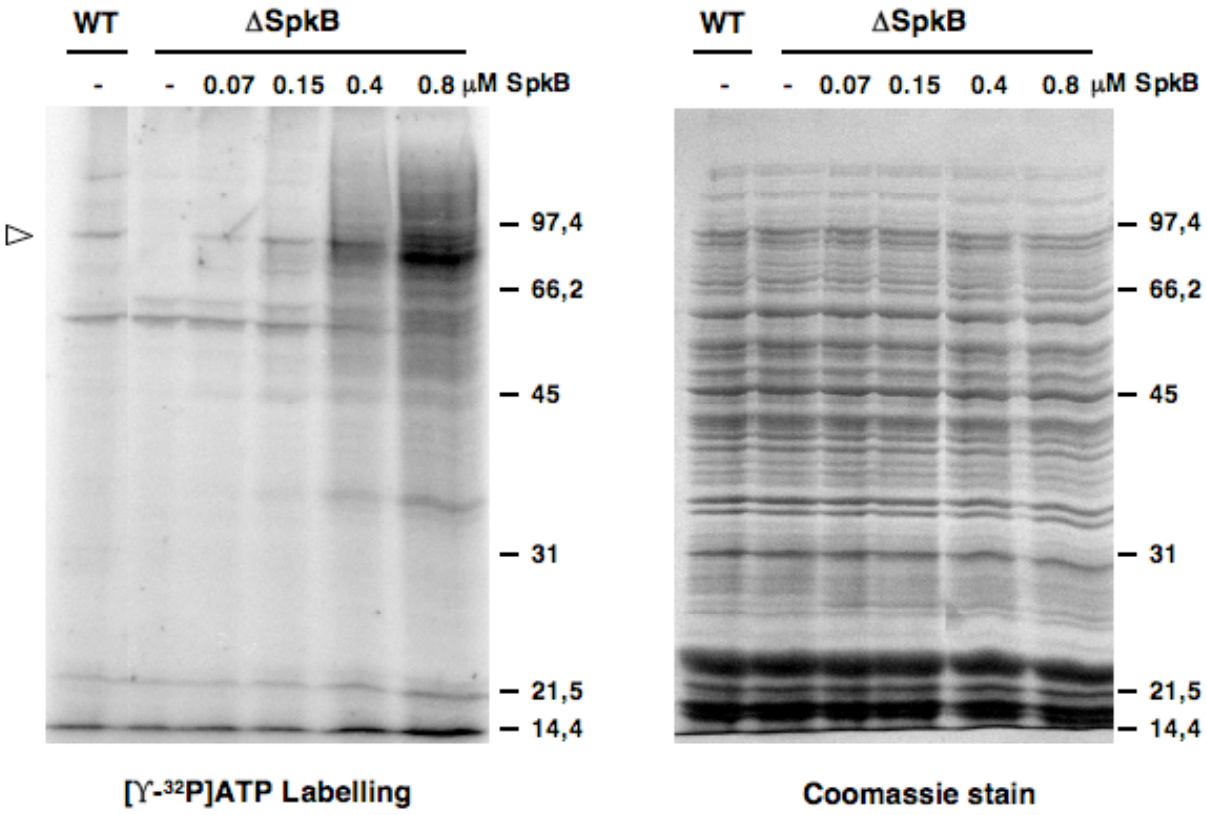

Figure 38. ΔSpkB mutant complementation with addition of exogenous purified SpkB. Increasing concentrations of partially purified SpkB (from 0 to 0.8 μM) were added to 150 μg of cytosolic extract of ΔSpkB strain in the phosphorylation assay. As control 150 μg of cytosolic extract of WT strain untreated and treated with 100 μM $CuCl_2$ were used in the phosphorylation assay. The white arrowhead indicates the location of the 90 kDa protein whose phosphorylation is sensitive to oxidation. The samples were resolved in 12% acrylamide gels, which were stained with coomassie (right panel) and the phosphorylated proteins were detected by autoradiography (left panel).

3. Identification of a target for SpkB phosphorylation

We had yet to determine the identity of the SpkB physiological target. To this end, the first step was to resolve the radioactively labelled cytosolic extracts from WT and ΔSpkB strains in an acrylamide gel by means of 2-DE, in which the first dimension consisted of a separation by the isoelectric point of proteins (pH 4.7 – 5.9). In the second dimension SDS-PAGE the proteins migrated according their molecular weight (Fig. 39). The resulting gels were CBB-stained and the phosphorylated proteins were detected by autoradiography. The comparative analyses of gels from both samples showed the lack of phosphorylation of a protein with the expected molecular weight in the mutant strain, being the apparent molecular weight about 85 kDa and the isoelectric point next to 4.7. Importantly, his loss did not correspond to the disappearance of the protein, but only its phosphorylation, since the Coomassie-stained spot remained similar in WT and mutant. The PMF identification of this spot revealed that the SpkB target is the glycyl t-RNA synthetase β-chain (GlyS). The theoretical molecular weight is 80.3 kDa and the isoelectric point is 4.7. The data of PMF for the spot identified as GlyS were MOWSE score: 248; number of peptides matched: 23; and sequence coverage: 33%.

The glycyl-tRNA synthetase catalyses the esterification of glycine with the terminal 3'-hydroxyl group of glycine transfer RNA resulting in the synthesis of glycyl-tRNA, which is required to introduce glycine into proteins. Besides, in a side reaction the enzyme also synthesises dinucleoside phosphate, which may participate in regulation of cell functions (Freist *et al*., 1996). Glycyl-tRNA synthetase is one of the few aminoacyl-tRNA synthetases that exhibits different oligomeric structures in different organisms. A tetrameric structure of the type $\alpha_2\beta_2$ has been suggested to be distributed only in bacteria and a dimeric structure of the type α_2 can be mainly observed in eukaryotes (Mazauric *et al*., 1998). The α-subunit and parts of the β-subunit are required for aminoacylation of tRNA and the α-chain contributes specifically to amino acid and ATP binding (Freist *et al*., 1996). Treatment with thiol-reductant and thiol-alkylating agents led to inhibition of the enzyme from *E. coli* (Ostrem and Berg, 1974; Profy and Schimmel, 1986), *S. aureus* (Niyomporn *et al*., 1968) and yeast (Kern *et al*., 1981). In general, this effect has been structurally interpreted as an inactivation by dissociation of the oligomer (Freist *et al*., 1996).

However, GlyS has been identified to possess a reactive thiol in *S. aureus* (Pöther *et al.*, 2009) as well as in *E. coli* (Hu *et al.*, 2010). This suggests a putative direct redox regulation of glycyl-tRNA synthetase. Phosphorylation also may be a means of regulation of this enzyme. Phosphorylated aminoacyl-tRNA synthetases have been isolated from uterus and liver cells of mice and some of these were activated by phosphorylation, while others were inactivated by this post-translational modification (Berg, 1977, 1978). Later studies showed that 15 different aminoacyl-tRNA synthetases, including glycyl-tRNA synthetase, from mouse liver were present in phosphorylated and non-phosphorylated forms (Berg, 1990).

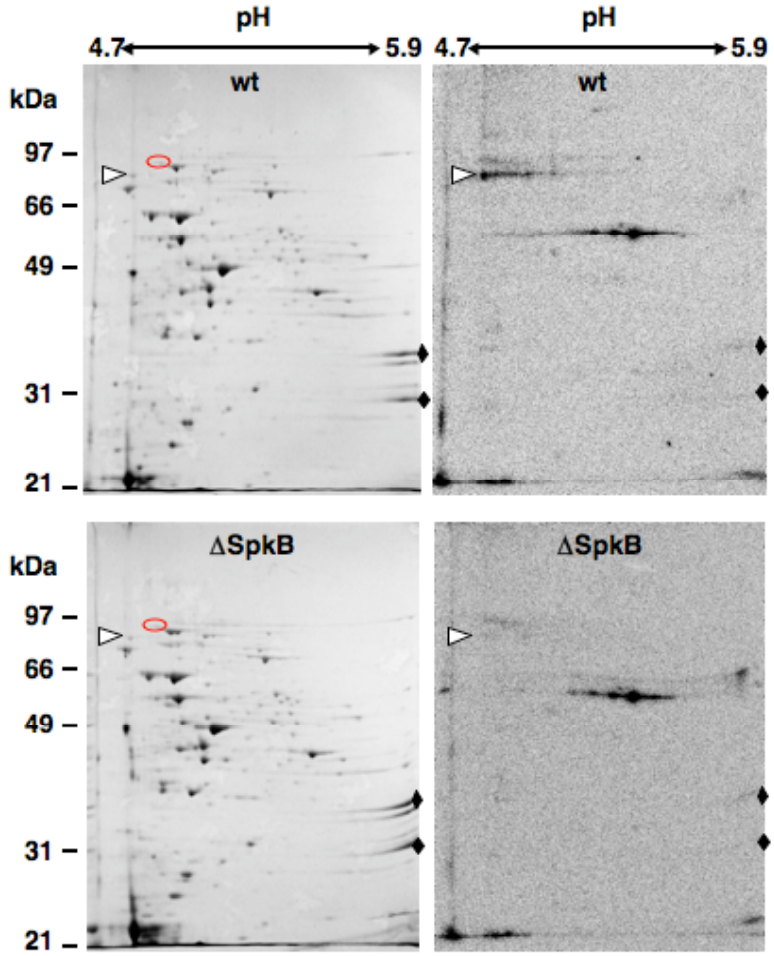

Figure 39. SpkB substrate identification. Four hundred μg of cytocolic protein extracts of WT and ΔSpkB strains were resolved in 2-D SDS-PAGE gels after the phosphorylation assay was performed incubating the samples with 0.5 mM ATP, 15 μCi [γ-^{32}P]ATP and 10 mM NaF in order to label the phospho-proteins present in the samples. The gels were stained with Coomassie (left panels) and the phosphorylated proteins were detected by autoradiography (right panels). White arrowhead marks the location of the endogenous SpkB substrate and the red ellipse localizes the Phenylalanyl-tRNA synthetase. Diamonds indicate the phycobilisome linker proteins, which are constitutively phosphorylated in *Synechocystis* (Piven *et al.*, 2005).

Synechocystis possesses in its genome two genes that codify for the α (GlyQ) and β (GlyS) subunits of glycyl-tRNA synthetase, indicating that the enzyme belongs to the $\alpha_2\beta_2$ type, as in the majority of prokaryotes. Surprisingly, looking at the genetic environment of SpkB we realised that an adjacent gene, which probably shares promotor with SpkB, was the phenylalanyl-tRNA synthetase β-chain (PheT). In *E. coli* the phenylalanyl-tRNA synthetase is also a $\alpha_2\beta_2$ type enzyme and exhibits similarities with GlyQS (Freist *et al*., 1996). In fact, despite little sequence homologies between the two enzymes, antibodies raised specifically against GlyQS displayed cross-reaction with phenylalanyl-tRNA synthetase (Nagel *et al*., 1988). To clarify the possible doubts about our SpkB target identification we localised PheT in the 2-D gel (Fig. 39). Hence, we ensured the loss of GlyS phosphorylation was real and it was not derived from a genetic effect on PheT in the ΔSpkB mutant strain. The CBB-stained 2-DE gel showed that PheT and GlyS were close, but far enough so as not to be confused. Moreover, the PheT protein was present in both strains in a similar quantity indicating that its expression was not altered in the mutant (Fig. 39). The data for the PheT identification by PMW were MOWSE score: 299; number of peptides matched: 26; and sequence coverage: 35%.

In order to verify *in vitro* the GlyS phosphorylation by SpkB we intended to purify recombinant GlyS. The ORF (*slr0220*) that codes for GlyS was cloned into the pET28a vector and expressed in *E. coli* but the protein produced was not soluble and impossible to purify in its native conformation. Since the glycyl-tRNA synthetase enzyme is composed by two subunits and maybe the solubility of the complex is higher than that of the separate subunits, we aimed at improving the solubility of GlyS co-expressing both subunits GlyS and GlyQ together. The *glyQ* gene (*slr0638*) was cloned into pET22b. pET28a vector confers resistance to kanamycin antibiotic and pET22b to ampicillin, hence the *E. coli* clone expressing both proteins was selected by growing with both antibiotics. In this manner we achieved partially soluble GlyS and GlyQ in cytosolic extracts used to obtain an enriched preparation of GlyQS through nickel affinity chromatography. The GlyQS preparation was used as substrate in a SpkB phosphorylation assay (Fig. 40). As a result, SpkB was proven able to phosphorylate GlyS *in vitro*. GlyQ was radioactively labelled in the presence and absence of SpkB. This would be expected since this is the ATP-binding subunit of GlyQS (Freist *et al*., 1996).

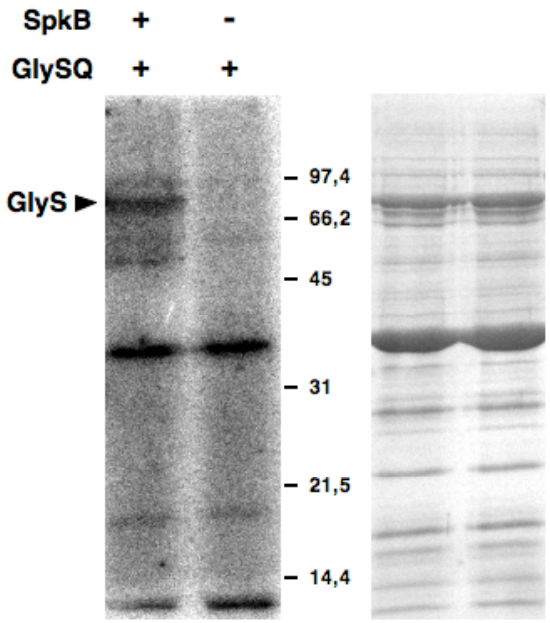

Figure 40. SpkB phosphorylates GlyS *in vitro*. His-tagged GlyS and GlyQ were cloned and co-expressed in *E. coli*. They were partially co-purified by nickel affinity chromatography. Ten μg of the recombinant GlyQS were used in a phosphorylation assay in the presence and absence of 0.5 μg of purified SpkB. The samples were by 1-D SDS-PAGE resolved in a 12% acrylamide gel and stained with Coomassie (right panel). The phosphorylated proteins were detected by autoradiography (left panel).

4. SpkB Cys-motif involvement in redox regulation

A truncated version of SpkB lacking the N-terminal Cys-motif was constructed in order to analyse the implications of this domain in the redox regulation of SpkB (Fig. 41A). The truncated SpkB was called β-SpkB. Because of the difficulty to purify these kinases we used extracts as in (Kamei *et al.*, 2001, 2002 and 2003) of *E. coli* expressing SpkB and β-SpkB to perform phosphorylation assays. Hence, we tested the kinase activity of β-SpkB and its sensitivity to redox treatments in comparison of WT SpkB (Fig. 41B). The amounts of SpkB and β-SpkB kinases were normalised based on western blot analyses of the respective *E. coli* extracts using α–His antibodies. Without any treatment, β-SpkB displayed a very weak casein kinase activity as compared with the WT kinase and no autophosphorylation was observed. However, the β-SpkB activity was inhibited by Cu^{2+} just like the WT SpkB. This result suggested that the Cys-motif was required for optimal catalytic activity, but not for redox regulation. The protein kinase G (PknG) from *Mycobacterium tuberculosis* (Scherr *et al.*, 2007) is structurally similar to SpkB. The so-called Cys-motif in SpkB is composed in PknG by

two iron-binding motifs (Cys-X-X-Cys-Gly, where X is any amino acid) characteristic for rubredoxins (Sieker *et al*., 1994), which for this reason is called rubredoxin domain in PknG from *M. tuberculosis* (Scherr *et al*., 2007). Rubredoxins are proteins that act as electron donors in electron transfer reactions (Sieker *et al*., 1997). When the four cysteines in the rubredoxin domain of PknG were mutated to serines the kinase was devoid of activity (Scherr *et al*., 2007). The authors proposed that the rubredoxin domain might modulate the kinase activity of PknG depending on the redox status of the environment (Scherr *et al*., 2007).

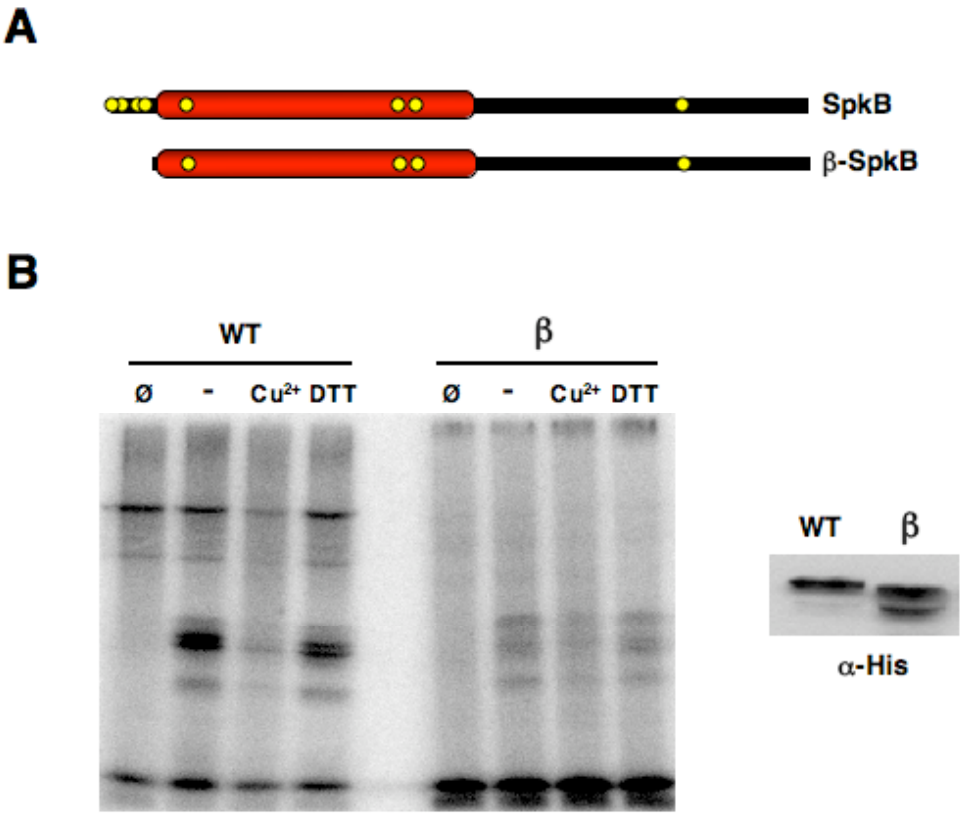

Figure 41. Kinase activity of the β version of SpkB. (A) Schematic representation of SpkB and β-SpkB. **(B)** The SpkB version lacking the two Cys motifs in the N-terminal region (β-SpkB) was expressed in *E. coli* and extracts of it were used to test the kinase activity. The quantity of extracts of *E. coli* expressing the WT and β versions of SpkB used in the phosphorylation assay were those in which the levels of the two versions of the kinase were similar (aprox. 20 μg). The kinase levels were balanced by means of western blot using specific anyibodies against His-tag in a dilution of 1:1000 (right panel). Before the phosphorylation assay with radioactive ATP both extracts were incubated 15 min with 100 μM $CuCl_2$ or 5 mM DTT. Two controls without any treatment (-) or lacking the casein (Ø) were carried out. All samples were resolved in a 12% acrylamide gel and phosphorylated proteins were detected by autoradiography (left panel).

Although the kinase activity of β-SpkB was almost abolished, the slight inhibition by $CuCl_2$ raised the possibility that the cysteine responsible for redox regulation is still present, though the lack of the Cys-motif leaves the enzyme almost completely oxidised. Therefore, we tested further whether this kinase was activated by reducing agents without oxidising pre-treatment. Thus, β-SpkB was incubated in presence of increasing concentrations of DTT and TrxA prior to the phosphorylation assay (Fig. 42). In the absence of reductant the kinase activity was hardly detectable, but the addition of DTT or TrxA restored the kinase activity. The treatment with TrxA as reducing agent was more efficient than that with the DTT alone, recovering a higher phosphorylation level. The reactivation was similar to those performed with the WT SpkB inhibited by $CuCl_2$ (Fig. 37), though higher Trx concentrations (2 μM) were needed to reach maximum activity. This result demonstrated that the Cys-motif is not required for catalytic activity, but for redox regulation.

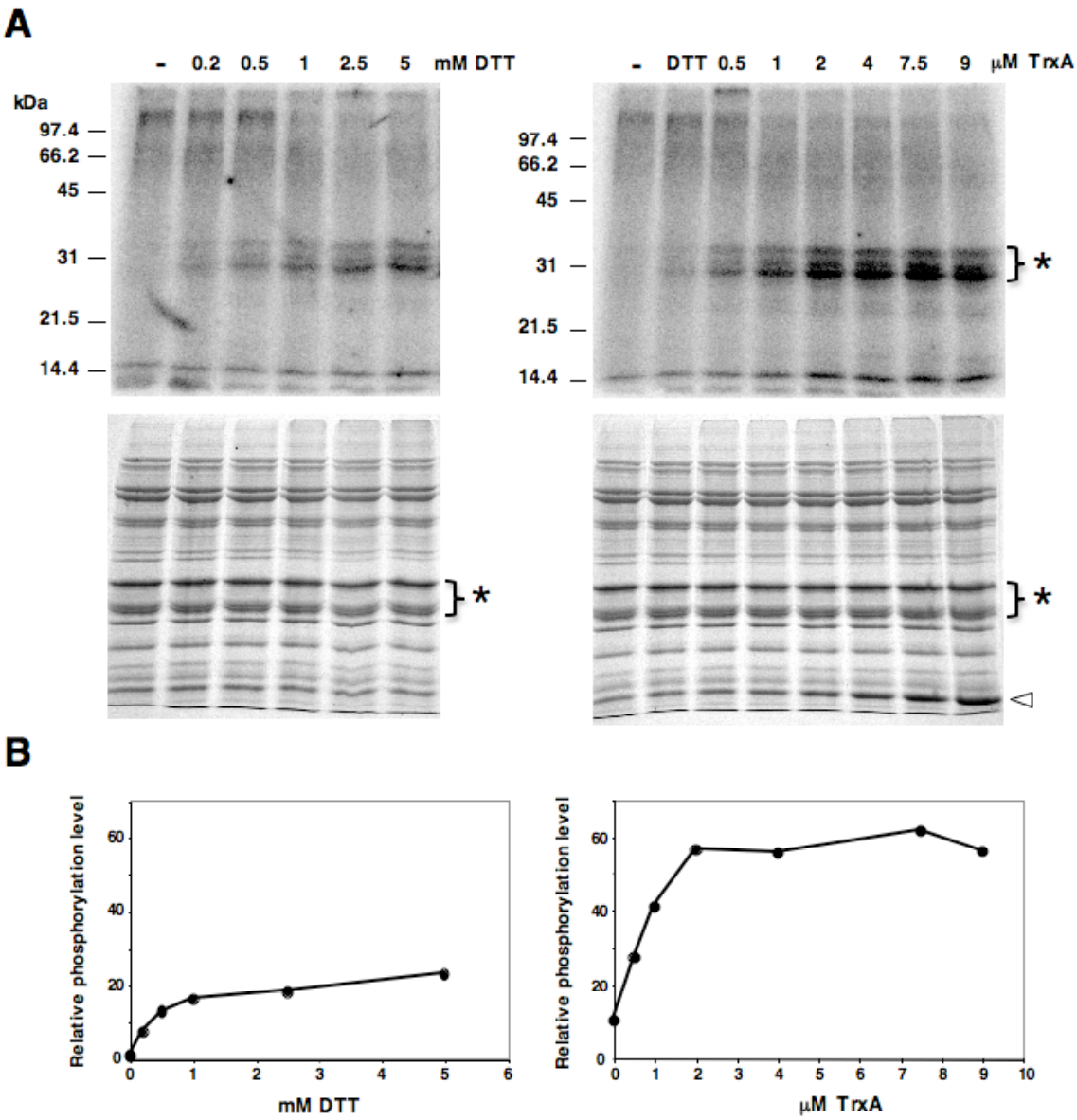

Figure 42. Kinase activity reactivation of β-SpkB. (A) Twenty µg of *E. coli* extracts expressing β-SpkB was incubated 15 min with growing concentrations of DTT (from 0 to 5 mM) and TrxA (from 0 to 9 µM), where 0.2 mM DTT was used as electron donor to TrxA. A control with 0.2 mM of DTT and whitout TrxA was performed (DTT). Casein 2.5 µg was used as phosphorylation substrate. The phosphorylation assay was performed incubating the samples with 0.5 mM ATP, 5 µCi [γ-^{32}P]ATP and 10 mM NaF. The samples were resolved in 12% acrylamide gels and stained with Coomassie (lower panels). Phosphorylated proteins were detected by autoradiography (upper panels). Asterisks indicate the casein and the white arrowhead marks the TrxA. **(B)** Graphic representation of the quantification of the radioactive signal in (A).

DISCUSSION

DISCUSSION

I - Membrane proteins from the cyanobacterium *Synchocystis* sp. PCC 6803 interacting with the thioredoxin

Gram-negative bacteria possess outer membranes and plasma membranes. Cyanobacteria are particular amongst the Gram-negative bacteria, since they possess an additional membrane system forming the thylakoids. One of the central processes in nature, the photosynthesis, takes place in the thylakoids. Furthermore, the cyanobacterial respiration occurs in thylakoids and shares some components with the photosynthetic electron transport. Hence, membranes in cyanobacteria have an important role. However, because of technical difficulties the characterisation of the membrane proteome in cyanobacteria has been very limited. About one-third of the more than 3000 ORFs present in the *Synechocystis* genome have been predicted to encode proteins that possess transmembrane domains (Wallin and von Heijne, 1998). In addition, there are peripheral membrane proteins, which are associated to membranes or to integral membrane proteins. Nevertheless, the number of integral membrane proteins identified exclusively by standard proteomic approaches is very low in this cyanobacterium, with only 66 out of the 706 predicted integral membrane proteins (Huang *et al*., 2002; Huang *et al*., 2006; Srivastava *et al*., 2005; Pisareva *et al*., 2007; Wang *et al*., 2009). The technical limitations for identification of large numbers of membrane proteins are related to the hydrophobic nature of transmembrane domains. Hydrophobic proteins may precipitate at their isoelectric points during the IEF separation process, resulting in sample loss and difficulties to perform the second dimension separation (Santoni *et al*., 2000). Moreover, in-gel tryptic digestion covers principally exposed hydrophilic domains of integral membrane proteins, leaving behind the hydrophobic transmembrane domains in the gel (Blackler *et al*., 2008). However, progress has been made for membrane proteome analyses. One of the solutions proposed involves a 2-D SDS-PAGE, where in the first dimension a cationic detergent is used and in the second an anionic detergent, thus avoiding the IEF separation (Zahedi *et al*., 2005). Another method developed is the Blue Native PAGE/SDS-PAGE in which the first dimension consists of a native electrophoresis in the presence of a negatively charged CBB, which binds to exposed hydrophobic surfaces of proteins (Schägger and von Jagow, 1991). In the past few years, a gel-free

technical platform has been developed for membrane proteome analyses (Wu and Yates, 2003; Weiner and Li, 2008). In this method the entire protein mixture is first digested and peptides are analysed by LC-MS/MS. A key step for the development of this method is finding a solvent for solubilisation of membrane proteins compatible with enzymatic or chemical protein digestion (Weiner and Li, 2008). An efficient means of degrading proteins into peptides of suitable length for LC separation and MS analysis is also vital for the success of the gel-free method (Weiner and Li, 2008). The methods used to study integral membrane proteins in *Synechocystis* include 1-DE of membrane preparations (Srivastava *et al*., 2005; Pisareva *et al*., 2007) or the analyses of the solubilised membrane proteins using classical proteomic prodedure (Huang *et al*., 2002 and 2006; Srivastava *et al*., 2005). Recently, a systematic analyses of *Synechocystis* membrane proteome has been reported, in which the isolated total membrane proteins underwent acid hydrolysis followed by trypsin or chymotrypsin digestion and LC-MS/MS analyses (Kwon *et al*., 2010). In this study 155 proteins containing at least 1 transmembrane domain and 36 peripheral membrane proteins were identified (Kwon *et al*., 2010), which makes this newly developed method twice as efficient as the classical ones.

The association of thioredoxin with membranes (Srivastava *et al*., 2005; DeRocher *et al*., 2008; Meng *et al*., 2010) as well as a thioredoxin-like membrane protein (Motohashi and Hisabori, 2006) have been reported. This fact has prompted the search for membrane proteins able to interact with thioredoxins. Two screening studies for Trx-targets in plant thylakoid membranes have been reported. In the first study, Triton X-100-solubilised proteins reduced by Trx were labelled with monobromobimane (mBBr) and separated using 2-DE, which led to the identification of 14 proteins (Balmer *et al*., 2006). Since the authors applied a classical 2-DE procedure with a first IEF step and a second SDS-PAGE separation, they probably only identified the most abundant proteins. In the second study, the authors used Trx-affinity chromatography to identify Trx-targets amongst octylglucoside solubilised membrane proteins (Motohashi and Hisabori, 2006). The proteins eluted from the chromatography were resolved using 1-DE. Hence, they identified 9 putative Trx-targets, 5 of which were predicted to have transmembrane domains. However, since both methods involve solubilisation prior to interaction with Trx, the exposure of normally buried cysteines might have resulted in identification of false positives.

Contrary to previous studies, in the approach that we developed for identification of membrane proteins interacting with Trx, the membranes were not solubilised prior to the procedure. Therefore, the monocysteinic Trx was only able to interact with the exposed cysteines *in situ*. After subsequent solubilisation, the Trx-target complexes were isolated and the separation of membrane proteins was performed by 2-D SDS-PAGE, and hence, the problems arising from the use of IEF were prevented. However, only 4 of the 50 Trx-targets detected were transmembrane proteins. This could mean that there is not a high number of Trx-targets amongst the integral membrane proteins or that we were not able to identify them, which would be consistent with the fact that we performed in-gel tryptic digestion and it has been demonstrated not to be the best for hydrophobic proteins (Blackler *et al*., 2008). FtsH is the only integral membrane protein in common between our study of cyanobacterial membranes and that of plant thylakoids made by Motashi and Hisabori, 2006. In the future, the new advances in the analysis of the membrane proteome could be applied to improve the screening for Trx-targets amongst integral membrane proteins.

In our study we identified 50 Trx-targets amongst the membrane bound proteins. Thirty-eight were identified for the first time, though 10 of these had been previously described to interact with Trx in other organisms (Table 3). Regarding the distribution of the total Trx-targets identified in *Synechocystis* (Lindahl and Florencio, 2003; Pérez-Pérez et al., 2006; and the present study) (Fig. 13), it is surprising that the number of targets associated to membranes is almost twice the number of the soluble targets. This could be representative for the real distribution of proteins in *Synechocystis* and emphasises the importance of the membranes in this kind of organisms. The overlap of identified targets between our analyses and those made by Motohashi and Hisabori, 2006, and Balmer *et al*., 2006 is minimal. The only target in common with the study of Balmer *et al*., 2006 is the ATP synthase β-subunit. This protein is also found in Motoashi and Hisabori, 2006, where other common targets are the ATP synthase α-subunit and FtsH. The large differences in total number of targets identified between our study and the other two may partially explain this divergence. One reason for the relatively low number of targets in Motohashi and Hisabori, 2006 is that they used as bait for Trx-chromatography the Trx-like protein HCF164, whereas we used a canonical Trx. An important difference with the procedure of Balmer *et al*.,

2006, is that they used a mBBr 2-DE approach, lacking an enrichment step, whereas we performed a Trx-chromatography, in which the targets were enriched prior to resolution.

It is striking that a large number of targets identified here are involved in amino acid- and protein metabolism. This may suggest a redox-dependent readjustment of amino acid and protein metabolism in response to *e.g.* oxidative stress, but further investigations are necessary to confirm it. Moreover, here we have identified as Trx-target the serine-O-acetyltransferase, which is involved in the production of cysteine. In addition, two enzymes involved in sulphur metabolism have been identified, ferredoxin-sulfite reductase (Lindahl and Florencio, 2003; and the present study) and sulfate adenylyltransferase (Lindahl and Florencio, 2003). This could indicate a putative redox regulation of the cysteine metabolism, which would be a useful mechanism of defence against oxidative stress. Another remarkable feature is the abundance of Trx-targets containing a conserved cysteine within an ATP-binding domain. This could indicate a putative regulation of the ATP-binding by redox modification of the cysteine. For example, the disulphide bond formation with another molecule, such as glutathione, or a protein, would block the binding of ATP. Another possibility would be the direct interaction of the cysteine with the ATP. Recently, the autophosphorylation of the resolving cysteine of the 2-Cys Prx from rapeseed has been reported (Aran *et al*., 2008). This study describes how the oxidised forms of cysteines are able to bind ATP and how this binding impairs the catalytic activity of 2-Cys Prx. Thus, it opens the possibility that cysteines are able to directly bind ATP and would represent the convergence between the redox and phosphorylation signalling.

Two of the targets analysed in the present work were the 1-Cys and 2-Cys Prx. 1-Cys Prx together with type II Prx have been reported as Trx-targets in previous proteomic studies in *Synechocystis* (Lindahl and Florencio, 2003; Pérez-Pérez *et al*., 2006; Florencio *et al*., 2006). However, 2-Cys Prx had never been detected and it had even been proposed to be anchored to membrane (Pérez-Pérez *et al*., 2006). Here, we have demonstrated that 2-Cys Prx is located in the cytosol and that its abundance is very low compared to 1-Cys Prx and type II Prx. This may be the reason why 1-Cys and type II Prxs had been detected, but not 2-Cys Prx. The difference of about 50 times in abundance could indicate a possible divergence in function between the different

peroxiredoxins, each one playing a different role in redox signalling and peroxide detoxification.

Aiming at verifying whether these two Prxs were truly Trx-targets in *Synechocystis*, we tested their interaction with TrxA35 *in vitro* using purified proteins and the capacity of TrxA to sustain their peroxidase activities. Eventually, we could conclude that 2-Cys Prx and 1-Cys Prx are able to interact with TrxA in *Synechocystis* and that these interactions are functional. Previously, a very low peroxidase activity of 1-Cys Prx using *x*-type Trx (TrxB) in *Synechocystis* (Hosoya-Matsuda, 2005) has been shown, and the 2-Cys Prx and 1-Cys Prx activities in *Synechococcus elongatus* PCC 7942 using the complete reducing system of *E. coli* TrxA (Stork *et al*., 2009). The activities calculated by Stork *et al*., 2009 were much higher than those measured here, but the difference between the activities of the two Prx was similar. However, none of them used the endogenous TrxA (*m*-type Trx) as electron donor and neither used the FOX method to monitor the peroxidase activity. In *Arabidopsis* the 2-Cys Prx was reduced by the *m*, *f* and *x*-types of Trx. However, the best reductant for this Prx was not the *m*-type Trx, but the *x*-type Trx (TrxB in *Synechocystis*) (Collin *et al*., 2004). These data are consistent with those obtained in our laboratory, which indicate that TrxB is the thioredoxin that binds with more affinity to the 2-Cys Prx in *Synechocystis*.

In Pérez-Pérez *et al*., 2009, we performed an extensive study of the peroxiredoxin system in *Synechocystis*. We have examined the interactions of all five *Synechocystis* Prx with the three different Trx from this organism with regard to affinity and catalytic efficiency. In addition, we have analysed the expression of *prx* and *trx* genes under different conditions in order to search for correlations between their expression patterns. In this study we concluded that all these Prx are expressed and are genuine Trx-dependent peroxidases, all of which are able to interact with and receive electrons from the different *Synechocystis* Trx (Pérez-Pérez *et al*., 2009). With respect to 2-Cys Prx, TrxB is the thioredoxin with the highest affinity, but TrxQ is the thioredoxin that reduces most efficiently this Prx. However, the 50-fold higher abundance of TrxA as compared to TrxQ could mean that *in vivo* TrxA would have more relative importance as electron donor for this Prx. In the case of 1-Cys Prx, TrxB is the Trx, which binds in with the highest affinity, but TrxA is the most efficient electron donor. 1-Cys Prx and TrxA coincided in the unusual expression pattern of

reduced transcription under conditions of elevated ROS concentrations (Pérez-Pérez *et al*., 2009). Thus, it seems very likely that TrxA is the electron donor for 1-Cys Prx *in vivo*. Since the catalase/peroxidase KatG has higher capacity for scavenging of H_2O_2 in *Synechocystis* as compared to the thiol peroxidases, this enzyme is responsible for the main peroxidase activity in the cell and for the high peroxide tolerance of this cyanobacterium (Tichy and Vermaas, 1999). Thus, although the role of the Prxs remains still unknown, it is possible that they do not participate in goal defence against ROS, but they could be involved in cellular signalling or in the local elimination of peroxides at low concentrations.

Other putative targets found in our screening, in which we were interested, were the Usp proteins, Usp1 and Usp2. We demonstrated that the cysteines present within the amino acid sequence of Usp1 played an important role in the oligomerisation of the Usp1 under oxidising conditions (Fig. 20 and 21). Therefore, the treatments with reductants, including TrxA, were able to reduce the homodimeric and oligomeric forms of Usp1 and to release the monomers. Interestingly, treatment with H_2O_2 specifically induces oligomerisation (Fig. 21), which suggests the presence of a redox-active cysteine that forms sulfenic acid reaction intermediates (Salsbury *et al*., 2008). Previously, the formation of homodimers of Usp proteins from diverse organisms has been reported (Sousa and McKay, 2001; Zarembinski *et al*., 1998; Weber and Jung, 2006) and also larger complexes in native *E. coli* protein extracts (Gustavsson *et al*., 2002). However, neither of them reported the involvement of cysteines in the oligomer formation. We have also demonstrated that the autophosphorylation activity of Usp1 was impaired by reduction (Fig. 22). The structure of one member of the UspA protein family from *Methanococcus jannaschii* was resolved by X-ray crystallography and this analysis demonstrated that the protein forms ATP-binding homodimers (Zarembinski *et al*., 1998). We observed that under oxidising conditions, when the oligomers are formed, is also when the Usp1 is phosphorylated. Hence, when the monomers appear after reducing treatment the autophosphorylation in inhibited. Therefore, the autophosphorylation could be regulated by the oligomeric state, which in turn could be regulated by the redox state of the cysteines. The Usp1 from *Synechocystis* is formed by two UspA-like domains in tandem and each UspA contain an ATP-binding motif, inside which is located one

cysteine. Thus again, we found an ATP-binding protein that is redox regulated, supporting the idea that this could be a general regulation mechanism.

Although diverse phenotypes of hypersensitivity to stress conditions have been assigned to the ΔUsp mutant strains (Nyström and Neidhart, 1994 and 1996; Gustavsson *et al*., 2002; Bochkareva *et al*., 2002; Nachin *et al*., 2005), the molecular mechanism for the function of these proteins remains certainly unknown. With respect to a possible role of Usp in response to oxidative stress, the *E. coli* UspA has been shown to be important for H_2O_2 resistance during growth (Nyström and Neidhart, 1996). In addition, the class I of Usp (UspA and UspD) from *E. coli* have also been suggested to play an important role in the resistance to superoxide of growing cells (Nachin *et al*., 2005). UspA has a single cysteine, which is highly conserved, whereas UspD has two cysteines, but only the second one, which corresponds to the conserved cysteine in UspA, is extensively conserved amongst diverse organisms.

FtsH was an interesting putative target of Trx, since it would imply a redox regulation of the photoinhibition process. Thus, under high light the Trx could reduce the only cysteine of FtsH located within the ATP-binding domain activating the protease activity of FtsH, which would participate in the D1 degradation. Under low light the cysteine could remain oxidased or forming a disulphide bond with another molecule, such as glutathione, which would block the ATP binding and the enzyme would be inactive. Our data strongly suggest an *in situ* interaction between TrxA and FtsH in *Synechocystis*. However, the data concerning the FtsH2 site directed mutant were not conclusive, since this would resemble the reduced form of FtsH2, and it had the same phenotype as WT strain. Since we were not able to purify FtsH2, we could not clarify the redox regulation of this enzyme and its putative inhibition by oxidation. Another possibility to explain the role of the only cysteine is that suggested in the Figures 22 and 23 in which the oxidation and reduction of the cysteine could modulate the involvement of FtsH in supercomplexes formation with other FtsH or with other kinds of protein, such as those reported in *E. coli* (Saikawa *et al*., 2004) and in yeast (Steglich *et al*., 1999). However, in this case the FtsH would be active when forming the complexes in its oxidised state, but this is not in accordance with our data in which the C266S-version of FtsH2 is as active as the WT, at least in the D1 repair mechanism.

Further investigations are necessary to completely elucidate whether the cysteine plays a role in the FtsH regulation.

II – Thioredoxin targets in the thylakoid lumen

Since it is not possible to isolate intact thylakoids from cyanobacteria, the thylakoid lumen proteome of cyanobacteria is not very well characterised, although some lumenal proteins have been identified (Mulo *et al*., 2008). Evidence for redox regulation in the thylakoid lumen of the chloroplast has been reported (Gopalan *et al*., 2004; Marchand *et al*., 2004; Marchand *et al*., 2006; Buchanan and Balmer, 2005), but no soluble Trx has been detected inside this compartment. However, HCF164, a Trx-like protein anchored to the thylakoid membrane was identified (Lennartz *et al*., 2001; Motohashi and Hisabori, 2006). This protein, which is homologous to *E. coli* DsbD, may be responsible for transduction of reducing equivalents across the thylakoid membrane through dithiol/disulphide exchange (Porat *et al*., 2004). The homologue of HCF164 in cyanobacteria was called TxlA (Collier and Grossman, 1995). This suggests a putative redox regulation in the thylakoid lumen of cyanobacteria. The disulphide proteome studies performed hitherto in cyanobacteria have used total cell extracts including soluble and membrane fractions (Florencio *et al*., 2006; and the present work). Thus, *a priori* lumenal Trx-targets could have been identified, but the fact is that none was detected. Therefore, it would be necessary to isolate the thylakoid to analyse the proteins contained, but since the thylakoid and plasma membrane are in close connection, in cyanobacteria is not possible to separate intact thylakoids from the rest of the cell. However, the chloroplast thylakoids are more independent compartments and, then, therefore they can be isolated. Thus, we decided to use chloroplast thylakoid preparations from *Arabidopsis* and the Trx-targets found were searched against the *Synechocystis* genome for comparison. Hence, we identified 12 putative Trx-targets that have homologues in *Synechocystis* (Table 6).

This screening forms part of a systematic study, in which complementary approaches have been used to discover lumenal Trx targets (Hall *et al*., 2010). Apart from the Trx affinity chromatography, here described, the methods used in this study are fluorescence labelling using mBBr and differential alkylation. The Trx affinity

chromatography was the procedure that has led to detection of the largest number of Trx-target proteins, a total of 14 lumenal proteins, whereas, the two other approaches combined detected 11 targets. Four stromal Trx-targets, which were contaminating the lumenal preparation, were identified namely, the RuBisCo large subunit, the two ferredoxin-NADP oxidoreductase FNR 1 and FNR 2, and the unknown protein encoded by the gene At3g15840.3. All these four contaminant proteins were detected by the Trx-affinity chromatography method, but only the RuBisCo large subunit and the FNR 1 were detected by differential alkylation. The location of the plastid lipid-associated protein is unknown in plants and was only identified in the Trx affinity approach. These data suggest that the method here explained was the most sensitive of the three used. Moreover, an advantage of this protocol is that it can discriminate between true targets and possible false positives that would be equally retained in both dimensions. Therefore, proteins that migrated exclusively along the diagonal are not considered as Trx targets.

The only two target proteins, which conserved the cysteines between *Arabidopsis* and *Synechocystis* were PsbO and PrxQ2 (Table 4). The two PsbO isoforms found as putative targets in the *Arabidopsis* preparation share the same homologue in *Synechocystis*. PsbO contains two conserved cysteines, which may form a disulphide bond that could function in the regulation of the oxygen-evolving activity. Moreover, PsbO is a highly flexible molecule that undergoes conformational changes and bound-unbound transitions of PsbO to PSII have been suggested (De Las Rivas and Barber, 2004). Under normal conditions the PsbO-proteins are very stable in isolated luminal preparations. However, the presence of possible degradation products of PsbO1 and PsbO2 in our eluates from Trx-affinity chromatography (Fig. 26B) raised the possibility that disulphide reduction promotes their degradation. Thus, we performed experiments *in vitro* and showed that the PsbO1 and PsbO2 subunits of the OEC in *Arabidopsis* undergo a pronounced Trx-dependent degradation (Hall *et al*., 2010). The reduction of the disulphide within the PsbO proteins could change their conformation and render them accessible to proteolysis. Taken into account the presence of two lumenal proteases, Deg1 and Deg5, among the Trx-targets found in the lumenal fraction from *Arabidopsis*, one could envisage a redox-regulated degradation of PsbO subunits involving the Deg proteases. Deg proteases have been proposed to be involved in heat and high light protection in cyanobacteria (Barker *et al*., 2006).

However, their physiological substrates have not been identified (Huesgen *et al*., 2009).

Another target that possesses conserved cysteines is the Trx-dependent peroxidase PrxQ. In plants the PrxQ is located in the chloroplast thylakoid lumen (Petersson *et al*., 2006), but in bacteria its localisation is controversial. It has been described as a periplasmic protein (Cha *et al*., 1995; Link *et al*., 1997) as well as cytosolic (Tao, 2008). *Synechocystis* has two PrxQ, named PrxQ1 and PrxQ2. We have reported here that PrxQ2 contains in its amino acid sequence a N-terminal signal peptide, which could direct the enzyme to the thylakoid lumen or the periplasm. Thus, it suggests that each PrxQ in *Synechocystis* is located in a different compartment; one in the cytosol and another probably in the thylakoid lumen. The phylogenetic analyses revealed that this dual localisation is very common amongst cyanobacteria (Fig. 26) and that the PrxQs containing signal peptides group together.

Here we have demonstrated that PrxQ2 is a functional Trx-dependent peroxidase. It is able to interact physically *in vitro* with TrxA (Fig. 27) and this thioredoxin is also an effective electron donor to PrxQ2 (Fig. 28). The peroxidase activity of PrxQ2 is intermediate between activities determined for 2-Cys Prx and 1-Cys Prx in this study. These activities are significantly lower than those calculated for *Anabaena* sp. PCC 7120 (Cha *et al*., 2007), *Synechococcus elongatus* (Stork *et al*., 2009) and *Arabidopsis* (Lamkemeyer *et al*., 2006). However, these values are not entirely comparable since the Trx system, Trx concentrations and the assay used in each case were different. For the PrxQ2 of *Anabaena* and *Synechocuccus* the *E. coli* TrxA reduction system (TrxA, Thioredoxin reductase, NADPH) was used, where the concentrations of TrxA were 5 μM and 3 μM, respectively. In the study of the *Arabidopsis* PrxQ, Trx *x* was used with 0.4 mM DTT as reductant. The thioredoxin concentration in this case was 10 μM, *i.e.* more than twice the concentration used here. The peroxidase activity was measured by the FOX assay also in *Anabaena* as in *Arabidopsis*, but in *Synechococcus* the absorption of NADPH at 340 nm was monitored. The Trx *x* of *Arabidopsis* was the only endogenous Trx used as an electron donor for the PrxQ2. However, it corresponds to the TrxB of *Synechocystis*, not to the TrxA, which is an *m*-type Trx. In Pérez-Pérez *et al*., 2009, we reported that TrxQ is the

Synechocystis Trx with highest affinity for PrxQ2, but that TrxB is the most efficient electron donor for PrxQ2.

Since the PrxQ2 seems to be located in the thylakoid lumen or in the periplasm, none of the Trx used as reductant in our assays would actually interact physiologically with this kind of peroxiredoxin. No soluble Trx has been shown to be located in the thylakoid lumen, and therefore this function may be attributed to the thylakoid membrane anchored thioredoxin-like protein HCF164. *Synechocystis* possesses in its genome two ORFs, *sll1980* and *sll0685*, which encode two proteins homologous to the *Arabidopsis* HCF164, and both contain a possible N-terminal signal peptides in their amino-acid sequences. Neither of these putative HCF164 have been characterised in *Synechocystis* or other cyanobacteria, with the exception of TxlA in *Synechococcus*, which was reported to be involved in redox regulation of the structure and function of photosynthetic apparatus, although the authors propose that TxlA acts as a protein disulphide isomerase more than a thioredoxin (Collier and Grossman, 1995). Definitely, this is only the beginning of the knowledge on redox regulation in the thylakoid lumen and further investigations are necessary to understand completely the thiol-dependent signalling in this compartment and across the thylakoid membrane.

III – Thioredoxin-mediated redox regulation of a eukaryote type Ser/Thr kinase in the cyanobacterium *Synechocystis* sp. PCC 6803

The presence of a mechanism in cyanobacteria similar to the state transition in plants (Piven *et al*., 2005) could suggest the existence of a redox regulated Ser/Thr kinase similar to the one in algae (Depège *et al*., 2003) and plants (Bellafiore *et al*., 2005). The first eukaryotic type Ser/Thr kinase in prokaryotes was reported in 1991 (Muñoz-Dorado *et al*., 1991). Since then, the number of genes predicted to encode bacterial Ser/Thr kinases has increased steadily and they are widespread amongst prokaryotic genomes (Krupa and Srinivasan, 2005). However, the function of these kinases is not well studied in bacteria and no regulation of these enzymes has been described. Two Ser/Thr kinases have been suggested to be involved in redox signalling in bacteria. The Pkn22 kinase (Alr2502) from *Anabaena* sp. PCC 7120 has

been reported to be induced by iron starvation and oxidative stress and shown to regulate the expression of *isiA*, which is required for cell growth under iron-limiting conditions (Xu *et al*., 2003). Pkn22 forms a cluster with the peroxiredoxin PrxQA, which is thought to play a role in oxidative stress protection (Latifi *et al*., 2007). This kinase possesses in its amino acid sequence a N-terminal "Cys-motif" containing four cysteines and a C-terminal PbHI domain, which is composed by parallel beta-helix repeats. Proteins containing these repeats are usually enzymes with polysaccharide substrates and some of them belong to the amino acid metabolism of arginine and proline (Jenkins *et al*., 1998). PknG is a Ser/Thr kinase from *Mycobacterium tuberculosis* and it is an essential virulence factor (Walburger *et al*., 2004). The N-terminal part of this protein contains four cysteines grouped into two iron-binding motifs (Cys-X-X-Cys-Gly) characteristic for rubredoxins (Scherr *et al*., 2007). Rubredoxins act as electron donors in electron transfer reactions, so this domain has been suggested to play a regulatory role (Sieker *et al*., 1994; Scherr *et al*., 2007). The mutant version of PknG, in which the four cysteines of the rubredoxin domain were replaced with serine residues, was devoid of kinase activity. This suggests that PknG activity might be redox regulated via the rubredoxin domain (Scherr *et al*., 2007).

With this background, we decided to undertake the search for a Ser/Thr kinase in *Synechosystis* that undergoes redox regulation. *A priori*, the search for a Ser/Thr kinase should be easier than of a His kinase due to the lower number of predicted genes in *Synechocystis* (Kaneko *et al*., 1996; Leonard *et al*., 1998; Murata and Suzuki, 2006) and since the phosphorylation of His residues is more labile (Matthews, 1995). Hence, we firstly identified a protein phosphorylation sensitive to copper treatment, which was restored by reductants (Fig. 31 and 33). The analyses of the Ser/Thr kinase mutant strains revealed that SpkB is responsible for this redox-dependent phosphorylation (Fig.34). All Pkn2 type Ser/Thr kinases, with the exception of SpkD, contain Cys residues within the kinase domain, but SpkB and SpkF possess an aditional Cys motif in the N-terminus in a manner similar to that of *M. tuberculosis* PknG (Fig. 34). This suggested that both could be redox regulated, but only SpkB showed an altered pattern of phosphorylation in the cytosol. Since SpkF is predicted to be an integral membrane protein (Fig. 34) it may be responsible for the phosphorylation inhibited by copper treatment in membrane preparations (Fig. 31). The treatment with oxidised glutathione also caused inhibition of phosphorylation in

cytoplasmic extracts (Fig. 32). However, this inhibition was more drastic and global at high concentrations than the one displayed by copper. Since most of the signal visualised in the autoradiography should correspond to Ser/Thr/Tyr phosphorylation, the global effect of GSSG might involve a general inhibition of the Ser/Thr kinases in *Synechocystis*. It is consistent with the presence of cysteines in the kinase domain of almost all Ser/Thr in *Synechocystis* and with the idea here suggested of a redox regulation of the ATP-binding and hydrolysis as a global mechanism. Curiously, all Spk proteins, with the exceptions of SpkE (which is not a functional kinase), SpkA and SpkD, contain a cysteine in the ATP-binding region. Thus, the glutathione could bind the thiol group and block the ATP binding and, then, inhibit the kinase activity. However, this hypothesis needs to be tested.

In order to characterise the redox regulation of SpkB *in vitro* we carried out phosphorylation assays using extracts of *E. coli* expressing SpkB as well as a preparation of partially purified SpkB. Hence, we demonstrated that this kinase is inhibited by oxidants and that its activity is restored by reductants. The titration with TrxA displayed a restored activity higher than the basal one before the inactivation with copper (Fig. 37). This may be explained by a progressive oxidation during the storage of semi-purified SpkB previous to the assay. In the case of the inactivation by GSSG complete restoration of activity could not be achieved. So far, we have not been able to obtain absolutely pure preparations of SpkB due to extremely low expression levels in *E. coli*. However, the appropriate controls using *E. coli* extracts from non-expressing cells and mock purifications have enabled us make conclusive experiments regarding SpkB activity.

In the cytosolic extracts of the *Synechocystis* WT strain treated with copper or in those of the ΔSpkB mutant strain the phosphorylation of a protein of about 90 kDa is missing. The phosphorylation of this protein was reconstituted in cytosolic extracts from the ΔSpkB mutant by addition of partially purified SpkB. Applying proteomic approaches combined with radioactive labelling we could identify this SpkB target as GlyS, the β–subunit of the glycyl-tRNA synthetase. This enzyme was suggested to be subjected to redox regulation in *E. coli* (Ostrem and Berg, 1974; Profy and Schimmel, 1986; Hu *et al*., 2010), as well as in *S. aureus* (Niyomporn *et al*., 1968; Pöther *et al*., 2009) and in yeast (Kern *et al*., 1981). In addition, the activity of some aminoacyl-

tRNA synthetases, including glycyl-tRNA synthetase, has been reported to be modulated by phosphorylation in mice (Berg, 1977, 1978, 1980). Therefore, this enzyme could undergo a double post-translational regulation by direct redox-control and redox-dependent phosphorylation. Taking into account the possible double redox-regulation of the glycyl-tRNA synthetase this suggests an important role in the cellular redox homeostasis.

Aiming at elucidating the implication of the Cys motif in the redox regulation of SpkB, we constructed a truncated version of the kinase lacking this motif, termed β–SpkB. The truncated version displayed a very reduced kinase activity that was still inactivated by the copper treatment (Fig. 41). This result suggested that the Cys-motif was not involved in the redox modulation of SpkB, but in the kinase activity. However, the β–SpkB kinase activity was efficiently restored by reductants, such as DTT and TrxA (Fig. 42), indicating that indeed the Cys-motif is implicated in the redox control. Thereby, this domain could have a trigger effect on other cysteines as an electron donor, so when it is absent, the kinase is inactive, but in the presence of an external reductant the activity is restored. The presence of a thiol oxidant, such as $CuCl_2$ or GSSG, has the same effect as the absence of the Cys-motif; the target cysteine stays oxidised and then the kinase inactivated. As in PknG from *M. tuberculosis,* the Cys-motif could be a metal ion-binding domain. If so, the Cys-motif is not exactly a rubredoxin domain since only two of the four cysteines form a canonical iron-binding domain. The possibility that SpkB binds iron or another metal cannot be discarded. If it were true, this kinase could be a metal sensor or use this domain to receive a redox signal that is translated into a phosphorylation signal. Maybe the reason why we need a high concentration of copper is due to this metal is competing with the metal coordinated by the four cysteines and copper actually is inhibiting by displacement of the other metal. Supporting the hypothesis of the iron sensor, a mutant strain of *Anabaena* sp. PCC 7120 lacking the Ser/Thr kinase Pkn22 was growth-deficient under iron starvation (Xu *et al*., 2003). Iron deficiency generates oxidative stress, so the cell needs to adapt to survive under this conditions. Hypothetically, SpkB could sense the environmental iron levels and trigger a cellular response by means of modification of the amino acid metabolism in order to increase the cysteine pool to protect the cell against oxidative damage. In that case under normal conditions SpkB would phosphorylate GlyS and this enzyme would be active transferring the Gly to the

corresponding tRNA and under oxidative stress generated by iron starvation SpkB would not phosphorylate GlyS leaving this inactive, and the Gly would not be incorporated to the tRNA increasing the pool of free Gly, which could be used to synthesise cysteines. Free cysteines or incorporated into some molecules such as glutathione play a protective role against oxidative damage. It is worth noting that SpkB in vivo is present in the completely reduced, active form under normal growth conditions. Notably, under normal growth conditions *Synechocystis* SpkB is fully active as shown by the fact that the DTT treatment has no effect on SpkB activity in cytosolic extracts (Fig. 33 and Fig. 34).

In mammals some Ser/Thr kinases undergoing redox regulation have been reported. Protein kinase C (PKC), MEKK1 and c-Abl have been described to be inhibited by glutathionylation (Ward *et al*., 1998; Cross and Templeton, 2004; Leonberg and Chai, 2007). Both regulatory and catalytic domains of PKC contain cysteine rich regions that are targets for redox regulation (Gopalakrishna *et al*., 1995). The cysteines within the regulatory domain coordinate zinc atoms and a redox modification of these cysteines releases zinc promoting structural changes, which lead to constitutive activation of PKC (Gopalakrishna and Jaken, 2000). On the other hand the cysteines within the catalytic domain are susceptible to react with alkylating agents and glutathione, which irreversibly inactivate the enzyme (Ward *et al*., 1998; Gopalakrishna and Jaken, 2000). PKC activity is also sensitive to other oxidizing agents such as H_2O_2 or other peroxides (Gopalakrishna and Jaken, 2000). MEKK1 and c-Abl are both inactivated by alkylation and glutathionylation but in theses cases the inhibition by glutathionylation is reversible by treatment with some reducing agents such as DTT or glutaredoxin (Cross and Templeton, 2004; Leonberg and Chai, 2007). The cysteine residue that undergoes glutathionylation in MEKK has been located within the ATP-binding pocket of the kinase, this is an unconserved residue in other kinases (Cross and Templeton, 2004). In the case of c-Abl, it was reported that glutathionylation affects a cysteine present in the catalytic domain (Leonberg and Chai, 2007). Glutathionylation of a cysteine anywhere within the interior of the catalytic domain has been proposed as a general regulatory mechanism for kinases in mammals (Anselmo and Cobb, 2004). The *Synechocystis* SpkB possesses three cysteines in the kinase domain, and one or more of them are likely to be responsible for the redox regulation here reported. Glutathione could be blocking the ATP binding

or another type of interaction or function inside the catalytic domain and thus the role of Cys-motif could be the release of glutathione to maintain active the kinase activity. It might explain the incapacity of GSH to reactive SpkB, since its presence would favour the process of glutathionylation (Fig. 37). However, a data that support the glutathionylation of MEKK was that GSH was capable of reactivate this kinase (Cross and Templeton, 2004). Nonetheless, the glutathionylation may occur by direct interaction between an oxidised sulphydryl radical and GSH (Dalle-Donne *et al*., 2007). Hence, the hypothesis of a glutathione molecule linked to a cysteine within the kinase domain that inhibits SpkB could not be discarded. However, the inactivation of the partially purified SpkB by Cu^{2+} alone speaks against an exclusive role of glutathione and glutathionylation.

Further investigation is needed to completely explain the redox regulation mechanism of SpkB in cyanobacteria.

MATERIALS AND METHODS

MATERIALS AND METHODS

1. Organisms and culture conditions

1.1. Cyanobacteria

1.1.1. Cyanobacterial strains

The present work has been carried out using the cyanobacterium *Synechocystis* strain sp. PCC 6803 (hereafter called *Synechocystis*). *Synechocystis* is a unicellular cyanobacterium unable to fix nitrogen and it belongs to the taxonomic Group I (formerly Chroococcales) (Rippka *et al*., 1979). *Synechocystis* can grow under diverse physiological conditions, such as photoauto-, mixo-, and heterotrophycally. During this research the WT strain was used as well as different mutant strains, some of which were constructed here and others were gifts. In the Table 7 the mutant strains used are listed with their principal features.

Table 7. *Synechocystis* mutant strains used in the thesis

Strain	Features	Source
GST-FtsH2	Δ*ftsH2*::*ftsH2-gst*	Provided by Peter Nixon's Lab.
ΔFtsH2	Δ*ftsH2*::*npt*, Km^r	Here constructed
FtsH266	Δ*ftsH2*::*ftsH2C266S*::*aadA*$^+$, Sp^r St^r	Here constructed
ΔSpkA	Δ*spkA::npt*, Km^r	Lab. collection
ΔSpkB	Δ*spkB::npt*, Km^r	Lab. collection
ΔSpkC	Δ*spkC::npt*, Km^r	Lab. collection
ΔSpkD	Δ*spkD::npt*, Km^r	Lab. collection
ΔSpkE	Δ*spkE::npt*, Km^r	Lab. collection
ΔSpkF	Δ*spkF::npt*, Km^r	Lab. collection
ΔSpkG	Δ*spkG::npt*, Km^r	Lab. collection

1.1.2 Cyanobacterial culture medium and conditions

The different *Synechocystis* strains were grown at axenic conditions in a medium based on the BG11 described in Rippka *et al.*, 1979. The BG11 composition is:

$NaNO_3$	17.6 mM	Ammonium iron(III) citrate	6 mg/l
$MgSO_4$	0.30 mM	$MnCl_2$	9.1 µM
$CaCl_2$	0.24 mM	Na_2-EDTA	2.4 µM
Na_2CO_3	0.20 mM	Na_2MoO4	1.6 µM
K_2HPO_4	0.20 mM	$ZnSO_4$	0.8 µM
H_3BO_3	46 µM	$CuSO_4$	0.3 µM
Citric acid	28.5 µM	$CoCl_2$	0.2 µM

This medium supplemented with $NaHCO_3$ 12 mM is denoted BG11C, which was the medium used here. The medium BG11C was prepared from a solution 100 times concentrated, containing all components except K_2HPO_4, $NaHCO_3$ and $NaNO_3$, which were added to the medium just before being sterilized. Sterilisation of media and materials was carried out during 20 min in an autoclave under one atmosphere of over-pressure and at 120 ^oC. Ten g/l (1% w/v) of agar (Bacto-Agar, Difco) were added to prepare solid medium and was sterilised separately.

The liquid *Syechocystis* cultures were grown in 250 ml E-flasks containing 50 to 100 ml of medium. E-flaks were incubated at 30 ^oC under continuous illumination (25-50 $\mu Em^{-2}s^{-1}$) and with 100 rpm of constant stirring in orbital shakers (Gallenkamp INR.401.W model). Alternatively, cultures were bubbled with a stream of 1% (v/v) CO_2 in air under continuous illumination at light intensity of 50 to 70 $\mu Em^{-2}s^{-1}$ provided by fluorescents lamps (Sylvania daylight F20w/D). The bubbled cultures were grown in volumes of 750 ml medium in Roux flasks or at 150 ml in cylindrical flasks. Petri plates with *Synechocystis* plated on solid medium were incubated at 30 ^oC under continuous illumination (25-30 $\mu Em^{-2}s^{-1}$).

Antibiotics were added to culture media after their sterilisation by filtration. The final concentrations used of each of them were:

Kanamycin	50 μg/ml
Streptomycin	2.5-5 μg/ml
Spectinomycin	2.5-5 μg/ml

1.2. *Escherichia coli*

1.2.1. Strains of *E. coli*

The *E. coli* strains used and their genotypes are listed in the Table 8.

Table 8. Stains of *E. coli* used in this work

Strains	Genotype	Reference
DH5α	*F-, endA1, hsdR17 (mK+,rK-) supE44, thi-1 recA1 gyrA96 relA1 ΔlacU169 (Ø80-lacZΔM15)*	(Hanahan, 1983)
BL21(DE3)	*hsdS gal (λcIts857 ind1 Sam7 nin5 lac UV5-T7 gene1)*	(Studier y Moffatt, 1986)

Generally, the DH5α strain was used for cloning and the BL21(DE3) strain was used for the expression of proteins cloned into the pET vectors.

1.2.2. *E. coli* culture medium and conditions

The normal culture medium for the growth of the *E. coli* strains was the Luria-Bertani (LB) (Sambrook, *et al*., 1989). The LB composition was:

NaCl	10 g/l
Tryptone	10 g/l
Yeast extract	5 g/l

In order to prepare solid medium, a final concentration of 15 g/l (1.5% w/v) of agar (Bacto-Agar, Difco) was added to the LB prior to sterilisation. The sterilisation

was performed using the same conditions described above for the BG11C.

In addition, the LB medium was supplemented with different antibiotics depending on the purpose. The final concentrations of antibiotics were:

Ampicillin	100 μg/ml
Kanamycin	50 μg/ml
Spectinomycin	100 μg/ml

Different volumes of culture were used in different recipients, tubes and flasks, depending on the objective. Small volumes were used for DNA cloning and manipulation and bigger volumes for protein expression. As a rule, the volume of medium to inoculate comprised 1/5 of the capacity of the recipient. The liquid cultures as well as solid cultures were incubated at 37 ºC. Liquid cultures were stirred continuously at 200 rpm in New Brunswick Scientific shakers, model G25.

1.3. Harvesting of cells

Cyanobacterial cells as well as *E. coli* cells were harvested by centrifugation. Depending on the volume of culture a micro-centrifuge Eppendorf (13000 x *g*, 3 min) was used or a Beckman refrigerated centrifuge (9000 x *g*, 10 min), model Avanti J-25. Centrifugation was performed either at room temperature or at 4 ºC depending on the requirements.

2. DNA analysis and manipulation

2.1. Plasmids and primers

Commercial and gifts plasmids as well as the plasmids constructed here are listed in the Tables 9 and 10, where some important characteristics are described.

Table 9. Commercial plasmids and gifts

Plasmid	Features	Reference	Resistance
pGEMT	This vector carries terminal thymidines in both ends that allow the ligation of PCR products. It also contains the β-lactamase coding region, which allows selection of positive clones.	Promega	Ap
pET28a	Expression vector. The expression is under control of the promoter of T7 phage. This vector encodes an N-terminal and an optional C-terminal His-Tag.	Novagen	Km
pET24a	Expression vector. The expression is under control of the promoter of T7 phage. This vector adds a C-terminal His-Tag to the gene products.	Novagen	Km
pET22b	Expression vector. The expression is under control of the promoter of T7 phage. This vector encodes a C-terminal His-Tag.	Novagen	Ap
pFNT4	This plasmid derived from a pBS vector containing the whole *trxA* gene from *Synechocystis*.	(Navarro and Florencio, 1996)	Ap
pTrxA35	This plasmid derived from pET22b, into which the *trxA35* gene has been cloned. The vector adds a C-terminal His-tag to the protein.	(Lindahl and Florencio, 2004)	Ap

Table 10. Plasmids constructed in this work

Plasmid	Features	Resistance
pTrxA	pET22b vector containing the whole *trxA* gene cloned from pFNT4 in the restriction sites NdeI-XhoI. This plasmid was constructed to express and purify the His-tagged TrxA.	Ap
p1CP	pET24a vector containing the *slr1198* gene cloned by PCR from *Synechocystis* gDNA. The gene was inserted into the NdeI-XhoI restriction sites. This plasmid was constructed to express and purify the His-tagged 1-Cys Prx.	Km

p2CP	pET28a vector containing the *sll0755* gene cloned by PCR from *Synechocystis* gDNA. The gene was inserted into the NdeI-XhoI restriction sites. This plasmid was constructed to express and purify the N-terminal His-tagged 2-Cys Prx.	Km
pPQ2	pET28a vector containing the *slr0221* gene cloned by PCR from *Synechocystis* gDNA. The gene was inserted into the NdeI-XhoI restriction sites. This plasmid was constructed to express and purify the His-tagged PrxQ2.	Km
pUSP1	pET28a vector containing the *slr0244* gene cloned by PCR from *Synechocystis* gDNA. The gene was inserted into the NdeI-XhoI restriction sites. This plasmid was constructed to express and purify the His-tagged Usp1.	Km
pFtsH2	pGEM-T carrying the PCR that contains the *slr0228* gene plus 500 pb prior and after the gene. This vector was constructed to make the FtsH2 knock out mutant strain.	Ap
pΔFtsH	pGEM-T carrying the partially deleted and interrupted *slr0228* gene plus 500 bp before and after the gene. The partial deletion of *slr0228* was carried out by fusing the PCR products corresponding to the beginning of the gene plus the 500 bp upstream and the end of the gene plus the 500 bp downstream. A StuI restriction site was introduced in the fusion in order to replace the deleted sequence by a Km resistance gene. This plasmid was used to transform *Synechocystis* to generate the ΔFtsH2 mutant strain.	Ap, Km
pFtsH266	pGEM-T carrying the directed site mutant *slr0228* gene plus 500 bp before and after the gene, in which the cysteine 266 is replaced by a serine. At the end of the gene, a Sp/St resistance gene was inserted in a BamHI restriction site generated by PCR. This plasmid was used to transform and generate the site directed mutant FtsH266 *Synechocystis* strain.	Ap, Sp, St
pSpkB	pET28a vector containing the *slr1697* gene cloned by PCR from *Synechocystis* gDNA. The gene was inserted into the NdeI-XhoI restriction sites. This plasmid was constructed to	Km

	express and purify the His-tagged SpkB.	
pβ-SpkB	pET28a vector containing the *slr1697* gene lacking the N-terminal Cys motif. It was cloned by PCR from *Synechocystis* gDNA and inserted into the plasmid in the NdeI-XhoI restriction sites. This plasmid was constructed to express and purify the His-tagged β-SpkB.	Km
pGlyS	pET28a vector containing the *slr0220* gene cloned by PCR from *Synechocystis* gDNA. The gene was inserted into the NdeI-XhoI restriction sites. This plasmid was constructed to express and purify the His-tagged GlyS.	Km
pGlyQ	pET22b vector containing the *slr0638* gene cloned by PCR from *Synechocystis* gDNA. The gene was inserted in NdeI-HindIII restriction sites. This plasmid was constructed to express and purify the His-tagged GlyQ.	Ap

The primers used in this work were synthesised by SIGMA-ALDRICH. They are detailed in the Table 11, including their sequences and their use.

Table 11. Synthetic primers used in this work

Primer	Sequence	Use
1CPF	5'-GCTACATATGGCCTTACAACTCGGTGATG-3'	Used to clone the *slr1198* gene into the pET24a vector
1CPR	5'-GCTACTCGAGCTTATTGGGTTGGGGGGTC-3'	
2CPF	5'-GCTACATATGACAGAGGTATTAAGGGTAG-3'	Used to clone the *sll0755* gene into the pET28a vector
2CPR	5'-GCTACTCGAGCTAAGGTTCCGCCACTGTCTC-3'	
PQ2F	5'-CCTGGGGCATATGCAACCAGAGTTG-3'	Used to clone the *slr0221* gene into the pET28a vector
PQ2R	5'-CGGGATTATTTACGTCGACGGGGAG-3'	
USP1F	5'-CAAGGAACTCAATTCATATGCTTAGCAAA-3'	Used to clone the *slr0244* gene into the pET28a vector
USP1R	5'-CCGGGAAACAAAGCTCGAGCTAAGCCTTG-3'	
FtsHUF	5'-GGTCAGAAATGTAGGTAACATC-3'	Used to clone the *slr0228* plus the 500 pb adjacent to both sides of the gene into the pGEN-T vector
FtsHLR	5'-CCGACGTGGGTTGCTGTGCAGAAG-3'	
FtsHUR	5'-GATAGGCCTTGGGGATTTAGTGTAATCGGTTAAC-3'	Used, along with FtsHUF and FtsHLR, to make the FtsH2 knock-out mutant
FtsHLF	5'-CCAAGGCCTATCCCAACCAATTTAGTATGGTCAG-3'	

		construction
FtsHCSF	5'-GAATGCCCCCAGTTTGATCTTC-3'	Used, along with FtsHUF and FtsHLR, to make the FtsH2 site directed mutant construction, in which the Cys 266 was replaced with a serine
FtsHCSR	5'-GAAGATCAAACTGGGGGCATTC-3'	
FtsHCSLF	5'-GATTCTTCGGATCCGGGCTTTTTTC-3'	
FtsHCSLR	5'-GAAAAAAGCCCGGATCCGAAGAATC-3'	
SpkBF	5'-CTGGTGAACCCATATGAGTTTTTGCG-3'	Used to clone the *slr1697* gene into the pET28a vector
SpkBR	5'-GCTTGGTTTGGTCAGAAACACTCGAGATT-3'	
β-SpkBF	5'-GTGGGCATATGCTGCGCCTC-3'	Used, along with SpkBR, to clone the *slr1697* gene lacking the Cys motif into the pET28a vector
GlySF	5'-GCTCCCTTGCCATATGCCCCTGC-3'	Used to clone the *slr0220* gene into the pET28a vector
GlySR	5'-GGAGGCCTCGAGGACATTTAAAAC-3'	
GlyQF	5'-CTTGTTGGCTTCATATGACCATTACTTTCC-3'	Used to clone the *slr0638* gene into the pET22b vector
GlyQR	5'-GTTTTTAAATCAAGCTTTACGAGGGAAA-3'	

2.2. DNA isolation

2.2.1. Plasmid DNA isolation from *E. coli*

In order to isolate plasmid DNA from *E. coli* at small scale we used a method developed by Birnboim and Doly, 1979, based on alkaline lysis of cells in the presence of sodium dodecyl sulphate (SDS) and NaOH. Genomic DNA as well as the proteins were removed by precipitation with potassium acetate. The procedure was carried out as described in Sambrook *et al.*, 1989. As an option, the plasmid DNA preparations were treated with a solution of phenol:chloroform (1:1, v/v) in order to reduce the protein content. The plasmid DNA was precipitated at -20 °C by 2.5 volumes of absolute ethanol. Thereafter, the DNA was resuspended in deionised water or in 10 mM Tris-HCl pH 8. To eliminate the RNA present in the sample the preparations were treated during 1 h at 37 °C with Ribonuclease A from bovine pancreas (SIGMA-ALDRICH). When a high quality preparation of plasmid DNA was required the commercial kit "GFX Micro Plasmid Prep Kit" (GE Healthcare, UK) was used following the manufacturer's instructions.

2.2.2. Cyanobacterial genome DNA isolation

The method used to isolate the gDNA from cyanobacteria was described in Cai and Wolk, 1990, and is based on cell lysis using glass beads. Cells were harvested from a 35 ml liquid BG11C culture by centrifugation at 4 ºC. The pellet of cells was resuspended in 400 μl TE (10 mM Tris-HCl pH 8, 0.1 mM EDTA pH 8). A volume of 150 μl of glass beads (diameter 0.25-0.3 mm, SIGMA-ALDRICH), 20 μl 10 % (w/v) SDS and 400 μl phenol:chloroform (1:1, v/v) were added to the cell suspension. This mixture was subjected to 10 cycles of vortexing 1 min followed by 1 min of incubation on ice. The lysate was centrifuged for 15 min at 4 ºC at 12000 x *g* and the supernatant was subjected to sucessive treatments with 400 μl phenol:chloroform (1:1, v/v). The released gDNA was precipitated with 2 volumes of cold ethanol and 0.3 M sodium acetate. Finally, the precipitated gDNA was resuspended in 50 μl TE and the remaining RNA was removed by Ribonuclease A from bovine pancreas (SIGMA-ALDRICH) treatment.

2.3. DNA analysis and quantification

2.3.1. DNA electrophoresis in agarose gels

Electrophoretic resolution of DNA in agarose gels was carried out as described in Sambrook *et al*., 1989. The gels were made in TBE 0.5X (45 mM Tris-borate, 1 mM EDTA, pH 8) buffer containing 0.7-1.5% (w/v) agarose and 5 μg/ml ethidium bromide. The electrophoresis was run in Mini Sub-cell GT systems (Bio-Rad). DNA loading buffer was added to every sample in a proportion of 1/10. The composition of loading buffer was 0.25% (w/v) bromophenol blue, 0.25% (w/v) xilene cyanol FF and 50% (v/v) glycerol. The molecular weight marker used to infer the molecular weight of the DNA molecules migrated was the 1kb DNA Ladder (Invitrogen). After the electrophoresis the DNA was visualised by illumination with UV light in a Bio-Rad transilluminator model GelDoc XR.

2.3.2. DNA quantification

The fluorescence emitted by the ethidium bromide intercalated into the double DNA helix is proportional to the amount of DNA. Thus, in order to estimate the DNA concentration, the fluorescence emitted by the samples under UV illumination was compared to that emitted by the molecular marker of known concentration.

DNA was also quantified spectrophotometrically. DNA absorbs at 260 nm wavelength and 1 unit of absorbance at 260 nm in a cuvette with 1 cm pathlength corresponds to 50 μg/ml of DNA.

2.3.3. DNA extraction from agarose gels

To purify DNA bands from the agarose gels we used the commercial system "GFX PCR and Gel Band purification" (GE Healthcare, UK) following the manufacturers' instructions.

2.3.4. Enzymatic manipulation of DNA

The DNA enzymatic digestions were carried out by restriction nucleases provided by Takara, Roche and New England BioLabs. The dephosphorylation of vector ends cut open with restriction enzymes was performed by treatment with alkaline phosphatase provided by Roche. For sticky end DNA fragments, cut with restriction enzymes leaving the 5'-strand protruding, filler treatments were performed with the Klenow fragment of DNA polymerase I from *E. coli* supplied by Promega. The ligation of DNA fragments was carried out by treatment with DNA ligase of phage T4 provided by Promega. In all cases the treatments were made according to the manufacturers' instructions.

2.4. Polymerase Chain Reaction (PCR)

PCR reactions were performed in a Mastercycler 5330 Eppendorf device. Each PCR reaction was performed in a volume of 100 μl containing 2.5 U of Biotaq

polymerase (Bioline), Biotaq buffer (supplied with enzyme) 1.5 mM $MgCl_2$, dNTPs at final concentrations of 0.2 mM each, 1.5 ng of template DNA and 50 pmol of each primer. Oligonucleotides used are listed in Table 11. Generally, the amplification program consisted of an initial denaturation cycle at 94 °C for 5 min, followed by 30 cycles of reaction and a final polymerization cycle at 72 °C for 10 min. Each reaction cycle consisted of a denaturing stage at 94 °C (1 min), a renaturation step at 45-65 °C (1 min) and a polymerization step at 72 °C (1 minute per kb of DNA to be amplified). The amplified DNA fragments were subjected to agarose gel electrophoresis and purified essentially as described in section 2.3.3.

2.5. DNA sequencing

The sequencings were carried out by the commercial service MWG Biotech (Germany). The samples were prepared to sequencing according to the service instructions.

2.6. Introduction of DNA into different organisms by transformation

2.6.1. *E. coli* transformation

Competent cells of the different strains of *E. coli* were supplied by the responsible service of the Instituto de Bioquímica Vegetal y Fotosíntesis. In order to transform the DH5α competent cells, the exogenous DNA (in a volume maximum volume of 10 μl) was gently mixed with an aliquot of competent cells (100 μl) thawed on ice. After 30 min incubation on ice, the mixture was subjected to 2 min heat shock at 42 °C followed by 2 min on ice. Subsequently, 0.9 ml of LB medium was added and, then, the mix was incubated for one hour at 37 °C. Then the cells were spread on solid LB medium with the antibiotic suitable for selecting transformants or were used to inoculate a liquid culture. When we used plasmids and *E. coli* strains, which allow identifying the clones carrying recombinant molecules due to inactivation by insertion of lacZ gene, the medium was supplemented with 0.2 mM IPTG and 40 mg/ml X-gal. Colonies with recombinant plasmids had white colour, whereas negative colonies

were blue.

The BL21(DE3) competent cells were transformed by electroporation. For this transformation, 1-2 μg of plasmid DNA, in a maximum volume of 5 μl, was mixed with 100 μl of competent cells and the mixture was incubated on ice for 5 min. Subsequently, it was transferred to a Gene Pulser cuvette (BioRad), which had 2 mm of distance between the electrodes, and was subjected to an electric pulse of 2500 V in a Easyject Optima (Equibio) device. Immediately, 1 ml of cold LB was added and the mixture was incubated 1 h at 37 °C. Finally, the cells were spread on LB plates with the appropiate antibiotic to select the transformant clones or they were inoculated directly in liquid LB cultures.

2.6.2. *Synechocystis* transformation

Synechocystis sp. PCC 6803 is naturally capable of incorporating into the cell DNA molecules from the culture medium. Once inside, if these DNA molecules have homology to any sequence of the genome, they are stably integrated into the genome by recombination. The principle for mutagenesis and introduction of exogenous DNA fragments in *Synechocystis* sp. PCC 6803 is based on this property. Therefore, if a fragment of DNA (exogenous DNA or an antibiotic resistance gene) is flanked by sequences homologous to the genome sequences, the exogenous DNA fragment is incorporated in at least one chromosome copy.

The *Synechocystis* transformation method is based on that described by Chauvat *et al*., 1986. Cultures were grown until they reached a OD_{580nm} equal to 1. A volume of 50 ml of culture was harvested by centrifugation and the cells were washed twice with fresh medium to eliminate possible extracellular nucleases. After washing, cells were resuspended in 1 ml fresh medium that was distributed in aliquots of 200 μl in polystyrene tubes of 10 ml (Soria Greiner S.A.) and the DNA was added. Each transformation was carried out typically with 2 μg of purified DNA. The cell and DNA mixture was incubated for 1.5 hours under normal light conditions. After this time, the cells were spread on solid BG11C plates, without antibiotics, over 85 mm diameter Nucleopore filters (Whatman). After a period of 20 h to allow the expression of resistance genes, introduced by the foreign DNA, the filters were moved to plates

containing the appropriate antibiotic, *e.g.* 50 μg/ml kanamycin or 2.5 μg/ml of spectinomycin and streptomycin. Antibiotic resistant colonies appeared after 8-10 days of incubation. To force segregation of mutant chromosome copies, filters were transferred to new plates with increasing concentrations of antibiotics.

The degree of segregation of mutant chromosomes was analysed by PCR, performed as explained in section 2.4., using gDNA isolated from the mutant strains using the primers listed in the Table 11.

2.7. Site directed mutagenesis

The site directed mutagenesis was performed using an overlapping PCR approach in which two complementary synthetic primers were designed containing the site directed mutation. These oligonucleotides, along with two other external primers, were used to amplify the gene of interest into two separate fragments. Based on these fragments we carried out the overlapping PCR that could be divided into three steps:

1. Overlapping of the complementary sequence. At this stage both PCR fragments were denatured and hybridised together through the complementary sequence, corresponding to the primers that carry the mutation. To facilitate the hybridisation, the temperature dropped gradually from 95 °C to 72 °C at a rate of 0.01 °C/s. The reaction mixture only contained in this step the enzyme buffer and the two PCR fragments in a proportion of 1:1.

2. Complementary chain polymerisation step. This phase completed the polymerisation of each DNA chain from its 3' end, generating a double-stranded fragment resulting from the merge of the two initial PCR fragments. At this stage the polymerase enzyme and the dNTPs were added to the reaction mix. The cycle ran for 10 min at 72 ° C.

3. Reaction cycles. The double-stranded fragment obtained in the previous

step was used as a template to start the typical PCR reaction cycles described above (2.4. section), which consists of denaturation, renaturation and polymerization. In this phase, the addition of specific external primers is necessary. After 30-35 cycles the PCR was completed with a polymerisation cycle of 5 min at 72 °C.

3. Protein synthesis, purification and analysis

3.1. Protein expression in *E. coli*

For the expression of various proteins used in this study we used a heterologous expression system in *E. coli*, cloning the gene under the control of the phage T7 promoter (pET series plasmids supplied by Novagen). To induce expression of the genes cloned, *E. coli* BL21 (DE3) cells were used, since they carry the gene encoding the T7 RNA polymerase under the control of the lacUV5 promoter. Thus, the gene is inducible by isopropyl-β-thio galactopyranoside (IPTG).

Transformed *E. coli* BL21 (DE3) cells were cultured at 37 °C in LB medium with the appropriate antibiotic until the culture reached an OD_{580nm} equal to 0.5. Subsequently, gene expression was induced by addition 1 mM IPTG and the culture incubation was continued for 2-4 hours, before collecting the cells.

3.2. Preparation of cell extracts

3.2.1. Cell lysis using glass beads

Generally, the cell extracts from *Synechocystis* and small quantities of *E. coli* were prepared by breakage with glass beads. To this end, cultures were harvested by centrifugation and the pellet was resuspended in a small volume of buffer 25 mM Tris-HCl pH 8, 50 mM NaCl. This suspension was divided into Eppendorf tubes in aliquots of a maximum volume of 500 μl and an amount equivalent to 50 μl of glass beads (0.25 to 0.30 mm in diameter, SIGMA-ALDRICH) per 100 μl of suspension was added. Phenyl

methyl sulfonyl fluoride (PMSF), a serine prtease inhibitor, was added to a final concentration of 1 mM. This mixture was subjected to ten pulses of 1 min of vigorous stirring alternating with periods of 1 min on ice. Cellular debris and insoluble proteins were separated from the soluble fraction by centrifugation for 30 minutes at 13000 x *g* at 4 °C. The supernatant constituted the cell-free crude soluble extract.

3.2.2. Cell lysis by sonication

This method was used for large volumes of *E. coli* cultures (1-1.5 l). The harvested cells were resuspended in 25 mM Tris-HCl pH 8, 50 mM NaCl buffer and PMSF was added to a final concentration of 1 mM. The cell suspension was kept on ice and sonicated in 6 pulses of 30 s separated by 30 s cooling intervals. The frequency of ultrasound produced by a Branson sonicator model B12, was 20 KHz and the power was 40 W. After lysis, the cell lysate was subjected to centrifugation for 30 minutes at 18 000 x *g* and 4 °C. The supernatant constituted the cell-free crude soluble extract.

3.2.3. Preparation of *Synechocystis* total membranes

Synechocystis cultures were grown photoautotrophically with bubbling at 30 °C under continuous illumination with white light at an intensity of 50 $\mu Em^{-2}s^{-1}$. Cells of exponentially growing cultures were harvested and broken with glass beads in a buffer containing 25 mM HEPES-NaOH pH 7.0, 15 mM $CaCl_2$, 5 mM $MgCl_2$, 15% (v/v) glycerol and 1 mM PMSF (Buffer A). Unbroken cells were removed by centrifugation at 2300 x *g* for 5 min and total membranes were thereafter pelleted by centrifugation at 16000 x *g* for 20 min. The pellet was washed once by resuspension in Buffer A and centrifugation at 16000 x *g* for 20 min. Finally, the membranes were resuspended in Buffer A to a chlorophyll concentration of 1 mg/mL, which corresponded to a protein concentration of 23 mg/ml. The chlorophyll concentration was measured as described in section 6.1., and the protein concentration was determined according to section 3.3.

3.3. Protein quantification

The protein concentration of intact cells, cell extracts and isolated proteins

were determined by applying the modification of the Lowry method (Lowry *et al*., 1951) described in Markwell *et al*., 1978. For this method the Folin-Ciocalteu's reagent (Merk, Germany) was used. The method described by Bradford (Bradford, 1976) was also used to quantify proteins. In this case we used a BioRad reagent according to the manufacturer's instructions. In both cases we used known concentrations of commercial BSA (Sigma) to make the calibration curve.

3.4. Protein electrophoresis

3.4.1. 1-D SDS-PAGE

The analytical separations of proteins using denaturing electrophoresis in polyacrylamide gels were performed based on the Laemmli system (Laemmli, 1970) as described in (Sambrook *et al*., 1989), using Miniprotean BioRad II or III apparatuses. Stacking and separating gels as well as electrode buffer contained 0.1% (w/v) SDS (sodium dodecyl sulphate). The concentration of polyacrylamide (acrylamide: bisacrylamide 29:1) in separating gels varied between 10 and 15% (w/v) depending on the molecular mass of the proteins analysed. Samples were mixed with an equal volume of solubilising buffer, containing: 0.125 M Tris-HCl pH 6.8, 20% glycerol (v/v), SDS 4% (w/v), 2-mercaptoethanol 10% (v/v) and bromophenol blue 0.0025% (w/v). When the SDS-PAGE was performed under non-reducing conditions the 2-mercaptoethanol was omitted. In some cases indicated in the text the 2-mercaptoethanol was replaced with 50 mM DTT to reach reducing conditions. Denaturation of samples was carried out by heating at 65 °C for 5 minutes and the electrophoresis was run at room temperature by applying a constant voltage of 200 V for 45-60 minutes.

We used the molecular mass standards Low Molecular Weight Range provided by BioRad, which contains the following proteins: rabbit muscle phosphorylase B (97.4 kDa), bovine serum albumin (BSA) (66.2 kDa), chicken ovalbumin (45.0 kDa), bovine carbonic anhydrase (31.0 kDa), soybean seed trypsinogen inhibitor (21.5 kDa) and hen egg lysozyme (14.4 kDa). The SeeBlue Pre-Stained Standard (Invitrogen) was also used, containing the following proteins: myosin (250 kDa), BSA (98 kDa),

glutamic dehydrogenase (64 kDa), alcohol dehydrogenase (50 kDa), carbonic anhydrase (36 kDa), myoglobin (30 kDa), lysozyme (16 kDa) aprotinin (6 kDa) and insulin, B chain (4 kDa).

3.4.2. Two dimensional protein electrophoresis

3.4.2.1. Non-reducing/reducing 2-D SDS-PAGE

This method was used to isolate the putative Trx-targets after purification of protein complexes by Ni-affinity chromatography. Thus, the imidazole eluates containing target-Trx mixed disulphides from Ni-affinity chromatography were subjected to 2-D SDS-PAGE under nonreducing/reducing conditions as described in Lindahl and Florencio, 2004. For the first dimension, 150 μl of eluate was mixed with 10 μl of SeeBlue Prestained protein standard (Invitrogen) and 50 μl of solubilising buffer without reductant consisting of 0.25 M Tris-HCl pH 6.8, 12.5% v/v glycerol and 10% w/v SDS. The mixture was loaded on a 10% acrylamide gel, 16 x 18 cm and 1.5 mm thick (Amersham Biosciences). The electrophoresis was carried out by applying a maximum voltage of 220 V and a constant current of 35 mA per gel at room temperature for about 4 h. The second dimension was carried out under reducing conditions, which allowed the release of the target proteins. The gel lanes containing the proteins were excised, incubated for 1 h at room temperature in solubilisation buffer diluted 2.5 times and supplemented with DTT to a final concentration of 100 mM and were mounted at the top of the second dimension 10% acrylamide gels. Electrophoresis was performed in the same way as for the first gel. The gels were run using a SE600 Hoefer system.

3.4.2.2. 2-D IEF/SDS-PAGE

The *Synechocystis* cytosolic extracts were prepared as described in 3.2.1. section. The protein samples were salt precipitated and washed by means of the commercial system 2-D Clean Up Kit (GE Healthcare) and resuspended in DeStreak rehydratation Solution (GE Healthcare) supplemented with ampholytes with a pH range of 3-10 (BioRad) at 0.5%, following the manufacturer's instructions. The samples were separated in the first dimension according to their isoelectric point,

using acrylamide strips with immobilized pH "DryStrips Immobiline gel (GE Healtcare) with pH range of 4-7. The sample was loaded by an active rehydration at 20 °C for 12 h. The IEF was performed applying the program according to the manufacturer's instruction depending on the strip used. For the indicated strips the focusing took place in four steps: S1: 250 V, 15 min, S2: 250 to 8000 V, 2 h 30 min; S3: 8000 V, 35000 Vh, S4: 500 V. Both rehydration and focusing were performed in a Protean IEF Cell (BioRad) device. After IEF, and before the second dimension, strips were immersed in equilibration solution (6 M Urea, 2% SDS (w/v), 375 mM Tris-HCl pH 8.8, 20% glycerol (p/v)) initially supplemented with 130 mM DTT for 15 min and subsequently with 135 mM IAA for 15 more min. The incubation with the SDS solution was necessary to confer a negative charge to the proteins and DTT treatment broke all disulfide bonds, leaving each protein in its reduced state. The IAA prevented the re-oxidation of proteins during electrophoresis. After that, the strips were washed in electrophoresis buffer and placed horizontally over the second dimension acrylamide gels and fixed with agarose solution (0.5% agarose (w/v) and 0.002 % bromophenol blue (w/v) in electrophoresis buffer). Acrylamide concentrations ranged between 10 and 15%. Thus, the second dimension was performed as a normal SDS-PAGE, in which proteins are separated according to their molecular mass, at a fixed current of 70 mA. The gels were run in a SE600 Hoefer system.

3.5. Protein staining

After the electrophoresis the proteins were visualised by CBB-staining. Hence, the gels were immersed in a solution of 0.1% (w/v) Coomassie blue R-250 (SIGMA-ALDRICH), 10% (v/v) acetic acid and 40% (v/v) methanol. After 15 minutes staining at room temperature, gels were washed several times with a 40% methanol (v/v) and 10% (v/v) acetic acid solution. After this treatment, the proteins appeared as blue bands or spots.

3.6. Protein identification by peptide mass fingerprinting (PMF)

CBB-stained proteins were excised manually from the gels, destained, dried

and digested with trypsin by rehydration in 100 μl of 50 mM NH_4HCO_3 with the addition of 15 μl of 0.1 mg/ml trypsin in 1 mM HCl overnight at 37 ºC. Peptides were extracted with 20 μl of 0.5 % TFA, 0.5 μl of each sample was applied on the sample plate and MALDI-TOF MS spectra were acquired on an Autoflex apparatus (Bruker Daltonics). External calibration was performed using Peptide Calibration Standard (Bruker Daltonics) and the trypsin autodigestion products of *m/z* values 842.5094 and 2211.1046 were used for internal calibration. Proteins were identified as the highest ranked result by searching the databases NCBInr 20061215 or MSDB 20050929, including all species, using the MASCOT search engine (Matrix Science). The search parameters included carbamidomethylation of cysteines, oxidation of methionines, one miscleavage by trypsin and between 30 and 80 ppm mass accuracy.

3.7. Protein inmunodetection (Western blot)

The proteins subjected to electrophoresis on polyacrylamide gel were transferred to nitrocellulose membranes (Bio-Rad) of 0.45 mm pore size, in a semidry transfer system (Biometrics), following the instructions of manufacturer. Both gel and nitrocellulose membrane were wet in transfer buffer (49.4 mM Tris pH 8.3, 39 mM glycine, 1.3 mM SDS and 20% methanol (v/v)) and, after that, the transfer was carried out at room temperature for 60-90 min, depending on size of the proteins to be transferred, at 2.5 mA per cm^2 of gel and a maximum of 20 V. The efficiency of transfer was checked by the disappearance of pre-stained standard from the gel. After the transfer, the membrane was incubated for at least 1 h in blocking solution consisting of 5% skimmed milk powder La Asturiana and 0.1% Tween 20 in PBS buffer (26 mM NaCl, 0.54 mM KCl, 0.8 mM Na_2HPO_4, 0.352 mM KH_2PO_4). Subsequently, the membrane was incubated with the antiserum appropriately diluted in blocking solution for 15 h at 4 °C and constant gentle shaking. Afterwards, the membrane was subjected to 4 washes of 15 min in washing solution, which consists of PBS buffer supplemented with 0.1% Tween 20 (v/v). After washing the incubation with the secondary antibody was performed. Hence, the goat anti-rabbit immunoglobulin G, conjugated with horse-radish peroxidase (Boehringer Mannheim) diluted (1:10000) in the blocking solution was incubated for 1 hour at room temperature and constant shaking. Then, the washing process was repeated as described above. The detection of peroxidase

activity was carried out using the commercial system ECL Plus (GE Healthcare) following the manufacturer's instructions.

3.8. Protein gel drying

The stained gels containing radioactively labelled proteins were dried before autoradiography. The gels were incubated in a 10 % glycerol solution for 30 min. Thereafter, the gels were placed between two sheets of Cellophane Support (BioRad) and they were dried in a Gel Dryer Model 583 (BioRad) for 2 h at 80 ºC.

3.9. Detection of radioactivity

To detect the radioactive signal of the radioactively labelled proteins separated in acrylamide gels we used the Cyclone Storage Phosphor autoradiography system (Packard). Alternatively, the dried gels were subjected to autoradiography by exposure of the Kodak film X-OMAT model S or X-OMAT model LS in an exposure cassette (SIGMA-ALDRICH) using Lightning Plus intensifying screens (Dupont) at -80 ºC. After the exposure time, the films were developed using developing and fixing reagents supplied by Kodak following the manufacturer's instructions.

3.10. Protein purification

3.10.1. Metal affinity chromatography

The His-tagged proteins were purified by nickel-affinity chromatography in a manual system using the matrix (His-Bind Resin, Novagen) packaged into a plastic column, Poly-Prep Chromatography Columns (BioRad), or by using 1 ml Hitrap columns connected to the Äkta FPLC system of Amersham Biosciences according to manufacturer's instructions. In both cases the columns were washed with 5 column volumes of distilled water, loaded with 50 mM $NiSO_4$ and the excess was washed off with 5 volumes of distilled water. For both purification methods the binding buffer

was composed of 20 mM Tris-HCl pH 8, 500 mM NaCl, and the elution buffer was composed of 20 mM Tris-HCl pH 8, 500 mM NaCl and 500 mM imidazole.

3.10.2. Gel filtration

We used a preparative column HiLoad 16/60 Superdex 75 (Amersham Biosciences) with an inner diameter of 16 mm, which was filled with porous agarose beads bound covalently to dextrane, that could separate proteins, the molecular mass of which are between 3000 and 70000 Da. The column was connected to a Äkta FPLC system (Amersham Biosciences) and a cooling bath for maintaining the temperature at 4 °C. The column was equilibrated with two volumes of a buffer containing 50 mM Tris-HCl pH 8 and 150 mM NaCl, previously filtered and vacuum degassed to remove impurities and gases. The sample was passed through a filter of 0.2 μm pore size before injection into the FPLC. The same buffer was used to elute the sample. Each protein eluted in fractions corresponding to its molecular mass.

3.10.3. Proteins purified in this work

In the Table 12 are listed the proteins purified during the course of this research along with the method used for purification.

Table12. Proteins purified during the course of this work

Protein	Plasmid	Purification method
TrxA	pTrxA	Ni-affinity chromatography
TrxA35	pTrxA35	Ni-affinity chromatography
		Gel filtration chromatography
1-Cys Prx	p1CP	Ni-affinity chromatography
2-Cys Prx	p2CP	Ni-affinity chromatography
PrxQ2	pPQ2	Ni-affinity chromatography
Usp1	pUSP1	Ni-affinity chromatography

SpkB	pSpkB	Ni-affinity chromatography
β-SpkB	pβ-SpkB	Ni-affinity chromatography
GlyS	pGlyS	Ni-affinity chromatography
GlyQ	pGlyQ	Ni-affinity chromatography

3.10.4. Trx-target isolation

3.10.4.1. Isolation of membrane-bound Trx-target protein complexes

A suspension of *Synechocystis* total membranes (See 3.2.3. section) in Buffer A (25 mM HEPES-NaOH pH 7.0, 15 mM $CaCl_2$, 5 mM $MgCl_2$, 15% (v/v) glycerol and 1 mM PMSF) at a protein concentration of 9.4 mg/ml was incubated in a final volume of 2.5 ml for 16 h at 4 ºC under gentle agitation with 2.5 mg of the His-tagged recombinant TrxA35, in which the second cysteine of the active site has been substituted for a serine. The suspension was centrifuged at 16000 x *g* for 30 min yielding a supernatant, which was denoted fraction I. The pellet was resuspended to 1.75 ml in 20 mM Tris-HCl pH 8.0, 0.75 M NaCl and 0.02% (v/v) Triton X-100, kept on ice for 30 min and centrifuged at 16000 x *g* for 30 min. The supernatant was collected and named fraction II. The pelleted membranes were resuspended to a volume of 800 μl in 20 mM Tris-HCl pH 8.0, an equal volume of 2.6% (w/v) *n*-dodecyl-β-D-maltoside (Roche Diagnostics) in 20 mM Tris-HCl pH 8.0 was added and the mixture was subsequently incubated for 30 min at 4 ºC under gentle agitation. The resulting solubilised membranes were named fraction III. Each of the fractions I, II and III were added to 500 μl of His-bind Ni-affinity matrix (Novagen) and incubated for 2 h at 4 ºC under gentle agitation. Following incubation, the His-bind resin was allowed to settle and the supernatant containing unbound proteins was removed. The His-bind matrix was washed four times with 1 ml of 20 mM Tris-HCl pH 8.0, 0.5 M NaCl (Buffer B) and thereafter three times with 0.5 ml of Buffer B containing 60 mM imidazole to remove weakly bound contaminants, and three more times in 1 ml Buffer B without supplements. Finally, the TrxA35-target protein complexes were released by addition of 120 μl Buffer B containing 1 M imidazole and incubated at 4 ºC with gentle agitation for 1 h. For fraction III, Buffer B was supplemented with 0.1% *n*-dodecylmaltoside. The

supernatant containing unbound proteins from fraction III was subjected to centrifugation at 16000 x *g* for 15 min. The pellet, which contained non-solubilised and/or precipitated membrane proteins was resuspended in 500 μl of 20 mM Tris-HCl pH 8.0 containing 8 M urea and centrifuged at 16000 x *g* for 15 min. The resulting clear supernatant, fraction IV, was added to 250 μl of His-bind matrix, which was thereafter treated as described above, except that Buffer B included 4 M urea.

3.10.4.2. Isolation of lumenal Trx-target proteins complexes

In each experiment 1 mg of recombinant histidine-tagged TrxA35 was bound to the Ni-affinity matrix and 10 ml of lumenal fraction containing about 2 mg of total protein was applied. After washes, the target-TrxA35 mixed disulphides were eluted in 250-μl fractions with binding buffer containing 1 M imidazole. The binding buffer composition was 20 mM Tris-HCl pH 8.0, 0.5 M NaCl. The wash buffer was binding buffer containing 60 mM imidazole.

3.11. Protein concentration

The concentration of proteins was carried out, either in Amicon concentrators (Millipore), using ultrafiltration membranes with a cut-off from 3 to 30 kDa, or using Vivaspin 500 (Sartorius Stedim Biotech) with a molecular mass cut-of of 30 to 50 kDa, in a refrigerated Eppendorf centrifuge. The method used, the time of concentration and the molecular mass cut-off depended on the protein, the starting volume and the desired final volume. These methods were also used for removal off salts, urea or imidazole from the protein preparations. The Vivaspin concentrators were also used to remove copper and GSSG after oxidative tretatments.

3.12. Production of polyclonal antibodies

Specific polyclonal antibodies against *Synechocystis* 2-Cys Prx were obtained at the Centro de Production y Experimentación Animal of the Universidad de Sevilla. In order to generate the antibodies, 0.75 mg of purified protein was injected

subcutaneously for each rabbit.

4. Enzymatic assays

4.1. Peroxidase assay

Peroxide decomposition catalyzed by Prx was measured using the ferrous ion oxidation (FOX) assay in the presence of xylenol orange as described in Wolff, 1994. The FOX1 reagent was composed of 100 μM xylenol orange (SIGMA-ALDRICH), 250 μM ammonium ferrous sulphate, 100 mM sorbitol and 25 mM H_2SO_4. Hydroperoxides oxidise selectively ferrous to ferric ions in dilute acid and the resultant ferric ions can be determined using ferric-sensitive dyes as an indirect measure of hydroperoxide concentration. Xylenol-orange binds ferric ion with high selectivity to produce a coloured (blue-purple) complex with an extinction coefficient of 1.5 $x10^4$ $M^{-1}cm^{-1}$ at 560 nm, the absorbance maximum. Hence, the H_2O_2 decomposition could be spectrophotometrically monitored at 560 nm. The assay mixture typically contained 50 mM HEPES-NaOH pH 7, 5 μM Prx, 4 μM TrxA, 0.2 mM DTT and 100 μM H_2O_2. The reaction was started with the addition of the H_2O_2 and its concentration was measured at different time points by withdrawing 50 μl of the assay mixture to 950 μl of FOX1 reagent. Trx was included as an electron donor and was kept reduced by addition of 0.2 mM DTT. Controls were performed omitting TrxA and in the absence of both Prx and TrxA.

4.2. Protein phosphorylation in cell extracts of *Synechocystis*

One hundred and eighty ml of growing cultures of *Synechocystis* in the exponential phase were harvested by centrifugation as described in 1.3. section and the cell extracts were prepared as described in 3.2. section with the difference that here we resuspend the cells in 25 mM Hepes-NaOH pH 7.6, 15 % (v/v) glycerol, 10 mM $MgCl_2$ (phosphorylation buffer) prior to lysis. After the corresponding pre-treatments during 15 min at room temperature, indicated in each experiment, the cell extracts were incubated for 30 min at 25 ºC with the phosphorylation mixture

composed of 0.5 mM ATP, 10 mM NaF and 5 μCi [γ-^{32}P]ATP. The radioactively labelled proteins were resolved in acrylamide gel electrophoresis according to section 3.4. using a Hoefer SE600 system.

For identification of the SpkB substrate 400 μg of cytosolic protein cell extract were used in the phosphorylation assay. In this case the [γ-^{32}P]ATP was increased to 15 μCi and the proteins were resolved in 2-D IEF/SDS-PAGE as described in 3.4.2.2.

The gels were dried as explained in 3.8. and the radioactivity was detected as described in 3.9. Proteins were identified by PMF as described in 3.6.

4.3. Assays for protein kinase activity

Autophosphorylation of USP and kinase activity of SpkB were assayed *in vitro* with [γ-^{32}P]ATP. Three μg of USP, 2 μg of SpkB or 20 μg of *E. coli* extracts expressing SpkB were used in the assays for kinase activity. In the case of SpkB 2.5 μg of casein or 10 μg of GlySQ were used as substrates. The mixtures were incubated for 15 min at room temperature in phosphorylation buffer with their respective redox treatments, indicated in each experiment. Subsequently, the phosphorylation mixture was added to the sample, including 2 μCi [γ-^{32}P]ATP to USP and 5 μCi [γ-^{32}P]ATP to SpkB, and were incubated at 25 °C for 30 min. The radioactively labelled proteins were resolved in acrylamide protein gels as described in 3.4. After drying the gels the radioactivity was visualised as explained in 3.9.

5. Bioinformatic methods

5.1. DNA and Protein sequences analysis

The sequences of the genes and proteins of *Synechocystis* and were obtained from the database Cyanobase (http://www.kazusa.or.jp/cyano.html) or from the database of NCBI (National Center for Biotechnology Information) (http://www.ncbi.nlm.nih.gov). To search for open reading frames, the location of

restriction sites and translation of nucleotide sequences to protein, we used DNA-Strider, version 1.3, designed by Christian Mark (Service of Biochimie, Centre d'Etudes Nucléaire de Saclay, France). The search for nucleotide or amino acid sequence similarity with the sequences available in databases was made using the BLAST application from NCBI (http://blast.ncbi.nlm.nih.gov/Blast.cgi) or Cyanobase (http://blast.kazusa.or.jp/blast_search/cyanobase/genes).

In order to predict transmembrane regions, the DAS server (http://www.sbc.su.se/~miklos/DAS/) as well as the TMHMM server (http://www.cbs.dtu.dk/services/TMHMM-2.0/) was used.

The presence of signal peptide was analysed by the SignalP (http://www.cbs.dtu.dk/services/SignalP/) and TargetP (http://www.cbs.dtu.dk/services/TargetP/) servers.

The patterns and motifs present within the amino acid sequences were analysed by diverse servers: ScanProsite (http://www.expasy.ch/tools/scanprosite/), Motif Scan (http://myhits.isb-sib.ch/cgi-bin/motif_scan) and Prosite Scan (http://npsa-pbil.ibcp.fr/cgi-bin/npsa_automat.pl?page=npsa_prosite.html).

The phylogenetic alignments and trees were carried out by using the Clustal X engine (European Bioinformatics Institute).

6. Other methods

6.1. Determination of chlorophyll concentration

The cellular content of chlorophyll was determined spectrophotometrically following the method described by MacKinney, 1941. The cells contained in 1 ml of culture were harvesyed by centrifugation at 12000 x *g*. The pellet was resuspended in 1 ml of 90 % methanol, and after mixing the solution by vigorous vortexing for 30 seconds, the sample was centrifuged for 2 minutes at 12000 x *g*. Finally, we determined the chlorophyll concentration in the supernatant measuring the

absorbance at 665 nm using a extinction coefficient of 74.46 mM^{-1} cm^{-1}.

6.2. Spectrophotometric measurements

The absorbance measurements of visible light or ultraviolet light were performed in a Biomat5 spectrophotometer (Thermo Electron Corporation).

6.3. pH measurements

The pH of the solutions was determined with a pH meter, equipped with digital scale, model pH Meter Basic 20 (Crison).

CONCLUSIONS

CONCLUSIONS

1. About one-third of the TrxA protein present in *Synechocystis* is associated with membranes. TrxA appears distributed in equal proportions between plasma membranes and thylakoids.

2. At least 50 Trx-targets are membranes-bound and 38 of these have not been previously reported as Trx-targets in *Synechocistis*. Only 10 of these Trx-targets have earlier been reported as such in other organisms. Four of the newly identified targets were predicted to be integral membrane proteins.

3. The distribution of all reported Trx-targets in *Synechocystis* shows that the majority are in association with membranes.

4. A large number of Trx-membrane targets identified here are involved in the amino acid- and protein metabolism. Proteins containing ATP-binding domain are highly represented amongst the detected targets.

5. 1-Cys Prx and 2-Cys Prx are two thiol peroxidases able to interact physically with TrxA. In both cases TrxA is able to sustain their peroxidase activities.

6. Oligomerisation as well as autophosphorylation activity of Usp1 is redox regulated. TrxA can reduce efficiently Usp1.

7. FtsH proteins are able to interact *in situ* with TrxA35 using total membrane preparations, but their redox regulation could not be demonstrated.

8. Using plant thylakoid lumen preparations we have inferred 7 potential luminal Trx-targets in *Synechocystis*.

9. *Synechocystis* possesses two PrxQ, PrxQ1 and PrxQ2. PrxQ2 contains in its amino acid sequence a signal peptide common to a subclass of cyanobacterial PrxQ. PrxQ2 is able to interact physically with TrxA, which sustains the PrxQ2 peroxidase activity.

10. The protein phosphorylation pattern of *Synechocystis* is altered by treatment with the oxidising agents copper and oxidised glutathione. Reducing treatments with DTT or TrxA restore this phosphorylation indicating redox regulation of protein phosphorylation in this prokaryote.

11. SpkB is a redox-regulated Ser/Thr kinase. The kinase activity of SpkB is inhibited by oxidising treatments with copper or oxidised glutathione and is restored upon reduction catalysed by TrxA *in vitro*. This kinase contains a Cys-motif in its N-terminus, which is involved in the redox regulation.

12. The physiological substrate of SpkB in *Synechocystis* is the glycyl-tRNA synthetase (GlyS), which has potential implications for indirect redox-regulation of its activity.

BIBLIOGRAPHY

BIBLIOGRAPHY

Akiyama Y, Yoshihisa T, Ito K (1995) FtsH, a membrane-bound ATPase, forms a complex in the cytoplasmic membrane of Escherichia coli. J Biol Chem 270:23485-23490

Alkhalfioui F, Renard M, Frendo P, Keichinger C, Meyer Y, Gelhaye E, Hirasawa M, Knaff DB, Ritzenthaler C, Montrichard F (2008) A novel type of thioredoxin dedicated to symbiosis in legumes. Plant Physiol 148:424-435

Allen JF (1992) How does protein phosphorylation regulate photosynthesis? Trends Biochem Sci 17:12-17

Aluru MR, Yu F, Fu A, Rodermel S (2006) Arabidopsis variegation mutants: new insights into chloroplast biogenesis. J Exp Bot 57:1871-1881

Anselmo AN and Cobb MH (2004) Protein kinase function and glutathionylation. Biochem J 381(Pt 3):e1-2

Aran M, Caporaletti D, Senn AM, Tellez de Iñon MT, Girotti MR, Llera AS, Wolosiuk RA (2008) ATP-dependent modulation and autophosphorylation of rapeseed 2-Cys peroxiredoxin. FEBS J 275:1450-1463

Aro EM, Virgin I, Andersson B (1993) Photoinhibition of photosystem II. Inactivation, protein damage and turnover. Biochim Biophys Acta 1143:113-134

Åslund F, Zheng M, Beckwith J, Storz G (1999) Regulation of the OxyR transcription factor by hydrogen peroxide and the cellular thiol-disulfide status. Proc Natl Acad Sci USA 96:6161–6165

Baier M and Dietz KJ (1996) Primary structure and expression of plant homologues of animal and fungal thioredoxin-dependent peroxide reductases and bacterial alkyl hydroperoxide reductases. Plant Mol Biol 31:553-564

Bailey S, Thompson E, Nixon PJ, Horton P, Mullineaux CW, Robinson C, Mann NH (2002) A critical role for the Var2 FtsH homologue of *Arabidopsis thaliana* in the photosystem II repair cycle in vivo. J Biol Chem 277:2006-2011

Bailey S, Melis A, Mackey KR, Cardol P, Finazzi G, van Dijken G, Berg GM, Arrigo K, Shrager J, Grossman A (2008) Alternative photosynthetic electron flow to oxygen in marine *Synechococcus*. Biochim Biophys Acta 1777:269-276

Balmer Y and Buchanan BB (2002) Yet another plant thioredoxin. Trends Plant Sci 7:191–193

Balmer Y, Koller A, del Val G, Manieri W, Schürmann P, Buchanan BB (2003) Proteomics gives insight into the regulatory function of chloroplast thioredoxins. Proc Natl Acad Sci USA 100:370-375

Balmer Y, Koller A, Val GD, Schürmann P, Buchanan BB (2004) Proteomics uncovers proteins interacting electrostatically with thioredoxin in chloroplasts. Photosynth Res 79:275–280

Balmer Y, Vensel WH, Tanaka CK, Hurkman WJ, Gelhaye E, Rouhier N, Jacquot JP, Manieri W, Schürmann P, Droux M, Buchanan BB (2004b) Thioredoxin links redox to the regulation of fundamental processes of plant mitochondria. Proc Natl Acad Sci USA 101:2642-2647

Balmer Y, Vensel WH, Hurkman WJ, Buchanan BB (2006) Thioredoxin target proteins in chloroplast thylakoid membranes. Antioxid Redox Signal 8:1829–1834

Barber J and Andersson B (1992). Too much of a good thing – Light can be bad for photosynthesis. Trends Biochem Sci 17:62-66

Barker M, de Vries R, Nield J, Komenda J, Nixon PJ (2006) The Deg proteases protect *Synechocystis* sp. PCC 6803 during heat and light stresses but are not essential for removal of damaged D1 protein during the photosystem two repair cycle. J Biol Chem 281:30347-30355

Baumann U and Juttner J (2002) Plant thioredoxins: the multiplicity conundrum. Cell Mol Life Sci 59:1042-1057

Bellafiore S, Barneche F, Peltier G, Rochaix JD (2005) State transitions and light

adaptation require chloroplast thylakoid protein kinase STN7. Nature 433:892-895

Bendall DS and Manasse RS (1995) Cyclic photophosphorylation and electron transport. Biochim Biophys Acta 1229: 23-38

Berg BH (1977) The early influence of 17-beta-oestradiol on 17 aminoacyl-tRNA synthetases of mouse uterus and liver. Phosphorylation as a regulation mechanism. Biochim Biophys Acta 479:152-171

Berg BH (1978) The role of cyclic 3',5'-AMP in the regulation of aminoacyl-tRNA synthetase activities in mouse uterus and liver following 17beta-oestradiol treatment. Activation of a phosphoaminoacyl-tRNA synthetase phosphatase by phosphorylation with cyclic 3',5'-AMP dependent protein kinase. Biochim Biophys Acta 521:274-287

Berg BH (1990) Chromatofocusing of aminoacyl-tRNA synthetases, extracted from NMRI mouse liver. Biochim Biophys Acta 1038:391-394

Bernroitner M, Zamocky M, Furtmüller PG, Peschek GA, Obinger C (2009) Occurrence, phylogeny, structure, and function of catalases and peroxidases in cyanobacteria. J Exp Bot 60:423-440

Birnboim HC and Doly J (1979) A rapid alkaline extraction procedure for screening recombinant plasmid DNA. Nucleic Acids Res 7: 1513-1523

Blackler AR, Speers AE, Ladinsky MS, Wu CC (2008) A shotgun proteomic method for the identification of membrane-embedded proteins and peptides. J Proteome Res 7:3028-3034

Bochkareva ES, Girshovich AS, Bibi E (2002) Identification and characterization of the *Escherichia coli* stress protein UP12, a putative in vivo substrate of GroEL. Eur J Biochem 269:3032-3040

Bockholt R, Masepohl B, Pistorius EK (1991) Insertional inactivation of the psbO gene encoding the manganese stabilizing protein of photosystem II in the cyanobacterium *Synechococcus* PCC7942. Effect on photosynthetic water oxidation and L-amino acid oxidase activity. FEBS Lett 294:59-63

Bradford MM (1976) A rapid and sensitive method for the quantitation of microgram quantities of protein utilizing the principle of protein-dye binding. Anal Biochem 72:248-254

Brandes N, Rinck A, Leichert LI, Jakob U (2007) Nitrosative stress treatment of E.coli targets distinct set of thiol containing proteins. Mol Microbiol 66:901-914

Bricker TM, Morvant J, Masri N, Sutton HM, Frankel LK (1998). Isolation of a highly active photosystem II preparation from *Synechocystis* 6803 using a histidine-tagged mutant of CP 47. Biochim Biophys Acta 1409:50–57

Broin M and Rey P (2003) Potato plants lacking the CDSP32 plastidic thioredoxin exhibit overoxidation of the BAS1 2-cysteine peroxiredoxin and increased lipid Peroxidation in thylakoids under photooxidative stress. Plant Physiol 132:1335-1343

Brown AH and Webster GC (1953) The influence of light on the rate of respiration of the blue-green alga Anabaena. Am J Bot 40: 753-758

Bonaventura C and Myers J (1969) Fluorescence and oxygen evolution from Chlorella pyrenoidosa. Biochim Biophys Acta 189:366-383.

Buchanan BB (1980) Role of light in the regulation of chloroplast enzymes. Annu Rev Plant Physiol 31:341–374

Buchanan BB, Schurmann P, Wolosiuk RA, Jacquot JP (2002) The ferredoxin/thioredoxin system: from discovery to molecular structures and beyond. Photosynth Res 73:215–222

Buchanan BB and Balmer Y (2005) Redox regulation: a broadening horizon. Annu Rev Plant Biol 56:187-220

Burnap RL and Sherman LA (1991) Deletion mutagenesis in *Synechocystis* sp. PCC6803 indicates that the Mn-stabilizing protein of photosystem II is not essential for O2 evolution. Biochemistry 30:440-446

Cai YP and Wolk CP (1990) Use of a conditionally lethal gene in *Anabaena* sp. strain PCC 7120 to select for double recombinants and to entrap insertion sequences. J Bacteriol 172: 3138-3145.

Cha MK, Kim HK, Kim IH (1995) Thioredoxin-linked "thiol peroxidase" from periplasmic space of Escherichia coli. J Biol Chem 270:28635-28641

Cha MK, Hong SK, Kim IH (2007) Four thiol peroxidases contain a conserved GCT catalytic motif and act as a versatile array of lipid peroxidases in *Anabaena* sp. PCC7120. Free Radic Biol Med 42:1736-1748

Chauvat F, Labarre J, Van der Ende A, Van Arkel G A (1986). Develoment of gene transfer system for the cyanobacterium *Synechocystis* sp. PCC 6803. Plant Physiol Biochem 26, 629-637

Choi YA, Kim SG, Kwon YM (1999) The plastidic glutamine synthetase activity is directly modulated by means of redox change at two unique cysteine residues. Plant Sci 149:175–182

Christman MF, Morgan RW, Jacobson FS, Ames BN (1985) Positive control of a regulon for defenses against oxidative stress and some heat-shock proteins in *Salmonella typhimurium*. Cell 41:753-762

Collier JL and Grossman AR (1995) Disruption of a gene encoding a novel thioredoxin-like protein alters the cyanobacterial photosynthetic apparatus. J Bacteriol 177:3269-3276

Collin V, Issakidis-Bourguet E, Marchand C, Hirasawa M, Lancelin JM, Knaff DB, Miginiac-Maslow M (2003) The *Arabidopsis* plastidial thioredoxins: new functions and new insights into specificity. J Biol Chem 278:23747-23752

Cotgreave IA, Gerdes R, Schuppe-Koistinen I, Lind C (2002) S-glutathionylation of glyceraldehyde-3-phosphate dehydrogenase: role of thiol oxidation and catalysis by glutaredoxin. Methods Enzymol 348:175-182

Cooper CE, Patel RP, Brookes PS, Darley-Usmar VM (2002) Nanotransducers in

cellular redox signaling: modification of thiols by reactive oxygen and nitrogen species. Trends Biochem Sci 27:489-492

Couturier J, Jacquot JP, Rouhier N (2009) Evolution and diversity of glutaredoxins in photosynthetic organisms. Cell Mol Life Sci 66:2539-2557

Cross JV and Templeton DJ (2004) Oxidative stress inhibits MEKK1 by site-specific glutathionylation in the ATP-binding domain. Biochem J 381:675-683

Dai S, Saarinen M, Ramaswamy S, Meyer Y, Jacquot JP, Eklund H (1996) Crystal structure of Arabidopsis thaliana NADPH dependent thioredoxin reductase at 2.5A resolution. J Mol Biol 264:1044–1110

Dalle-Donne I, Rossi R, Giustarini D, Colombo R, Milzani A (2007) S-glutathionylation in protein redox regulation. Free Radic Biol Med 43:883-898

D'Andrea LD and Regan L (2003) TPR proteins: the versatile helix. Trends Biochem Sci 28:655-662

D'Autréaux B and Toledano MB (2007) ROS as signalling molecules: mechanisms that generate specificity in ROS homeostasis. Nat Rev Mol Cell Biol 8:813-824

De la Rosa MA, Navarro JA, Díaz-Quintana A, De la Cerda B, Molina-Heredia FP, Balme A, Murdoch Pdel S, Díaz-Moreno I, Durán RV, Hervás M (2002) An evolutionary analysis of the reaction mechanisms of photosystem I reduction by cytochrome c(6) and plastocyanin. Bioelectrochemistry 55:41-45

De Las Rivas J and Barber J (2004) Analysis of the Structure of the PsbO Protein and its Implications. Photosynth Res 81:329-343

Debus RJ (2000) The polypeptides of Photosystem II and their influence on manganotyrosyl/based oxygen evolution. Met Ions Biol Syst 37:657–711

Depège N, Bellafiore S, Rochaix JD (2003) Role of chloroplast protein kinase Stt7 in LHCII phosphorylation and state transition in Chlamydomonas. Science 299:1572-1575

Demmig B, Winter K, Krüger A, Czygan FC (1987) Photoinhibition and zeaxanthin formation in intact leaves. A possible role of the xanthophyll cycle in the dissipation of excess light. Plant Physiol 84:218–224

DeRocher AE, Coppens I, Karnataki A, Gilbert LA, Rome ME, Feagin JE, Bradley PJ, Parsons M (2008) A thioredoxin family protein of the apicoplast periphery identifies abundant candidate transport vesicles in *Toxoplasma gondii*. Eukaryot Cell 7:1518-1529

DeRuyter YS and Fromme P (2008) Molecular structure of the photosynthetic apparatus. In Herrero A and Flores E (ed.), The Cyanobacteria: Molcular Biology, Genomics and Evolution. Caister Academic Press, Norfolk, UK . p 217-270

Dufresne A, Garczarek L, Partensky F (2005) Accelerated evolution associated with genome reduction in a free-living prokaryote. Genome Biol 6:R14

Eaton-Rye JJ (2005) Requirements for different combinations of the extrinsic proteins in specific cyanobacterial Photosystem II mutants. Photosynth Res 84:275–281

Edge R, McGarvey DJ, Truscott TG (1997) The carotenoids as anti-oxidants--a review. J Photochem Photobiol B 41:189-200

Ellis HR and Poole LB (1997) Roles for the two cysteine residues of AhpC in catalysis of peroxide reduction by alkyl hydroperoxide reductase from *Salmonella typhimurium*. Biochemistry 36:13349–13356

Enami I, Iwai M, Akiyama A, Suziki T, Okumura A, Katoh T, Tada O, Ohta H, Shen JR (2003) Comparison of binding and functional properties of two extrinsic components, Cyt c550 and a 12 kDa protein, in cyanobacterial PSII with those in read algal PSII. Plant Cell Physiol 44:820–827

Fay P (1992) Oxygen relations of nitrogen fixation in cyanobacteria. Microbiol Rev 56:340-373

Florencio FJ, Yee BC, Johnson TC, Buchanan BB (1988) An NADP/ thioredoxin system in leaves: purification and characterization of NADP-thioredoxin reductase and thioredoxin h from spinach. Arch Biochem Biophys 266:496–507

Florencio FJ, Gadal P, Buchanan BB (1993) Thioredoxin-linked activation of the chloroplast and cytosolic forms of Chlamydomonas reinhardtii glutamine synthetase. Plant Physiol Biochem 31:649–655

Florencio JF, Pérez-Pérez ME, López-Maury L, Mata-Cabana A, Lindahl M (2006) The diversity and complexity of the cyanobacterial thioredoxin systems. Photosynth Res 89:157-171

Flores E and Herrero A (1994) Assimilatory nitrogen metabolism and its regulation. In Bryant DA (ed.), Advances in Photosynthesis. The molecular biology of cyanobacteria. Kluwer Academic Publishers, Dordretch, Holland. p 487-517

Flores E, and Wolk CP (1985) Identification of facultatively heterotrophic, N2-fixing cyanobacteria able to receive plasmid vectors from Escherichia coli by conjugation. J Bacteriol 162: 1339-1341.

Forman HJ, Fukuto JM, Torres M (2004) Redox signaling: thiol chemistry defines which reactive oxygen and nitrogen species can act as second messengers. Am J Physiol Cell Physiol 287:C246-56

Freestone P, Nyström T, Trinei M, Norris V (1997) The universal stress protein, UspA, of *Escherichia coli* is phosphorylated in response to stasis. J Mol Biol 274:318-324

Freist W, Logan DT, Gauss DH (1996) Glycyl-tRNA synthetase. Biol Chem Hoppe Seyler 377:343-356

Fromme P and Grotjohann I (2008a) Structure of Photosystems I and II. Results Probl Cell Differ 45:33-72

Fromme P and Grotjohann I (2008b) Overview of photosynthesis. In Fromme P (ed.), Photosynthetic Protein Complex. WILEY-VCH Verlag GmbH and Co. KGaA, Weinheim, Germany. p 1-22

Funk C and Vermaas W (1999) A cyanobacterial gene family coding for single-helix proteins resembling part of the light-harvesting proteins from higher plants. Biochemistry

38:9397-9404

Gaber A, Yoshimura K, Tamoi M, Takeda T, Nakano Y, Shigeoka S (2004) Induction and functional analysis of two reduced nicotinamide adenine dinucleotide phosphate-dependent glutathione peroxidase-like proteins in *Synechocystis* PCC 6803 during the progression of oxidative stress. Plant Physiol 136:2855-2861

Gantt E (1994) Supramolecular membrane organization. In Bryant DA (ed.), Advances in Photosynthesis. The molecular biology of cyanobacteria. Kluwer Academic Publishers, Dordretch, Holland. p 409-435

Gleason FK and Holmgren A (1981) Isolation and characterization of thioredoxin from the cyanobacterium, *Anabaena* sp. J Biol Chem 256:8306-8309

Gleason FK (1996) Glucose-6-phosphate dehydrogenase from the cyanobacterium, *Anabaena* sp. PCC 7120: purification and kinetics of redox modulation. Arch Biochem Biophys 334: 277-283.

Gonzalez Porqué P, Baldesten A, Reichard P (1970) The involvement of the thioredoxin system in the reduction of methionine sulfoxide and sulfate. J Biol Chem 245:2371-2374

Gopalakrishna R, Chen ZH, Gundimeda U (1995) Modifications of cysteine-rich regions in protein kinase C induced by oxidant tumor promoters and enzyme-specific inhibitors. Methods Enzymol 252:132-146

Gopalakrishna R and Jaken S (2000) Protein kinase C signaling and oxidative stress. Free Radic Biol Med 28:1349-1361

Gopalan G, He Z, Balmer Y, Romano P, Gupta R, Héroux A, Buchanan BB, Swaminathan K, Luan S (2004) Structural analysis uncovers a role for redox in regulating FKBP13, an immunophilin of the chloroplast thylakoid lumen. Proc Natl Acad Sci USA 101:13945-13950

Granlund I, Storm P, Schubert M, García-Cerdán JG, Funk C, Schröder WP (2009) The TL29 protein is lumen located, associated with PSII and not an ascorbate peroxidase. Plant Cell Physiol 50:1898-1910

Guerrero MG and Lara C (1987) Assimilation of inorganic nitrogen. In Fay P and van Baalen C (ed.), The cyanobacteria. Elsevier Science Publishers, New York, USA. p 163-186

Gustavsson N, Diez AA, Nyström T (2002) The universal stress protein paralogues of *Escherichia coli* are co-ordinately regulated and co-operate in the defence against DNA damage. Mol Microbiol 43:107-117

Hall M, Mata-Cabana A, Akerlund HE, Florencio FJ, Schröder WP, Lindahl M, Kieselbach T (2010) Thioredoxin targets of the plant chloroplast lumen and their implications for plastid function. Proteomics 10:987-1001

Hägglund P, Bunkenborg J, Maeda K, Svensson B (2008) dentification of thioredoxin disulfide targets using a quantitative proteomics approach based on isotope-coded affinity tags. J Proteome Res 7:5270-5276

Han G, Zhang CC (2001) On the origin of Ser/Thr kinases in a prokaryote. FEMS Microbiol Lett 200:79-84

Hankamer B, Morris E, Nield J, Carne A, Barber J (2001) Subunit positioning and transmembrane helix organisation in the core dimer of Photosystem II. FEBS Lett 504:142–151

Heide H, Kalisz HM, Follmann H (2004) The oxygen evolving enhancer protein 1 (OEE) of photosystem II in green algae exhibits thioredoxin activity. J Plant Physiol 161:139-149

Herranen M, Battchikova N, Zhang P, Graf A, Sirpiö S, Paakkarinen V, Aro EM (2004) Towards functional proteomics of membrane protein complexes in *Synechocystis* sp. PCC 6803. Plant Physiol 134:470-481

Hishiya S, Hatakeyama W, Mizota Y, Hosoya-Matsuda N, Motohashi K, Ikeuchi M, Hisabori T (2008) Binary reducing equivalent pathways using NADPH-thioredoxin reductase and ferredoxin-thioredoxin reductase in the cyanobacterium Synechocystis sp. strain PCC 6803. Plant Cell Physiol 49:11-18

Hochgräfe F, Mostertz J, Albrecht D, Hecker M (2005) Fluorescence thiol modification assay: oxidatively modified proteins in Bacillus subtilis. Mol Microbiol 58:409-425

Hochgräfe F, Mostertz J, Pöther DC, Becher D, Helmann JD, Hecker M (2007) S-cysteinylation is a general mechanism for thiol protection of Bacillus subtilis proteins after oxidative stress. J Biol Chem 282:25981-25985

Hoiczyk E and Hansel A (2000) Cyanobacterial cell walls: news from an inusual prokaryotic envelope. J Bacteriol 182: 1191–1199

Hondorp ER and Matthews RG (2004) Oxidative stress inactivates cobalamin-independent methionine synthase (MetE) in Escherichia coli. PLoS Biol 2:e336

Hosoya-Matsuda N, Motohashi K, Yoshimura H, Nozaki A, Inoue K, Ohmori M, Hisabori T (2005) Anti-oxidative stress system in cyanobacteria. Significance of type II peroxiredoxin and the role of 1-Cys peroxiredoxin in *Synechocystis* sp. strain PCC 6803. J Biol Chem 280:840-846

Hosoya-Matsuda N, Inoue K, Hisabori T (2009) Roles of thioredoxins in the obligate anaerobic green sulfur photosynthetic bacterium Chlorobaculum tepidum. Mol Plant 2:336-343

Huang F, Parmryd I, Nilsson F, Persson AL, Pakrasi HB, Andersson B, Norling B (2002) Proteomics of *Synechocystis* sp. strain PCC 6803: identification of plasma membrane proteins. Mol Cell Proteomics 1:956-966

Huang F, Hedman E, Funk C, Kieselbach T, Schröder WP, Norling B (2004) Isolation of outer membrane of Synechocystis sp. PCC 6803 and its proteomic characterization. Mol Cell Proteomics 3:586-595

Huang F, Fulda S, Hagemann M, Norling B (2006) Proteomic screening of salt-stress-induced changes in plasma membranes of *Synechocystis* sp. strain PCC 6803. Proteomics 6:2733-2745

Huber HE, Russel M, Model P, Richardson CC (1986) Interaction of mutant thioredoxins of *Escherichia coli* with the gene 5 protein of phage T7. J Biol Chem 261:15006-15012

Huber HE, Tabor S, Richardson CC (1987) Escherichia coli thioredoxin stabilizes complexes of bacteriophage T7 DNA polymerase and primed templates. J Biol Chem 262:16224-16232

Huesgen PF, Schuhmann H, Adamska I (2009) Deg/HtrA proteases as components of a network for photosystem II quality control in chloroplasts and cyanobacteria. Res Microbiol 160:726-732

Ikegami A, Yoshimura N, Motohashi K, Takahashi S, Romano PG, Hisabori T, Takamiya K, Masuda T (2007) The CHLI1 subunit of Arabidopsis thaliana magnesium chelatase is a target protein of the chloroplast thioredoxin. J Biol Chem 282:19282–19291

Imlay JA (2003) Pathways of oxidative damage. Annu Rev Microbiol 57:395–418

Ishikawa Y, Schröder WP, Funk C (2005) Functional analysis of the PsbP-like protein (sll1418) in *Synechocystis* sp. PCC 6803. Photosynth Res 84:257-262

Jacquot JP, Eklund H, Rouhier N, Schürmann P (2009) Structural and evolutionary aspects of thioredoxin reductases in photosynthetic organisms. Trends Plant Sci 14:336-343

Jahns P, Latowski D, Strzalka K (2009) Mechanism and regulation of the violaxanthin cycle: the role of antenna proteins and membrane lipids. Biochim Biophys Acta 1787:3-14

Jakob U, Muse W, Eser M, Bardwell JC (1999) Chaperone activity with a redox switch. Cell 96:341-352

Jang HH, Lee KO, Chi YH, Jung BG, Park SK, Park JH, Lee JR, Lee SS, Moon JC, Yun JW, Choi YO, Kim WY, Kang JS, Cheong GW, Yun DJ, Rhee SG, Cho MJ, Lee SY (2004) Two enzymes in one; two yeast peroxiredoxins display oxidative stress-dependent switching from a peroxidase to a molecular chaperone function. Cell 117:625-635

Jeanjean R, Latifi A, Matthijs HC, Havaux M (2008) The PsaE subunit of photosystem I prevents light-induced formation of reduced oxygen species in the cyanobacterium *Synechocystis* sp. PCC 6803. Biochim Biophys Acta 1777:308-316

Jenkins J, Mayans O, Pickersgill R (1998) Structure and evolution of parallel beta-helix proteins. J Struct Biol 122:236-246

Kamei A, Yuasa T, Orikawa K, Geng XX, Ikeuchi M (2001) A eukaryotic-type protein kinase, SpkA, is required for normal motility of the unicellular cyanobacterium *Synechocystis* sp. strain PCC 6803. J Bacteriol 183:1505-1510

Kamei A, Yuasa T, Geng X, Ikeuchi M (2002) Biochemical examination of the potential eukaryotic-type protein kinase genes in the complete genome of the unicellular cyanobacterium *Synechocystis* sp. PCC 6803. DNA Res 9:71-78

Kamei A, Yoshihara S, Yuasa T, Geng X, Ikeuchi M (2003) Biochemical and functional characterization of a eukaryotic-type protein kinase, SpkB, in the cyanobacterium, *Synechocystis* sp. PCC 6803. Curr Microbiol 46:296-301

Kaneko T, Sato S, Kotani H, Tanaka A, Asamizu E, Nakamura Y, Miyajima N, Hirosawa M, Sugiura M, Sasamoto S, Kimura T, Hosouchi T, Matsuno A, Muraki A, Nakazaki N, Naruo K, Okumura S, Shimpo S, Takeuchi C, Wada T, Watanabe A, Yamada M, Yasuda M, Tabata S (1996) Sequence analysis of the genome of the unicellular cyanobacterium *Synechocystis* sp. strain PCC6803. II. Sequence determination of the entire genome and assignment of potential protein-coding regions. DNA Res 3:109–136

Kaneko T, Nakamura Y, Wolk CP, Kuritz T, Sasamoto S, Watanabe A, Iriguchi M, Ishikawa A, Kawashima K, Kimura T, Kishida Y, Kohara M, Matsumoto M, Matsuno A, Muraki A, Nakazaki N, Shimpo S, Sugimoto M, Takazawa M, Yamada M, Yasuda M, Tabata S (2001) Complete genomic sequence of the filamentous nitrogen-fixing cyanobacterium *Anabaena* sp. strain PCC 7120. DNA Res 8:205–213, 227–253

Kanesaki Y, Yamamoto H, Paithoonrangsarid M, Shoumskaya M, Suzuki I, Hayashi H, Murata N (2007) Histidine kinases play important roles in the perception and signal transduction of hydrogen peroxide in the cyanobacterium, *Synechocystis* sp. PCC 6803.

Plant J 49: 313–324

Kashino Y, Lauber WM, Carroll JA, Wang Q, Whitmarsh J, Satoh K, Pakrasi HB (2002) Proteomic analysis of a highly active Photosystem II preparation from the cyanobacterium *Synechocystis* sp. PCC 6803 reveals the presence of novel polypeptides. Biochemistry 41:8004–8012

Kern D, Giegé R, Ebel JP (1981) Glycyl-tRNA synthetase from baker's yeast. Interconversion between active and inactive forms of the enzyme. Biochemistry 20:122-131

Kieselbach T and Schröder WP (2003) The proteome of the chloroplast lumen of higher plants. Photosynth Res 78:249-264

Kimura Y, Kakemizu A, Matsubara Y, Takegawa K (2009) Enzymatic characteristics of a Ser/Thr protein kinase, SpkA, from *Myxococcus xanthus*. J Biosci Bioeng 107:10-15

Kirilovsky D (2007) Photoprotection in cyanobacteria: the orange carotenoid protein (OCP)-related non-photochemical-quenching mechanism. Photosynth Res 93:7-16

Klughammer B, Baier M, Dietz KJ (1998) Inactivation by gene disruption of 2-cysteine-peroxiredoxin in *Synechocystis* sp. PCC 6803 leads to increased stress sensitivity. Physiol Plant 104: 699–706

Klumpp S, Krieglstein J (2002) Phosphorylation and dephosphorylation of histidine residues in proteins. Eur J Biochem 269:1067-1071

Knoll AH (2008) Cyanobacteria and Earth History. In Herrero A and Flores E (ed.), The Cyanobacteria: Molcular Biology, Genomics and Evolution. Caister Academic Press, Norfolk, UK . p 1-19

Kobayashi M, Ishizuka T, Katayama M, Kanehisa M, Bhattacharyya-Pakrasi M, Pakrasi HB, Ikeuchi M (2004) Response to oxidative stress involves a novel peroxiredoxin gene in the unicellular cyanobacterium *Synechocystis* sp. PCC 6803. Plant Cell Physiol 45: 290–299

Komenda J, Barker M, Kuviková S, DeVries R, Mullineaux CW, Tichy M, Nixon PJ (2006). The FtsH protease *slr0228* is important for quality control of photosystem II in the thylakoid membrane of *Synechocystis* PCC 6803. J Biol Chem 281:1145-1151

König J, Baier M, Horling F, Kahmann U, Harris G, Schürmann P, Dietz KJ (2002) The plant-specific function of 2-Cys peroxiredoxin-mediated detoxification of peroxides in the redox-hierarchy of photosynthetic electron flux. Proc Natl Acad Sci USA 99:5738-5743

Koonin EV (1993) A common set of conserved motifs in a vast variety of putative nucleic acid-dependent ATPases including MCM proteins involved in the initiation of eukaryotic DNA replication. Nucleic Acids Res 21: 2541-2547

Krone FA, Westphal G, Meyer HE, Schwenn JD (1990) PAPS-reductase of Escherichia coli. Correlating the N-terminal amino acid sequence with the DNA of gene cys H. FEBS Lett 260:6–9

Krupa A and Srinivasan N (2005) Diversity in domain architectures of Ser/Thr kinases and their homologues in prokaryotes. BMC Genomics 6:129

Kumar JK, Tabor S, Richardson CC (2004) Proteomic análisis of thioredoxin-targeted proteins in Escherichia coli. Proc Natl Acad Sci U S A 101:3759-3764

Kvint K, Nachin L, Diez A, Nyström T (2003) The bacterial universal stress protein: function and regulation. Curr Opin Microbiol 6:140-145

Kwon J, Oh J, Park C, Cho K, Kim SI, Kim S, Lee S, Bhak J, Norling B, Choi JS (2010) Systematic cyanobacterial membrane proteome analysis by combining acid hydrolysis and digestive enzymes with nano-liquid chromatography-Fourier transform mass spectrometry. J Chromatogr A 1217:285-293

Labarre J, Chauvat F, Thuriaux P (1989) Insertional mutagenesis by random cloning of antibiotic resistance genes into the genome of the cyanobacterium *Synechocystis* strain PCC 6803. J Bacteriol 171:3449-3457

Laemmli UK (1970) Cleavage of structural proteins during the assembly of the head of bacteriophage T4. Nature 227:680-685

Laloi C, Rayapuram N, Chartier Y, Grienenberger JM, Bonnard G, Meyer Y (2001) Identification and characterization of a mitochondrial thioredoxin system in plants. Proc Natl Acad Sci USA 98:14144–14149

Lamkemeyer P, Laxa M, Collin V, Li W, Finkemeier I, Schottler MA, Holtkamp V, Tognetti VB, Issakidis-Bourguet E, Kandlbinder A, Weis E, Miginiac-Maslow M, Dietz KJ (2006) Peroxiredoxin Q of Arabidopsis thaliana is attached to the thylakoids and functions in context of photosynthesis. Plant J 45:968-981

Lamparter T (2004) Evolution of cyanobacterial and plant phytochromes. FEBS Lett 573:1-5

Latifi A, Ruiz M, Jeanjean R, Zhang CC (2007) PrxQ-A, a member of the peroxiredoxin Q family, plays a major role in defense against oxidative stress in the cyanobacterium Anabaena sp. strain PCC7120. Free Radic Biol Med 42:424-431

Latifi A, Ruiz M, Zhang CC (2009) Oxidative stress in cyanobacteia. FEMS Microbiol Rev 33:258-278

Laurent TC, Moore EC, Reichard P (1964) Enzymatic synthesis of deoxyribonucleotides. IV. Isolation and characterization of thioredoxin, the hydrogen donor from *Escherichia coli* B. J Biol Chem 239:3436–3444

Lee SP, Hwang YS, Kim YJ, Kwon KS, Kim HJ, Kim K, Chae HZ (2001) Cyclophilin a binds to peroxiredoxins and activates its peroxidase activity. J Biol Chem 276:29826-29832

Leichert LI, Scharf C, Hecker M (2003) Global characterization of disulfide stress in Bacillus subtilis. J Bacteriol 185:1967-1975

Leichert LI and Jakob U (2004) Protein thiol modifications visualized in vivo. PLOS Biol 2:1723-1737

Leichert LI, Gehrke F, Gudiseva HV, Blackwell T, Ilbert M, Walker AK, Strahler JR, Andrews PC, Jakob U (2008) Quantifying changes in the thiol redox proteome upon

oxidative stress in vivo. Proc Natl Acad Sci USA 105:8197-8202

Lemaire SD, Guillon B, Le Maréchal P, Keryer E, Miginiac-Maslow M, Decottignies P (2004) New thioredoxin targets in the unicellular photosynthetic eukaryote *Chlamydomonas reinhardtii*. Proc Natl Acad Sci USA 101:7475–7480

Lemaire SD, Michelet L, Zaffagnini M, Massot V, Issakidis-Bourguet E (2007) Thioredoxins in chloroplasts. Curr Genet 51:343-365

Lennartz K, Plücken H, Seidler A, Westhoff P, Bechtold N, Meierhoff K (2001) HCF164 encodes a thioredoxin-like protein involved in the biogenesis of the cytochrome b(6)f complex in Arabidopsis. Plant Cell 13:2539-2551

Lennon BW, Williams CH Jr, Ludwig ML (2000) Twists in catalysis: alternating conformations of Escherichia coli thioredoxin reductase. Science 289:1190–1194

Leonard CJ, Aravind L, Koonin EV (1998) Novel families of putative protein kinases in bacteria and archaea: evolution of the "eukaryotic" protein kinase superfamily. Genome Res 8:1038-1047

Leonberg AK and Chai YC (2007) The functional role of cysteine residues for c-Abl kinase activity. Mol Cell Biochem. 304:207-212

Li H, Singh AK, McIntyre LM, Sherman LA (2004) Differential gene expression in response to hydrogen peroxide and the putative PerR regulon of *Synechocystis* sp. strain PCC 6803. J Bacteriol 186:3331–3345

Liberton M, Howard Berg R, Heuser J, Roth R, Pakrasi HB (2006) Ultrastructure of the membrane systems in the unicellular cyanobacterium *Synechocystis* sp. strain PCC 6803. Protoplasma 227:129-138

Lichter A and Häberlein I (1998) A light-dependent redox signal participates in the regulation of ammonia fixation in chloroplasts of higher plants – ferredoxin: glutamate synthase is a thioredoxin-dependent enzyme. J Plant Physiol 153:83–90

Liebeke M, Pöther DC, van Duy N, Albrecht D, Becher D, Hochgräfe F, Lalk M,

Hecker M, Antelmann H (2008) Depletion of thiol-containing proteins in response to quinones in Bacillus subtilis. Mol Microbiol 69:1513-1529

Lillig CH, Prior A, Schwenn JD, Åslund F, Ritz D, Vlamis-Gardikas A, Holmgren A (1999) New thioredoxins and glutaredoxins as electron donors of 3'-phosphoadenylylsulfate reductase. J Biol Chem 274:7695-7698

Lindahl M, Tabak S, Cseke L, Pichersky E, Andersson B, Adam Z (1996) Identification, characterization and molecular cloning of a homologue of the bacterial FtsH protease in chloroplasts of higher plants. J Biol Chem 271:29329-29334

Lindahl M, Spetea C, Hundal T, Oppenheim AB, Adam Z, Andersson B (2000) The thylakoid FtsH protease plays a role in the light-induced turnover of the photosystem II D1 protein. Plant Cell 12:419-431

Lindahl M and Florencio FJ (2003) Thioredoxin-linked processes in cyanobacteria are as numerous as in chloroplasts, but targets are different. Proc Natl Acad Sci USA 100:16107–16112

Lindahl M and Florencio FJ (2004) Systematic screening of reactive cysteine proteomes. Proteomics 4:448–450

Lindahl M and Kieselbach T (2009) Disulphide proteomes and interactions with thioredoxin on the track towards understanding redox regulation in chloroplasts and cyanobacteria. J Proteomics 72:416-438

Link AJ, Robison K, Church GM (1997) Comparing the predicted and observed properties of proteins encoded in the genome of Escherichia coli K-12. Electrophoresis 18:1259-1313

Liu XG, Zhao JJ, Wu QY (2005) Oxidative stress and metal ions effects on the cores of phycobilisomes in *Synechocystis* sp. PCC 6803. FEBS lett 579: 4571–4576

López-Maury L, Sánchez-Riego AM, Reyes JC, Florencio FJ (2009) The glutathione/glutaredoxin system is essential for arsenate reduction in *Synechocystis* sp. strain PCC 6803. J Bacteriol 191:3534-3543

Lowry OH, Rosebrough NJ, Farr AL, Randall RJ (1951) Protein measurement with the Folin phenol reagent. J Biol Chem 193: 265-275

Lu JZ, Fujiwara T, Komatsuzawa H, Sugai M, Sakon J (2006) Cell wall-targeting domain of glycylglycine endopeptidase distinguishes among peptidoglycan cross-bridges. J Biol Chem 281:549-558

Lundin B, Thuswaldner S, Shutova T, Eshaghi S, Samuelsson G, Barber J, Andersson B, Spetea C (2007) Subsequent events to GTP binding by the plant PsbO protein: structural changes, GTP hydrolysis and dissociation from the photosystem II complex. Biochim Biophys Acta 1767:500-508

Mackinney G (1941) Absorption of light by chlorophyll solutions. J Biol Chem 140:109-112.

Mann NH, Novac N, Mullineaux CW, Newman J, Bailey S, Robinson C (2000) Involvement of an FtsH homologue in the assembly of functional photosystem I in the cyanobacterium *Synechocystis* sp. PCC 6803. FEBS Lett 479:72-77

Marchand C, Le Maréchal P, Meyer Y, Miginiac-Maslow M, Issakidis-Bourguet E, Decottignies P (2004) New targets of Arabidopsis thioredoxins revealed by proteomic analysis. Proteomics 4:2696-2706

Marchand C, Le Maréchal P, Meyer Y, Decottignies P (2006) Comparative proteomic approaches for the isolation of proteins interacting with thioredoxin. Proteomics 6:6528-6537

Markwell MA, Haas SM, Bieber LL, Tolbert NE (1978) A modification of the Lowry procedure to simplify protein determination in membrane and lipoprotein samples. Anal Biochem 87: 206-210

Marx C, Wong JH, Buchanan BB (2003) Thioredoxin and germinating barley: targets and protein redox changes. Planta 216:454-460

Masip L, Veeravalli K, Georgiou, G (2006) The many faces of glutathione in bacteria.

Antiox Redox Signal 8:753-762

Matthews HR (1995) Protein kinases and phosphatases that act on histidine, lysine, or arginine residues in eukaryotic proteins: a possible regulator of themitogen-activated protein kinase cascade. Pharmac Ther 67:323-350

Mazauric MH, Keith G, Logan D, Kreutzer R, Giegé R, Kern D (1998) Glycyl-tRNA synthetase from *Thermus thermophilus*--wide structural divergence with other prokaryotic glycyl-tRNA synthetases and functional inter-relation with prokaryotic and eukaryotic glycylation systems. Eur J Biochem 251:744-57

Meng L, Wong JH, Feldman LJ, Lemaux PG, Buchanan BB (2010) A membrane-associated thioredoxin required for plant growth moves from cell to cell, suggestive of a role in intercellular communication. Proc Natl Acad Sci USA 107:3900-3905

Meyer Y, Reichheld JP, Vignols F (2005) Thioredoxins in Arabidopsis and other plants. Photosynth Res 86:419–433

Meyer Y, Buchanan BB, Vignols F, Reichheld JP (2009) Thioredoxins and glutaredoxins: unifying elements in redox biology. Annu Rev Genet 43:335-367

Michelet L, Zaffagnini M, Massot V, Keryer E, Vanacker H, Miginiac-Maslow M, Issakidis-Bourguet E, Lemaire SD (2006) Thioredoxins, glutaredoxins and glutathionylation: new crosstalks to explore. Photosynth Res 89:225-245

Mikkelsen R, Mutenda KE, Mant A, Schürmann P, Blennow A (2005) Alpha-glucan, water dikinase (GWD): a plastidic enzyme with redox-regulated and coordinated catalytic activity and binding affinity. Proc Natl Acad Sci USA 102:1785-1790

Mizuno T, Kaneko T, Tabata S (1996) Compilation of all genes encoding bacterial two-component signal transducers in the genome of the cyanobacterium, *Synechocystis* sp. strain PCC 6803. DNA Res 3:407-414

Motohashi K, Kondoh A, Stumpp MT, Hisabori T (2001) Comprehensive survey of proteins targeted by chloroplast thioredoxin. Proc Natl Acad Sci USA 98:11224-11229

Motohashi K, Koyama F, Nakanishi Y, Ueoka-Nakanishi H, Hisabori T (2003) Chloroplast cyclophilin is a target protein of thioredoxin. Thiol modulation of the peptidyl-prolyl cis-trans isomerase activity. J Biol Chem 278:31848-31852

Motohashi K and Hisabori T (2006) HCF164 receives reducing equivalents from stromal thioredoxin across the thylakoid membrane and mediates reduction of target proteins in the thylakoid lumen. J Biol Chem 281:35039–35047

Montrichard F, Alkhalfioui F, Yano H, Vensel WH, Hurkman WJ, Buchanan BB (2009) Thioredoxin targets in plants: the first 30 years. J Proteomics 72:452-474

Mullineux CW (2008) Biogenesis and Dynamics of Thylakoid Membranes and the Photosynthetic Apparatus. In Herrero A and Flores E (ed.), The Cyanobacteria: Molcular Biology, Genomics and Evolution. Caister Academic Press, Norfolk, UK . p 289-303

Mulo P, Sirpiö S, Suorsa M, Aro EM (2008) Auxiliary proteins involved in the assembly and sustenance of photosystem II. Photosynth Res 98:489-501

Muñoz-Dorado J, Inouye S, Inouye M (1991) A gene encoding a protein serine/threonine kinase is required for normal development of *M. xanthus*, a gram-negative bacterium. Cell 67:995-1006

Murata N (1969) Control of excitation transfer in photosynthesis. I. Light-induced change of chlorophyll a fluorescence in Porphyridium cruentum. Biochim Biophys Acta 172:242-251

Murata N and Suzuki I (2006) Exploitation of genomic sequences in a systematic analysis to access how cyanobacteria sense environmental stress. J Exp Bot 57:235-247

Mutsuda M, Ishikawa T, Takeda T, Shigeoka S (1996) The catalase-peroxidase of Synechococcus PCC 7942: purification, nucleotide sequence analysis and expression in Escherichia coli. Biochem J 316:251-257

Nachin L, Nannmark U, Nyström T (2005) Differential roles of the universal stress proteins of *Escherichia coli* in oxidative stress resistance, adhesion and motility. J Bacteriol 187:6265-6272

Nagel GM, Johnson MS, Rynd J, Petrella E, Weber BH (1988) Glycyl-tRNA synthetase of Escherichia coli: immunological homology with phenylalanyl-tRNA synthetase. Arch Biochem Biophys 262:409-415

Neuwald AF, Aravind L, Spouge JL, Koonin EV (1999) AAA+: A class of chaperone-like ATPases associated with the assembly, operation and disassembly of protein complexes. Genome Res 9:27-43

Nield J, Morris EP, Bibby TS, Barber J (2003) Structural analysis of the photosystem I supercomplex of cyanobacteria induced by iron deficiency. Biochemistry 42:3180-3188

Nishiyama Y, Allakhverdiev SI, Murata N (2006) A new paradigm for the action of oxygen species in the photoinhibition of photosystem II. Biochm Biophy Acta 1757:742–749

Niyogi KK, Grossman AR, Björkman O (1998) Arabidopsis mutants define a central role for the xanthophyll cycle in the regulation of photosynthetic energy conversion. Plant Cell 10:1121–1134

Nixon PJ, Barker M, Boehm M, deVries R, Komenda J (2005) FtsH-mediated repair of the photosystem two complex in response to light stress in the cyanobacterium *Synechocystis* sp. PCC 6803. J Exp Bot 56:347-356

Nixon PJ, Michoux F, Yu J, Boehm M, Komenda J (2010) Recent advances in understanding the assembly and repair of photosystem II. Ann Bot 106:1-16

Niyomporn B, Dahl JL, Strominger JL (1968) Biosynthesis of the peptidoglycan of bacterial cell walls. IX. Purification and properties of glycyl transfer ribonucleic acid synthetase from Staphylococcus aureus. J Biol Chem 243:773-778

Norling B, Zak E, Andersson B, Pakrasi H (1998) 2D-isolation of pure plasma and thylakoid membranes from the cyanobacterium *Synechocystis* sp. PCC 6803. FEBS Lett 436:189-192

Nyström T and Neidhardt FC (1994) Expression and role of the universal stress

protein, UspA, of *Escherichia coli* during growth arrest. Mol Microbiol 11:537–544

Nystrom T and Neidhardt FC (1996) Effects of overproducing the universal stress protein UspA, in *Escherichia coli* K-12. J Bacteriol 178:927–930

Obinger C, Regelsberger G, Strasser G, Burner U, Peschek GA (1997) Purification and characterization of a homodimeric catalase-peroxidase from the cyanobacterium Anacystis nidulans. Biochem Biophys Res Commun 235:545-552

Ogura T and Wilkinson AJ (2001) AAA^+ superfamily ATPases: common structure – diverse function. Genes Cells 6:575-597

Ostrem DL and Berg P (1974) Glycyl transfer ribonucleic acid synthetase from Escherichia coli: purification, properties, and substrate binding. Biochemistry 13:1338-1348

Panichkin VB, Arakawa-Kobayashi S, Kanaseki T, Suzuki I, Los DA, Shestakov SV, Murata N (2006) Serine/threonine protein kinase SpkA in *Synechocystis* sp. strain PCC 6803 is a regulator of expression of three putative pilA operons, formation of thick pili, and cell motility. J Bacteriol 188:7696-7699

Paumann M, Regelsberger G, Obinger C, Peschek GA (2005) The bioenergetic role of dioxygen and the terminal oxidase(s) in cyanobacteria. Biochim Biophys Acta 1707:231-253

Pe'er I, Felder CE, Man O, Silman I, Sussman JL, Beckmann JS (2004) Proteomic signatures: Amino acid and oligopeptide compositions differentiate among phyla. Proteins 54:20-40

Peltier JB, Emanuelsson O, Kalume DE, Ytterberg J, Friso G, Rudella A, Liberles DA, Söderberg L, Roepstorff P, von Heijne G, van Wijk KJ (2002) Central functions of the lumenal and peripheral thylakoid proteome of *Arabidopsis* determined by experimentation and genome-wide prediction. Plant Cell 14:211-236

Perelman A, Uzan A, Hacohen D, Schwarz R (2003) Oxidative stress in *Synechococcus* sp. strain PCC 7942: various mechanisms for H2O2 detoxification with

different physiological roles. J Bacteriol 185:3654-3660

Pérez-Pérez ME, Florencio FJ, Lindahl M (2006) Selecting thioredoxins for disulphide proteomics: target proteomes of three thioredoxins from the cyanobacterium *Synechocystis* sp. PCC 6803. Proteomics 6 (Suppl 1):S186–195

Pérez-Pérez ME, Mata-Cabana A, Sánchez-Riego AM, Lindahl M, Florencio FJ (2009) A comprehensive analysis of the peroxiredoxin reduction system in the Cyanobacterium Synechocystis sp. strain PCC 6803 reveals that all five peroxiredoxins are thioredoxin dependent. J Bacteriol 191:7477-7489

Pérez-Ruiz JM, Spínola MC, Kirchsteiger K, Moreno J, Sahrawy M, Cejudo FJ (2006) Rice NTRC is a high-efficiency redox system for chloroplast protection against oxidative damage. Plant Cell 18:2356-2368

Petersson UA, Kieselbach T, García-Cerdán JG, Schröder WP (2006) The Prx Q protein of *Arabidopsis thaliana* is a member of the luminal chloroplast proteome. FEBS Lett 580:6055-6061

Pisareva T, Shumskaya M, Maddalo G, Ilag L, Norling B (2007) Proteomics of *Synechocystis* sp. PCC 6803. Identification of novel integral plasma membrane proteins. FEBS J 274:791-804

Piven I, Ajlani G, Sokolenko A (2005) Phycobilisome linker proteins are phosphorylated in *Synechocystis* sp. PCC 6803. J Biol Chem 280:21667-21672

Poole LB, Karplus PA, Claiborne A (2004) Protein sulfenic acids in redox signaling. Annu Rev Pharmacol Toxicol 44:325-47

Poole LB (2005) Bacterial defenses against oxidants: mechanistic features of cysteine-based peroxidases and their flavoprotein reductases. Arch Biochem Biophys 433:240-254

Poole LB (2007) The catalytic mechanism of peroxiredoxins. Subcell Biochem 44:61–81

Poole LB and Nelson KJ (2008) Discovering mechanisms of signaling-mediated cysteine oxidation. Curr Opin Chem Biol 12:18-24

Porat A, Cho SH, Beckwith J (2004) The unusual transmembrane electron transporter DsbD and its homologues: a bacterial family of disulfide reductases. Res Microbiol 155:617-622

Pöther DC, Liebeke M, Hochgräfe F, Antelmann H, Becher D, Lalk M, Lindequist U, Borovok I, Cohen G, Aharonowitz Y, Hecker M (2009) Diamide triggers mainly S Thiolations in the cytoplasmic proteomes of Bacillus subtilis and Staphylococcus aureus. J Bacteriol 191:7520-7530

Price GD, Badger MR, Woodger FJ, Long BM (2008) Advances in understanding the cyanobacterial CO2-concentrating-mechanism (CCM): functional components, Ci transporters, diversity, genetic regulation and prospects for engineering into plants. J Exp Bot 59:1441-1461

Profy AT and Schimmel P (1986) A sulfhydryl presumed essential is not required for catalysis by an aminoacyl-tRNA synthetase. J Biol Chem 261:15474-15479

Rey P, Cuiné S, Eymery F, Garin J, Court M, Jacquot JP, Rouhier N, Broin M (2005) Analysis of the proteins targeted by CDSP32, a plastinic thioredoxin participating in oxidative stress responses. Plant J 41:31–42

Rhee KY, Erdjument-Bromage H, Tempst P, Nathan CF (2004) S-nitroso proteome of Mycobacterium tuberculosis: Enzymes of intermediary metabolism and antioxidant defense. Proc Natl Acad Sci USA 102:467-472

Rintamäki E, Martinsuo P, Pursiheimo S, Aro EM (2000) Cooperative regulation of light-harvesting complex II phosphorylation via the plastoquinol and ferredoxin-thioredoxin system in chloroplasts. Proc Natl Acad Sci USA 97:11644-11649

Rippka R, Deruelles J, Waterbury JB, Herman M, Stanier RY (1979) Generic assignments, strain histories and properties of pure cultures of cyanobacteria. J Gen Microbiol 111:1–61

Rouhier N, Gelhaye E, Sautiere PE, Brun A, Laurent P, Tagu D, Gerard J, de Faÿ E, Meyer Y, Jacquot JP (2001) Isolation and characterization of a new peroxiredoxin from poplar sieve tubes that uses either glutaredoxin or thioredoxin as a proton donor. Plant Physiol 127:1299-1309

Rouhier N, Gelhaye E, Gualberto JM, Jordy MN, De Fay E, Hirasawa M, Duplessis S, Lemaire SD, Frey P, Martin F, Manieri W, Knaff DB, Jacquot JP (2004) Poplar peroxiredoxin Q. A thioredoxin-linked chloroplast antioxidant functional in pathogen defense. Plant Physiol 134:1027-1038

Russel M, Model P (1985) Thioredoxin is required for filamentous phage assembly. Proc Natl Acad Sci USA 82:29-33

Saikawa N, Akiyama Y, Ito K (2004) FtsH exists as an exceptionally large complex containing HflKC in the plasma membrane of *Escherichia coli*. J Struct Biol 146:123-129

Sakamoto W, Zaltsman A, Adam Z, Takahashi Y (2003) Coordinated regulation and complex formation of yellow variegated1 and yellow variegated2, chloroplastic FtsH metalloproteases involved in the repair cycle of photosystem II in Arabidopsis thylakoid membranes. Plant Cell 15:2843-2855

Sakamoto W (2006) Protein degradation machineries in plastids. Annu Rev Plant Biol 57:599-621

Salsbury FR Jr, Knutson ST, Poole LB, Fetrow JS (2008) Functional site profiling and electrostatic analysis of cysteines modifiable to cysteine sulfenic acid. Protein Sci 17:299-312

Sambrook J, Fritsch EF, Maniatis T (1989) Molecular Cloning: A Laboratory Manual. Cold Spring Harbor, N. Y.: Cold Spring Harbor Laboratory

Santoni V, Molloy M, Rabilloud T (2000) Membrane proteins and proteomics: Un amour impossible?. Electrophoresis 21:1054-1070

Schägger H and von Jagow G (1991) Blue native electrophoresis for isolation of membrane protein complexes in enzymatically active form. Anal Biochem 199:223-231

Scherr N, Honnappa S, Kunz G, Mueller P, Jayachandran R, Winkler F, Pieters J, Steinmetz MO (2007) Structural basis for the specific inhibition of protein kinase G, a virulence factor of *Mycobacterium tuberculosis*. Proc Natl Acad Sci USA 104:12151-12156

Schilling B, Yoo CB, Collins CJ, Gibson BW (2004) Determining cysteine oxidation status using differential alkylation. Int J Mass Spectrom 236:117-127

Schneider GJ, Tumer NE, Richaud C, Borbely G, Haselkorn R (1987) Purification and characterization of RNA polymerase from the cyanobacterium *Anabaena* 7120. J Biol Chem 262: 14633-14639

Schriek S, Aguirre-von-Wobeser E, Nodop A, Becker A, Ibelings BW, Bok J, Staiger D, Matthijs HC, Pistorius EK, Michel KP (2008) Transcript profiling indicates that the absence of PsbO affects the coordination of C and N metabolism in *Synechocystis* sp. PCC 6803. Physiol Plant 133:525-543

Schubert H, Matthijs HCP, Mur LR (1995) In vivo assay of P700 redox changes in the cyanobacterium *Fremyella diplosiphon* and the role of cytochrome-C-oxidase in regulation of photosynthetic electron-transfer. Photosynthetica 31:517-527

Schubert M, Petersson UA, Haas BJ, Funk C, Schröder WP, Kieselbach T (2002) Proteome map of the chloroplast lumen of Arabidopsis thaliana. J Biol Chem 277:8354-8365

Schürmann P, Buchanan BB (2008) The ferredoxin/thioredoxin system of oxygenic photosynthesis. Antioxid Redox Signal 10:1235-1274

Schürmann P, Jacquot JP (2000) Plant thioredoxin systems revisited. Annu Rev Plant Physiol Plant Mol Biol 51:371–400

Serrato AJ, Pérez-Ruiz JM, Spinola MC, Cejudo FJ (2004) A novel NADPH thioredoxin reductase, localized in the chloroplast, which deficiency causes hypersensitivity to abiotic stress in Arabidopsis thaliana. J Biol Chem 279:43821-43827

Sétif P, Fischer N, Lagoutte B, Bottin H, Rochaix JD (2002) The ferredoxin docking site of photosystem I. Biochim Biophys Acta 1555:204-209

Sevier CS and Kaiser CA (2002) Formation and transfer of disulphide bonds in living cells. Nat Rev Mol Cell Biol 3:836-847

Shi J, Vlamis-Gardikas A, Aslund F, Holmgren A, Rosen BP (1999) Reactivity of glutaredoxins 1, 2, and 3 from *Escherichia coli* shows that glutaredoxin 2 is the primary hydrogen donor to ArsC-catalyzed arsenate reduction. J Biol Chem 274:36039–36042

Sieker LC, Stenkamp RE, LeGall J (1994) Rubredoxin in crystalline state. Methods Enzymol 243:203-216

Silva P, Thompson E, Bailey S, Kruse O, Mullineaux CW, Robinson C, Mann NH, Nixon PJ (2003) FtsH is involved in the early stages of repair of photosystem II in *Synechocystis* sp. PCC 6803. Plant Cell 15:2152-2164

Simon RD (1976) The biosynthesis of multi-L-arginyl-poly(L-aspartic acid) in the filamentous cyanobacterium *Anabaena cylindrica*. Biochim Biophys Acta 422: 407-418

Simon RD (1987) Inclusion bodies in the cyanobacteria: cyanophycin, polyphosphate, polyhedral bodies. In Fay P and Van Baalen C (ed.) The Cyanobacteria. Elsevier, Amsterdam, Netherlands. p 199–225

Singh AK and Sherman LA (2000) Identification of iron-responsive, differential gene expression in the cyanobacterium *Synechocystis* sp. strain PCC 6803 with a customized amplification library. J Bacteriol 182:3536-3543

Singh AK and Sherman LA (2002) Characterization of a stress-responsive operon in the cyanobacterium *Synechocystis* sp. strain PCC 6803. Gene 297:11-19

Sippola K and Aro EM (1999) Thiol redox state regulates expression of psbA genes in *Synechococcus* sp. PCC 7942. Plant Mol Biol 41: 425-433

Smulevich G, Jakopitsch C, Droghetti E, Obinger C (2006) Probing the structure and bifunctionality of catalase-peroxidase (KatG). J Inorg Biochem 100:568-85

Sousa MC and McKay DB (2001) Structure of the universal stress protein from *Haemophilus influenzae.* Structure 9:1135–1141

Srivastava R, Pisareva T, Norling, B (2005) Proteomic studies of the thylakoid membrane of *Synechocystis* sp. PCC 6803. Proteomics 5:4905-4916

Stacy RA, Munthe E, Steinum T, Sharma B, Aalen RB (1996) A peroxiredoxin antioxidant is encoded by a dormancy-related gene, Per1, expressed during late development in the aleurone and embryo of barley grains. Plant Mol Biol 31:1205-1216

Stacy RA, Nordeng TW, Culiáñez-Macià FA, Aalen RB (1999) The dormancy-related peroxiredoxin anti-oxidant, PER1, is localized to the nucleus of barley embryo and aleurone cells. Plant J 19:1-8

Stanier RY, Cohen-Bazire G (1977) Phototrophic prokaryotes: the cyanobacteria. Annu Rev Microbiol 31: 225-274

Steglich G, Neupert W, Langer T (1999) Prohibitins regulate membrane protein degradation by the m-AAA protease in mitochondria. Mol Cell Biol 19:3435-3442

Stewart WD (1980) Some aspects of structure and function in N2-fixing cyanobacteria. Annu Rev Microbiol 34: 497-536

Stock JB, Stock AM, Mottonen JM (1990) Signal transduction in bacteria. Nature 344:395-400

Stork T, Michel KP, Pistorius EK, Dietz KJ (2005) Bioinformatic analysis of the genomes of the cyanobacteria *Synechocystis* sp. PCC 6803 and *Synechococcus elongatus* PCC 7942 for the presence of peroxiredoxins and their transcript regulation under stress. J Exp Bot 56:3193-3206

Stork T, Laxa M, Dietz MS, Dietz KJ (2009) Functional characterisation of the peroxiredoxin gene family members of *Synechococcus elongatus* PCC 7942. Arch Microbiol 191:141-151

Storz G and Imlay JA (1999) Oxidative stress. Curr Opi Microbiol 2:188–194

Ströher E and Dietz KJ (2008) The dynamic thiol-disulphide redox proteome of the Arabidopsis thaliana chloroplast as revealed by differential electrophoretic mobility.

Physiol Plant 133:566-583

Sugishima M, Migita CT, Zhang X, Yoshida T, Fukuyama K (2004) Crystal structure of heme oxygenase-1 from cyanobacterium *Synechocystis* sp. PCC 6803 in complex with heme. Eur J Biochem 271:4517-4525

Sun QA, Kirnarsky L, Sherman S, Gladyshev VN (2001) Selenoprotein oxidoreductase with specificity for thioredoxin and glutathione systems. Proc Natl Acad Sci U. S. A. 98: 3673–3678

Sveshnikov D, Funk C, Schröder WP (2007) The PsbP-like protein (sll1418) of *Synechocystis* sp. PCC 6803 stabilises the donor side of Photosystem II. Photosynth Res 93:101-109

Tao K (2008) Subcellular localization and in vivo oxidation-reduction kinetics of thiol peroxidase in Escherichia coli. FEMS Microbiol Lett 289:41-45

Thiel T and Poo H (1989) Transformation of a filamentous cyanobacterium by electroporation. J Bacteriol 171: 5743-5746

Thornton LE, Ohkawa H, Roose JL, Kashino Y, Keren N, Pakrasi HB (2004) Homologs of plant PsbP and PsbQ proteins are necessary for regulation of photosystem ii activity in the cyanobacterium *Synechocystis* 6803. Plant Cell 16:2164-75

Tichy M and Vermaas W (1999) In vivo role of catalase-peroxidase in *Synechocystis* sp. strain PCC 6803. J Bacteriol 181:1875-1882

Ting CS, Rocap G, King J, Chisholm SW (2002) Cyanobacterial photosynthesis in the oceans: the origins and significance of divergent lightharvesting strategies. Trends Microbiol 10: 134–142

Tomitani A, Knoll AH, Cavanaugh CM, Ohno T (2006) The evolutionary diversification of cyanobacteria: molecular-phylogenetic and paleontological perspectives. Proc Natl Acad USA 103:5442-5447

Tsiotis G, Haase W, Engel A, Michel H (1995) Isolation and structural

characterization of trimeric cyanobacterial photosystem I complex with the help of recombinant antibody fragments. Eur J Biochem 231:823-830

van de Meene AM, Hohmann-Marriott MF, Vermaas WF, Roberson RW (2006) The three-dimensional structure of the cyanobacterium *Synechocystis* sp. PCC 6803. Arch Microbiol 184:259-270

Vassiliev S and Bruce D (2008) Toward understanding molecular mechanisms of light harvesting and charge separation in photosystem II. Photosynth Res 97:75-89

Verdoucq L, Vignols F, Jacquot JP, Chartier Y, Meyer Y (1999) In vivo characterization of a thioredoxin h target protein defines a new peroxiredoxin family. J Biol Chem 274:19714-19722.

Walburger A, Koul A, Ferrari G, Nguyen L, Prescianotto-Baschong C, Huygen K, Klebl B, Thompson C, Bacher G, Pieters J (2004) Protein kinase G from pathogenic mycobacteria promotes survival within macrophages. Science 304:1800-1804

Walker JE, Saraste M, Runswick MJ, Gay NJ (1982) Distantly related sequences in the α- and β-subunits of ATP synthase, myosin, kinases and other ATP-requiring enzymes and a common nucleotide binding fold. EMBO J 1:945-951

Wallin E, and von Heijne G (1998) Genome-wide analysis of integral membrane proteins from eubacterial, archaean and eukaryotic organisms. Prot Sci 7:1029-1038

Walters EM, Garcia-Serres R, Jameson GN, Glauser DA, Bourquin F, Manieri W, Schürmann P, Johnson MK, Huynh BH (2005) Spectroscopic characterization of sitespecific [Fe(4)S(4)] cluster chemistry in ferredoxin:thioredoxin reductase: implications for the catalytic mechanism. J Am Chem Soc 127:9612–9624

Wang Y, Xu W, Chitnis PR (2009) Identification and bioinformatic analysis of the membrane proteins of *Synechocystis* sp. PCC 6803. Proteome Sci 7:11

Ward NE, Pierce DS, Chung SE, Gravitt KR, O'Brian CA (1998) Irreversible inactivation of protein kinase C by glutathione. J Biol Chem 273:12558-12566

Weber A and Jung K (2006) Biochemical properties of UspG, a universal stress protein of *Escherichia coli*. Biochemistry 45:1620-1628

Weber M, Suter M, Brunold C, Kopriva S (2000) Sulfate assimilation in higher plants characterization of a stable intermediate in the adenosine 5'-phosphosulfate reductase reaction. Eur J Biochem 267:3647-3653

Weber H, Engelmann S, Becher D, Hecker M (2004) Oxidative stress triggers thiol oxidation in the glyceraldehydes-3-phosphate dehydrogenase of *Staphylococcus aureus*. Mol Microbiol 52:133-140

Weiner JH and Li L (2008) Proteome of the *Escherichia coli* envelope and technological challenges in membrane proteome analysis. Biochim Biophys Acta 1778:1698-16713

Wieles B, van Soolingen D, Holmgren A, Offringa R, Ottenhoff T, Thole J (1995) Unique gene organization of thioredoxin and thioredoxin reductase in Mycobacterium leprae. Mol Microbiol 16:921–929

Wolf C, Hochgräfe F, Kusch H, Albrecht D, Hecker M, Engelmann S (2008) Proteomic analysis of antioxidant strategies of Staphylococcus aureus: diverse responses to different oxidants. Proteomics 8:3139-3153

Wolff SP (1994) Ferrous ion oxidation in presence of ferric ion indicator xylenol orange for measurement of hydroperoxides. Methods Enzymol 233:182–189

Wolk CP (1982) Heterocysts. In Carr NG and Whitton BA (ed.), The biology of cyanobacteria. Blackwell Scientific Publications, Oxford, UK. p 359-386

Wolk CP, Vonshak A, Kehoe P, Elhai J (1984) Construction of shuttle vectors capable of conjugative transfer from Escherichia coli to nitrogen-fixing filamentous cyanobacteria. Proc Natl Acad Sci U S A 81: 1561-1565.

Wong JH, Balmer Y, Cai N, Tanaka CK, Vensel WH, Hurkman WJ, Buchanan BB (2003) Unraveling thioredoxin-linked metabolic processes of cereal starchy endosperm using proteomics. FEBS Lett 547:151-156

Wood ZA, Schröder E, Robin Harris J, Poole LB (2003) Structure, mechanism and regulation of peroxiredoxins. Trends Biochem Sci 28:32-40

Wu CC and Yates III JR (2003) The application of mass spectrometry to membrane proteomics. Nat Biotechnol 21:262-267

Wu G, Ortiz-Flores G, Ortiz-Lopez A, Ort DR (2007) A pointmutation in atpC1 raises the redox potential of the Arabidopsis chloroplast ATP synthase -subunit regulatory disulphide above the range of thioredoxin modulation. J Biol Chem 282:36782–36789

Xu H, Vavilin D, Funk C, Vermaas W (2004) Multiple deletions of small Cab-like proteins in the cyanobacterium *Synechocystis* sp. PCC 6803: consequences for pigment biosynthesis and accumulation. J Biol Chem 279:27971-9

Xu WL, Jeanjean R, Liu YD, Zhang CC (2003) *pkn22* (*alr2502*) encoding a putative Ser/Thr kinase in the cyanobacterium *Anabaena* sp. PCC 7120 is induced by both iron starvation and oxidative stress and regulates the expression of isiA. FEBS Lett 553:179-182

Yamamoto H, Miyake C, Dietz KJ, Tomizawa K, Murata N, Yokota A (1999) Thioredoxin peroxidase in the cyanobacterium *Synechocystis* sp. PCC 6803. FEBS Lett 447: 269-273

Yano H, Wong JH, Lee YM, Cho MJ, Buchanan BB (2001) A strategy for the identification of proteins targeted by thioredoxin. Proc Natl Acad Sci USA 98:4794-4799

Yano H, Kuroda S, Buchanan BB (2002) Disulfide proteome in the analysis of protein function and structure. Proteomics 2:1090-1096

Yee BC, de la Torre A, Crawford NA, Lara C, Carlson DE, Buchanan BB (1981) The ferredoxin/thioredoxin enzyme regulation in a cyanobacterium. Arch Microbiol 130:14-18

Zahedi RP, Meisinger C, Sickmann A (2005) Two-dimensional benzyldimethyl-n-hexadecylammonium chloride/SDS-PAGE for membrane proteomics. Proteomics 5:3581-3588

Zarembinski TI, Hung LW, Müller-Dieckmann HJ, Kim KK, Yokota H, Kim R, Kim SH (1998) Structure-based assignment of the biochemical function of a hypothetical protein: a test of structural genomics. Proc Natl Acad Sci USA 95:15189–15193

Zeller T, Klug G (2006) Thioredoxins in bacteria: functions in oxidative stress response and regulation of thioredoxin genes. Naturwissenschaften 93:259-266

Zhang CC (1993) A gene encoding a protein related to eukaryotic protein kinases from the filamentous heterocystous cyanobacterium *Anabaena* PCC 7120. Proc Natl Acad Sci USA 90:11840-11844

Zhang X, Zhao F, Guan X, Yang Y, Liang C, Qin S (2007) Genome-wide survey of putative serine/threonine protein kinases in cyanobacteria. BMC Genomics 8:395

Zheng M, Åslund F, Storz G (1998) Activation of the OxyR transcription factor by reversible disulfide bond formation. Science 279:1718-1721